UNIVERSITÉ PARIS 6
PIERRE ET MARIE CURIE

École doctorale de Paris centre

Thèse de Doctorat

Spécialité: Mathématiques

Tiehong Zhao

Géométries des réseaux hyperboliques complexes

sous la direction d'Elisha Falbel
John Parker

Soutenue le 19 Octobre 2011 devant le jury composé de :

Gilles Courtois	Université Paris VI
Martin Deraux	Institut Fourier
Elisha Falbel	Université Paris VI
Ruth Kellerhals	Université de Fribourg
John R Parker	University of Durham

au vu des rapports de:

Martin Deraux	Institut Fourier, France
Ruth Kellerhals	Université de Fribourg, Suisse

Institut de Mathématiques de Jussieu
175, rue du chevaleret
75 013 Paris

École doctorale Paris centre Case 188
4 place Jussieu
75 252 Paris cedex 05

献给我最亲爱的爸爸妈妈

女朋友赵凌燕

Remerciements

Je tiens tout d'abord à exprimer ma profonde reconnainssance envers Elisha Falbel. Je le remercie d'avoir accepé d'encadrer cette thèse. J'ai pu béneficier de son intuition mathématique, en particulier, sa vision géométrique des problèmes. Je voudrais le remercier pour tous ses encouragements constants, sa disponibilité et sa profonde gentillesse qui m'ont permis d'avancer sereinement dans mon travail.

J'aimerais aussi exprimer ma gratitude à John Parker pour avoir dirigé mon travail. En particulier, je le remercie de m'avoir suggéré le sujet qui fait l'objet la cinquième chapitre de ma thèse et de m'avoir invité à l'Université de Durham pour trois mois. Je remercie aussi James Thompson pour nos discussions et les problèmes de géométrie hyperbolique complexe qui'il m'a proposé pendent ce sejour.

Martin Deraux et Ruth Kellerhals ont accepté d'être rapporteurs de cette thèse et participer au jury. Je les remercie pour les remarques et suggestions qu'ils ont faites sur mon travail. Merci également à John Parker et Gilles Courtois d'avoir accepté d'être membre de mon jury.

Je voudrais remercier les persones qui ont partagé avec discussions mathématiques. Nicolas Bergron pour m'avoir expliqué les outils cohomologique nécessaire au dernier chapitre de ma thèse. Maxime Wolff pour ses précisions sur le théorie de Teichmüller et les représentations de groupe de surface, ainsi que Juliette Genzmer, ma grande sœur de thèse.

Je tiens à remercier Madame Soizic Merle qui m'a patiemment enseigné le français et aussi m'a invité chez elle.

Je voudrais remercier mes collègues dans bureau 7C10 qui m'ont accompagné pendant les deux premières années de ma thèse à chevaleret : Runqiang, Jiao, Banafsheh, Luc, Mirjam et en particulier Benjamin pour toutes les fois où il m'a aidé. Après le déménagement à Jussieu, j'ai connu des nouvaux collègues dans bureau 1516-5-15 : Fei, Jenney, Maksim et en particulier Charles qui je remercie pour les nombreuses fois où il m'a aidé.

Je remercie mes amis chinois de Paris pour l'ambiance amicale qu'ils ont créée, je pense à Dai Xiaoying, Fang Xin, Fu Lie, Guo Lingyan, Lu Yong, Qin Botao, Qin Fan, Sun Fei, Qiu Yanqi, Wang Haoran, Wang Xiaoyi, Wang Zhiqiang, Zhu Jialin et bien d'autres. Je remercie aussi le Professeur Xiaonan Ma de m'avoir beaucoup aidé quand je suis arrivé à Paris.

Je voudrais aussi remercier Yueping Jiang sans qui cette thèse m'aurait jamais vu le jour et Yuming Chu qui a su m'apprendre comment rédiger un texte mathématique.

Je voudrais enfin remercier mes parents qui m'ont toujours soutenu.

Résumé

Dans cette thèse, nous nous intéressons à l'étude des géométries des réseaux dans $PU(2,1)$, en d'autres termes, construction des domaines fondamentaux de ces réseaux pour leur action dans l'espace hyperbolique complexe. Dans le troisième chapitre, nous construisons un domaine fondamental pour la sœur du groupe modulaire d'Eisenstein-Picard et calculatons le volume de son orbifold de quotient par la fomula de Gauss-Bonnet. Dans le quatrième chapitre nous donnons les generateurs des groupes modulaires euclidiens de Picard $PU(2,1;\mathcal{O}_d)$ où $d = 2, 7, 11$. De plus, domaines fondamentaux des stabilisateurs de l'infini sont obtenu ainsi que de leurs présentations. Dans le cinquième chapitre nous donnons une nouvelle construction des domaines fondamentaux pour certains groupes de Mostow, qui sont engendrés par trois réflexions complexe d'ordre 3. Ces domaines sont une généralisation naturelle du domaine de la sœur du groupe modulaire d'Eisenstein-Picard. Comme application, nous calculons la cohomologie de la surface d'Eisenstein-Picard et sa soeur à coefficients locaux dans le dernier chapitre.

Mots-clefs

Réseaux · Space hyperbolique complexe · Domaine fondamental · Bisecteur · Groupes modulaires de Picard · Groupes de Mostow · Cohomologie · Coefficients locaux

---

Geometry of complex hyperbolic lattices

Abstract

This thesis concerns the study of the geometry of lattices in $PU(2,1)$, in other words, construction of fundamental domains for these lattices for their action in complex hyperbolic space. In the third chapter we construct a fundamental domain for the sister of Eisenstein-Picard modular group and compute the volume of its quotient orbifold by Gauss-Bonnet fomula. In the fourth chapter we give the generators of the Euclidean Picard modular groups $PU(2,1;\mathcal{O}_d)$ where $d = 2, , 7, 11$. Furthermore, fundamental domains of their stabilizers of the infinity are obtained as well as their presentations. In the fifth chapter we give a new construction of fundamental domains for certain Mostow groups, that are generated by three braiding complex reflections of order 3. These fundamental domains are a natural generalization of the domain for the sister of Eisenstein-Picard modular group. As an application, we compute the cohomology of Eisenstein-Picard modular surface and its sister with local coefficients in the last chapter.

Keywords

Lattices · Complex hyperbolic space · Fundamental domain · Bisector · Picard modular groups · Mostow groups · Cohomology · Local coefficients

Contents

0.1 Introduction en français

Cette thèse consiste en l'étude de la géométrie de certains réseaux de $PU(2,1)$, à travers leur action sur l'espace hyperbolique complexe.

Un réseau dans un groupe topologique localement compact G muni de la mesure de Haar est un sous-groupe discret Γ de G tel que le quotient $\Gamma\backslash G$ soit de volume fini. Nous nous intéressons en particulier au cas où le groupe de Lie associé est le groupe des isométries holomorphes de l'espace hyperbolique complexe $\mathbf{H}^2_{\mathbb{C}}$, et un *réseau hyperbolique complexe* est un sous-groupe discret Γ de $PU(2,1)$ tel que le volume du quotient $\mathbf{H}^2_{\mathbb{C}}/\Gamma$ est fini pour la métrique de Bergman.

- Un réseau est dit *uniforme* ou *cocompact* si le quotient $\mathbf{H}^2_{\mathbb{C}}/\Gamma$ est compact, c'est-à-dire, s'il existe un domaine fondamental compact de Γ, et est appelé *non-uniforme* ou de *covolume infinite* sinon.

- Un réseau $\Gamma \subset G$ est *réductible* si G admet sous-groupes normaux connexes H, H' tel que $HH' = G$, $H \cap H'$ est discret et $\Gamma/(\Gamma \cap H) \cdot (\Gamma \cap H')$ est fini. Un réseau est *irréductible* s'il n'est pas réductible. En outre, l'irréductibilité est équivalente à la condition que pour tout sous-groupe normal connexe $H \subset G$ et $\pi : G \to G/H$ est la projection naturelle, $\pi(\Gamma)$ est dense.

- Deux sous-groupes H_1 et H_2 d'un groupe sont *commensurables* si leur intersection $H_1 \cap H_2$ est d'indice fini dans H_1 et H_2. Soit $G \subset \mathrm{GL}_n(\mathcal{K})$ un groupe algébrique linéaire défini sur un corps de nombres $\mathcal{K}$. Un sous-groupe $\Gamma \subset G(\mathcal{K})$ est dit *arithmétique* s'il est commensurable avec $G(\mathcal{O})$, où $\mathcal{O}$ est l'anneau des entiers de $\mathcal{K}$.

Les réseaux des espaces symétriques de rang un ont été étudiés depuis longtemps avec des résultats importants de rigidité et d'arithméticité. Un problème fondamental dans l'étude des espaces symétriques est la relation entre groupes arithmétiques et réseaux. En général, Borel et Harish-Chandra [BHC62] ont pouvé que dans tout espace symétrique de type non-compact, les groupes arithmétiques sont des réseaux. En revanche, Margulis [Mar84] a montré que lorsque le rang de l'espace symétrique est au moins deux, tous les réseaux irréductibles sont arithmétiques.

Des progrès ont été faits pour les espaces symétriques de rang un de type non-compact, par exemple, les espaces symétriques suivants :

$$\mathbf{H}^n_{\mathbb{R}} \quad \mathbf{H}^n_{\mathbb{C}} \quad \mathbf{H}^n_{\mathbb{H}} \quad \mathbf{H}^n_{\mathbb{O}}$$

lesquels sont les espaces hyperboliques respectivement réel, complexe et quaternionique de dimension n ainsi que le plan hyperbolique sur les octonions de Cayley (voir le chapitre 19 du livre [Mos83]). Dans ces cas, Corlette [Cor92] et Gromov et Schoen [GS92] ont montré que dans $\mathbf{H}^n_{\mathbb{H}}$ pour $n \geq 2$ et dans $\mathbf{H}^2_{\mathbb{O}}$ tous les réseaux sont arithmétiques. En plus, Gromov et Piatetski-Shapiro [GPS87] ont donné des exemples des réseaux non-arithmétiques de $\mathbf{H}^n_{\mathbb{R}}$ pour tout $n \geq 2$. L'existence de réseaux non-arithmétiques dans la géométrie hyperbolique complexe n'a pas été démontrée complètement. Plus précisément, Mostow [Mos80] a construit une famille de réseaux non-arithmétiques dans le plan hyperbolique complexe $\mathbf{H}^2_{\mathbb{C}}$ dont nous parlerons ci-dessous. Deligne et Mostow [DM86] ont trouvé un réseau non-arithmétique de $\mathbf{H}^3_{\mathbb{C}}$. La question de savoir s'il existe des réseaux non-arithmétiques de $\mathbf{H}^n_{\mathbb{C}}$ avec $n \geq 4$ est encore ouverte. Il s'agit peut-être de la question ouverte le puls importante du domaine.

Il existe quatre méthodes de construction de réseaux dans l'espace hyperbolique complexe : les constructions arithmétiques, l'utilisation de différents espaces de modules, la géométrie algébrique et la construction des domaines fondamentaux ; voir la papier [Par09] pour l'étude préliminaire et ses références pour plus de détails. Nous nous intéressons en particulier aux réseaux dans $PU(2,1)$ par la construction d'un domaine fondamental dans $\mathbf{H}^2_{\mathbb{C}}$. En d'autres termes, il faut trouver un ensemble ouvert connexe $D \in \mathbf{H}^2_{\mathbb{C}}$ tel que $D \cap \gamma(D) = \emptyset$ pour tout $\gamma \in \Gamma - \{Id\}$ et $\bigcup_{\gamma\in\Gamma} \gamma(\overline{D}) = \mathbf{H}^2_{\mathbb{C}}$, où $\overline{D}$ est la clôture de D dans $\mathbf{H}^2_{\mathbb{C}}$. Une difficulté de cette construction est qu'il n'existe pas d'hypersurfaces réelles totalement géodésiques en géométrie hyperbolique complexe, et en particulier pas de notions naturelles de polyèdres.

Une méthode simple de la construction de domaines fondamentaux est de construire le domaine de Dirichlet centré en un point $p_0 \in \mathbf{H}^n_{\mathbb{C}}$. Le domaine de Dirichlet est l'ensemble des points de $\mathbf{H}^n_{\mathbb{C}}$ qui sont plus proches de p_0 que de tout autre point dans la Γ-orbite de p_0. C'est-à-dire, l'objet principal dans cette construction est l'ensemble des points équidistants à deux points donnés, qu'on l'appele un *bissecteur*. Le premier exemple de domaine de Dirichlet hyperbolique complexe est attribué à Giraud [Gir21] ; voir également l'annexe A de Goldman [Gol99]. Une généralisation naturelle du domaine de Dirichlet est le *domaine de Ford*, voir la section 9.3 de [Gol99]. Ici le point z_0 se trouve sur $\partial\mathbf{H}^n_{\mathbb{C}}$ et la distance est remplacée par une fonction de Busemann centrée en z_0. Les courbes de niveau d'une fonction de Busemann sont les *horosphères*. Les faces du domaine de Ford sont contenues dans des bissecteurs appelés *sphères isométriques* par rapport à la métrique de Cygan, une métrique naturelle sur le groupe de Heisenberg. Comme le stabilisateur de z_0 est infini, on peut obtenir un domaine fondamental en considérant l'intersection du domaine de Ford avec un domaine fondamental du stabilisateur.

Typiquement, un domaine fondamental est un polyèdre localement fini D muni d'une structure combinatoire. Les faces de codimension 1 de D, appelées faces, peuvent être parmi une grande variété d'hypersurfaces réelles (par exemple des bissecteurs, $\mathbb{C}$-sphères et $\mathbb{R}$-sphères), mais il doit exister des *isométries d'appariement*: chaque face doit être envoyée bijectivement sur une face (peut-être lui-même) par une isométrie d'appariement dans $PU(2,1)$. *Le théorème du polyèdre de Poincaré* donne les conditions permettant d'affirmer que le groupe engendré par les isométries d'appariement est discret, que D est un domaine fondamental et on obtient une présentation de ce groupe. Une autre conséquence du théorème de Poincaré, est qu'on peut obtenir la caractéristique d'Euler de l'orbifold et ainsi de calculer le volume par la version hyperbolique complexe du théorème de Gauss-Bonnet. Nous donnons quelques exemples de domaines fondamentaux explicites qui ont été construits pour des réseaux de $PU(2,1)$.

- L'un des réseaux arithmétiques les plus simples de $PU(2,1)$ est le *groupe modulaire d'Eisenstein-Picard* $PU(2,1,\mathbb{Z}[\omega])$ comprenant des matrices dont les entrées sont toutes dans les coefficients d'Eisenstein $\mathbb{Z}[\omega]$ où ω est une racine cubique de l'unité. C'est l'un des premiers exemples de Picard [Pic83] dans $PU(2,1)$ et c'est la généralisation naturelle du groupe modulaire classique $\mathrm{PSL}(2,\mathbb{Z})$ dans $\mathrm{PSL}(2,\mathbb{R})$. En fait, Picard [Pic83, Pic84] construit une famille de réseaux arithmétiques notés $PU(2,1;\mathcal{O}_d)$, ce qu'on appelle *groupes modulaires de Picard*, où $\mathcal{O}_d$ est l'anneau des entiers dans le corps de nombres quadratique imaginaire $\mathbb{Q}(i\sqrt{d})$. La géométrie du groupe $PU(2,1,\mathbb{Z}[\omega])$ a été étudiée par Falbel et Parker dans [FP06]. En d'autres termes, ils ont construit un domaine fondamental muni de la structure combinatoire la plus simple possible. Ce domaine est un 4-simplexe, qui est un cône géodésique construit à partir d'un 3-simplexe avec un sommet idéal (le point fixé parabolique).

Cette construction est tout à fait analogue au 2-simplexe avec un sommet idéal qui est le domaine fondamental pour le groupe modulaire classique $PSL(2,\mathbb{Z})$ dans le plan hyperbolique $\mathbf{H}^1_{\mathbb{C}}$.

- Un autre groupe modulaire de Picard est appelé *groupe modulaire de Gauss-Picard* dont l'anneau associé est $\mathbb{Z}[i]$, noté $PU(2,1;\mathbb{Z}[i])$. Francsics et Lax ont décrit dans [FL05, FLa05] un domaine fondamental pour ce groupe. Leur domaine fondamental est seulement semi-explicite et ne comprend pas l'analyse de la combinatoire. Plus récemment, Falbel, Francsics, Lax et Parker [FFP10, FFLP11] en construisent un domaine fondamental à partir du domaine de Ford, qui est analogue au cas de $PU(2,1,\mathbb{Z}[\omega])$. Il peut être obtenu par l'intersection du domaine de Ford avec un domaine fondamental pour le stabilisateur. La différence est principalement due au fait qu'il y a trois arêtes compactes qui sont contenues dans trois sphères isométrique respectivement.

- Dans son célèbre article [Mos80], Mostow a étudié de nouveaux exemples de sous-groupes de $PU(2,1)$ engendrés par trois réflexions complexes d'ordre p ($p = 3,4,5$) et a montré que ces sont des réseaux hyperboliques complexes en construisant des domaines fondamentaux de Dirichlet. Toutes les faces de codimension 1 sont contenues dans des bissecteurs. Comme nous l'avons mentionné, l'absence d'hypersurfaces réelles totalement géodésiques donne lieu à la difficulté de comprendre l'intersection de deux bissecteurs. Il y a eu quelques erreurs mineures dans la construction de Mostow, voir [Der05]. Une autre de construction des domaines fondamentaux pour les mêmes groupes a été proposée par Deraux, Falbel et Paupert [DFP05].

- Ron Livné dans sa thèse [Liv81] a construit une famille de réseaux dans $PU(2,1)$ par utilisant des techniques issues de la géométrie algébrique. Parker [Par06] a utilisé la méthode de Thurston pour donner une construction géométrique des réseaux de Livné. Plus précisément, il a construit un polyèdre fondamental pour les groupes de Livné, chaque arête de laquelle est contenue dans un bissecteur. Un lien entre les groupes de Livné et le groupe modulaire d'Eisenstein-Picard provient de la description du domaine fondamental. Le polyèdre fondamental dans [Par06] est un cône géodésique obtenu à partir d'un tétraèdre vers un triangle géodésique sur une droite complexe. Si cette droite complexe dégénère en un sommet idéal, les groupes de Livné devient le groupe modulaire d'Eisenstein-Picard. En d'autres termes, cette configuration limite correspond à un domaine fondamental pour le groupe modulaire d'Eisenstein-Picard qui est différente de celle de [FP06]. Plus récemment, Boadi dans sa thèse [Bo11] a utilisé la même approche que pour les groupes de Livné pour construire des domaines fondamentaux pour les groupes de Mostow du premier type mentionné dans [Par09]. Le domaine fondamental, dans la construction de Boadi, est composé de deux simplexes en dimension 4 recollés sur la face commune en dimension 3.

- D'autres exemples viennent de représentations de groupes triangulaires hyperboliques dans $PU(2,1)$. Par convention, nous adoptons les notations suivantes pour ces réseaux. Soit (p,q,r) un *groupe triangulaire hyperbolique* avec $1/p + 1/q + 1/r < 1$, défini comme étant le groupe de Coxeter avec la présentation,

$$\left\langle a_1, a_2, a_3 |\ a_1^2, a_2^2, a_3^2, (a_2a_3)^p, (a_3a_1)^q, (a_1a_2)^r \right\rangle.$$

  Nous pouvons considèrer une famille de représentations $\rho_t : (p,q,r) \to PU(2,1)$. Nous définissons $\Gamma(p,q,r;n)$ comme l'image d'une représentation non-fidèle $\rho_t(p,q,r)$

où $\rho_t(a_1a_3a_2a_3)$ est un élément elliptique d'ordre n. Deraux montre dans [Der06] que le groupe $\Gamma(4,4,4;5)$ est un réseau cocompact de $PU(2,1)$. Parker et Thompson [PT10] ont construit un domaine fondamental pour le réseau de Deraux et ont donné la présentation

$$\left\langle a_1, a_2, a_3 |\ a_i^2, (a_ia_j)^4, (a_ia_ja_k)^{10}, (a_ia_ja_ka_j)^5 \right\rangle.$$

De plus, Thompson dans sa thèse [Tho10] a découvert deux nouveaux réseaux déformés du groupe trianglaire hyperbolique, $\Gamma(3,3,4;7)$ et $\Gamma(3,3,5;5)$. Il a construit conjecturalement leur domaines fondamentaux. La même construction des domaines fondamentaux pourrait être effectuée pour tout $\Gamma(p,q,r;n)$ où $a_1a_2a_3$ est un élément elliptique régulier d'ordre fini. Plus explicitement, le domaine fondamental consiste en un cône de dimension 4 sur une région de dimension 3 connexe bornée de $\mathbf{H}^2_{\mathbb{C}}$ avec un point cône (le point fixé de $a_1a_2a_3$).

Soit $X = G/K$ un espace symétrique de type non compact, où G est le groupe des points réels d'un groupe algébrique semi-simple $\mathbf{G}$ défini sur $\mathbb{Q}$. Soit $\Gamma \subset G$ un réseau arithmétique et (E,ρ) un Γ-module. Comme l'espace localement symétrique $\Gamma\backslash X$ est un $K(\Gamma,1)$, le groupe de cohomologie Γ est isomorphe à la cohomologie de l'espace localement symétrique, c.-à-d.

$$H^*(\Gamma, E) \cong H^*(\Gamma\backslash X; \mathbb{E}),$$

où $\mathbb{E}$ désigne le faisceau associé au système local sur (le variété ou l'orbifold) $\Gamma\backslash X$ défini par (E,ρ). Une *épine* est un déformation rétracte Γ-équivariante $X_0 \subset X$ telle que $\Gamma\backslash X_0$ est compact s'il existe. Des exemples d'épines explicites ont été construits pour quelques Γ. Par exemple, Soulé dans [Sou78] a trouvé une épine pour $SL_3(\mathbb{Z})$ et le cas des groupes euclidiens de Bianchi $SL_2(\mathcal{O}_d)$ (où $d = 1,2,3,7,11$) a été traité par Mendoza dans [Men79]. Plus généralement, Ash [As77, As84] a utilisé la méthode de *well-rounded retract* pour construire une épine pour tous les espaces symétriques linéaires. Cette méthode peux être appliquée pour les groupes algébriques où les points réels sont isomorphes à un produit des groupes suivants [FK94] :

- $GL_n(\mathbb{R})$;
- $GL_n(\mathbb{C})$;
- $GL_n(\mathbb{H})$;
- $O(1,n-1)\times\mathbb{R}^\times$;
- Le groupe de Lie noncompact d'algèbre de Lie $\mathfrak{e}_{6(-26)} \oplus \mathbb{R}$.

Pour quelques exemples en petite dimension, la cohomologie a été calculée combinatoirement à partir de la structure cellulaire d'une épine dans [As80, Men79, Sou78, SV83].

Plus récemment, Yasaki a construit dans [Yas06] une rétraction sur une épine pour groupes en $\mathbb{Q}$-rang 1. Comme application, il a construit dans [Yas08] une épine explicite pour $\Gamma = SU(2,1;\mathbb{Z}[i])$ et calcule la cohomologie de $\mathbf{H}^2_{\mathbb{C}}/\Gamma$ à coefficients locaux.

Plan de thèse

Le plan de cette thèse est le suivant. Les principaux résultats se répartissent en trois grands chapitres, tous les trois indépendants, comportant chacun une introduction.

Dans le premier chapitre nous rappelons les deux modèles du plan hyperbolique complexe $\mathbf{H}^2_{\mathbb{C}}$, les isométries hyperboliques complexes et leur classification. Trois types de sous-variétés totalement géodésiques seront décrites. En plus, nous discutons de la projection orthogonale sur une géodésique complexe qui sera utilisée dans la thèse. Le domaine de Siegel a la même structure que le modèle du demi-espace supérieur de l'espace hyperbolique réel. De plus, le bord s'identifie au compactifié en un point du groupe de Heisenberg. Nous définissons la métrique de Cygan sur le groupe de Heisenberg et de la sphère de Cygan. La référence générale pour ce chapitre est le livre de Goldman [Gol99] ou Parker [Par10].

Nous passons en revue, dans le deuxième chapitre, la définition d'un bissecteur qui est l'ensemble points à égales distances de deux points donnés. Un bissecteur est une hypersurfaces analytiques réelles dans $\mathbf{H}^2_{\mathbb{C}}$, ce qui est difféomorphe à $\mathbb{R}^3$. Ces hypersurfaces jouissent de deux décompositions naturelles dans les sous-variétés totalement géodésiques ; voir[Mos80, Gol99]. Les sphères isométriques sont des exemples des bissecteurs. Nous construisons des polyèdres dont les faces de codimension un peuvent être contenues dans des bissecteurs ou sphères isométriques dans les chapitres suivants. Nous passons en revue le théorème du polyèdre de Poincaré qui sera d'usage constant tout au long de la thèse.

Dans le troisième chapitre, nous construisons un domaine fondamental explicitement pour un groupe (que nous appelons la sœur du groupe modulaire d'Eisenstein-Picard) noté G_2. Ce groupe a d'abord été défini par Parker dans [Par98], où il montre que les surfaces modulaires d'Eisenstein-Picard et $\mathbf{H}^2_{\mathbb{C}}/G_2$ sont des candidats pour être l'orbifold hyperbolique complexe avec cusp de volume minimal. Stover dans son article [Sto10] a affirmé que ce sont précisément les deux orbifolds hyperboliques complexes de volume minimal. Nous énonçons le résultat principal de ce chapitre :

Théorème 0.1.1. *Il existe un domaine fondamental pour G_2, qui est un cône géodésique sur un prisme (voir la Figure 3.6) vers q_∞, avec les isométries d'appariement I_1, R, S et T. Par conséquent, le groupe G_2 engendré par I_1, R, S, T est discret et a la présentation :*

$$G_2 = \left\langle I_1, R, S, T \middle| \begin{array}{l} R^6 = (R^{-1}S)^3 = [R,T] = S^2T^{-1} \\ = (T^{-1}I_1)^3 = (S^{-1}I_1)^3 = R^{-1}I_1^2 = Id \end{array} \right\rangle.$$

Ce troisième chapitre a été publié dans *Mathematical Proceedings of Cambridge Philosophical Society* [Zh11].

Le quatrième chapitre est consacré à donner les générateurs des groupes modulaires de Picard $PU(2,1;\mathcal{O}_d)$ où l'anneau d'entier $\mathcal{O}_d$ est Euclidien, c'est à dire $d = 1, 2, 3, 7, 11$. En particulier, le cas de $\mathcal{O}_1$ et $\mathcal{O}_3$ ont déja été étudiés dans de nombreux aspects. Par exemple, le domaine fondamental explicite de ces deux groupes a été obtenu dans [FFP10, FP06]. Il y a peu de résultats pour les autres groupes modulaires de Picard. Chaque élément du groupe modulaire de Gauss-Picard peut être décomposé en un produit des générateurs par un algorithme simple [FFLP11]. Nous avons commencé par essayer de construire les domaines fondamentaux pour ces groupes $PU(2,1;\mathcal{O}_d)$ d'après la méthode utilisée par Falbel et Parker dans [FP06]. Cela a conduit à un domaine qui était trop complexe à comprendre. Enfin, un résultat de construction de domaine fondamental nous permet de donner les générateurs pour les groupes modulaires euclidiens de Picard de manière géométrique. Nous énoncons plus précisément :

Théorème 0.1.2. *Les groupes modulaires euclidiens de Picard $PU(2,1;\mathcal{O}_d)$ où $d = 2, 3, 7$ sont engendrés par une involution, une rotation de Heisenberg, deux rotations spirales de Heisenberg et une translation verticale.*

Essentiellement, cette méthode peut être appliquée sur le cas de $\mathcal{O}_d$ dont le nombre de classe est un. Cette classe est plus grande que celle des $\mathcal{O}_d$ où $\mathcal{O}_d$ est Euclidien. Toutefois, il est plus difficile de déterminer la collection finie des sphères spinales contenant le domaine fondamental pour le groupe cuspidal lorsque d est plus grand.

Ce chapitre a été accepté pour publication dans *Transactions of American Mathematical Society.*

Le cinquième chapitre consiste en l'étude des réseaux de Mostow $\Gamma(p,k)$, basée sur le fait que la sœur du groupe modulaire d'Eisenstein-Picard qui est un cas particulier du réseau de Mostow $\Gamma(3,6)$. Mostow [Mos80] a considéré tout d'abord une famille remarquable des groupes engendrés par trois réflexions complexes R_1, R_2, R_3 d'ordre p où $p=3,4,5$. Le fait que ces groupes soient discrets a été vérifié par la construction d'un domaine fondamental pour leur action. Après le travail de Mostow, Deraux, Falbel et Paupert [DFP05] ont construit un nouveau domaine fondamental qui est plus simple que celui de Mostow, mais surtout qui permet l'utilisation de la synthèse des arguments géométriques. Nous donnons maintenant une autre construction de nouveaux domaines fondamentaux pour certains réseaux de Mostow $\Gamma(3,k)$ où les valeurs de k satisfont $1/k+1/l=1/6$ pour un entier l. L'idée principale de ce chapitre est inspirée par la construction de [Par06]. Plus de motivations et de résultats peuvent être trouvés dans l'introduction détaillée de ce chapitre, ainsi que quelques notations. Le groupe Γ_k est l'un des réseaux de Mostow que nous considérons avec les générateurs géométriques I_1, R, S et T. Notez bien que nous utilisons les mêmes notations que dans le troisième chapitre, mais ces générateurs sont des produits de R_1, R_2, R_3 et J, qui sont les générateurs de l'article original [Mos80]. Nous résumons les résultats :

Théorème 0.1.3. *Le groupe $\Gamma_k \subset PU(2,1)$ est discret s'il existe un entier l tel que $1/k+1/l=1/6$, c.-à-d., la paire ordonnée (k,l) est dans la liste*

$$(7,42),\ (8,24),\ (9,18),\ (10,15),\ (12,12),\ (15,10),\ (18,9),\ (24,8),\ (42,7).$$

Dans ce cas, il existe un domaine fondamental $\mathbf{D}$ avec les isométries d'appariement donnée par $R=(JR_1^{-1}J)^2$, $S=JR_1^{-1}$, $T=(JR_1^{-1})^2$, $I_1=JR_1^{-1}J$ et les relations cycle donnent la présentation suivante:

$$\Gamma_k=\left\langle R,S,T,I_1 \;\middle|\; \begin{array}{l} R^k=T^l=(R^{-1}S)^3=(T^{-1}I_1)^3=(S^{-1}I_1)^3 \\ =[R,T]=Id, \quad T=S^2, \quad R=I_1^2 \end{array} \right\rangle.$$

Le dernier chapitre, motivé par le travail de Yasaki dans [Yas08], est consacré de calculer la cohomologie de la surface d'Eisenstein-Picard et sa soeur à coefficients locaux. Cette méthode peut être généralisée au domaine fondamental d'un cusp. Nous donnons la cohomologie à $\mathbb{Z}$-coefficients triviaux suivant:

Théorème 0.1.4. *A coefficients triviaux,*

$$\begin{aligned} H^i(\mathbf{H}^2_{\mathbb{C}}/G_1;\mathbb{Z}) &= \begin{cases} \mathbb{Z}, & i=0 \\ 0, & i\geq 1. \end{cases} \\ H^i(\mathbf{H}^2_{\mathbb{C}}/G_2;\mathbb{Z}) &= \begin{cases} \mathbb{Z}, & i=0,2 \\ 0, & i=1 \text{ or } i\geq 3. \end{cases} \end{aligned}$$

0.2 Introduction in English

This thesis consists in the study of the geometry of some lattices in $PU(2,1)$ by means of their action on the complex hyperbolic space.

A lattice in a locally compact topological group G with Haar measure is a discrete subgroup Γ of G such that the quotient $\Gamma\backslash G$ has finite volume. In our particular case of interest where the associated Lie group is the holomorphic isometry group of complex hyperbolic space $\mathbf{H}^2_{\mathbb{C}}$, a *complex hyperbolic lattice* is a discrete subgroup Γ of $PU(2,1)$ such that the volume of the quotient $\mathbf{H}^2_{\mathbb{C}}/\Gamma$ is finite with respect to the Bergman metric.

- A lattice is said to be *uniform* or *cocompact* if the quotient $\mathbf{H}^2_{\mathbb{C}}/\Gamma$ is compact, namely, there exists a compact fundamental domain of Γ and is called *non-uniform* or *coinfinite-volume* otherwise.

- A lattice $\Gamma \subset G$ is *reducible* if G admits connected normal subgroups H, H' such that $HH' = G$, $H \cap H'$ is discrete and $\Gamma/(\Gamma \cap H) \cdot (\Gamma \cap H')$ is finite. A lattice is *irreducible* if it is not reducible. Also, irreducibility is equivalent to the condition that for any connected normal subgroup $H \subset G$ and $\pi : G \to G/H$ is the natural projection, $\pi(\Gamma)$ is dense.

- Two subgroups H_1 and H_2 of a group are *commensurable* if their intersection $H_1 \cap H_2$ has finite index in both H_1 and H_2. Let $G \subset \mathrm{GL}_n(\mathcal{K})$ be a linear algebraic group defined over a number field $\mathcal{K}$. A subgroup $\Gamma \subset G(\mathcal{K})$ is an *arithmetic* subgroup if it is commensurable with $G(\mathcal{O})$, where $\mathcal{O}$ is the ring of integers of $\mathcal{K}$.

Lattices in rank one symmetric spaces have been studied for a long time with important results concerning rigidity and arithmeticity. A fundamental problem in the study of symmetric spaces is the relationship between arithmetic groups and lattices. In general, Borel and Harish-Chandra [BHC62] proved that in all symmetric spaces of non-compact type all arithmetic groups are lattices. In contrast, Margulis [Mar84] showed that when the rank of symmetric space is at least two then all irreducible lattices are arithmetic.

More progress has been made in rank one symmetric space of non-compact type, for example, the following symmetric spaces:

$$\mathbf{H}^n_{\mathbb{R}} \quad \mathbf{H}^n_{\mathbb{C}} \quad \mathbf{H}^n_{\mathbb{H}} \quad \mathbf{H}^n_{\mathbb{O}}$$

which are hyperbolic spaces of dimension n over the reals, complex numbers quaternions respectively, and the hyperbolic plane over the Cayley octonions (see Chapter 19 of book [Mos83]). In these cases, Corlette [Cor92] and Gromov and Schoen [GS92] have shown that in $\mathbf{H}^n_{\mathbb{H}}$ for $n \geq 2$ and in $\mathbf{H}^2_{\mathbb{O}}$ all lattices are arithmetic. Furthermore, Gromov and Piatetski-Shapiro [GPS87] have given examples of non-arithmetic lattices in $\mathbf{H}^n_{\mathbb{R}}$ for all $n \geq 2$. The existence of non-arithmetic lattices in complex hyperbolic geometry has not completely been settled. More explicitly, Mostow [Mos80] constructed a family of non-arithmetic lattices in complex hyperbolic plane $\mathbf{H}^2_{\mathbb{C}}$ which we will discuss below. Deligne and Mostow [DM86] found a non-arithmetic lattice in $\mathbf{H}^3_{\mathbb{C}}$. The question whether there exist non-arithmetic lattices in $\mathbf{H}^n_{\mathbb{C}}$ with $n \geq 4$ is still open. This is perhaps the most important open question in the field.

There are four major methods of constructing lattices in complex hyperbolic space such as arithmetic constructions, use of moduli of different objects, algebraic geometry and

construction of fundamental domains; see the introductory survey paper [Par09] and its references for further details. Our particular case of interest is to study lattices in $PU(2,1)$ by building a fundamental domain acting on $\mathbf{H}^2_{\mathbb{C}}$. In other words, one must find an open connected set $D \in \mathbf{H}^2_{\mathbb{C}}$ so that $D \cap \gamma(D) = \emptyset$ for all $\gamma \in \Gamma - Id$ and $\bigcup_{\gamma\in\Gamma} \gamma(\overline{D}) = \mathbf{H}^2_{\mathbb{C}}$, where $\overline{D}$ is the closure of D inside $\mathbf{H}^2_{\mathbb{C}}$. The difficulty of constructing a fundamental domain is mostly due to the fact that there are no totally geodesic real hypersurfaces in complex hyperbolic geometry, and in particular no natural notion of polyhedra.

One simple method of constructing fundamental domains is to construct the Dirichlet domain based at a *central* point $p_0 \in \mathbf{H}^n_{\mathbb{C}}$. The Dirichlet domain is the set of points in $\mathbf{H}^n_{\mathbb{C}}$ that are closer to p_0 than to any other point in the Γ-orbit of p_0. Namely, the basic object in this construction is the set of points equidistant from two given points, which is called a *bisector*. The first example of complex hyperbolic Dirichlet domain was due to Giraud [Gir21]; see also Appendix A of Goldman [Gol99]. A natural generalization of the Dirichlet domain is the *Ford domain*, see Section 9.3 of [Gol99]. Here the point z_0 lies on $\partial\mathbf{H}^n_{\mathbb{C}}$ and the distance is replaced with a Busemann function based at z_0. The level sets of a Busemann function are horospheres. The sides of the Ford domain are contained in bisectors called *isometric spheres* with respect to the Cygan metric, a natural metric on the Heisenberg group. As the stabilizer of z_0 is infinite, one may obtain a fundamental domain by intersecting the Ford domain with a fundamental domain for the stabiliser.

Typically, a fundamental domain is a locally finite polyhedron D with some combinatorial structure. The codimension one faces of D, called *sides*, may be contained in a wide variety of real hypersurfaces (for example bisectors, $\mathbb{C}$-spheres and $\mathbb{R}$-spheres), but there should exist a set of *side pairing maps*: each side should be mapped bijectively to another side (possibly itself) by a map in $PU(2;1)$. *Poincaré's polyhedron theorem* gives conditions under which the group generated by the side pairing maps is discrete with D as a fundamental domain and moreover one obtains a presentation for this group. Another consequence of Poincaré's theorem, is that can obtain the orbifold Euler characteristic of the quotient and so calculate its volume by the complex hyperbolic version of Gauss-Bonnet theorem. We give some examples of explicit fundamental domains which have been constructed for lattices in $PU(2,1)$.

- One of the simplest arithmetic lattices in $PU(2,1)$ is the *Eisenstein-Picard modular group* $PU(2,1,\mathbb{Z}[\omega])$ comprising matrices whose entries are all in the Eisenstein integers $\mathbb{Z}[\omega]$ where ω is the cube-root of unity. This is one of Picard's first examples [Pic83] in $PU(2,1)$ and is the natural generalization of the classic modular group $\mathrm{PSL}(2,\mathbb{Z})$ in $\mathrm{PSL}(2,\mathbb{R})$. In fact, Picard [Pic83, Pic84] constructed a family of arithmetic lattices $PU(2,1;\mathcal{O}_d)$, so-called *Picard modular groups*, where $\mathcal{O}_d$ is the ring of integers in the imaginary quadratic number field $\mathbb{Q}(i\sqrt{d})$. The geometry of the group $PU(2,1,\mathbb{Z}[\omega])$ has been studied by Falbel and Parker [FP06]. In other words, they constructed a fundamental domain with the simplest possible combinatorial structure, which is 4-simplex, itself a geodesic cone based on 3-simplex with an ideal cone point (the parabolic fixed point). This construction is completely analogous to the 2-simplex with one ideal vertex which is the fundamental domain for the classical modular group $\mathrm{PSL}(2,\mathbb{Z})$ in the hyperbolic plane $\mathbf{H}^1_{\mathbb{C}}$.

- Another Picard modular group is called *Gauss-Picard modular group* where the associated ring is $\mathbb{Z}[i]$. Francsics and Lax [FL05, FLa05] described a fundamental domain for this group $PU(2,1;\mathbb{Z}[i])$. Their fundamental domain is only semi-explicit and did not include analysis of the combinatorics of the fundamental domain. More re-

cently, Falbel, Francsics, Lax and Parker [FFP10, FFLP11] construct a fundamental domain from the Ford domain, which is analogous to the case of $PU(2,1,\mathbb{Z}[\omega])$. The fundamental domain for $PU(2,1;\mathbb{Z}[i])$ may be obtained by intersecting the Ford domain with a fundamental domain for the stabiliser. The difference is mostly due to the fact that there are three compact sides which are contained in three isometric spheres respectively.

- In his famous paper [Mos80], Mostow studied new examples of subgroups of $PU(2,1)$ generated by three complex reflections of order p ($p = 3,4,5$) and showed that these are complex hyperbolic lattices by building fundamental domains, specifically, Dirichlet domains. All the codimension-1 faces are contained in bisectors. As we have mentioned, the absence of totally geodesic real hypersurfaces gives rise to the difficulty of understanding the intersection of two bisectors. There were some minor errors in Mostow's construction; see [Der05] . Another construction of fundamental domains for the same groups was given by Deraux, Falbel and Paupert [DFP05].

- Ron Livné in his thesis [Liv81] constructed a family of lattices in $PU(2,1)$ by using techniques from algebraic geometry. Parker [Par06] used Thurston's method to give a geometrical construction of Livné's lattices. Specifically, he constructed a fundamental polyhedron for Livné's groups, each side of which is contained a bisector. A link between Livné's groups and the Eisenstein-Picard modular group comes from the description of fundamental domain. The pattern of the fundamental polyhedra in [Par06] is a geodesic cone starting from a tetrahedron pointing to a geodesic triangle on a complex line. As this complex line degenerates to an ideal vertex, Livné's group becomes the Eisenstein-Picard modular group. In other words, this limiting configuration corresponds to a fundamental domain for the Eisenstein-Picard modular group which is different from that in [FP06]. More recently, Boadi in his thesis [Bo11] used the same approach as for Livné's groups to construct fundamental domains for Mostow groups of the first kind mentioned in [Par09]. The fundamental domain, in Boadi's construction, is made up of two 4-dimensional simplices glued along a common 3-dimensional face.

- Other examples come from the representation of hyperbolic triangle groups in $PU(2,1)$. For convenience, we adopt the following notations for these lattices. Let (p,q,r) be a *hyperbolic triangle group* with $1/p+1/q+1/r<1$, that is defined to be the Coxeter group with presentation,

$$\left\langle a_1,a_2,a_3|\ a_1^2,a_2^2,a_3^2,(a_2a_3)^p,(a_3a_1)^q,(a_1a_2)^r\right\rangle.$$

  We may consider a family of representations $\rho_t : (p,q,r)\to PU(2,1)$. We define $\Gamma(p,q,r;n)$ to be the image of a non-faithful representation $\rho_t(p,q,r)$ where $\rho_t(a_1a_3a_2a_3)$ is an elliptic element of order n. The group $\Gamma(4,4,4;5)$ is a cocompact lattice in $PU(2,1)$ due to Deraux [Der06]. Parker and Thompson [PT10] have constructed a fundamental domain for Deraux's lattice and give the presentation

$$\left\langle a_1,a_2,a_3|\ a_i^2,(a_ia_j)^4,(a_ia_ja_k)^{10},(a_ia_ja_ka_j)^5\right\rangle.$$

  Furthermore, Thompson in his thesis [Tho10] discovered two new deformed triangle group lattices, $\Gamma(3,3,4;7)$ and $\Gamma(3,3,5;5)$. He constructed conjectural fundamental domains for them. The same construction of fundamental domains could be carried out for any $\Gamma(p,q,r;n)$ with $a_1a_2a_3$ finite order regular elliptic element. Specifically,

the fundamental domain consists of a 4-dimensional cone over a connected bounded 3-dimensional region of $\mathbf{H}^2_{\mathbb{C}}$ with a cone point (the fixed point of $a_1a_2a_3$).

Let $X = G/K$ be a symmetric space of non-compact type, where G is the group of real points of an semisimple algebraic group $\mathbf{G}$ defined over $\mathbb{Q}$. Let $\Gamma \subset G$ be an arithmetic lattice and (E, ρ) be a Γ-module. Since the locally symmetric space $\Gamma\backslash X$ is a $K(\Gamma, 1)$, the group cohomology of Γ is isomorphic to the cohomology of the locally symmetric space, namely

$$H^*(\Gamma, E) \cong H^*(\Gamma\backslash X; \mathbb{E}),$$

where $\mathbb{E}$ denotes the sheaf associated to the local system on (the manifold or the orbifold) $\Gamma\backslash X$ defined by (E, ρ). A *spine* is a Γ-equivariant deformation retract $X_0 \subset X$ such that $\Gamma\backslash X_0$ is compact if it exists. Explicit examples of spines have been constructed for various Γ. For example, Soulé [Sou78] found a spine for $SL_3(\mathbb{Z})$ and the case of the Euclidean Bianchi groups $SL_2(\mathcal{O}_d)$ (for $d = 1, 2, 3, 7, 11$) was treated by Mendoza in [Men79]. More generally, Ash [As77, As84] used the *well-rounded retract* method for constructing a spine for all linear symmetric spaces. This covers algebraic groups where the real points are isomorphic to a product of the following groups [FK94]:

- $GL_n(\mathbb{R})$;
- $GL_n(\mathbb{C})$;
- $GL_n(\mathbb{H})$;
- $O(1, n-1) \times \mathbb{R}^\times$;
- The non-compact Lie group with Lie algebra $\mathfrak{e}_{6(-26)} \oplus \mathbb{R}$.

For some low-dimensional examples, the cohomology has been computed combinatorially from the cellular structure of a spine [Sou78, As80, Men79, SV83].

More recently, Yasaki constructed in [Yas06] a retraction onto a spine for $\mathbb{Q}$-rank 1 groups. As an application, he [Yas08] constructed an explicit spine for $\Gamma = SU(2, 1; \mathbb{Z}[i])$ and computed the cohomology of $\mathbf{H}^2_{\mathbb{C}}/\Gamma$ with local coefficients.

Plan of thesis

The thesis is organized as follows. The main results will fall into three large chapters, each of which is conceived to be self-contained, with its own introduction.

In the first chapter we recall the two models of complex hyperbolic plane $\mathbf{H}^2_{\mathbb{C}}$, complex hyperbolic isometries and their classification. Three types of totally geodesic submanifolds will be described. Moreover, we discuss the orthogonal projection into a complex geodesic which will be used in the thesis. The Siegel domain has the same structure as the upper half-space model of real hyperbolic space. Further to say that the boundary is identified with the one-point compactification of the Heisenberg group. We define the Cygan metric on the Heisenberg group and Cygan spheres. The general reference for this chapter is the book of Goldman [Gol99] or Parker [Par10].

We review, in the second chapter, the definition of a bisector which is the equidistant between two distinct points. A bisector is a real analytic hypersurfaces in $\mathbf{H}^2_{\mathbb{C}}$ which is diffeomorphic to $\mathbb{R}^3$. These hypersurfaces come about as close as possible to being totally geodesic. Specifically, they enjoy two natural decompositions into totally geodesic submanifolds, called *slice* and *meridian* decompositions [Mos80, Gol99]. Isometric spheres

are examples of bisectors. We will build the polyhedra whose codimensional 1 faces may be contained in bisectors or isometric spheres in later chapters. We review Poincaré's polyhedron theorem as the main technical tool throughout the thesis.

In the third chapter we construct an explicit fundamental domain for the group (we call the sister of Eisenstein-Picard modular group) denoted by G_2. This group was first defined by Parker in [Par98], in which he showed that Eisenstein-Picard modular surfaces and $\mathbf{H}^2_{\mathbb{C}}/G_2$ are candidates for the cusped, complex hyperbolic orbifold of minimal volume. Stover in his article [Sto10] affirmed that they are precisely the two of orbifolds with minimal volume. We state the main result of this chapter as follows:

Theorem 0.2.1. *There is a fundamental domain for G_2, that is a geodesic cone over a prism (see Figure 3.6) pointing to q_∞, with the side-pairing maps I_1, R, S and T. As the consequence, the group G_2 generated by I_1, R, S, T is discrete and has the presentation:*

$$G_2 = \left\langle I_1, R, S, T \;\middle|\; \begin{array}{l} R^6 = (R^{-1}S)^3 = [R,T] = S^2T^{-1} \\ = (T^{-1}I_1)^3 = (S^{-1}I_1)^3 = R^{-1}I_1^2 = Id \end{array} \right\rangle.$$

This third chapter has been published in *Mathematical Proceedings of the Cambridge Philosophical Society* [Zh11].

This fourth chapter is devoted to give the generators of the Picard modular groups $PU(2,1;\mathcal{O}_d)$ where the integer ring $\mathcal{O}_d$ is Euclidean, i.e. $d = 1, 2, 3, 7, 11$. In particular, the cases of $\mathcal{O}_1$ and $\mathcal{O}_3$ have been studied in many aspects. For example, the explicit fundamental domain for these two groups were obtained in [FFP10, FP06]. There are few results for other picard modular groups. Each element of the Gauss-Picard modular group can be decomposed as a product of the generators by a simple algorithm [FFLP11]. We began by trying to construct fundamental domain for these groups $PU(2,1;\mathcal{O}_d)$ following the method used by Falbel and Parker in [FP06]. This leads to a domain that was much to complicated to understand. However, a result of constructing fundamental domain enables us to give the generators for the Euclidean Picard modular groups in a geometric way. We state explicitly as follows:

Theorem 0.2.2. *The Euclidean Picard modular groups $PU(2,1;\mathcal{O}_d)$ where $d = 2, 3, 7$ are generated by an involution, a Heisenberg rotation, two screw Heisenberg rotations and a vertical translation.*

Essentially, this method can be implemented on the case of $\mathcal{O}_d$ with class number one. This is a larger collection of $\mathcal{O}_d$ than the Euclidean ring. However it is more complicated to determine the finite collection of spinal spheres containing the fundamental domain for the cusp group as d becoming large.

This chapter has been accepted for publication in *Transactions of the American Mathematical Society.*

The fifth chapter consists in the study of Mostow's lattices $\Gamma(p,k)$, based on the relationship that the sister of Eisenstein-Picard modular group corresponds to one of Mostow's lattices $\Gamma(3,6)$. Mostow [Mos80] considered firstly a remarkable family of groups generated by three braiding complex reflections R_1, R_2, R_3 of order p where $p = 3, 4, 5$. The discreteness of these groups was verified by building a fundamental domain for their action. After Mostow's work, Deraux, Falbel and Paupert [DFP05] constructed a new fundamental domain which is simpler than Mostow's, but mostly which allows the use of synthetic geometric arguments. We now give another new construction of fundamental domains for certain Mostow's lattices $\Gamma(3,k)$ where the values of k satisfy $1/k + 1/l = 1/6$ for

an integer l. The main idea of this chapter is inspired by the construction of [Par06]. Further motivations and results can be found in the detailed introduction to that chapter, as well as some notations. The group Γ_k is one of Mostow's lattices we consider with the geometric generators I_1, R, S and T. Note that we use the same notations as in the third chapter but these generators are the product of R_1, R_2, R_3 and J which are the generators coming from the original article [Mos80]. We summarizes the result in the following:

Theorem 0.2.3. *The group $\Gamma_k \subset PU(2,1)$ is discrete if there is an integer l such that $1/k + 1/l = 1/6$, namely, the ordered pair (k,l) is in the list*

$$(7,42),\ (8,24),\ (9,18),\ (10,15),\ (12,12),\ (15,10),\ (18,9),\ (24,8),\ (42,7).$$

In that case, there is a fundamental domain $\mathbf{D}$ with side pairings given by $R = (JR_1^{-1}J)^2$, $S = JR_1^{-1}$, $T = (JR_1^{-1})^2$, $I_1 = JR_1^{-1}J$ and the cycle relations give the following presentation of the group

$$\Gamma_k = \left\langle R, S, T, I_1 \;\middle|\; \begin{array}{l} R^k = T^l = (R^{-1}S)^3 = (T^{-1}I_1)^3 = (S^{-1}I_1)^3 \\ = [R,T] = Id, \quad T = S^2, \quad R = I_1^2 \end{array} \right\rangle.$$

The last chapter, motivated by the Yasaki's work [Yas08], is devoted to compute the cohomology of Eisenstein-Picard modular surface and its sister with local coefficients. This method can be generalized to the case of fundamental domain with one cusp. We give the cohomology with trivial $\mathbb{Z}$-coefficients as follows:

Theorem 0.2.4. *With trivial coefficients,*

$$\begin{aligned} H^i(\mathbf{H}^2_{\mathbb{C}}/G_1;\mathbb{Z}) &= \begin{cases} \mathbb{Z}, & i = 0 \\ 0, & i \geq 1. \end{cases} \\ H^i(\mathbf{H}^2_{\mathbb{C}}/G_2;\mathbb{Z}) &= \begin{cases} \mathbb{Z}, & i = 0, 2 \\ 0, & i = 1 \text{ or } i \geq 3. \end{cases} \end{aligned}$$

Chapter 1

Complex hyperbolic space

In this chapter we review some basic features of complex hyperbolic geometry which may be needed later on; we will mainly focus on the case of (complex) dimension 2. The material is completely standard and may be found in more details in the book of Goldman [Gol99] and the forthcoming book of Parker [Par10] or in the article of Chen and Greenberg [CG74].

Let $\mathbb{C}^{n,1}$ be the complex vector space $\mathbb{C}^{n+1}$ of dimension $n+1$ equipped with a non-degenerate, indefinite Hermitian form $\langle \cdot, \cdot \rangle$ of signature $(n,1)$. Here $\langle \cdot, \cdot \rangle$ is given by a non-singular $(n+1) \times (n+1)$ Hermitian matrix H with n positive eigenvalues and 1 negative eigenvalue, which is

$$H = \begin{bmatrix} 1 & \cdots & 0 & 0 \\ \vdots & \ddots & & \vdots \\ 0 & & 1 & 0 \\ 0 & \cdots & 0 & -1 \end{bmatrix}.$$

Specifically, $\langle \mathbf{z}, \mathbf{w} \rangle = \mathbf{w}^* H \mathbf{z}$ where $\mathbf{z}, \mathbf{w}$ are column vectors in $\mathbb{C}^{n+1}$ and the operator * is the *Hermitian transpose*. Thus we may define subsets V_-, V_0 and V_+ of $\mathbb{C}^{n,1}$ by

$$\begin{aligned} V_- &= \{\mathbf{z} \in \mathbb{C}^{n,1} | \langle \mathbf{z}, \mathbf{z} \rangle < 0\}, \\ V_0 &= \{\mathbf{z} \in \mathbb{C}^{n,1} | \langle \mathbf{z}, \mathbf{z} \rangle = 0\}, \\ V_+ &= \{\mathbf{z} \in \mathbb{C}^{n,1} | \langle \mathbf{z}, \mathbf{z} \rangle > 0\}. \end{aligned}$$

A vector $\mathbf{z} \in \mathbb{C}^{n,1}$ is negative (respectively null, positive) if and only if $\langle \mathbf{z}, \mathbf{z} \rangle < 0$ (respectively $\langle \mathbf{z}, \mathbf{z} \rangle = 0$, $\langle \mathbf{z}, \mathbf{z} \rangle > 0$).

Let $\mathbb{P} : \mathbb{C}^{n,1} \backslash \{0\} \longmapsto \mathbb{CP}^n$ denote the standard projection map defined by $\mathbb{P}(\mathbf{z}) = [\mathbf{z}]$ where $[\mathbf{z}]$ is the equivalence class of $\mathbf{z}$. On the chart of $\mathbb{C}^{n,1}$ with $z_{n+1} \neq 0$ the projection map $\mathbb{P}$ is given by

$$\mathbb{P} : \begin{bmatrix} z_1 \\ \vdots \\ z_n \\ z_{n+1} \end{bmatrix} \longmapsto \begin{bmatrix} z_1/z_{n+1} \\ \vdots \\ z_n/z_{n+1} \end{bmatrix} \in \mathbb{C}^n.$$

The projective model of complex hyperbolic space $\mathbf{H}^n_{\mathbb{C}}$ is defined to be the collection of negative lines in $\mathbb{C}^{n,1}$ and its boundary is defined to be the collection of null lines. In other words $\mathbf{H}^n_{\mathbb{C}}$ is $\mathbb{P}V_-$ and $\partial \mathbf{H}^n_{\mathbb{C}}$ is $\mathbb{P}V_0$.

For the projective model the metric on $\mathbf{H}^n_{\mathbb{C}}$, called the *Bergman metric* is given by

$$ds^2 = \frac{-4}{\langle \mathbf{z}, \mathbf{z} \rangle^2} \det \begin{pmatrix} \langle \mathbf{z}, \mathbf{z} \rangle & \langle d\mathbf{z}, \mathbf{z} \rangle \\ \langle \mathbf{z}, d\mathbf{z} \rangle & \langle d\mathbf{z}, d\mathbf{z} \rangle \end{pmatrix}.$$

The distance between points $w, u \in \mathbf{H}^n_{\mathbb{C}}$ is given by the formula

$$\cosh^2 \left(\frac{\rho(w,u)}{2} \right) = \frac{\langle \mathbf{w}, \mathbf{u} \rangle \langle \mathbf{u}, \mathbf{w} \rangle}{\langle \mathbf{w}, \mathbf{w} \rangle \langle \mathbf{u}, \mathbf{u} \rangle}$$

where $\mathbf{w}, \mathbf{u}$ are the lift of w, u in $\mathbb{C}^{n+1}$. This formula is independent of which lifts $\mathbf{z}$ and $\mathbf{w}$ in $\mathbb{C}^{n,1}$ of z and w we choose.

For each element A of $PU(n,1)$, A is unitary with respect to $\langle \cdot, \cdot \rangle$, namely, A acts isometrically on the projective model of complex hyperbolic space. Thus the Lie group $PU(n,1)$ is a subgroup of the complex hyperbolic isometry group. There are isometries of $\mathbf{H}^n_{\mathbb{C}}$ not in $PU(n,1)$ for instance the complex conjugation $z \mapsto \overline{z}$. All of the isometries of $\mathbf{H}^n_{\mathbb{C}}$ will be described in the following theorem.

Theorem 1.0.5. *(see [Gol99]) The holomorphic isometries of $\mathbf{H}^n_{\mathbb{C}}$ are given by the matrices in $PU(n,1)$; all other isometries are antiholomorphic which are obtained by composing an element of $PU(n,1)$ with complex conjugation. The group of all the isometries of $\mathbf{H}^n_{\mathbb{C}}$, denoted by $\widehat{PU(n,1)}$, is generated by $PU(n,1)$ and the complex conjugation.*

We have defined the projective model and then go on to specialize to the unit ball model and the Siegel domain model. This is simultaneously a complex version of the projective and Klein-Beltrami models of ordinary (real) hyperbolic space and also a generalization to higher complex dimensions of the Poincaré disc and half plane models of the hyperbolic plane. In what follows we restrict ourselves to the case of complex hyperbolic 2-space.

1.1 Complex hyperbolic plane

Different choices of Hermitian forms will lead to different models of complex hyperbolic plane $\mathbf{H}^2_{\mathbb{C}}$. We describe the following two models, which will be most useful.

1.1.1 The unit ball model

In this section, the representative matrix of the Hermitian form is chosen as follows

$$H_1 = \begin{bmatrix} 1 & 0 & 0 \\ 0 & 1 & 0 \\ 0 & 0 & -1 \end{bmatrix},$$

namely, for all $\mathbf{z} \in \mathbb{C}^{2,1}$, the first Hermitian product $\langle \mathbf{z}, \mathbf{z} \rangle_1 = |z_1|^2 + |z_2|^2 - |z_3|^2$. On the chart of $\mathbb{P}(V_-)$ with $z_3 = 1$, complex hyperbolic plane is given by

$$\mathbf{H}^2_{\mathbb{C}} = \mathbb{B}^2 = \{(z_1, z_2) : |z_1|^2 + |z_2|^2 < 1\}.$$

Its boundary $\mathbb{P}(V_0)$ is homeomorphic to the sphere S^3:

$$\partial \mathbf{H}^2_{\mathbb{C}} = \{(z_1, z_2) : |z_1|^2 + |z_2|^2 = 1\}.$$

This model is a generalization of Poincaré disc model for complex hyperbolic line, which we will mention later.

1.1.2 The Siegel domain model

Let $\langle \cdot, \cdot \rangle_2$ denote the second Hermitian form associated to the following matrix

$$H_2 = \begin{bmatrix} 0 & 0 & 1 \\ 0 & 1 & 0 \\ 1 & 0 & 0 \end{bmatrix}.$$

For the second Hermitian form, the standard lift of z is negative if and only if

$$z_1 + |z_2|^2 + \overline{z}_1 = 2\Re(z_1) + |z_2|^2 < 0.$$

Thus $\mathbb{P}(V_-)$ is a paraboloid in $\mathbb{C}^2$, called the *Siegel domain*. Likewise, its boundary $\mathbb{P}(V_0)$ satisfies

$$2\Re(z_1) + |z_2|^2 = 0.$$

However, not all points in $\mathbb{P}(V_0)$ lie in $\mathbb{C}^2 \subset \mathbb{CP}^2$. We have to add an extra point, denoted q_∞, on the boundary of the Siegel domain. The standard lift of q_∞ is

$$\begin{bmatrix} 1 \\ 0 \\ 0 \end{bmatrix}.$$

Recall that one of the important models of real hyperbolic 3-space $\mathbf{H}^3_{\mathbb{R}}$ is the upper half space in $\mathbb{R}^3$. The boundary of this model is the one point compactification of $\mathbb{C}$ regarded as the extended complex plane $\mathbb{C} \cup \{\infty\}$ (or Riemann sphere). The Siegel domain model has an analogous construction.

Fix $u \in \mathbb{R}_+$ and consider the standard lift $\mathbf{z}$ of $z \in \mathbf{H}^2_{\mathbb{C}}$ satisfying $\langle \mathbf{z}, \mathbf{z} \rangle = -u$. In other words, $2\Re(z_1) = -|z_2|^2 - u$. We rewrite $z_2 = \zeta \in \mathbb{C}$ which means that $z_1 = (-|\zeta|^2 - u + iv)/2$. Thus for a $(\zeta, v, u) \in \mathbb{C} \times \mathbb{R} \times \mathbb{R}_+$ corresponds to

$$\mathbf{z} = \begin{bmatrix} (-|\zeta|^2 - u + iv)/2 \\ \zeta \\ 1 \end{bmatrix} \in \mathbf{H}^2_{\mathbb{C}}.$$

In this way we can identify a point $\mathbf{z}$ in the Siegel domain with $(\zeta, v, u) \in \mathbb{C} \times \mathbb{R} \times \mathbb{R}_+$, called the *horospherical coordinate* of $\mathbf{z}$.

Definition 1.1.1. *The set of points of the Siegel domain $H_u = \mathbb{C} \times \mathbb{R} \times \{u\}$ is called the horosphere of height u. Likewise, the horoball U_t of height t is defined to be the union of all horospheres of height $u > t$.*

The finite boundary points $\mathbf{z} \in \partial\mathbf{H}^2_{\mathbb{C}} - \{q_\infty\}$ is the horosphere of height zero $(\zeta, v, 0)$, that can be parameterized by $(\zeta, v) \in \mathbb{C} \times \mathbb{R}$. Therefore we can identify the boundary of the Siegel domain with the one-point compactification of $\mathbb{C} \times \mathbb{R}$. Furthermore, consider a family of the maps that fix the infinity and sends the origin to the point (ζ, v) given by

$$T(\zeta, v) = \begin{bmatrix} 1 & -\overline{\zeta} & (-|\zeta|^2 + iv)/2 \\ 0 & 1 & \zeta \\ 0 & 0 & 1 \end{bmatrix}.$$

In terms of their action on the boundary, $\mathbb{C} \times \mathbb{R}$ has a group law which gives the structure of the Heisenberg group $\mathcal{N}$ as follows

$$(\zeta, v) \diamond (\xi, t) = (\zeta + \xi, v + t + 2\Im(\overline{\xi}\zeta)).$$

Remark 1.1.2. There are other Hermitian forms which are widely used in the literature (see page 67 of [CG74]). The one given by the matrix

$$\begin{bmatrix} 0 & -1 & 0 \\ -1 & 0 & 0 \\ 0 & 0 & 1 \end{bmatrix}$$

will be seen in the study of complex hyperbolic triangle groups. Following Mostow, it is most convenient to use the Gram matrix as the Hermitian form. This form will always be defined, but only for certain points in the parameter space will it have the correct signature (see [PPa09]). Furthermore, using this Hermitian form, calculations in complex hyperbolic geometry have a tendency to become extremely complicated but only the simple matrix representation for the group, refer to Chapter 5.

1.1.3 Cayley-transform associated to two models

Analogous to the map

$$z \longmapsto -i\frac{z+i}{z-i}$$

passing from the Poincaré disc to the upper half plane, the following Cayley-transform interchanges the first and second Hermitian forms

$$C = \frac{1}{\sqrt{2}} \begin{bmatrix} 1 & 0 & 1 \\ 0 & \sqrt{2} & 0 \\ 1 & 0 & -1 \end{bmatrix}.$$

The map C conjugates H_1 and H_2 with $C^2 = Id$, in other words, $H_2 = C^* H_1 C$.

On the affine chart with $z_3 = 1$ of $\mathbb{CP}^2$, we see that

$$C : (z_1, z_2) \longrightarrow \left(\frac{z_1+1}{z_1-1}, \sqrt{2}\frac{z_2}{z_1-1}\right).$$

The Cayley transform leads to a generalized form of the *stereographic projection*. This mapping $\pi : S^3 \setminus \{e_2\} \to \mathbb{R}^3$, where $S^3 = \partial\mathbb{B}^2$ and $e_2 = (1,0) \in \mathbb{C}^2$, is defined as the composition of the Cayley transform restricted $S^3 \setminus \{e_2\}$ followed by the projection

$$\begin{cases} z_1 \to 2\Im(z_1), \\ z_2 \to z_2. \end{cases}$$

The stereographic projection π can be extended to a mapping from S^3 onto the one-point compactification $\overline{\mathbb{R}}^3$ of $\mathbb{R}^3$, given by

$$\pi(z_1, z_2) = \left[\frac{\sqrt{2}z_2}{z_1-1}, \frac{-4\Im(z_1)}{|z_1-1|^2}\right].$$

Using the stereographic projection, we can identify $S^3 \setminus \{e_2\}$ with $\mathcal{N}$ and S^3 with the one-point compactification $\overline{\mathcal{N}}$ of $\mathcal{N}$. The inverse function of the stereographic projection is given by

$$\pi^{-1}([z,t]) = \left(\frac{-|z|^2+it+2}{-|z|^2+it-2}, \frac{2\sqrt{2}z}{-|z|^2+it-2}\right).$$

1.2 Totally geodesic submanifolds

In the general theory of symmetric spaces, one can readily prove that the only totally geodesic subspaces of $\mathbf{H}^2_{\mathbb{C}}$ are either complex linear subspaces or totally real totally geodesic submanifolds. There are only four types of totally geodesic subspaces in $\mathbf{H}^2_{\mathbb{C}}$:

- the points
- the geodesics
- $\mathbb{C}$-planes
- $\mathbb{R}$-planes

In particular, it doesn't exist totally geodesic real hypersurface in complex hyperbolic space. A sketch of the proof can be found in the Section 3.1.11 of [Gol99].

1.2.1 Geodesics

There exists a unique geodesic joining a pair of distinct points in $\mathbf{H}^2_{\mathbb{C}} \cup \partial\mathbf{H}^2_{\mathbb{C}}$ (see Theorem 3.1.11 of [Gol99]). Let z and w two points in $\partial\mathbf{H}^2_{\mathbb{C}}$, up to normalization, we suppose that their lifts $\mathbf{z}$ and $\mathbf{w}$ in V_0 satisfy $\langle \mathbf{z}, \mathbf{w}\rangle = -1$. The geodesic joining z and w can be described in the following proposition.

Proposition 1.2.1. *(see [Par10]) Let $\mathbf{z}, \mathbf{w} \in V_0$ be null vectors with $\langle \mathbf{z}, \mathbf{w}\rangle = -1$. The geodesic $\sigma(t)$ with endpoints z and w is the collection of points in $\mathbf{H}^2_{\mathbb{C}}$ corresponding to the vector $e^{t/2}\mathbf{z} + e^{-t/2}\mathbf{w}$ in $\mathbb{C}^{2,1}$ where t is the arc length parameter.*

The following proposition describes the expression for the geodesic connecting two distinct points in $\mathbf{H}^2_{\mathbb{C}}$.

Proposition 1.2.2. *(see Proposition 5.2, [Par10]) Let $\sigma(t)$ be a geodesic parameterized by arc length t joining z and w in $\mathbf{H}^2_{\mathbb{C}}$. Suppose that $\sigma(r) = z$ and $\sigma(s) = w$ such that their lifts $\mathbf{z}, \mathbf{w}$ satisfy $\langle \mathbf{z}, \mathbf{z}\rangle = \langle \mathbf{w}, \mathbf{w}\rangle = -2$ and $\langle \mathbf{z}, \mathbf{w}\rangle$ is real and negative. Then $\sigma(t)$ is given by the vector*

$$\frac{\sinh((t-s)/2)}{\sinh((r-s)/2)}\mathbf{z} + \frac{\sinh((r-t)/2)}{\sinh((r-s)/2)}\mathbf{w}. \tag{1.1}$$

1.2.2 $\mathbb{C}$-planes

Definition 1.2.3. *A complex line (or $\mathbb{C}$-plane) of $\mathbf{H}^2_{\mathbb{C}}$ is the intersection with $\mathbf{H}^2_{\mathbb{C}}$ of a complex projective line of $\mathbb{CP}^2$ (when this intersection is not empty).*

Such a $\mathbb{C}$-plane is an embedded copy of $\mathbf{H}^1_{\mathbb{C}}$ (more precisely, in the ball model, it carries the Poincaré model of real hyperbolic plane, with constant curvature -1, see [Gol99] and [Par10]). Each $\mathbb{C}$-plane is also the fixed-point set of a one-parameter family of (holomorphic) isometries, one of which is an involution, so that $\mathbb{C}$-planes are totally geodesic.

We denote $\mathbf{n}^\perp = \{\mathbf{z} \in \mathbb{C}^{2,1} : \langle \mathbf{n}, \mathbf{z}\rangle = 0\}$. The following proposition shows the duality between $\mathbb{P}(V_+)$ and the set of complex lines.

Proposition 1.2.4.

- *Each complex line Σ of $\mathbf{H}^2_{\mathbb{C}}$ is associated to a unique point $n \in \mathbb{P}(V_+)$ such that $\Sigma = \mathbf{n}^\perp \cap \mathbf{H}^2_{\mathbb{C}}$ where $\mathbf{n}$ is a lift of n in $\mathbb{C}^{2,1}$. Such a vector $\mathbf{n}$ is called the **polar vector** to Σ.*
- *For all points n in $\mathbb{P}(V_+)$, the intersection $\mathbf{n}^\perp \cap \mathbf{H}^2_{\mathbb{C}}$ is a complex line of $\mathbf{H}^2_{\mathbb{C}}$ which does not depend on the choice of lift $\mathbf{n}$.*

The elements of $PU(2,1)$ act on $\mathbb{P}(V_+)$ transitively. As a consequence, we have

Proposition 1.2.5. *The group $PU(2,1)$ acts transitively on the set of $\mathbb{C}$-planes, with isotropy group a conjugate of $P(U(1) \times U(1,1))$.*

Example 1.2.6. In the unit ball model, the vector

$$\mathbf{n} = \begin{bmatrix} 0 \\ 1 \\ 0 \end{bmatrix}$$

is polar to the complex line $\{(z_1, 0) : |z_1| < 1\}$. Observe that the vector $\mathbf{n}$ is fixed by the Cayley transformation. In the Siegel domain model, it corresponds to the complex line given in horospherical coordinates by

$$\{(0, v, u) : v \in \mathbb{R}, u \in \mathbb{R}_+\}.$$

1.2.3 $\mathbb{R}$-planes

Definition 1.2.7. *A Lagrangian plane (or $\mathbb{R}$-plane) is a maximal totally real subspace of $\mathbf{H}^2_{\mathbb{C}}$, that is the projective image of a real 3-subspace L of $\mathbb{C}^{2,1}$ such that $\langle v, w\rangle \in \mathbb{R}$ for all $v, w \in L$ (and such that $L \cap \mathbf{H}^2_{\mathbb{C}} \neq \emptyset$).*

Such a $\mathbb{R}$-plane is an embedded copy of $\mathbf{H}^2_{\mathbb{R}}$ (more precisely, in the ball model, it carries the Klein-Beltrami model of real hyperbolic plane, with constant curvature $-1/4$, see [Gol99] and [Par10]). Each $\mathbb{R}$-plane is also the fixed-point set of a unique (antiholomorphic) isometry, which is an involution. In particular, $\mathbb{R}$-planes are also totally geodesic.

Example 1.2.8. In the unit ball model, a standard example of $\mathbb{R}$-plane is

$$L_0 = \{(z_1, z_2) \in \mathbf{H}^2_{\mathbb{C}} : z_1, z_2 \in \mathbb{R}\},$$

that is a copy of real hyperbolic plane $\mathbf{H}^2_{\mathbb{R}}$. In the Siegel domain model, it becomes $\{(x, 0, u) : x \in \mathbb{R}, u \in \mathbb{R}_+\}$ in horospherical coordinates.

We show the action of $PU(2,1)$ on the $\mathbb{R}$-planes of $\mathbf{H}^2_{\mathbb{C}}$ in the following proposition.

Proposition 1.2.9. *The group $PU(2,1)$ acts transitively on the set of $\mathbb{R}$-planes, with isotropy group a conjugate of $PO(2,1)$.*

1.2.4 Orthogonal projection onto $\mathbb{C}$-planes

In the following we describe the orthogonal projection of geodesics onto a complex line that will be used later. The sketch of the proof follows from geometric facts and refers to the same situation in [Tho10] for calculations.

Lemma 1.2.10. *Let Π_Σ be the orthogonal projection of complex hyperbolic space onto a complex line Σ and σ be a geodesic.*

- *Then the image $\Pi_\Sigma(\sigma)$ is a single point*
- *or an arc of a geometric circle in Σ. In particular, if $\sigma \cap \Sigma \neq \emptyset$, then $\Pi_\Sigma(\sigma)$ is the segment of a geodesic in Σ.*

Proof. Using the ball model of $\mathbf{H}^2_{\mathbb{C}}$, we may assume that $\Sigma = \{(z_1, 0) | z_1 \in \mathbb{C}\}$. This makes the orthogonal projection linear, that is $\Pi_\Sigma(z_1, z_2) = z_1$. We also assume $z_1 \neq$ const otherwise the geodesic will be contained in the $\mathbb{C}$-line $\{(a, z_2) | a = \text{constant}, z_2 \in \mathbb{C}\}$), so σ will be projected to a single point.

Recall, a complex line is the non-empty intersection of a complex projective line with $\mathbf{H}^2_{\mathbb{C}}$ and a geodesic is the locus of a quadratic equation with respect to the real and imaginary parts of coordinates in a $\mathbb{C}$-line. From this, we see that $\Pi_\Sigma(\sigma)$ is the locus of a quadratic equation with respect to $\Re(z_1)$ and $\Im(z_1)$, which is a geometric circle in Σ.

To see this is true for a general $\mathbb{C}$-line, recall that a $\mathbb{C}$-line is an embedded copy of $\mathbf{H}^1_{\mathbb{C}}$, an element of $PU(2,1)$ sending a $\mathbb{C}$-line to another is an isometry of $\mathbf{H}^1_{\mathbb{C}}$. Isometries of $\mathbf{H}^1_{\mathbb{C}}$ is a Möbius transformation, which sends circles to circles. For the particular case of $\sigma \cap \Sigma \neq \emptyset$, the result follows from the fact that the linear projection preserves the straight line. □

Corollary 1.2.11. *In the ball model of $\mathbf{H}^2_{\mathbb{C}}$, let Σ_1 and Σ_2 be $\mathbb{C}$-planes, γ a hypercycle in Σ_2 and Π_{Σ_1} be the orthogonal projection map onto Σ_1. Then $\Pi_{\Sigma_1}(\gamma)$ is an arc of a geometric circle in Σ_1 or a point if Σ_1 and Σ_2 are orthogonal.*

Proof. Note that the hypercycle is the arc of a Euclidean circle in the Poincaré disc (see Proposition 2.1.8). This corollary follows from the same argument as Lemma 1.2.10. □

Lemma 1.2.12. *Let σ be a geodesic and p, q be two points on σ. Then the geodesic segment $[p, q]$ projects to the shorter arc of a geometric circle in a coordinate axis.*

Proof. Let Σ be a complex line containing the geodesic σ. Using the ball model of $\mathbf{H}^2_{\mathbb{C}}$, we know that Σ is an embedded copy of Poincaré disc in $\mathbf{H}^2_{\mathbb{C}}$. We consider the extension to projective space of σ and Σ, denoted by $\overline{\sigma}$ and $\overline{\Sigma}$ respectively. There is an involution fixing S^3 (the boundary of $\partial\mathbf{H}^2_{\mathbb{C}}$) in $\mathbb{C}^2$

$$(z_1, z_2) \longrightarrow \left(\frac{z_1}{|z_1|^2 + |z_2|^2}, \frac{z_2}{|z_1|^2 + |z_2|^2}\right),$$

which preserves the extension $\overline{\Sigma}$ and swaps the two parts $\overline{\sigma}\backslash\sigma$ and σ. It follows (like in Poincaré disc) that σ is shorter than $\overline{\sigma}\backslash\sigma$ with respect to the Euclidean metric. By Lemma 1.2.10, the projection of $\overline{\sigma}$ is a geometrical circle in a $\mathbb{C}$-line. Furthermore, the orthogonal projection on a coordinate axis is linear, which implies that it preservers the angle. As a consequence, the projection sends the geodesic σ to the shorter arc of a geometric circle. So does each geodesic segment $[p, q]$. □

1.3 Complex hyperbolic isometries

Let $U(2,1)$ be the group of matrices that are unitary with respect to the Hermitian form $\langle\cdot,\cdot\rangle$. The group of holomorphic isometries of complex hyperbolic space is the projective unitary group $PU(2,1) = U(2,1)/U(1)$, with a natural identification $U(1) = \{e^{i\theta}I, \theta \in [0, 2\pi)\}$ where I is the identity matrix in $U(2,1)$. It will be useful to consider $SU(2,1)$, the group of matrices with determinant 1 which are unitary with respect to $\langle\cdot,\cdot\rangle$. Then the group $SU(2,1)$ is a 3-fold covering of $PU(2,1)$, that is

$$PU(2,1) = SU(2,1)/\{I, \omega I, \omega^2 I\}$$

where $\omega = (-1 + i\sqrt{3})/2$ is a cube root of unity.

1.3.1 Classification of the elements of $SU(2,1)$

In this section we recall briefly the different types of isometries of $\mathbf{H}^2_{\mathbb{C}}$. A holomorphic complex hyperbolic isometry of $\mathbf{H}^2_{\mathbb{C}}$ is said to be:

(i) *loxodromic* if it fixes exactly two points of $\partial\mathbf{H}^2_{\mathbb{C}}$;

(ii) *parabolic* if it fixes exactly one point of $\partial\mathbf{H}^2_{\mathbb{C}}$;

(iii) *elliptic* if it fixes at least one point in $\mathbf{H}^2_{\mathbb{C}}$.

Following Chen and Greenberg [CG74], we now give the first criterion for classifying the elements of $SU(2,1)$.

Proposition 1.3.1. *Let g be a holomorphic isometry of $\mathbf{H}^2_{\mathbb{C}}$ and A a lift of g in $U(2,1)$, then*

- *g is elliptic if A is semisimple with eigenvalues of norm 1;*

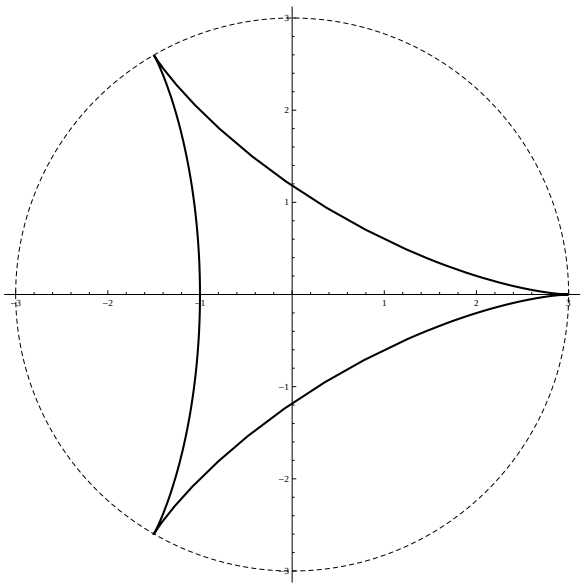

FIGURE 1.1: The deltoid given by $f(\tau) = 0$. Its interior corresponds to $f(\tau) < 0$ and its exterior corresponds to $f(\tau) > 0$.

- *g is loxodromic if A is semisimple with two eigenvalues λ and $\overline{\lambda}^{-1}$ where $|\lambda| \neq 1$;*
- *g is parabolic if A is not semisimple. In this case, its eigenvalues are of norm 1.*

Definition 1.3.2.
- *An elliptic element g is called **regular elliptic** if and only if its eigenvalues are distinct. In the other case, we say that g is **special**.*
- *A parabolic element g is called **pure parabolic** if it can be represented by a unipotent element of $U(2,1)$, that is, a linear transformation having 1 as its only eigenvalue. In the other case, we say that g is **screw-parabolic**.*

Definition 1.3.3. *The map $\tau : SU(2,1) \longrightarrow \mathbb{C}$ is defined to be the trace of matrices in $SU(2,1)$. Let f be the polynomial*

$$f(z) = |z|^4 - 8\Re(z^3) + 18|z|^2 - 27.$$

Let $\mathbb{U}_3 \subset \mathbb{C}$ denote the set of cube roots of unity. The second criterion is described in the following theorem.

Theorem 1.3.4. *(see [Gol99], Chapter 6) Let A be a matrix of $SU(2,1)$ and g be the isometry of $\mathbf{H}^2_{\mathbb{C}}$ associated to A. Then*

(i) g is regular elliptic if and only if $f(\tau(A)) < 0$;

(ii) g is loxodromic if and only if $f(\tau(A)) > 0$;

(iii) g is screw-parabolic if and only if g is not elliptic and $\tau(A) \in f^{-1}(0) - 3\mathbb{U}_3$;

(iv) g a complex reflection (about either a point or a complex geodesic) if and only if A is elliptic and $\tau(A) \in f^{-1}(0) - 3\mathbb{U}_3$;

(v) $\tau(A) \in 3\mathbb{U}_3$ if and only if A represents a unipotent automorphism of $\mathbf{H}^2_{\mathbb{C}}$.

Figure 1.1 depicts the level set $f^{-1}(0)$ of f, which is a classical curve called a *deltoid* (see Chapter 8 of Lockwood [Loc61] or page 26 of Kirwan [Kir92] where it is written in terms of $x = \Re(\tau)$ and $y = \Im(\tau)$). The interior of the deltoid corresponds to conjugacy classes of elliptic elements and its exterior corresponds to conjugacy classes of loxodromic elements. Its boundary corresponds to various parabolic conjugacy classes and complex reflections, its three cusps correspond to the central elements and various unipotent conjugacy classes.

1.3.2 The elliptic elements

In the unit ball model, up to conjugation, a lift of an elliptic transformation in $SU(2,1)$ is

$$A = \begin{bmatrix} e^{i\theta_1} & 0 & 0 \\ 0 & e^{i\theta_2} & 0 \\ 0 & 0 & e^{-i(\theta_1+\theta_2)} \end{bmatrix}. \tag{1.2}$$

In this case A fixes the center of the ball, corresponding to the vector $[0,0,1]^T$, and preserves the double axis of coordinates. The two quantities $2\theta_1 + \theta_2$ and $\theta_1 + 2\theta_2$ in the range of $[0, 2\pi)$, called the *angles* of the elliptic element, determine the conjugacy class of an elliptic element.

Example 1.3.5. Using the unit ball model, in homogeneous coordinates, the function

$$(z_1, z_2) \longmapsto (e^{i\alpha} z_1, e^{i\beta} z_2)$$

is elliptic and fixes only the origin if $e^{i\alpha}$ and $e^{i\beta}$ are different from 1.

The regular elliptic elements

If $A \in SU(2,1)$ is a lift of regular elliptic g, then g has three fixed points in $\mathbb{CP}^2$, which are the images of eigenvectors of A under the projection.

- One of these fixed points is in $\mathbf{H}^2_{\mathbb{C}}$.
- The two other points are in $\mathbb{P}(V_+)$ which are polar to the preserved complex lines.

The special elliptic elements

A special elliptic element has a repeated eigenvector. In this case, the angles can be divided into two types:

- $\{0, \varphi\}$, in this case we call it *complex reflection*: g fixes a complex line Σ and acts on the complex line orthogonal to Σ as a rotation with angle φ.
- $\{\varphi, \varphi\}$, in this case we call it *complex reflection* in a point: g preserves each of the complex lines passing through this point in $\mathbf{H}^2_{\mathbb{C}}$ and acts on each of these complex lines as a reflection with angle φ.

More precisely, the following proposition gives the formula of a complex reflection in $\mathbf{H}^2_{\mathbb{C}}$.

Proposition 1.3.6. *Let Σ be a complex line with polar vector $\mathbf{n}$. Then the complex reflection with angle φ fixing Σ is given in $U(2,1)$ by*

$$R(\mathbf{z}) = \mathbf{z} + (e^{i\varphi} - 1)\frac{\langle \mathbf{z}, \mathbf{n}\rangle}{\langle \mathbf{n}, \mathbf{n}\rangle}\mathbf{n}.$$

In particular, R is represented by a matrix in $SU(2,1)$ as follows,

$$R(\mathbf{z}) = e^{-i\varphi/3}\mathbf{z} + (e^{2i\varphi/3} - e^{-i\varphi/3})\frac{\langle \mathbf{z}, \mathbf{n}\rangle}{\langle \mathbf{n}, \mathbf{n}\rangle}\mathbf{n}.$$

Remark 1.3.7. If $\varphi = \pi$, this reflection is called *involution* or half-turn, given by

$$(z_1, z_2) \longmapsto (-z_1, -z_2).$$

For every point $z \in \mathbf{H}^2_{\mathbb{C}}$ there is a unique half-turn fixing z whose differential equals $-I$ on $T_z\mathbf{H}^2_{\mathbb{C}}$. These involutions equip $\mathbf{H}^2_{\mathbb{C}}$ with the structure of a Riemannian symmetric space (see [Gol99], page 82).

1.3.3 The loxodromic elements

Let g be a loxodromic element of $\mathbf{H}^2_{\mathbb{C}}$ and A a lift of g in $SU(2,1)$. Let z_g and w_g be the two fixed points of g in $\partial\mathbf{H}^2_{\mathbb{C}}$.

Definition 1.3.8. *The geodesic σ_g joining z_g and w_g is called the **axis** of g. The complex line Σ_g containing the geodesic σ_g is called the **complex axis** of g.*

The geodesic σ_g and complex line Σ_g are preserved by g. As a result, the polar vector $u_g = \Sigma_g^{\perp}$ to the complex line Σ_g is fixed by g. We describe this in the following proposition.

Proposition 1.3.9. *A loxodromic element of $PU(2,1)$ has three fixed points in $\mathbb{CP}^2$, two of which are lying in the boundary of $\mathbf{H}^2_{\mathbb{C}}$ and the third in $\mathbb{P}(V_+)$.*

Let $\mathbf{z}_g, \mathbf{w}_g$ and $\mathbf{u}_g$ be lifts of z_g, w_g and u_g respectively. We suppose that, up to conjugation, their lifts in $\mathbb{C}^3$ are

$$\mathbf{z}_g = \begin{bmatrix} 0 \\ 0 \\ 1 \end{bmatrix}, \mathbf{w}_g = \begin{bmatrix} 1 \\ 0 \\ 0 \end{bmatrix}, \mathbf{u}_g = \begin{bmatrix} 0 \\ 1 \\ 0 \end{bmatrix},$$

then A is the matrix

$$A = \begin{bmatrix} \lambda & 0 & 0 \\ 0 & \overline{\lambda}/\lambda & 0 \\ 0 & 0 & 1/\overline{\lambda} \end{bmatrix}. \tag{1.3}$$

If $|\lambda| > 1$, then z_g is an attractive fixed point and w_g is a repulsive fixed point. Otherwise, the situations are just converse. Since A acts on the geodesic as a translation, the quantity $\rho(w, A(w))$ on every point of σ_g is called *length of translation*, denoted l_g. The relation of l_g and λ is give by

$$\cosh\left(\frac{l_g}{2}\right) = \frac{1}{2}\left(|\lambda|^2 + \frac{1}{|\lambda|^2}\right).$$

1.3.4 The parabolic elements

A parabolic element fixes exactly one point in the boundary. Up to conjugation, we can suppose that it fixes ∞. From Lemma 1.3.10, we write the matrix of $SU(2,1)$ fixing ∞ which is not loxodromic as follows

$$A = e^{-i\theta/3} \begin{bmatrix} 1 & -e^{i\theta}\overline{z} & (-|z|^2 + it)/2 \\ 0 & e^{i\theta} & z \\ 0 & 0 & 1 \end{bmatrix} \tag{1.4}$$

with $z \in \mathbb{C}$ and $t \in \mathbb{R}$.

Lemma 1.3.10. *(see [Par10]) Suppose that $A \in SU(2,1)$ has the standard matrix form $(z_{jk})^{3\times 3}$. Then the following are equivalent:*

1. *A fixes ∞;*
2. *A is upper triangular;*
3. *z_{31}=0.*

A pure parabolic element has a lift in $SU(2,1)$ which is unipotent. A unipotent matrix A of $SU(2,1)$ is one such that $A - I$ is nilpotent, in other words, such that some power $(A-I)^n$ is zero. The smallest such n is sometimes called the degree of unipotency of $A-I$. We can classify, in terms of degree, the conjugacy class of pure parabolic isometries:

Proposition 1.3.11. *All pure parabolic isometries can be divided into two conjugacy class in $\widehat{PU(2,1)}$:*

1. *The first conjugacy class consists of the isometries which lift to a unipotent matrix A in $SU(2,1)$ such that the degree of unipotency of $A - I$ is two. Writing $z = 0, t = 1, \theta = 0$ in the matrix form (1.4), we obtain a representation with shortest length of translation. There are two candidates in $PU(2,1)$ for this conjugacy class, denoted by A_+ and A_-:*
$$A_\pm = \begin{bmatrix} 1 & 0 & \pm i/2 \\ 0 & 1 & 0 \\ 0 & 0 & 1 \end{bmatrix}.$$
2. *For the isometries which lift to a unipotent matrix A in $SU(2,1)$ such that the degree of $A - I$ is three. The conjugacy class is represented by*
$$A = \begin{bmatrix} 1 & -1 & -1/2 \\ 0 & 1 & 1 \\ 0 & 0 & 1 \end{bmatrix}.$$

Definition 1.3.12. *In the previous proposition, the parabolic isometries of the first conjugacy class will be denoted by **parabolic transformations of vertical type**, and the second class will be called **horizontal type**.*

For the screw-parabolic isometries, up to conjugation, we can suppose that the positive eigenvector is $[0,1,0]^T$. Under this condition, a matrix representation of a conjugacy class is

$$A = \begin{bmatrix} e^{-i\theta/3} & 0 & -e^{-i\theta/3}i/2 \\ 0 & e^{2i\theta/3} & 0 \\ 0 & 0 & e^{-i\theta/3} \end{bmatrix}.$$

Remark 1.3.13. Both screw-parabolic isometries and parabolic isometries of vertical type preserve a complex line where they act as a translation. Furthermore, screw-parabolic elements rotate around the preserved complex line with an angle θ.

1.4 The action on $\partial\mathbf{H}^2_{\mathbb{C}}$

In this section we work in the boundary of the Siegel domain model and discuss the classification of elements of $PU(2,1)$ in terms of their action on the boundary. Recall that $\mathbb{R}^3 \cup \{q_\infty\}$ in the Siegel's domain model is naturally equipped with the structure of the Heisenberg group on $\mathbb{C} \times \mathbb{R}$. In other words, the boundary of the Siegel domain is identified with the one-point compactification of the Heisenberg group.

1.4.1 The Heisenberg group

Definition 1.4.1. *The Heisenberg group $\mathcal{N}$ of dimension 3 is $\mathbb{C} \times \mathbb{R}$ equipped with the group law*

$$(\zeta, v) \diamond (\xi, t) = (\zeta + \xi, v + t + 2\Im(\zeta\overline{\xi})).$$

We remark that $\Im(\zeta\overline{\xi}) = \omega(\zeta, \xi)$ where ω is the standard symplectic form on $\mathbb{C}$. The Heisenberg group is 2-step nilpotent. Observe that

$$(\zeta, v) \diamond (\xi, t) \diamond (-\zeta, -v) \diamond (-\xi, -t) = (0, 4\Im(\zeta, \overline{\xi}))$$

where $(-\zeta, -v)$ is the inverse of the element (ζ, v). Therefore the center of $\mathcal{N}$ consists of the form $(0, v)$ and the commutator of any two elements lies in the center.

The stabilizer of q_∞

We now describe the action of the stabilizer of q_∞ on the Heisenberg group.

Definition 1.4.2. *We denote $Sim(\mathcal{N})$ the group of the restrictions of elements of $PU(2,1)$ fixing q_∞ on the Heisenberg group. The elements of $Sim(\mathcal{N})$ will be called **Heisenberg similarities**. (The elements are similarities with respect to the Cygan metric which we will mention a little later.)*

If A fixes q_∞ then it is upper triangular. As a matrix in $SU(2,1)$, it is given by

$$A = \begin{bmatrix} \lambda & -\overline{\lambda}\overline{z}/\lambda & (-|z|^2 + it)/2\overline{\lambda} \\ 0 & \overline{\lambda}/\lambda & z/\overline{\lambda} \\ 0 & 0 & 1/\overline{\lambda} \end{bmatrix}$$

with $\lambda \in \mathbb{C}^*$ and $(z, t) \in \mathbb{C} \times \mathbb{R}$. More precisely,

(I) The Heisenberg group acts on itself by *Heisenberg translations*. This is a normal subgroup of the group $Sim(\mathcal{N})$. For $(z_0, t_0) \in \mathcal{N}$, this is

$$T_{(z_0,t_0)} : (z, t) \mapsto (z + z_0, t + t_0 + 2\Im(\overline{z}z_0)) = (z_0, t_0) \diamond (z, t).$$

As a matrix in $SU(2,1)$ this is

$$\begin{bmatrix} 1 & -\overline{z}_0 & (-|z_0|^2 + it_0)/2 \\ 0 & 1 & z_0 \\ 0 & 0 & 1 \end{bmatrix}.$$

Heisenberg translation by $(0, t_0)$ for any $t \in \mathbb{R}$ is called *vertical translation* by t_0.

(II) The unitary group $U(1)$ acts on the Heisenberg group by *Heisenberg rotations*. For $e^{i\theta} \in U(1)$, the rotation fixing $q_0 = (0,0,0)$ is given by

$$\begin{bmatrix} 1 & 0 & 0 \\ 0 & e^{i\theta} & 0 \\ 0 & 0 & 1 \end{bmatrix}.$$

In Heisenberg coordinates, this Heisenberg rotation is given by

$$R_\theta : (z,t) \mapsto (e^{i\theta}z, t).$$

All other Heisenberg rotations may be obtained from these by conjugating by a Heisenberg translation.

(III) For $\lambda \in \mathbb{R}_+$, *Heisenberg dilation* by λ fixing q_∞ and $q_0 = (0,0,0) \in \partial\mathbf{H}^2_{\mathbb{C}}$ is given by

$$\begin{bmatrix} \lambda & 0 & 0 \\ 0 & 1 & 0 \\ 0 & 0 & \lambda^{-1} \end{bmatrix}.$$

In Heisenberg coordinates, the Heisenberg dilation is given by

$$D_\lambda : (z,t) \mapsto (\lambda z, \lambda^2 t).$$

All other Heisenberg dilations fixing q_∞ may be obtained by conjugating by a Heisenberg translation.

The stabilizer of q_∞ in $PU(2,1)$ is generated by all Heisenberg translations, rotations and dilations. However, only Heisenberg translations and rotations are isometric with respect to various natural metrics on $\mathcal{N}$. For this reason the group generated by all Heisenberg translations and rotations, which is the semidirect product $U(1) \ltimes \mathcal{N}$, is called the *Heisenberg isometry group* $Isom(\mathcal{N})$. The nontrivial central elements of the Heisenberg isometry group are precisely the vertical translations.

The vertical projection

Geometrically, we think of the $\mathbb{C}$-factor of $\mathcal{N}$ as being horizontal and the $\mathbb{R}$-factor as being vertical. There is a canonical projection from $\mathcal{N}$ to $\mathbb{C}$ called *vertical projection* and denoted by Π, given by $\Pi : (z,t) \longmapsto z$. Using the exact sequence

$$0 \longrightarrow \mathbb{R} \longrightarrow \mathcal{N} \xrightarrow{\Pi} \mathbb{C} \longrightarrow 0,$$

we obtain the exact sequence (see Scott [Sco83] page 467)

$$0 \longrightarrow \mathbb{R} \longrightarrow Isom(\mathcal{N}) \xrightarrow{\Pi_*} Isom(\mathbb{C}) \longrightarrow 1. \tag{1.5}$$

Here $Isom(\mathbb{C}) = \mathbb{C} \rtimes U(1)$ is the group of orientation preserving Euclidean isometries of $\mathbb{C}$.

Observe the elements in $Isom(\mathbb{C})$ can be represented by matrices in $GL(2,\mathbb{C})$ of the form

$$\begin{bmatrix} e^{i\theta} & z_0 \\ 0 & 1 \end{bmatrix} \begin{bmatrix} z \\ 1 \end{bmatrix} = \begin{bmatrix} e^{i\theta}z + z_0 \\ 1 \end{bmatrix}$$

Therefore, the map Π_* can be given by

$$\Pi_* : \begin{bmatrix} 1 & -\overline{z}_0 e^{i\theta} & (-|z_0|^2 + it_0)/2 \\ 0 & e^{i\theta} & z_0 \\ 0 & 0 & 1 \end{bmatrix} \longrightarrow \begin{bmatrix} e^{i\theta} & z_0 \\ 0 & 1 \end{bmatrix}. \tag{1.6}$$

It is clear that

$$\mathrm{Ker}(\Pi_*) = \left\{ \begin{bmatrix} 1 & 0 & it_0/2 \\ 0 & 1 & 0 \\ 0 & 0 & 1 \end{bmatrix} : t_0 \in \mathbb{R} \right\}$$

is the group of vertical translations fixing q_∞.

1.4.2 The Cygan metric

In this section we define a metric on the Heisenberg group, *the Cygan metric*. The Cygan metric can be extended to an incomplete metric on $\mathbf{H}^2_{\mathbb{C}}$ which agrees with the Cygan metric on each horosphere. This metric should be thought of as the counterpart to the Euclidean metric on the upper half space model of real hyperbolic space.

Recall that the Heisenberg norm is given by

$$|(z,t)| = \left||z|^2 - it\right|^{1/2}.$$

Definition 1.4.3. *The Cygan metric on $\mathcal{N}$ is defined to be*

$$\rho_0((z_1,t_1),(z_2,t_2)) = \left|(z_1,t_1)\diamond(z_2,t_2)^{-1}\right|.$$

In other words,

$$\rho_0((z_1,t_1),(z_2,t_2)) = \left||z_1-z_2|^2 - it_1 + it_2 - 2i\Im(z_1\overline{z}_2)\right|^{1/2}. \tag{1.7}$$

Remark 1.4.4. We remark that the Cygan metric defined by (1.7) is not a path metric. In other words, there exist pairs of points such that the Cygan distance between them is strictly shorter than the Cygan length of any path joining them (see the proof of [Par10]).

We extend the Cygan metric to an incomplete metric on $\overline{\mathbf{H}^2_{\mathbb{C}}} - \{q_\infty\}$ as follows

$$\widetilde{\rho}_0((z_1,t_1,u_1),(z_2,t_2,u_2)) = \left||z_1-z_2|^2 + |u_1-u_2| - it_1 + it_2 - 2i\Im(z_1\overline{z}_2)\right|^{1/2} \tag{1.8}$$

We now show that the extended Cygan metric on $\overline{\mathbf{H}^2_{\mathbb{C}}} - \{q_\infty\}$ is exactly a metric. Naturally the restriction on $\partial\mathbf{H}^2_{\mathbb{C}} - \{q_\infty\}$ is also metric.

Proposition 1.4.5. *(c.f. [Par10]) The function $\widetilde{\rho}_0(\cdot,\cdot)$ on $\overline{\mathbf{H}^2_{\mathbb{C}}} - \{q_\infty\}$ given by (1.8) is a metric.*

Proof. It obviously satisfies the properties of non-negativity, identity of indiscernible and symmetry. It suffices to verify the triangle inequality. That is,

$$\begin{aligned}
&\widetilde{\rho}_0^2\left((z_1,t_1,u_1),(z_2,t_2,u_2)\right) \\
&= \left||z_1-z_2|^2 + |u_1-u_2| - it_1 + it_2 - 2i\Im(z_1\overline{z}_2)\right| \\
&\leq \left||z_1-z_3|^2 + |u_1-u_3| - it_1 + it_3 - 2i\Im(z_1\overline{z}_3)\right| \\
&\quad +2|z_1-z_3||z_3-z_2| + \left||z_3-z_2|^2 + |u_3-u_2| - it_3 + it_2 - 2i\Im(z_3\overline{z}_2)\right| \\
&\leq \left(\widetilde{\rho}_0\left((z_1,t_1,u_1),(z_3,t_3,u_3)\right) + \widetilde{\rho}_0\left((z_3,t_3,u_3),(z_2,t_2,u_2)\right)\right)^2.
\end{aligned}$$

□

We conclude this section by considering spheres with respect to the Cygan metric.

Definition 1.4.6. *The **Cygan sphere** of radius $r \in \mathbb{R}_+$ and center $w_0 = (z_0, t_0) = (z_0, t_0, 0) \in \partial\mathbf{H}^2_{\mathbb{C}}$ is defined by*

$$S_r(w_0) = \{w = (z, t, u) : \widetilde{\rho}_0(w, w_0) = r\}.$$

In other words, $S_r(w_0)$ is given by

$$S_r(w_0) = \{w = (z, t, u) : \Big||z - z_0|^2 + u + it - it_0 - 2i\Im(z\overline{z}_0)\Big| = r^2\}.$$

A simple lemma will be useful in the Chapter 4, we state it as follows.

Lemma 1.4.7. *(c.f. [FFP10]) All Cygan balls are affinely convex.*

Proof. The Cygan ball of radius r centered at $o = (0, 0, 0)$ is given by

$$S_r(o) = \{(z, t, u) \in \mathbf{H}^2_{\mathbb{C}} : \ \Big(|z|^2 + u\Big)^2 + t^2 \leq r^4\}.$$

For $\lambda \in (0, 1)$ and $(z_1, t_1, u_1), (z_2, t_2, u_2) \in S_r(o)$, a simple calculation gives rise to

$$\begin{aligned}
&\Big(|\lambda z_1 + (1-\lambda)z_2|^2 + \lambda u_1 + (1-\lambda)u_2\Big)^2 + (\lambda t_1 + (1-\lambda)t_2)^2 \\
&\leq \ \Big(\lambda(|z_1|^2 + u_1) + (1-\lambda)(|z_2|^2 + u_2)\Big)^2 + (\lambda t_1 + (1-\lambda)t_2)^2 \\
&\leq \ \lambda\Big((|z_1|^2 + u_1)^2 + t_1^2\Big) + (1-\lambda)\Big((|z_1|^2 + u_1)^2 + t_1^2\Big) \\
&\leq \ \lambda r^4 + (1-\lambda)r^4 = r^4.
\end{aligned}$$

Clearly $S_r(o)$ is affinely convex. Any other Cygan ball is the image of one centred at o under a Heisenberg translation. Since Heisenberg translations are affine motions, the image is still affinely convex. □

Remark 1.4.8. The boundary of a Cygan sphere on $\partial\mathbf{H}^2_{\mathbb{C}}$ is called a *spinal sphere*.

- For $z_0 = 0$. Spinal spheres centered at $w_0 = (0, t_0)$ are ovoids with the property that along the locus $z = 0$ they have fourth order contact with their tangent plane. The diameter of their equator, that is the points (z, t) with $|z| = r$, grows linearly with r. On the other hand, the diameter of their meridians, that is the points $(0, t)$ with $|t - t_0| = r^2$, grows quadratically with r. Geometrically, as r tends to zero, spinal spheres become very short and fat, lie a *pancake*, see Figure 1.2(a). Conversely, as r tends to infinity, spinal spheres become very long and thin, like a *cigar*, see Figure 1.2(b).

- For $z_0 \neq 0$. Cygan spheres are *sheared ovoids*, see Figure 1.2(c), the magnitude of the shear being proportional to $|z_0|$. Otherwise they enjoy the same properties as the case $z_0 = 0$.

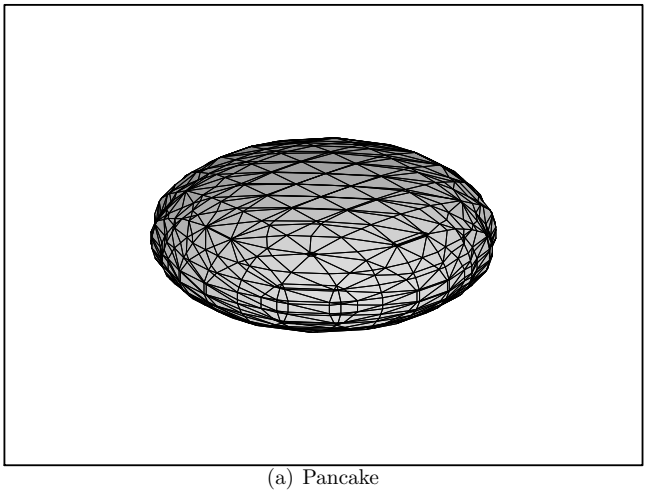

(a) Pancake

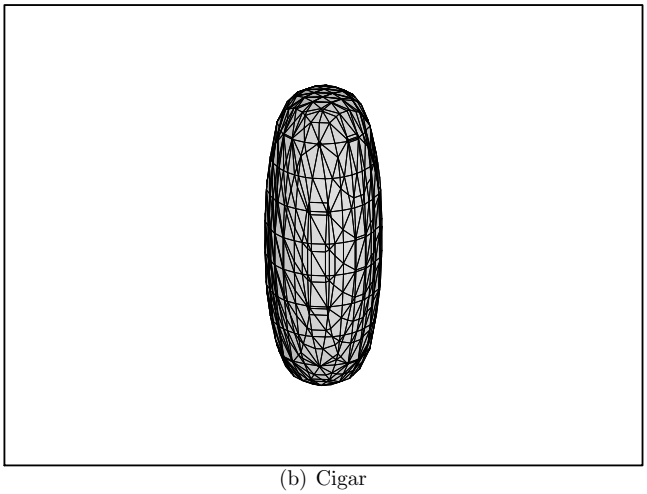

(b) Cigar

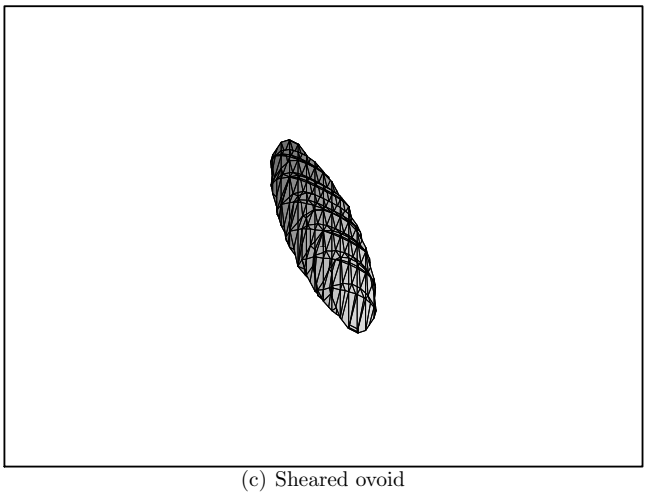

(c) Sheared ovoid

FIGURE 1.2: The shapes of spinal spheres in the Heisenberg group.

Chapter 2

Geometric technique

In this chapter we mostly state some geometric objects which are used to construct a polyhedron. There are no totally geodesic real hypersurfaces in $\mathbf{H}^2_{\mathbb{C}}$. The lack of totally geodesic real hypersurfaces complicates the construction of fundamental domains. However there is a three dimensional submanifold that is foliated by totally geodesic subspaces in two different ways. Throughout the thesis, the basic idea of constructing a fundamental domain is to verify the conditions of Poincaré's polyhedron theorem. As well, we can obtain a geometric presentation for the group we consider by the Poincaré's polyhedron theorem.

2.1 Bisectors

A bisector is the locus of points in complex hyperbolic space equidistant from a given, pair of points in complex hyperbolic space, say p and q. By the normalization of p and q such that $\langle \mathbf{p}, \mathbf{p} \rangle = \langle \mathbf{q}, \mathbf{q} \rangle$, we give the definition as follows:

Definition 2.1.1. *The bisector equidistant from p and q is defined as*

$$\mathcal{B}_{p,q} = \left\{ z \in \mathbf{H}^2_{\mathbb{C}} : |\langle \mathbf{z}, \mathbf{p} \rangle| = |\langle \mathbf{z}, \mathbf{q} \rangle| \right\}. \tag{2.1}$$

Remark 2.1.2. This definition of a bisector only depends on $\langle \mathbf{p}, \mathbf{p} \rangle = \langle \mathbf{q}, \mathbf{q} \rangle$ and not on whether this quantity is positive, negative or zero. If $\langle \mathbf{p}, \mathbf{p} \rangle = \langle \mathbf{q}, \mathbf{q} \rangle > 0$, then p and q are polar vectors to complex lines $\mathcal{C}_p$ and $\mathcal{C}_q$. Thus $\mathcal{B}_{p,q}$ is equidistant from two complex lines $\mathcal{C}_p$ and $\mathcal{C}_q$. In other words, for each $z \in \mathcal{B}_{p,q}$ the distance from z to the closest point of $\mathcal{C}_p$ is the same as the distance from z to the closest point of $\mathcal{C}_q$.

Definition 2.1.3.

- *The points p and q lie in a unique complex line Σ, called the **complex spine** of the bisector $\mathcal{B}_{p,q}$.*
- *We call **spine** the geodesic σ in Σ that is equidistant from our pair of points with respect to the natural Poincaré metric on Σ. It is given by*

$$\sigma = \Sigma \cap \mathcal{B}_{p,q} = \{ z \in \Sigma : \rho(z, p) = \rho(z, q) \}.$$

Bisectors are not totally geodesic in complex hyperbolic space, but can be described in terms of a foliation by totally geodesic subspaces in two different ways.

Theorem 2.1.4. ***(Mostow,Goldman)***([Mos80, Gol99])

1. *Let $\Pi_\Sigma : \mathbf{H}^2_{\mathbb{C}} \mapsto \Sigma$ be the orthogonal projection map onto Σ. Then $\mathcal{B}$ is the preimage of σ under Π_Σ,*

$$\mathcal{B} = \Pi_\Sigma^{-1}(\sigma) = \bigcup_{s \in \sigma} \Pi_\Sigma^{-1}(s).$$

   *Each fibre of this map, that is, each complex line that is the preimage of a point of σ, is a **slice** of $\mathcal{B}$.*

2. *The bisector $\mathcal{B}$ is the union of all Lagrangian planes that contain σ. These Lagrangian planes are called **meridians** of $\mathcal{B}$.*

Corollary 2.1.5.

- *A bisector is uniquely determined by its real spine.*
- *The bisector $\mathcal{B}$ is preserved under a complex involution in any of its slices.*
- *The bisector $\mathcal{B}$ is preserved under an anti-holomorphic involution in any of its meridians.*

Definition 2.1.6. *Let $\mathcal{B}$ be a bisector. The intersection $S = \overline{\mathcal{B}} \cap \partial\mathbf{H}^2_{\mathbb{C}}$ is called a **spinal sphere**. Suppose that σ is the spine of $\mathcal{B}$, the two points of $\overline{\sigma} \cap \partial\mathbf{H}^2_{\mathbb{C}}$ are called the **vertices** of bisector.*

2.1.1 Intersection of bisectors

The intersection of two or more bisectors can be very complicated, in general it is not necessarily connected or contained in a totally geodesic subspace. We adopt the following notation and recall several results which allow us to understand bisector intersections.

Definition 2.1.7. *Let $\mathcal{B}_1$ and $\mathcal{B}_2$ denote bisectors with complex spines Σ_1 and Σ_2.*

1. *We call $\mathcal{B}_1$ and $\mathcal{B}_2$ **cospinal** if and only if $\Sigma_1 = \Sigma_2$;*
2. *We call $\mathcal{B}_1$ and $\mathcal{B}_2$ **coequidistant** if and only if Σ_1 and Σ_2 intersect outside the real spines;*
3. *We call $\mathcal{B}_1$ and $\mathcal{B}_2$ **cotranchal** if and only if they share a common slice;*
4. *We call $\mathcal{B}_1$ and $\mathcal{B}_2$ **comeridanal** if and only it they share a common meridian.*

In terms of the slice decomposition for bisectors, the following result helps us to understand bisector intersections.

Proposition 2.1.8. *([Mos80]) Let $\mathcal{B}$ be a bisector and $\mathcal{C}$ be a complex line such that $\mathcal{B} \cap \mathcal{C} \neq \emptyset$, then $\mathcal{C} \subset \mathcal{B}$ (in which case $\mathcal{C}$ is a slice of $\mathcal{B}$) or $\mathcal{C} \cap \mathcal{B}$ is a hypercycle in $\mathcal{C}$. In the ball model a hypercycle is an arc of a Euclidean circle intersecting the boundary.*

We remark that a hypercycle in $\mathcal{C}$ is a curve with constant geodesic curvature (i.e. the magnitude of the mean curvature is constant). In particular, unless the two bisectors share a common slice, Proposition 2.1.8 implies that each connected component of the intersection $\mathcal{B}_1 \cap \mathcal{B}_2$ is a disk which is foliated by arcs of circles. It can be proven that there are at most two connected components. If the bisectors are coequidistant, there is a remarkable result due to Giraud.

Proposition 2.1.9. *([Gir21, Gol99]) Let $\mathcal{B}_1$ and $\mathcal{B}_2$ be two coequidistant bisectors with complex spines Σ_1 and Σ_2 respectively, then $\mathcal{B}_1 \cap \mathcal{B}_2$ is a smooth disk, moreover there exists one (and no more) bisector containing $\mathcal{B}_1 \cap \mathcal{B}_2$ other than $\mathcal{B}_1$ and $\mathcal{B}_2$.*

This intersection is not totally geodesic, we call it a *Giraud disc*. In particular, we can find the third bisector passing through the Giraud disc using the following proposition, see also [Tho10] and Figure 2.1.

Proposition 2.1.10. *Let $\mathcal{B}_1$ and $\mathcal{B}_2$ be a pair of coequidistant bisectors with respective complex (real) spines Σ_1 and Σ_2 (σ_1 and σ_2) such that their intersection is a Giraud disc $\mathcal{G}$. The third bisector $\mathcal{B}_3$ containing $\mathcal{G}$ can be defined as the following procedure. We denote $\Sigma_1 \cap \Sigma_2 = p_0$ and let R_{σ_i} be the unique reflection fixing σ_i for $i = 1, 2$. Suppose that $p_1 = R_{\sigma_1}(p_0)$ and $p_2 = R_{\sigma_2}(p_0)$, then*

$$\begin{aligned} \mathcal{B}_1 &= \mathcal{B}_{p_0,p_1} = \{z \in \mathbf{H}^2_{\mathbb{C}} : \rho(z, p_0) = \rho(z, p_1)\}, \\ \mathcal{B}_2 &= \mathcal{B}_{p_0,p_2} = \{z \in \mathbf{H}^2_{\mathbb{C}} : \rho(z, p_0) = \rho(z, p_2)\}, \\ \mathcal{B}_3 &= \mathcal{B}_{p_1,p_2} = \{z \in \mathbf{H}^2_{\mathbb{C}} : \rho(z, p_1) = \rho(z, p_2)\} \end{aligned}$$

and

$$\mathcal{G} = \{z \in \mathbf{H}^2_{\mathbb{C}} : \rho(z, p_0) = \rho(z, p_1) = \rho(z, p_3)\}.$$

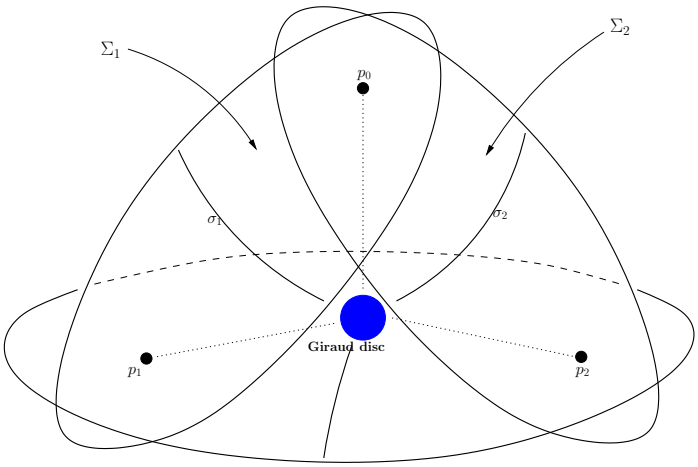

FIGURE 2.1: The schematic view of Giraud disc.

2.1.2 Intersection with geodesics

Proposition 2.1.11. *(see Theorem 5.5.1, [Gol99]) A real geodesic σ is contained in $\mathcal{B}$ if and only if σ is contained in either a slice or a meridian of $\mathcal{B}$.*

If the geodesic σ is not entirely contained in $\mathcal{B}$, the following proposition shows how to see the number of intersection points between σ and $\mathcal{B}$.

Proposition 2.1.12. *Let $\mathcal{B}$ be a bisector and σ a geodesic, σ not contained $\mathcal{B}$, then $\sigma \cap \Sigma$ consists of at most two points. Moreover the number of intersection points between σ and $\mathcal{B}$ is equal to the number of intersection points between $\sigma_{\mathcal{B}}$ (the real spine of $\mathcal{B}$) with $\Pi_\Sigma(\sigma)$ (the image of σ under orthogonal projection onto the complex spine of $\mathcal{B}$).*

Corollary 2.1.13. *Let $\mathcal{B}$ be a bisector, with complex spine Σ and σ a geodesic. If $\sigma \cap \Sigma \neq \emptyset$ and σ is not contained in $\mathcal{B}$, then σ intersects $\mathcal{B}$ in at most one point.*

2.2 Isometric spheres

2.2.1 Busemann function

We compute the Busemann function in the Siegel domain model in order to define the isometric spheres. Consider a unit speed geodesic $\sigma_t \in \mathbf{H}^2_{\mathbb{C}}$ such that $\lim_{t\to\infty} \sigma_t = q_\infty$. The corresponding *Busemann function* (see [BGS85, Gol99]) is defined as

$$h_\infty(z) = \lim_{t\to\infty} (\rho(z, \sigma_t) - t).$$

Explicitly, the points in the Siegel domain corresponding to the vectors

$$\widetilde{\sigma}_t = \begin{bmatrix} -e^{t/2}/2 \\ 0 \\ e^{-t/2} \end{bmatrix}$$

move (as $t \to \infty$) at unit speed along a geodesic towards q_∞ corresponding to

$$Q_\infty = \begin{bmatrix} 1 \\ 0 \\ 0 \end{bmatrix}.$$

Let $\mathbf{z}$ be the standard lift of z and $\langle \mathbf{z}, \mathbf{z} \rangle < 0$. As $t \to \infty$, we see that

$$\begin{aligned} \rho(z, \widetilde{\sigma}_t) &= 2\cosh^{-1} \frac{\left| -e^{t/2}/2 + z_1 e^{-t/2} \right|}{\sqrt{-2\Re(z_1) - |z_2|^2}} \\ &\sim 2\cosh^{-1} \left(\frac{e^{t/2}}{2\sqrt{-2\Re(z_1) - |z_2|^2}} \right) \\ &\sim 2\log \left(\frac{e^{t/2}}{\sqrt{-2\Re(z_1) - |z_2|^2}} \right) \\ &= t + \log \frac{1}{-2\Re(z_1) - |z_2|^2}. \end{aligned}$$

Definition 2.2.1. *The **Busemann function** in Siegel domain is given by*

$$h_\infty(z) = \log \frac{1}{-(2\Re(z_1) + |z_2|^2)} = -\log \Psi_\infty(z)$$

where

$$\Psi_\infty(z) = \frac{-\langle \mathbf{z}, \mathbf{z} \rangle}{\langle \mathbf{z}, Q_\infty \rangle \langle Q_\infty, \mathbf{z} \rangle}.$$

Recall that the *horosphere* (centered at q_∞) of height u is the set of points satisfying $\langle \mathbf{z}, \mathbf{z} \rangle = u$, that is the corresponding level sets $h_\infty^{-1}(-\log u)$ of $h_\infty(z)$. For $z_0 \in \mathbf{H}^2_{\mathbb{C}}$ and $A \in PU(2,1)$, then $\mathcal{B}(z_0, A^{-1}(z_0))$ is a bisector equidistant between z_0 and $A^{-1}(z_0)$. As z_0 tends to the boundary, then the distance in $\mathcal{B}(z_0, A^{-1}(z_0))$ is replaced with a *Busemann function* based at z_0. We have

Definition 2.2.2. *Given an element $A \in PU(2,1)$ such that $A(q_\infty) \neq q_\infty$, the **isometric sphere** of A is defined to be the hypersurface*

$$\{z \in \boldsymbol{H}^2_{\mathbb{C}} : \ h_\infty(z) = h_\infty(A(z))\}.$$

In other words,

$$\{z \in \boldsymbol{H}^2_{\mathbb{C}} : \ |\langle \mathbf{z}, Q_\infty \rangle| = |\langle \mathbf{z}, A^{-1}(Q_\infty) \rangle|\}$$

where $\mathbf{z}$ and Q_∞ are respectively the standard lifts of z and q_∞ in $\mathbb{C}^{2,1}$.

Example 2.2.3. The isometric sphere of

$$I_0 = \begin{bmatrix} 0 & 0 & 1 \\ 0 & -1 & 0 \\ 1 & 0 & 0 \end{bmatrix}$$

is

$$\mathcal{S} = \{(z, t, u) : \ \left| |z|^2 + u - it \right| = 2\} \tag{2.2}$$

in horospherical coordinates or

$$\mathcal{S} = \{[z_1, z_2, z_3] \in \mathbf{H}^2_{\mathbb{C}} : \ |z_1| = |z_3|\} \tag{2.3}$$

in homogeneous coordinates.

Remark 2.2.4.

- The isometric sphere $\mathcal{S}$ is the Cygan sphere at the origin, called the *standard* isometric sphere. All other isometric spheres are images of $\mathcal{S}$ by Heisenberg dilations, rotations and translations. Thus the isometric sphere with radius r and center $(z_0, t_0, 0)$ is given by

$$\left\{(z,t,u):\ \left||z-z_0|^2+u+it-it_0+2i\Im(z\overline{z}_0)\right|=r^2\right\}.$$

- If A has the matrix form as

$$\begin{bmatrix} a & b & c \\ d & e & f \\ g & h & j \end{bmatrix}, \tag{2.4}$$

then $A(q_\infty) \neq q_\infty$ if and only if $g \neq 0$; see Lemma 1.3.10. The isometric sphere of A has radius $r = \sqrt{2/|g|}$ and center $A^{-1}(q_\infty)$, which in horospherical coordinates is

$$(z_0, t_0, 0) = \left(\frac{\overline{h}}{\overline{g}}, 2\Im\Big(\frac{\overline{j}}{\overline{g}}\Big), 0\right).$$

2.2.2 Dirichlet and Ford domains

The simplest type of fundamental polyhedra for discrete groups are *Dirichlet* and *Ford* fundamental polyhedra.

Suppose $\Gamma \subset PU(2,1)$ is a discrete group of isometries of $\mathbf{H}^2_{\mathbb{C}}$ and choose a point $z_0 \in \mathbf{H}^2_{\mathbb{C}}$, called the *base point* of the polyhedron.

Definition 2.2.5. *The **Dirichlet domain** for Γ centered at z_0 is defined as*

$$\mathfrak{D}_{z_0}(\Gamma) = \{z \in \mathbf{H}^2_{\mathbb{C}}|\ \rho(z,z_0) < \rho(z,\gamma(z_0)) \quad \forall \gamma \in \Gamma\backslash\{Id\}\}.$$

In other words, $\mathfrak{D}_{z_0}(\Gamma)$ is the intersection of equidistant half-spaces

$$\mathfrak{D}_{z_0}(\Gamma) = \bigcap_{\gamma \neq id} H(z_0, \gamma(z_0))$$

where the equidistant half-space is defined by

$$H(u,v) = \{z \in \mathbf{H}^2_{\mathbb{C}}|\ \rho(z,u) < \rho(z,v)\}.$$

Remark 2.2.6. The base point should not be fixed by any element of Γ. If so, the *Dirichlet domain* is exactly a fundamental domain otherwise a fundamental domain of Γ is the intersection of a fundamental domain for Γ_0 (the stabilizer of the base point) and Dirichlet domain for $\Gamma - \Gamma_0$.

We define the *Ford domain* when the base point z_0 tends to an ideal point by using Busemann function. Here the boundary of Ford domain become the union of parts of isometric spheres. As well, the Dirichlet fundamental domains converge to Ford fundamental domains. Replace z_0 by q_∞ and the Bergman metric ρ by Busemann function in the previous definition.

Definition 2.2.7. *The **Ford domain** is defined as*

$$\mathfrak{F}_\infty(\Gamma) = \{z \in \mathbf{H}^2_{\mathbb{C}}|\ h_\infty(z) < h_\infty(\gamma(z))\}.$$

In other words, $\mathfrak{F}_\infty(\Gamma)$ is the intersection of isometric spheres of all elements not fixing infinity, that is,

$$\mathfrak{F}_\infty(\Gamma) = \{z \in \mathbf{H}^2_{\mathbb{C}}|\ |\langle \mathbf{z}, Q_\infty\rangle| < |\langle \mathbf{z}, \gamma^{-1}(Q_\infty)\rangle|\}.$$

2.2.3 The geographical coordinates

Isometric spheres are examples of *bisectors* and, as such, have a very nice foliation by two different families of totally geodesic submanifolds,

- the slices,
- the meridians.

The real geodesic passing through two vertices of a bisector is called the *spine* of the bisector.

Together the slices and meridians give *geographical coordinates* on the bisector (see [FP06]). In order to parameterize the standard isometric sphere $\mathcal{S}$, we write

$$|z|^2 + u - it = 2e^{i\theta}$$

for $\theta \in [-\pi/2, \pi/2]$ (in particular, $|z| \leq \sqrt{2\cos\theta}$) and

$$z = re^{i\alpha + i\theta/2}$$

for $r \in \left[-\sqrt{2\cos(\theta)}, \sqrt{2\cos(\theta)}\right]$ and $\alpha \in [-\pi/2, \pi/2)$.

Definition 2.2.8. *In geographical coordinates, $\mathcal{S}$ is parameterized by*

$$\left\{ \begin{bmatrix} -e^{i\theta} \\ re^{i\alpha+i\theta/2} \\ 1 \end{bmatrix} : \theta \in \left[-\frac{\pi}{2}, \frac{\pi}{2}\right], \alpha \in \left[-\frac{\pi}{2}, \frac{\pi}{2}\right), r \in \left[-\sqrt{2\cos(\theta)}, \sqrt{2\cos(\theta)}\right] \right\}. \tag{2.5}$$

In horospherical coordinates, the point of $\mathcal{S}$ with geographical coordinates (r, θ, α) is given by $(re^{i\alpha+i\theta/2}, -2\sin(\theta), 2\cos(\theta) - r^2)$. The spine, slices and meridians of $\mathcal{S}$ are given in the next proposition in terms of geographical coordinates.

Proposition 2.2.9. *(cf. [FP06]) The isometric sphere of I_0, $\mathcal{S}$, with coordinates given by (2.5) is a bisector. Moreover*

(i) the spine of $\mathcal{S}$ is given by $r = 0$;

(ii) the slices of $\mathcal{S}$ are given by $\theta = \theta_0$ for fixed $\theta_0 \in [-\pi/2, \pi/2]$;

(iii) the meridians of $\mathcal{S}$ are given by $\alpha = \alpha_0$ for fixed $\alpha_0 \in [-\pi/2, \pi/2)$.

Proof. The spine of $\mathcal{S}$ passes through its vertices q_∞ and $I_0(q_\infty)$. Thus the spine lies in the complex line spanned by q_∞ and $I_0(q_\infty)$, that is the equation $z = 0$ and the first part follows.

A slice is the preimage of a point of the spine under orthogonal projection onto the complex spine. When we orthogonally project onto the complex spine $z = 0$, we throw away the second coordinate in the vector and leave the other entries unchanged. For each point $(0, -2\sin(\theta_0), 2\cos(\theta_0))$ on the spine, the points of slice are given by

$$\left\{ \begin{bmatrix} -e^{i\theta_0} \\ z \\ 1 \end{bmatrix} \in \mathbf{H}^2_{\mathbb{C}} \right\}.$$

The second part follows immediately.

The meridians of $\mathcal{S}$ are the fixed-point of antiholomorphic involutions fixing the spine. For $\alpha_0 \in [-\pi/2, \pi/2)$, these maps are given by

$$\ell_{\alpha_0} : \begin{bmatrix} z_1 \\ z_2 \\ z_3 \end{bmatrix} \longmapsto \begin{bmatrix} \overline{z}_3 \\ -e^{2i\alpha_0}\overline{z}_2 \\ \overline{z}_1 \end{bmatrix}.$$

By applying ℓ_{α_0} on the points of $\mathcal{S}$, we see that

$$\ell_{\alpha_0} : \begin{bmatrix} -e^{i\theta} \\ re^{i\alpha+i\theta/2} \\ 1 \end{bmatrix} \longmapsto \begin{bmatrix} 1 \\ -re^{2i\alpha_0-i\alpha-i\theta/2} \\ -e^{-i\theta} \end{bmatrix} \sim \begin{bmatrix} -e^{i\theta} \\ re^{2i\alpha_0-i\alpha+i\theta/2} \\ 1 \end{bmatrix}.$$

Therefore, the fixed-points by ℓ_{α_0} is given by $\alpha = \alpha_0$, that is the meridian. □

2.3 Poincaré's polyhedron theorem

Definition 2.3.1. *Let Γ be a discrete group of complex hyperbolic isometries. A subset $\mathbf{\Delta}$ of $\mathbf{H}^2_{\mathbb{C}}$ is called a* **fundamental domain** *for Γ if the following satisfy.*

- *$\mathbf{\Delta}$ is a domain in $\mathbf{H}^2_{\mathbb{C}}$, that is an open connected set;*
- *$\mathbf{\Delta} \cap \gamma(\mathbf{\Delta}) = \emptyset$ for all $\gamma \in \Gamma \setminus \{id\}$;*
- *$\bigcup_{\gamma\in\Gamma} \gamma(\overline{\mathbf{\Delta}}) = \mathbf{H}^2_{\mathbb{C}}$;*
- *the complex hyperbolic volume of $\partial\mathbf{\Delta}$ is 0.*

In this section we establish a Poincaré's polyhedron theorem suitable for our purposes, compare [FZ99, PPl06]. We will follow the formulation given by Mostow in [Mos80] and also refer to [DFP05, FP06, Par06]. In what follows our polyhedron $\mathbf{D}$ constructed in the thesis is homeomorphic to the combinatorial model, we will use a form of Poincaré's polyhedron theorem to show that $\mathbf{D}$ is a fundamental domain and obtain a geometric presentation for the group.

Definition 2.3.2. *A polyhedron is a cellular complex homeomorphic to a (compact) polytope, with the properties that there is only one cell of highest dimension and that each codimension-two cell is contained in exactly two codimension-one cells (noncompact if possible). Then its realization as a cell complex in a space X is called a* ***polyhedron****.*

Each of its codimension-2 cells, called *faces*, is contained in exactly two codimension-1 cells, called *sides*. A polyhedron is smooth if its cells are smooth. For the boundary of polyhedron, the sides contained in bisectors are naturally smooth. Nevertheless, the sides of our polyhedron not contained in bisectors (see Figure 5.7) are foliated by geodesic triangular cones, which gives rise to their smoothness. Moreover, their faces foliated by geodesics are also smooth.

Definition 2.3.3. *A Poincaré polyhedron is a smooth polyhedron D in a manifold X with sides S_j and side-pairing maps $g_j \in Isom(X)$ satisfying:*

(I) The sides of polyhedron are paired by a set Λ of homeomorphisms $g_{ij} : S_i \longrightarrow S_j$ of X called the ***side-pairing transformations****, which respect the cell structure. We assume that if $g_{ij} \in \Lambda$, $g_{ij}^{-1} = g_{ji} \in \Lambda$.*

(II) For every $g_{ij} \in \Lambda$ such that $S_i = g_{ij}(S_j)$, then $g_{ij}(\overline{D}) \cap \overline{D} = S_i$.

Remark 2.3.4. If $S_i = S_j$ (that is, a side-pairing maps one side to itself), then we impose the restriction that $g_{ii} : S_i \longrightarrow S_i$ is of order two, and we call it a reflection. In this case, the relation $g_{ii}^2 = 1$ is called a *reflection relation.*

Let S_1 be a side of D and F_1 be a face contained in F_1. Let S_1' be the other side containing F_1. Let S_2 be the side paired to S_1' by g_1 and $F_2 = g_1(F_1)$. Again, there exists only one other side containing F_2, which we call F_2'. We define recursively g_i and F_i, so that $g_{i-1} \circ \cdots \circ g_1(F_1) = F_i$.

Definition 2.3.5. ***Cyclic condition***
Cyclic is the condition that for each pair (F_1, S_1) (a face contained in a side), there exists $n \geq 1$ such that, in the construction in the previous paragraph, $g_n \circ \cdots \circ g_1(S_1) = S_1$ and $g_n \circ \cdots \circ g_1$ restricted to F_1 is the identity. Moreover, writing $g = g_n \circ \cdots \circ g_1$, there exists a positive integer m such that $g^m = 1$ and

$$g_1^{-1}(D) \cup (g_2 \circ g_1)^{-1}(D) \cup \cdots \cup g^{-1}(D) \cup$$

$$(g_1 \circ g)^{-1}(D) \cup (g_2 \circ g_1 \circ g)^{-1}(D) \cup \cdots \cup (g^2)^{-1}(D)$$

$$\vdots$$

$$(g_1 \circ g^{m-1})^{-1}(D) \cup (g_2 \circ g_1 \circ g^{m-1})^{-1}(D) \cup \cdots \cup (g^m)^{-1}(D)$$

is a cover of a closed neighborhood of the interior of F_1 by D and its images.

The relation $g^m = (g_n \circ \cdots \circ g_1)^m = Id$ is called a ***cycle relation****.*

We now state Poincaré's polyhedron theorem:

Theorem 2.3.6. ***(Poincaré's polyhedron theorem)*** *Let D be a compact Poincaré polyhedron with side-pairing transformations $\Lambda \subset Isom(\mathbf{H}^2_{\mathbb{C}})$ in $\mathbf{H}^2_{\mathbb{C}}$ satisfying the cyclic condition. Let Γ be the group generated by Λ. Then*

- *Γ is a discrete subgroup of $Isom(\mathbf{H}^2_{\mathbb{C}})$,*
- *D is a fundamental domain, and*
- *Γ has a presentation given by*

$$\Gamma = \langle\ \Lambda \mid \textit{reflection relations, cycle relations} \rangle.$$

Chapter 3

A minimal volume arithmetic cusped complex hyperbolic orbifold

This chapter has been published in *Mathematical Proceedings of the Cambridge Philosophical Society* (see reference [Zh11] in the bibliography).

3.1 Introduction

Picard modular groups for $\mathcal{O}_d$, denoted by $PU(2,1,\mathcal{O}_d)$, are the subgroups of $PU(2,1)$ with entries in $\mathcal{O}_d$ where $\mathcal{O}_d$ be the ring of integers in the imaginary quadratic number field $\mathbb{Q}(i\sqrt{d})$. The general family of arithmetic groups $PU(2,1,\mathcal{O}_d)$ gives the simplest lattices known and they are due to Picard [Pic83, Pic84]. In particular, the case of $\mathcal{O}_3 = \mathbb{Z}[\omega]$, where ω is a cube root of unity was treated in [FP06] whose fundamental domain is a 4-simplex with one ideal vertex. A description of the fundamental domain in the case $\mathcal{O}_1 = \mathbb{Z}[i]$ was obtained in [FFP10, FL05, FLa05]. In [FFP10], Falbel, Francsics and Parker describe a fundamental domain for the group $PU(2,1;\mathcal{O}_1)$ and analyze the combinatorics of the fundamental domain to obtain a presentation of the group.

Recently, Stover [Sto10] has studied volumes of Picard modular surfaces. One of his main results is that there are exactly only two of arithmetic cusped complex hyperbolic orbifolds with minimal volume, namely, whose corresponding fundamental groups are the Eisenstein-Picard modular group and its sister. The sister of Eisenstein-Picard modular group $PU(2,1,\mathbb{Z}[\omega])$ was defined by Parker in [Par98]. It is convenient to adopt the following notation for 3×3 complex matrices:

$$\begin{bmatrix} z_{11} & z_{12} & z_{13} \\ z_{21} & z_{22} & z_{23} \\ z_{31} & z_{32} & z_{33} \end{bmatrix}.$$

Following notations as in [Par98], we denote the Eisenstein-Picard modular group by G_1 and its sister by G_2 in this chapter. Let G_2 be the collection of all elements of $PU(\mathbb{Q}(i\sqrt{3}))$ whose entries in the above form have z_{11}, z_{12}, $z_{13}(i\sqrt{3})$, $z_{21}/(i\sqrt{3})$, z_{22}, z_{23}, $z_{31}/(i\sqrt{3})$, $z_{32}/(i\sqrt{3})$, and z_{33} all in $\mathcal{O}_3$. In other words,

(i) $z_{13} = x_{13}/2 + iy_{13}/2\sqrt{3}$, where x_{13} and y_{13} are integers of the same parity;

(ii) $z_{jk} = x_{jk}/2 + i\sqrt{3}y_{jk}/2$ for all other j,k, where x_{jk} and y_{jk} are integers of the same parity;

(iii) x_{21}, x_{31} and x_{32} are all divisible by 3.

By construction, G_1 and G_2 are commensurable. Furthermore, they have a common subgroup $G_1 \cap G_2$ of index 4 in both G_1 and G_2; see [Par98]. As a consequence, one of the main results in [Par98] is as follows:

Theorem 3.1.1. *[Par98] Let G_1 and G_2 be as above. The orbifolds $\mathbf{H}^2_{\mathbb{C}}/G_1$ and $\mathbf{H}^2_{\mathbb{C}}/G_2$ are distinct and have volumes*

$$\mathrm{Vol}(\mathbf{H}^2_{\mathbb{C}}/G_1) = \mathrm{Vol}(\mathbf{H}^2_{\mathbb{C}}/G_2) = \frac{\pi^2}{27}.$$

However, neither Parker nor Stover give an explicit fundamental domain or a presentation for G_2.

The first part of this chapter is devoted to construct an explicit fundamental domain for the action of G_2 on $\mathbf{H}^2_{\mathbb{C}}$. The special feature which simplifies the analysis is that the quotient $\mathbf{H}^2_{\mathbb{C}}/G_2$ has only one cusp. The main idea (inspired by the analogous construction

of G_1 [FP06]) is to obtain a fundamental domain from the Ford domain instead of the Dirichlet domain. The Ford domain is the intersection of the exteriors of isometric spheres of all elements not fixing infinity, that is also a fundamental domain for the coset space of $(G_2)_\infty$ (the stabilizer of the point at infinity). In order to construct a fundamental domain, we must intersect the Ford domain with a suitable fundamental domain for $(G_2)_\infty$. Using the complex hyperbolic version of Poincaré's polyhedron theorem, we show their intersection gives a fundamental domain, from which we obtain a presentation. The main difference between the fundamental domain we construct and the one for $PU(2,1,\mathbb{Z}[\omega])$ is that our domain comprises two compact sides which are paired.

The second part of this chapter is devoted to use a form of Gauss-Bonnet theorem to calculate the volume of the orbifold $\mathbf{H}^2_{\mathbb{C}}/G_2$, which is the known value of the volume of the quotient orbifold (see Theorem 3.1.1). In order to do this we have to analyze the stabilizers and orbits of all n-dimensional faces of our fundamental polyhedron.

3.2 The group G_2

In this section we describe some general features of the group G_2. In particular, we find a set of generators and describe a fundamental domain for the stabilizer of infinity.

Let ω denote the cube root of unity $(-1+i\sqrt{3})/2$. The group G_2 comprises all matrices in $U(2,1)$ (preserving the second Hermitian form) of the form

$$A = \begin{bmatrix} a & b & ci/\sqrt{3} \\ di\sqrt{3} & e & f \\ gi\sqrt{3} & hi\sqrt{3} & j \end{bmatrix}$$

where $a, b, \cdots, h, j$ are all elements of $\mathbb{Z}[\omega]$.

3.2.1 The stabilizer $(G_2)_\infty$ of q_∞

First, we want to analyze $(G_2)_\infty$, the stabilizer of q_∞. Every element of $(G_2)_\infty$ is upper triangular, and its diagonal entries are units in $\mathbb{Z}[\omega]$. Therefore, $(G_2)_\infty$ contains no dilations and so is a subgroup of $Isom(\mathcal{N})$; and fits into the exact sequence (1.5) as

$$0 \longrightarrow \mathbb{R} \cap (G_2)_\infty \longrightarrow (G_2)_\infty \xrightarrow{\Pi_*} \Pi_*((G_2)_\infty) \longrightarrow 1.$$

We can find explicitly the kernel and image of $(G_2)_\infty$ as in [FP06].

Proposition 3.2.1. *The stabilizer $(G_2)_\infty$ of q_∞ in G_2 satisfies*

$$0 \longrightarrow \frac{2}{\sqrt{3}}\mathbb{Z} \longrightarrow (G_2)_\infty \xrightarrow{\Pi_*} \triangle(2,3,6) \longrightarrow 1,$$

where $\triangle(2,3,6)$ denotes the triangle group comprising orientation-preserving symmetries of $\mathbb{Z}[\omega]$.

Proof. From the explicit construction (1.6) of Π_*, we see that for $A \in (G_2)_\infty$,

$$\Pi_*(A) = \begin{bmatrix} (-\omega)^n & z_0 \\ 0 & 1 \end{bmatrix},$$

where $z_0 \in \mathbb{Z}[\omega]$. It follows from Proposition 3.1 of [FP06] that $\Pi_*((G_2)_\infty)$ is generated by $R_*(z) = -\overline{\omega}z$ and $S_*(z) = -z + 1$, which is the triangle group $\triangle(2,3,6) = \{R_*, S_* |\ R_*^6 = S_*^2 = (R_*S_*)^3 = 1\}$.

Likewise, the kernel of Π_* is easily seen to consist of those vertical translations in $(G_2)_\infty$, that is , Heisenberg translation by $(0, 2n/\sqrt{3}) \in \mathcal{N}$ for $n \in \mathbb{Z}$. □

The following proposition gives the generators of $(G_2)_\infty$.

Proposition 3.2.2. *$(G_2)_\infty$ is generated by*

$$R = \begin{bmatrix} 1 & 0 & 0 \\ 0 & -\overline{\omega} & 0 \\ 0 & 0 & 1 \end{bmatrix}, \quad S = \begin{bmatrix} 1 & 1 & -\overline{\omega}i/\sqrt{3} \\ 0 & -1 & 1 \\ 0 & 0 & 1 \end{bmatrix}.$$

Proof. The triangle group $\triangle(2,3,6)$ is generated by

$$\Pi_*(R) = R_* : z \longrightarrow -\overline{\omega}z, \qquad \Pi_*(S) = S_* : z \longrightarrow -z + 1.$$

Hence we only need to show that R and S generate $\mathbb{R} \cap (G_2)_\infty \simeq \frac{2}{\sqrt{3}}\mathbb{Z}$. Observe that

$$S^2 = \begin{bmatrix} 1 & 0 & i/\sqrt{3} \\ 0 & 1 & 0 \\ 0 & 0 & 1 \end{bmatrix} = T, \tag{3.1}$$

which is precisely the generator of $\frac{2}{\sqrt{3}}\mathbb{Z} \cap (G_2)_\infty$. Therefore $(G_2)_\infty$ is generated by R and S. □

We first construct a fundamental domain for the parabolic subgroup $(G_2)_\infty$ acting on the Heisenberg group. We want to describe the action of R and S on each horosphere. Recall that complex hyperbolic space can be parameterized in horospherical coordinates $(z,t,u) \in \mathbb{C} \times \mathbb{R} \times \mathbb{R}^+$ by:

$$(z,t,u) \longrightarrow \begin{bmatrix} (-|z|^2 - u + it)/2 \\ z \\ 1 \end{bmatrix}.$$

Then, using the matrices of R and S, we obtain the following action of R,

$$\begin{bmatrix} 1 & 0 & 0 \\ 0 & -\overline{\omega} & 0 \\ 0 & 0 & 1 \end{bmatrix} \begin{bmatrix} (-|z|^2 - u + it)/2 \\ z \\ 1 \end{bmatrix} = \begin{bmatrix} (-|z|^2 - u + it)/2 \\ -\overline{\omega}z \\ 1 \end{bmatrix}$$

and S,

$$\begin{aligned} &\begin{bmatrix} 1 & 1 & -\overline{\omega}i/\sqrt{3} \\ 0 & -1 & 1 \\ 0 & 0 & 1 \end{bmatrix} \begin{bmatrix} (-|z|^2 - u + it)/2 \\ z \\ 1 \end{bmatrix} \\ &= \begin{bmatrix} (-|z|^2 - u + it)/2 + z - \overline{\omega}i/\sqrt{3} \\ -z + 1 \\ 1 \end{bmatrix} \\ &= \begin{bmatrix} \left(-|-z+1|^2 - u + i\left[t + 2\Im(z) + 1/\sqrt{3}\right]\right)/2 \\ -z + 1 \\ 1 \end{bmatrix}. \end{aligned}$$

We also introduce two elliptic elements fixing q_∞ used in later:

$$RS^{-1} = \begin{bmatrix} 1 & 1 & \omega i/\sqrt{3} \\ 0 & \overline{\omega} & 1 \\ 0 & 0 & 1 \end{bmatrix} \quad \text{and} \quad R^{-1}S = \begin{bmatrix} 1 & 1 & -\overline{\omega} i/\sqrt{3} \\ 0 & \omega & -\omega \\ 0 & 0 & 1 \end{bmatrix}. \tag{3.2}$$

Therefore, we have the properties of those matrices:

(i) R has order 6 and rotates the complex line spanned by 0 and ∞ by $\pi/3$, that is, it acts on horospherical coordinates by

$$R : (z, t, u) \longmapsto (-\overline{\omega} z, t, u).$$

(ii) T is the shortest vertical translation. Its action on horospherical coordinates is given by

$$T : (z, t, u) \longmapsto (z, t + 2/\sqrt{3}, u).$$

(iii) S has a screw parabolic map with axis the complex line through $z = 1/2$. It acts on horospherical coordinates by

$$S : (z, t, u) \longmapsto (-z + 1, t + 2\Im(z) + 1/\sqrt{3}, u)$$

(iv) RS^{-1} has order 3 and rotates the complex line through $z = 1/2 + i/2\sqrt{3}$ by $2\pi/3$. It acts on horospherical coordinates by

$$RS^{-1} : (z, t, u) \longmapsto (\overline{\omega} z - \overline{\omega}, t + 2\Im(\omega z) - 1/\sqrt{3}, u).$$

(v) $R^{-1}S$ also has order 3 and rotates the complex line through $z = 1/2 - i/2\sqrt{3}$ by $2\pi/3$. It acts on horospherical coordinates by

$$R^{-1}S : (z, t, u) \longmapsto (\omega z - \omega, t + 2\Im(z) + 1/\sqrt{3}, u).$$

These actions preserve each horosphere, that is, the set of points where u is constant. Thus we may drop the dependence on u, and we obtain the action on $\mathcal{N} = \mathbb{C} \times \mathbb{R}$.

We now construct a fundamental domain for the action of $(G_2)_\infty$ on $\mathcal{N}$. We know that $\Pi_*((G_2)_\infty = \triangle(2, 3, 6)$ is a triangle group of $\mathbb{Z}[\omega]$. A fundamental domain for this group is the triangle in $\mathbb{C}$ with vertices at $0, 1/2 - i/2\sqrt{3}$ and $1/2 + i/2\sqrt{3}$; see Figure 3.1. Side pairing maps are given by

$$R_* = \begin{bmatrix} -\overline{\omega} & 0 \\ 0 & 1 \end{bmatrix}, \qquad S_* = \begin{bmatrix} -1 & 1 \\ 0 & 1 \end{bmatrix}.$$

The first of these is a rotation of order 6 fixing 0 and the second is a rotation of order 2 fixing 1/2.

A fundamental domain for $(G_2)_\infty$ can be constructed by the intersection of preimages of this triangle under vertical projection Π and a fundamental domain for $\ker(\Pi_*)$. The inverse image of the triangle under Π is an infinite prism. The kernel of Π_* is the infinite cycle group generated by T, the vertical translation by $(0, 2/\sqrt{3})$. So a fundamental domain for this group is the set of points where $-1/\sqrt{3} < t < 1/\sqrt{3}$. Hence a fundamental

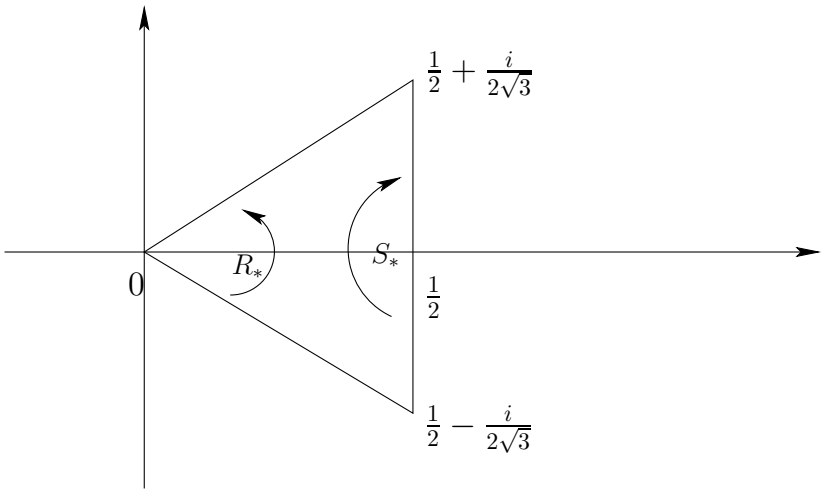

FIGURE 3.1: Fundamental domain for $\Delta(2,3,6)$ in $\mathbb{C}$. The map R_* rotates by $\pi/3$ about the origin and the map S_* rotates by π about $1/2$.

domain for $(G_2)_\infty$ is the prism in $\mathcal{N}$ with vertices at $(0, \pm 1/\sqrt{3})$, $(1/2 - i/2\sqrt{3}, \pm 1/\sqrt{3})$, $(1/2+i/2\sqrt{3}, \pm 1/\sqrt{3})$; see Figure 3.2. The side pairings act on points $(z,t) \in \mathcal{N}$ as follows:

$$\begin{aligned} R(z,t) &= (-\overline{\omega}z, t), \\ S(z,t) &= (-z+1, t+2\Im(z)+1/\sqrt{3}), \\ T(z,t) &= (z, t+2/\sqrt{3}). \end{aligned}$$

We can see the action of S on the triangle $(\hat{z}_1^+, \hat{z}_1^-, \hat{z}_2^-)$ is the composition of a reflection on the edge $\hat{z}_1^+\hat{z}_2^-$ and a clockwise rotation. We summarize the side-pairing maps by acting on the vertices of the prism:

$$\begin{aligned} R &: (\hat{z}_0^+, \hat{z}_0^-, \hat{z}_1^-, \hat{z}_1^+) \longmapsto (\hat{z}_0^+, \hat{z}_0^-, \hat{z}_2^-, \hat{z}_2^+), \\ S &: (\hat{z}_1^+, \hat{z}_1^-, \hat{z}_2^-) \longmapsto (\hat{z}_2^+, \hat{z}_2^-, \hat{z}_1^+), \\ T &: (\hat{z}_0^-, \hat{z}_1^-, \hat{z}_2^-) \longmapsto (\hat{z}_0^+, \hat{z}_1^+, \hat{z}_2^+). \end{aligned}$$

Denoting all the edges by the ordered pairs of their endpoints, we can also consider the edge cycles given by these side-pairings are

$$\begin{aligned} (\hat{z}_0^+, \hat{z}_0^-) &\xrightarrow{R} (\hat{z}_0^+, \hat{z}_0^-), \\ (\hat{z}_1^+, \hat{z}_1^-) &\xrightarrow{S} (\hat{z}_2^+, \hat{z}_2^-) \xrightarrow{R^{-1}} (\hat{z}_1^+, \hat{z}_1^-), \\ (\hat{z}_1^-, \hat{z}_2^-) &\xrightarrow{S} (\hat{z}_2^-, \hat{z}_1^+) \xrightarrow{S} (\hat{z}_1^+, \hat{z}_2^+) \xrightarrow{T^{-1}} (\hat{z}_1^-, \hat{z}_2^-), \\ (\hat{z}_0^-, \hat{z}_1^-) &\xrightarrow{R} (\hat{z}_0^-, \hat{z}_2^-) \xrightarrow{T} (\hat{z}_0^+, \hat{z}_2^+) \xrightarrow{R^{-1}} (\hat{z}_0^+, \hat{z}_1^+) \xrightarrow{T^{-1}} (\hat{z}_0^-, \hat{z}_1^-). \end{aligned}$$

This has used all the edges of fundamental domain. The first of these cycles gives the relation $R^6 = I$, the second gives the relation $(R^{-1}S)^3 = I$, the third gives the relation $S^2 = T$ and the last gives the relation $T^{-1}R^{-1}TR = I$. These relations can directly follow from the properties of matrices (3.1) and (3.2).

This enables us to give the following proposition.

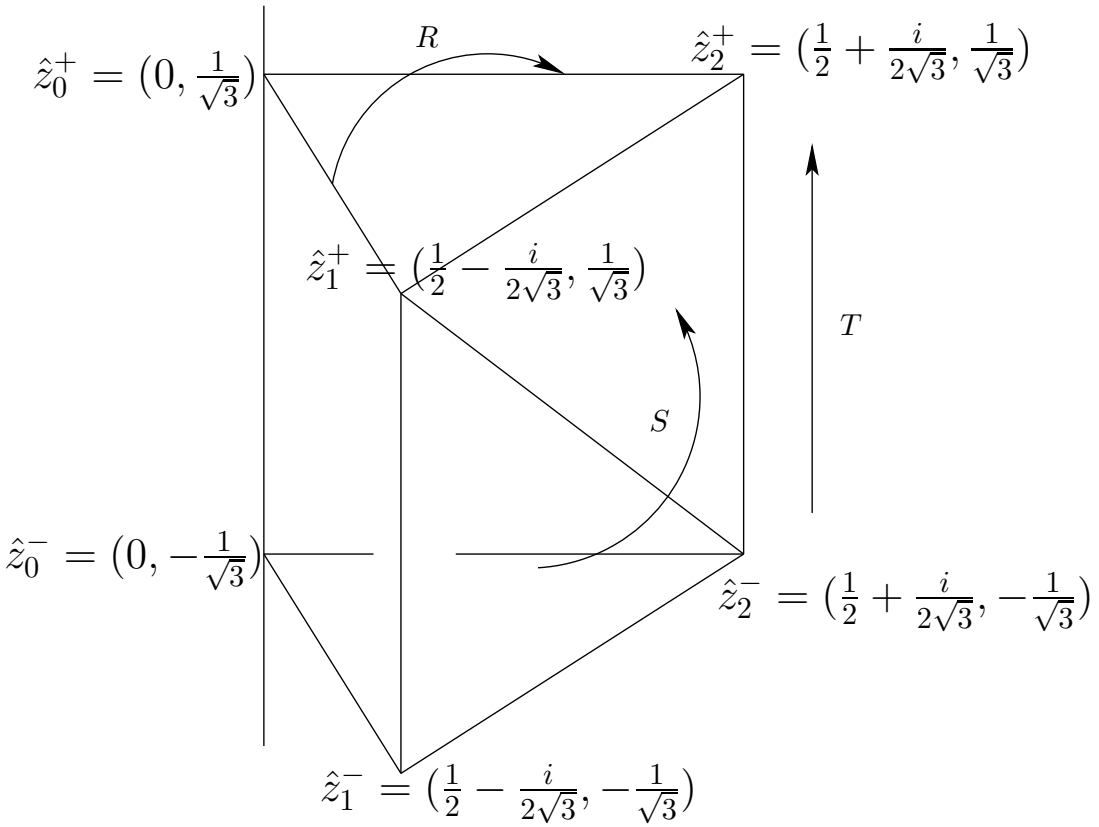

FIGURE 3.2: Fundamental domain for $(G_2)_\infty$ in the Heisenberg group: the map R rotates through $\pi/3$ about $z = 0$; the map S is a screw Heisenberg rotation through π about $z = 1/2$ followed by an upward vertical translation by $1/\sqrt{3}$; the map T translates along t-axis by $2/\sqrt{3}$.

Proposition 3.2.3. *A fundamental domain for $(G_2)_\infty$ is the prism with vertices (in Heisenberg coordinates) $(z,t) = (0, \pm 1/\sqrt{3})$, $(1/2 - i/2\sqrt{3}, \pm 1/\sqrt{3})$, $(1/2 + i/2\sqrt{3}, \pm 1/\sqrt{3})$.*

A presentation is given by

$$(G_2)_\infty = \langle R, S, T |\ R^6 = (R^{-1}S)^3 = [R,T] = \mathit{identity},\ S^2 = T \rangle.$$

3.2.2 Generators of G_2

First consider the map

$$I_1 = \begin{bmatrix} 0 & 0 & i/\sqrt{3} \\ 0 & -\omega & 0 \\ i\sqrt{3} & 0 & 0 \end{bmatrix},$$

it has the isometric sphere $\mathcal{S}_0$ given in horospherical coordinates by

$$\mathcal{S}_0 = \{(z,t,u) : \left| |z|^2 + u - it \right| = 2/\sqrt{3}\} \tag{3.3}$$

or in geographical coordinates $\mathcal{S}_0$ is parameterized by

$$\left\{ \begin{bmatrix} -e^{i\theta}/\sqrt{3} \\ re^{i\alpha+i\theta/2} \\ 1 \end{bmatrix} : \theta \in [-\pi/2, \pi/2], \alpha \in [-\pi/2, \pi/2), r \in \left[-\sqrt{\frac{2\cos\theta}{\sqrt{3}}}, \sqrt{\frac{2\cos\theta}{\sqrt{3}}} \right] \right\}. \quad (3.4)$$

Observe that the action of I_1 on $\mathcal{S}_0$ is given by

$$\begin{bmatrix} 0 & 0 & i/\sqrt{3} \\ 0 & -\omega & 0 \\ i\sqrt{3} & 0 & 0 \end{bmatrix} \begin{bmatrix} -e^{i\theta}/\sqrt{3} \\ re^{i\alpha+i\theta/2} \\ 1 \end{bmatrix} = \begin{bmatrix} i/\sqrt{3} \\ re^{i\alpha+i\theta/2-i\pi/3} \\ -ie^{i\theta} \end{bmatrix} = -ie^{i\theta} \begin{bmatrix} -e^{-i\theta}/\sqrt{3} \\ re^{i(\alpha+\pi/6)-i\theta/2} \\ 1 \end{bmatrix}$$

We see that I_1 maps $\mathcal{S}_0$ to itself, sending the point with coordinates (r, θ, α) to the point with coordinates $(r, -\theta, \alpha + \pi/6)$ when $-\pi/2 \leq \alpha < \pi/3$ or the point with coordinates $(-r, -\theta, \alpha - 5\pi/6)$ when $\pi/3 \leq \alpha < \pi/2$. Therefore I_1 is an elliptic element of order 12. Moreover, I_1 swaps the inside and the outside of $\mathcal{S}_0$.

Proposition 3.2.4. *Let $(G_2)_\infty$ be the stabilizer of q_∞ in G_2. Then there exists a fundamental domain for the action of $(G_2)_\infty$ on $\partial \boldsymbol{H}^2_{\mathbb{C}}$ whose interior lies inside the ball in $\partial \boldsymbol{H}^2_{\mathbb{C}}$ whose boundary is $\partial\mathcal{S}_0$.*

Proof. The same results are proved for the Eisenstein-Picard group in [FP06] and Gauss-Picard group in [FFP10]. As in the proof of Proposition 3.2.3, the prism with vertices (in Heisenberg coordinates) $(0, \pm 1/\sqrt{3})$, $(1/2 - i/2\sqrt{3}, \pm 1/\sqrt{3})$, $(1/2 + i/2\sqrt{3}, \pm 1/\sqrt{3})$ is a fundamental domain for $(G_2)_\infty$. All these vertices lie inside $\partial\mathcal{S}_0$ in Heisenberg group. Since $\partial\mathcal{S}_0$ is affinely convex (c.f. Lemma 1.4.7), the whole prism lies inside $\partial\mathcal{S}_0$. □

We now show that adjoining I_1 to $(G_2)_\infty$ gives the full group G_2. In order to prove that, we should show that $\langle R, S, T, I_1 \rangle$ has only one cusp. The fact that G_2 has only one cusp is already known we refer the reader to [Par98].

Proposition 3.2.5. *The group G_2 is generated by T, R, S and I_1.*

Proof. (cf. [FP06, FFP10]) The same result for the Eisenstein-Picard group and Gauss-Picard group. Since a fundamental domain for $\langle R, S, T, I_1 \rangle$ lies outside the isometric sphere of I_1 and inside the fundamental domain for $\langle R, S, T \rangle$. The Proposition 3.2.4 implies $\langle R, S, T, I_1 \rangle$ has only one cusp. The fact that G_2 has the same cusp as the group generated by T, R, S and I_1 implies that they are the same. □

3.3 Construction of a prism

In this section, we will construct a prism $\mathbf{P}_0$ by the intersection of isometric spheres. In fact, the prism $\mathbf{P}_0$ is the compact part of the boundary of a fundamental domain for G_2. To have a global view of the prism we refer the readers to Figures 3.3 and 3.6. The prism contains two compact sides of the fundamental domain and the other sides are cones based at the faces of this prism with cone point the ideal vertex.

We begin by investigating the intersection of $\mathcal{S}_0$ with its neighboring isometric spheres.

3.3.1 The intersection of $\mathcal{S}_0$ and its neighbors

Here we will use some isometric spheres and their intersections to define the compact sides. The bisectors we need are the following:

$$\mathcal{S}_0,\ T(\mathcal{S}_0),\ T^{-1}(\mathcal{S}_0),\ S(\mathcal{S}_0),\ S^{-1}(\mathcal{S}_0),\ RS^{-1}(\mathcal{S}_0),\ R^{-1}S(\mathcal{S}_0)$$

which are, respectively, the isometric spheres of

$$I_1,\ \ TI_1T^{-1},\ \ T^{-1}I_1T,\ \ SI_1S^{-1},\ \ S^{-1}I_1S,\ \ RS^{-1}I_1SR^{-1},\ \ R^{-1}SI_1S^{-1}R.$$

In particular, it suffices to determine

$$T^{\pm}(\mathcal{S}_0)\cap\mathcal{S}_0,\quad S^{\pm}(\mathcal{S}_0)\cap\mathcal{S}_0.$$

The other intersections are easily obtained from these. For example,

$$R^{-1}S(\mathcal{S}_0)\cap\mathcal{S}_0 = R^{-1}(S(\mathcal{S}_0)\cap\mathcal{S}_0).$$

We need to investigate the intersection of these bisectors with $\mathcal{S}_0$. A direct computation shows that $T(\mathcal{S}_0), T^{-1}(\mathcal{S}_0), S(\mathcal{S}_0), S^{-1}(\mathcal{S}_0)$ are given by

$$T(\mathcal{S}_0) = \left\{(z,t,u) : \left|\ |z|^2+u-it+2i/\sqrt{3}\right| = 2/\sqrt{3}\right\}, \tag{3.5}$$

$$T^{-1}(\mathcal{S}_0) = \left\{(z,t,u) : \left|\ |z|^2+u-it-2i/\sqrt{3}\right| = 2/\sqrt{3}\right\}, \tag{3.6}$$

$$S(\mathcal{S}_0) = \left\{(z,t,u) : \left|\ |z|^2-2z+u+1-it+i/\sqrt{3}\right| = 2/\sqrt{3}\right\}, \tag{3.7}$$

$$S^{-1}(\mathcal{S}_0) = \left\{(z,t,u) : \left|\ |z|^2-2z+u+1-it-i/\sqrt{3}\right| = 2/\sqrt{3}\right\}. \tag{3.8}$$

We start to describe the intersection of these bisectors. Note that $T^{\pm}$ and $S^{\pm}$ will be denoted by T, T^{-1} and S, S^{-1} respectively in Lemmas 3.3.1 and 3.3.2.

Lemma 3.3.1. *In geographical coordinates, a point (r,θ,α) of $\mathcal{S}_0$ with $\theta\in[-\pi/6,\pi/6]$ does not intersect the interior of $T(\mathcal{S}_0)$ and $T^{-1}(\mathcal{S}_0)$. Furthermore, $T^{\pm}(\mathcal{S}_0)\cap\mathcal{S}_0$ is a common slice of the bisectors $T^{\pm}(\mathcal{S}_0)$ and $\mathcal{S}_0$ which corresponds to $\theta=\mp\pi/6$.*

Proof. Recall that a point of $\mathcal{S}_0$ is given by

$$\begin{bmatrix} -e^{i\theta}/\sqrt{3} \\ re^{i\alpha+i\theta/2} \\ 1 \end{bmatrix}.$$

In horospherical coordinates, it is given by $\left(re^{i\alpha+i\theta/2}, -2\sin\theta/\sqrt{3}, 2\cos\theta/\sqrt{3}-r^2\right)$, where $\theta\in[-\pi/2,\pi/2]$, $\alpha\in[-\pi/2,\pi/2)$, $r\in\left[-\sqrt{(2\cos\theta)/\sqrt{3}},\sqrt{(2\cos\theta)/\sqrt{3}}\right]$. Therefore, a point of $\mathcal{S}_0$ does not intersect the interior of $T(\mathcal{S}_0)$ if and only if

$$\left|r^2+\frac{2}{\sqrt{3}}\cos\theta-r^2+i\frac{2}{\sqrt{3}}\sin\theta+i\frac{2}{\sqrt{3}}\right|\geq\frac{2}{\sqrt{3}}.$$

A simple computation implies that $\sin\theta\geq -1/2$, i.e. $\theta\in[-\pi/6,\pi/2]$. Similarly, a point of $\mathcal{S}_0$ does not intersect the interior of $T^{-1}(\mathcal{S}_0)$ if and only if $\theta\in[-\pi/2,\pi/6]$. Therefore, $T^{\pm}(\mathcal{S}_0)\cap\mathcal{S}_0$ are respectively the slices $\theta=\mp\pi/6$. This completes the result. □

Lemma 3.3.2. *$S^{\pm}(\mathcal{S}_0) \cap \mathcal{S}_0$ is a topological disk.*

Proof. In fact in horospherical coordinates (z, t, u) of the bisector $\mathcal{S}_0$, the intersection is foliated by arcs of circles, each contained in a slice of height t. We show it explicitly as follows. Recall that the coordinates (z, t), with that $|z|^4 + t^2 < 4/3$, parameterize the bisector $\mathcal{S}_0$ whose equation, in horospherical coordinates, are $(|z|^2 + u)^2 + t^2 = 4/3$. As vectors in $\mathbb{C}^{2,1}$ we obtain therefore

$$\begin{bmatrix} (-|z|^2 - u + it)/2 \\ z \\ 1 \end{bmatrix} = \begin{bmatrix} (-\sqrt{4/3 - t^2} + it)/2 \\ z \\ 1 \end{bmatrix}.$$

Then we have

$$\begin{aligned} & S \cdot \begin{bmatrix} (-\sqrt{4/3 - t^2} + it)/2 \\ z \\ 1 \end{bmatrix} \\ &= \begin{bmatrix} 1 & 1 & -\overline{\omega}i/\sqrt{3} \\ 0 & -1 & 1 \\ 0 & 0 & 1 \end{bmatrix} \begin{bmatrix} (-\sqrt{4/3 - t^2} + it)/2 \\ z \\ 1 \end{bmatrix} \\ &= \begin{bmatrix} (-\sqrt{4/3 - t^2} + it)/2 + z - \overline{\omega}i/\sqrt{3} \\ z \\ 1 \end{bmatrix}. \end{aligned}$$

The condition that such a point lies in $\mathcal{S}_0$ is that the first entry has absolute value $1/\sqrt{3}$, that is,

$$\left| \frac{-\sqrt{4/3 - t^2} + it}{2} + z - \frac{\overline{\omega}i}{\sqrt{3}} \right| = \frac{1}{\sqrt{3}}.$$

For each fixed height (with $-2/\sqrt{3} < t < 2/\sqrt{3}$), the intersection lies on the circle centered at $(\sqrt{4/3 - t^2} - it)/2 + \overline{\omega}i/\sqrt{3}$ with radius $1/\sqrt{3}$. The condition for the existence of an intersection between this circle and the slice of height t is that the sum of the radii of these two circles, $1/\sqrt{3} + (4/3 - t^2)^{1/4}$, be greater than the distance between the centers, that is, $|(\sqrt{4/3 - t^2} - it)/2 + \overline{\omega}i/\sqrt{3}|$. That gives the equation

$$\left[\frac{1}{\sqrt{3}} + \left(\frac{4}{3} - t^2 \right)^{1/4} \right]^2 > \left| \frac{\overline{\omega}i}{\sqrt{3}} + \frac{\sqrt{4/3 - t^2} - it}{2} \right|^2$$

whose solution is

$$-\frac{2}{\sqrt{3}} < t < \frac{(291\sqrt{3} + 504)^{1/3}}{3} + \frac{1}{(291\sqrt{3} + 504)^{1/3}} - \frac{4\sqrt{3}}{3} < \frac{2}{\sqrt{3}}.$$

This shows that the intersection is foliated by a one-parameter family of arcs of circles and therefore is a topological disc. Observe that $S^{-1}(\mathcal{S}_0) \cap \mathcal{S}_0 = S^{-1}(\mathcal{S}_0 \cap S(\mathcal{S}_0)$ implies that is also a topological disk. □

We describe this intersection in more details below.

3.3.2 The vertices

In this section we define the vertices of the prism, all of them will correspond to vertices of the fundamental domain for $(G_2)_\infty$ in the Heisenberg group. In fact, the vertical projection $(z,t,u) \to (z,t)$ which projects the geodesic passing through (z,t,u) to q_∞ to its end point (z,t) maps the vertices of this prism to the vertices of fundamental domain for $(G_2)_\infty$.

We start to define the vertices of the prism as points of $\mathbb{C}^{2,1}$ and discuss their horospherical and geographical coordinates. There are three vertices lying on the common slice of $\mathcal{S}_0$ and $T(\mathcal{S}_0)$, which are denoted by $z_j^+, j = 0,1,2$. Let z_0^+ define the intersection of the spine of $\mathcal{S}_0$ and the common slice $\theta = -\pi/6$ (that is height $t = 1/\sqrt{3}$ in the Heisenberg group $\mathcal{N}$). Other two vertices are the intersection of four bisectors, that are given by

$$\begin{aligned} z_1^+ &= \mathcal{S}_0 \cap T(\mathcal{S}_0) \cap S^{-1}(\mathcal{S}_0) \cap R^{-1}S(\mathcal{S}_0), \\ z_2^+ &= \mathcal{S}_0 \cap T(\mathcal{S}_0) \cap S(\mathcal{S}_0) \cap RS^{-1}(\mathcal{S}_0). \end{aligned}$$

Similarly, three vertices lie on the common slice of $\mathcal{S}_0$ and $T^{-1}(\mathcal{S}_0)$, which are denoted by $z_j^-, j = 0,1,2$. Let z_0^- define the intersection of the spine of $\mathcal{S}_0$ and the common slice $\theta = \pi/6$ (that is height $t = -1/\sqrt{3}$ in $\mathcal{N}$). Other two vertices are given by

$$\begin{aligned} z_1^- &= \mathcal{S}_0 \cap T^{-1}(\mathcal{S}_0) \cap S^{-1}(\mathcal{S}_0) \cap R^{-1}S(\mathcal{S}_0), \\ z_2^- &= \mathcal{S}_0 \cap T^{-1}(\mathcal{S}_0) \cap S(\mathcal{S}_0) \cap RS^{-1}(\mathcal{S}_0). \end{aligned}$$

We now list all the vertices as points of $\mathbb{C}^{2,1}$:
The vertices on the common slice of $\mathcal{S}_0$ and $T(\mathcal{S}_0)$ are

$$z_0^+ = \begin{bmatrix} -\frac{1}{2} + \frac{i}{2\sqrt{3}} \\ 0 \\ 1 \end{bmatrix}, \quad z_1^+ = \begin{bmatrix} -\frac{1}{2} + \frac{i}{2\sqrt{3}} \\ \frac{1}{2} - \frac{i}{2\sqrt{3}} \\ 1 \end{bmatrix}, \quad z_2^+ = \begin{bmatrix} -\frac{1}{2} + \frac{i}{2\sqrt{3}} \\ \frac{1}{2} + \frac{i}{2\sqrt{3}} \\ 1 \end{bmatrix}.$$

The vertices on the common slice of $\mathcal{S}_0$ and $T^{-1}(\mathcal{S}_0)$ are

$$z_0^- = \begin{bmatrix} -\frac{1}{2} - \frac{i}{2\sqrt{3}} \\ 0 \\ 1 \end{bmatrix}, \quad z_1^- = \begin{bmatrix} -\frac{1}{2} - \frac{i}{2\sqrt{3}} \\ \frac{1}{2} - \frac{i}{2\sqrt{3}} \\ 1 \end{bmatrix}, \quad z_2^- = \begin{bmatrix} -\frac{1}{2} - \frac{i}{2\sqrt{3}} \\ \frac{1}{2} + \frac{i}{2\sqrt{3}} \\ 1 \end{bmatrix}.$$

In horospherical and geographical coordinates of these vertices $z_j^\pm$ points are given by

	z	t	u	r	θ	α
z_0^+	0	$1/\sqrt{3}$	1	0	$-\pi/6$	
z_1^+	$1/2 - i/2\sqrt{3}$	$1/\sqrt{3}$	$2/3$	$1/\sqrt{3}$	$-\pi/6$	$-\pi/12$
z_2^+	$1/2 + i/2\sqrt{3}$	$1/\sqrt{3}$	$2/3$	$1/\sqrt{3}$	$-\pi/6$	$\pi/4$
z_0^-	0	$-1/\sqrt{3}$	1	0	$\pi/6$	
z_1^-	$1/2 - i/2\sqrt{3}$	$-1/\sqrt{3}$	$2/3$	$1/\sqrt{3}$	$\pi/6$	$-\pi/4$
z_2^-	$1/2 + i/2\sqrt{3}$	$-1/\sqrt{3}$	$2/3$	$1/\sqrt{3}$	$\pi/6$	$\pi/12$

By computation we verify that $z_1^+, z_2^- \in S(\mathcal{S}_0) \cap S^{-1}(\mathcal{S}_0)$.

3.3.3 The edges

We first investigate the intersection of $\mathcal{S}_0$ and $S(\mathcal{S}_0), S^{-1}(\mathcal{S}_0)$ more closely than before. We compute it explicitly in geographical coordinates and show the following result.

Lemma 3.3.3. *A point (r,θ,α) of $\mathcal{S}_0$ in geographical coordinates with $-\pi/12 \leq \alpha \leq \pi/4$ does not intersect the interior of $S(\mathcal{S}_0)$, provided that*

$$r \leq \frac{1}{\sqrt{3}}\left[2\cos\left(\frac{\theta}{2}-\frac{\pi}{12}\right)\cos\left(\alpha-\frac{\pi}{12}\right)-\sqrt{1-4\cos^2\left(\frac{\theta}{2}-\frac{\pi}{12}\right)\sin^2\left(\alpha-\frac{\pi}{12}\right)}\right]$$

with equality if and only if the point lies in $\mathcal{S}_0 \cap S(\mathcal{S}_0)$.

Proof. A point of $\mathbf{H}^2_{\mathbb{C}}$ does not lie in the interior of $S(\mathcal{S}_0)$ (cf. 3.7) if satisfies

$$\frac{2}{\sqrt{3}} \leq \left||z|^2-2z+u+1-it+\frac{i}{\sqrt{3}}\right|. \tag{3.9}$$

If such a point lies on $\mathcal{S}_0$, we can write it in geographical coordinates. Substituting in (3.9) gives

$$1 \leq \left|-\sqrt{3}re^{i(\alpha+\theta/2)}+e^{i\theta}+e^{i\pi/6}\right| = \left|\sqrt{3}re^{i(\alpha-\pi/12)}-2\cos\left(\frac{\theta}{2}-\frac{\pi}{12}\right)\right|. \tag{3.10}$$

We have equality in (3.10) if and only if the point lies in $\mathcal{S}_0 \cap S(\mathcal{S}_0)$. Expanding out the right-hand side of (3.10), we see that is equivalent to

$$3r^2-4\sqrt{3}r\cos\left(\frac{\theta}{2}-\frac{\pi}{12}\right)\cos\left(\alpha-\frac{\pi}{12}\right)+4\cos^2\left(\frac{\theta}{2}-\frac{\pi}{12}\right)-1 \geq 0. \tag{3.11}$$

By solving this inequality, we know that all points of $\mathcal{S}_0$ do not intersect the interior of $S(\mathcal{S}_0)$ if satisfy with

$$r \leq \frac{1}{\sqrt{3}}\left[2\cos\left(\frac{\theta}{2}-\frac{\pi}{12}\right)\cos\left(\alpha-\frac{\pi}{12}\right)-\sqrt{1-4\cos^2\left(\frac{\theta}{2}-\frac{\pi}{12}\right)\sin^2\left(\alpha-\frac{\pi}{12}\right)}\right]$$

or

$$r \geq \frac{1}{\sqrt{3}}\left[2\cos\left(\frac{\theta}{2}-\frac{\pi}{12}\right)\cos\left(\alpha-\frac{\pi}{12}\right)+\sqrt{1-4\cos^2\left(\frac{\theta}{2}-\frac{\pi}{12}\right)\sin^2\left(\alpha-\frac{\pi}{12}\right)}\right].$$

We claim that the second of these solutions is always greater than $\sqrt{2\cos(\theta)/\sqrt{3}}$ as $-\pi/12 \leq \alpha \leq \pi/4$ and so does not correspond to a point of $\mathcal{S}_0$. In order to see this, observe that $-\pi/12 \leq \alpha \leq \pi/4$ implies $2\cos(\alpha/2-\pi/12) \geq \sqrt{3}$ and $4\sin^2(\alpha-\pi/12) \leq 1$. Thus

$$\begin{aligned}
&\frac{1}{\sqrt{3}}\left[2\cos\left(\frac{\theta}{2}-\frac{\pi}{12}\right)\cos\left(\alpha-\frac{\pi}{12}\right)+\sqrt{1-4\cos^2\left(\frac{\theta}{2}-\frac{\pi}{12}\right)\sin^2\left(\alpha-\frac{\pi}{12}\right)}\right]\\
&\geq \frac{1}{\sqrt{3}}\left[\sqrt{3}\cos\left(\frac{\theta}{2}-\frac{\pi}{12}\right)-\sin\left(\frac{\theta}{2}-\frac{\pi}{12}\right)\right]\\
&= \frac{2}{\sqrt{3}}\cos\left(\frac{\theta}{2}+\frac{\pi}{12}\right)\\
&= \sqrt{\frac{2}{\sqrt{3}}\left[\frac{\cos(\theta+\pi/6)+1}{\sqrt{3}}\right]}\\
&\geq \sqrt{\frac{2\cos\theta}{\sqrt{3}}}.
\end{aligned}$$

In fact,

$$\begin{aligned}\frac{\cos(\theta+\pi/6)+1}{\sqrt{3}}-\cos\theta &= \frac{1}{\sqrt{3}}\left[\frac{\sqrt{3}}{2}\cos\theta-\frac{1}{2}\sin\theta+1-\sqrt{3}\cos\theta\right]\\ &= \frac{1-\sin(\theta+\pi/3)}{\sqrt{3}}\geq 0.\end{aligned}$$

Note that when $\theta=\pi/6$ and $\alpha=\pi/12$ or $\pi/4$, then we have equality in both inequalities above. But in this case $1=4\cos^2(\theta/2-\pi/12)\sin^2(\alpha-\pi/12)$, so the quadratic equation (3.11) has a repeated root. □

Similarly, we can also obtain the following results.

Lemma 3.3.4. *A point (r,θ,α) of $\mathcal{S}_0$ in geographical coordinates with $-\pi/4\leq\alpha\leq\pi/12$ does not intersect the interior of $S^{-1}(\mathcal{S}_0)$, provided that*

$$r\leq\frac{1}{\sqrt{3}}\left[2\cos\left(\frac{\theta}{2}+\frac{\pi}{12}\right)\cos\left(\alpha+\frac{\pi}{12}\right)-\sqrt{1-4\cos^2\left(\frac{\theta}{2}+\frac{\pi}{12}\right)\sin^2\left(\alpha+\frac{\pi}{12}\right)}\right]$$

with equality if and only if the point lies in $\mathcal{S}_0\cap S^{-1}(\mathcal{S}_0)$.

We should understand the intersection of $\mathcal{S}_0$ and $R^{-1}S(\mathcal{S}_0), RS^{-1}(\mathcal{S}_0)$ and observe that $R^{-1}S(\mathcal{S}_0)\cap\mathcal{S}_0=R^{-1}(S(\mathcal{S}_0)\cap\mathcal{S}_0), RS^{-1}(\mathcal{S}_0)\cap\mathcal{S}_0=R(S^{-1}(\mathcal{S}_0)\cap\mathcal{S}_0)$. The following lemmas can be derived from Lemma 3.3.3 and Lemma 3.3.4.

Lemma 3.3.5. *A point (r,θ,α) of $\mathcal{S}_0$ in geographical coordinates with $-\pi/4\leq\alpha\leq-\pi/12$ does not intersect the interior of $R^{-1}S(\mathcal{S}_0)$, provided that*

$$r\leq\frac{1}{\sqrt{3}}\left[2\cos\left(\frac{\theta}{2}-\frac{\pi}{12}\right)\cos\left(\alpha+\frac{\pi}{4}\right)-\sqrt{1-4\cos^2\left(\frac{\theta}{2}-\frac{\pi}{12}\right)\sin^2\left(\alpha+\frac{\pi}{4}\right)}\right]$$

with equality if and only if the point lies in $\mathcal{S}_0\cap R^{-1}S(\mathcal{S}_0)$.

Lemma 3.3.6. *A point (r,θ,α) of $\mathcal{S}_0$ in geographical coordinates with $-\pi/12\leq\alpha\leq5\pi/12$ does not intersect the interior of $RS^{-1}(\mathcal{S}_0)$, provided that*

$$r\leq\frac{1}{\sqrt{3}}\left[2\cos\left(\frac{\theta}{2}+\frac{\pi}{12}\right)\cos(\alpha-\frac{\pi}{4})-\sqrt{1-4\cos^2\left(\frac{\theta}{2}+\frac{\pi}{12}\right)\sin^2\left(\alpha-\frac{\pi}{4}\right)}\right]$$

with equality if and only if the point lies in $\mathcal{S}_0\cap RS^{-1}(\mathcal{S}_0)$.

We can now characterize the edges of the prism not containing q_∞. Some edges are obtained by intersecting three bisectors. Some edges are contained in geodesic arcs by construction. We now list them in the following lemma.

Lemma 3.3.7. *(i) The edge joining z_0^+ and z_0^- is contained in the spine of $\mathcal{S}_0$.*

(ii) The edge joining $z_0^\pm$ and $z_j^\pm$ for $j=1,2$ is a geodesic arc.

(iii) The edge joining z_1^+ and z_2^+ is given by points in geographical coordinates

$$\theta=-\frac{\pi}{6},\quad r=\cos\left(\alpha-\frac{\pi}{12}\right)-\sqrt{\frac{1}{3}-\sin^2\left(\alpha-\frac{\pi}{12}\right)},\quad -\frac{\pi}{12}\leq\alpha\leq\frac{\pi}{4}.$$

(iv) The edge joining z_1^- and z_2^- is given by points in geographical coordinates

$$\theta = \frac{\pi}{6}, \quad r = \cos\left(\alpha + \frac{\pi}{12}\right) - \sqrt{\frac{1}{3} - \sin^2\left(\alpha + \frac{\pi}{12}\right)}, \quad -\frac{\pi}{4} \leq \alpha \leq \frac{\pi}{12}.$$

(v) The edge joining z_1^+ and z_1^- is given by points in geographical coordinates

$$r = \frac{1}{\sqrt{3}}, \quad \alpha = -\frac{\theta}{2} - \frac{\pi}{6} \quad \textit{and} \quad -\frac{\pi}{6} \leq \theta \leq \frac{\pi}{6}.$$

Notice that the complex line $z = re^{i\alpha + i\theta/2} = 1/2 - i/2\sqrt{3}$ contains this edge.

(vi) The edge joining z_2^+ and z_2^- is given by points in geographical coordinates

$$r = \frac{1}{\sqrt{3}}, \quad \alpha = \frac{\pi}{6} - \frac{\theta}{2} \quad \textit{and} \quad -\frac{\pi}{6} \leq \theta \leq \frac{\pi}{6}.$$

Notice that this edge lies in the complex line $z = 1/2 - i/2\sqrt{3}$.

(vii) The edge joining z_1^+ and z_2^- is given by points in geographical coordinates

$$r = \frac{1}{\sqrt{3}}, \quad \alpha = \frac{\theta}{2} \quad \textit{and} \quad -\frac{\pi}{6} \leq \theta \leq \frac{\pi}{6}.$$

Proof. Parts (i) and (ii) follow by construction.

We prove (iii) and then (iv) follows similarly. The edge joining z_1^+ and z_2^+ is defined to the common intersection of the bisectors $\mathcal{S}_0, T(\mathcal{S}_0), S(\mathcal{S}_0)$. Being in the first two of these implies that $\theta = -\pi/6$ following from Lemma 3.3.1. Substituting in Lemma 3.3.3 and requiring equality gives

$$\begin{aligned} r &= \frac{1}{\sqrt{3}}\left[\sqrt{3}\cos\left(\alpha - \frac{\pi}{12}\right) - \sqrt{1 - 3\sin^2\left(\alpha - \frac{\pi}{12}\right)}\right] \\ &= \cos\left(\alpha - \frac{\pi}{12}\right) - \sqrt{\frac{1}{3} - \sin^2\left(\alpha - \frac{\pi}{12}\right)}. \end{aligned}$$

We know that $\alpha = -\pi/12$ at z_1^+ and $\alpha = \pi/4$ at z_2^+. Moreover, $r = 1/\sqrt{3}$ at both z_1^+ and z_2^+.

We now prove (vi) and then (v), (vii) follows similarly. The edge joining z_2^+ and z_2^- is defined to the common intersection of the bisectors $\mathcal{S}_0, S(\mathcal{S}_0), RS^{-1}(\mathcal{S}_0)$. As in the proof of Lemma 3.3.3, the intersection of $\mathcal{S}_0$ and $S(\mathcal{S}_0)$ implies that

$$3r^2 - 4\sqrt{3}r\cos\left(\frac{\theta}{2} - \frac{\pi}{12}\right)\cos\left(\alpha - \frac{\pi}{12}\right) + 4\cos^2\left(\frac{\theta}{2} - \frac{\pi}{12}\right) - 1 = 0. \tag{3.12}$$

Similarly, the intersection of $RS^{-1}(\mathcal{S}_0)$ with $\mathcal{S}_0$ implies another equality

$$3r^2 - 4\sqrt{3}r\cos\left(\frac{\theta}{2} + \frac{\pi}{12}\right)\cos\left(\alpha - \frac{\pi}{4}\right) + 4\cos^2\left(\frac{\theta}{2} + \frac{\pi}{12}\right) - 1 = 0. \tag{3.13}$$

First we write $\phi = \alpha - \pi/6$. Then subtracting the equations (3.12) and (3.13) gives

$$\sqrt{3}r\sin\left(\frac{\theta}{2} - \phi\right) = \sin\theta. \tag{3.14}$$

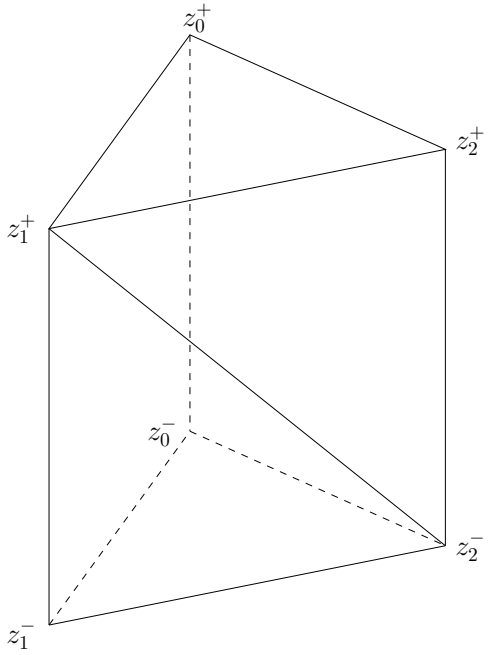

FIGURE 3.3: A schematic view of 1-skeleton of the prism $\mathbf{P}_0$. The compact sides are contained in the isometric sphere $\mathcal{S}_0$ and the noncompact sides of the fundamental domain are cones over the faces of the prism with cone point ∞.

Furthermore, adding the equations (3.12) and (3.13) derives

$$\begin{aligned} 0 &= 3r^2 - 2\sqrt{3}r\cos\left(\frac{\theta}{2}+\phi\right) - 3r\cos\left(\frac{\theta}{2}-\phi\right) + \sqrt{3}\cos\theta + 1 \\ &= 3r^2 - \sqrt{3}r(2\cos\theta+\sqrt{3})\cos\left(\frac{\theta}{2}-\phi\right) - 2\sqrt{3}r\sin\theta\sin\left(\frac{\theta}{2}-\phi\right) + \sqrt{3}\cos\theta + 1 \end{aligned} \tag{3.15}$$

Combining with the equation (3.14), we can simplify the equation (3.15) that

$$\sqrt{3}r\left(2\cos\theta+\sqrt{3}\right)\cos\left(\frac{\theta}{2}-\phi\right) = 3r^2 - 1 + \left(2\cos\theta+\sqrt{3}\right)\cos\theta. \tag{3.16}$$

Making use of the equalities (3.14) and (3.16), we see that

$$\begin{aligned} 3r^2\left(2\cos\theta+\sqrt{3}\right)^2 &= 3r^2\left(2\cos\theta+\sqrt{3}\right)^2\cos^2\left(\frac{\theta}{2}-\phi\right) \\ &\qquad +3r^2\left(2\cos\theta+\sqrt{3}\right)^2\sin^2\left(\frac{\theta}{2}-\phi\right) \\ &= \left[3r^2 - 1 + \left(2\cos\theta+\sqrt{3}\right)\cos\theta\right]^2 + \left(2\cos\theta+\sqrt{3}\right)^2(1-\cos^2\theta) \\ &= (3r^2-1)^2 + 2(3r^2-1)^2\left(2\cos\theta+\sqrt{3}\right)\cos\theta + \left(2\cos\theta+\sqrt{3}\right)^2. \end{aligned}$$

Taking all terms to the right of the equation and simplifying, we can obtain

$$0 = (3r^2-1)\left(3r^2 - 2\sqrt{3}\cos\theta - 4\right).$$

Thus, we can get the solution that

$$3r^2 = 1 \quad \text{or} \quad 3r^2 = 2\sqrt{3}\cos\theta + 4,$$

of which the latter is impossible since $3r^2 \leq 2\sqrt{3}\cos\theta$. So $r = 1/\sqrt{3}$. Substituting $r = 1/\sqrt{3}$ in the equation (3.14), it is easy to get $\phi = -\theta/2$, that is, $\alpha = \pi/6 - \theta/2$. This proves the result. □

Remark 3.3.8. The edges $z_1^+z_1^-, z_1^+z_2^-$ and $z_2^+z_2^-$ lie on the surface of cylinder which is given in the Euclidian coordinates (x, y, z) by

$$\begin{cases} x^2 + y^2 = 1/3, \\ -\pi/6 \leq z \leq \pi/6. \end{cases}$$

However, two faces (z_1^+, z_1^-, z_2^-) and (z_1^+, z_2^-, z_2^+) don't lie on the surface of cylinder.

3.3.4 Compact sides

In this section, we define two compact sides for the fundamental domain contained in the isometric sphere $\mathcal{S}_0$. For the sake of convenience, two compact sides are denoted by $\mathbf{F}_7, \mathbf{F}_8$ and the non-compact sides will be denoted by $\mathbf{F}_i, 1 \leq i \leq 6$.

Definition 3.3.9. *In geographical coordinates from (3.4), the compact sides are the points in $\mathcal{S}_0$ given by*

$$\begin{array}{ll} \mathbf{F}_7: & 0 \leq r \leq \rho_1(\theta,\alpha), \quad -\pi/6 \leq \theta \leq \pi/6, \quad -\theta/2 - \pi/6 \leq \alpha \leq \theta/2, \\ \mathbf{F}_8: & 0 \leq r \leq \rho_2(\theta,\alpha), \quad -\pi/6 \leq \theta \leq \pi/6, \quad \theta/2 \leq \alpha \leq \pi/6 - \theta/2, \end{array}$$

where

$$\rho_1(\theta,\alpha) = \frac{1}{\sqrt{3}}\left[2\cos\left(\frac{\theta}{2}+\frac{\pi}{12}\right)\cos\left(\alpha+\frac{\pi}{12}\right) - \sqrt{1-4\cos^2\left(\frac{\theta}{2}+\frac{\pi}{12}\right)\sin^2\left(\alpha+\frac{\pi}{12}\right)}\right],$$

$$\rho_2(\theta,\alpha) = \frac{1}{\sqrt{3}}\left[2\cos\left(\frac{\theta}{2}-\frac{\pi}{12}\right)\cos\left(\alpha-\frac{\pi}{12}\right) - \sqrt{1-4\cos^2\left(\frac{\theta}{2}-\frac{\pi}{12}\right)\sin^2\left(\alpha-\frac{\pi}{12}\right)}\right].$$

A realistic view of $\mathbf{F}_7$ and $\mathbf{F}_8$ is given in Figure 3.4. We next describe explicitly all the faces of $\mathbf{F}_7$ and $\mathbf{F}_8$.

(i) The face $\mathcal{F}_1 = (z_0^+, z_0^-, z_1^-, z_1^+)$ of $\mathbf{F}_7$ is union of geodesics arcs with endpoints in edges $(z_0^+z_0^-)$ and (z_1^+, z_1^-) on each slice. Therefore, its points are parameterized by

$$0 \leq r \leq \frac{1}{\sqrt{3}}, \quad \alpha = -\frac{\theta}{2} - \frac{\pi}{6} \quad \text{and} \quad -\frac{\pi}{6} \leq \theta \leq \frac{\pi}{6}.$$

We remark the projection of $\mathcal{F}_1$ on the Heisenberg group is the same as the face $(\hat{z}_0^+, \hat{z}_0^-, \hat{z}_1^-, \hat{z}_1^+)$ of the prism in Figure 3.2, which corresponds to $\arg(z) = -\pi/6$.

(ii) The common face $\mathcal{F}' = (z_0^+, z_1^+, z_2^-, z_0^-)$ of $\mathbf{F}_7$ and $\mathbf{F}_8$ is the union of geodesics arcs with endpoints in edges $(z_0^+z_0^-)$ and (z_1^+, z_2^-) on each slice. Therefore, its points are parameterized by

$$0 \leq r \leq \frac{1}{\sqrt{3}}, \quad \alpha = \frac{\theta}{2} \quad \text{and} \quad -\frac{\pi}{6} \leq \theta \leq \frac{\pi}{6}.$$

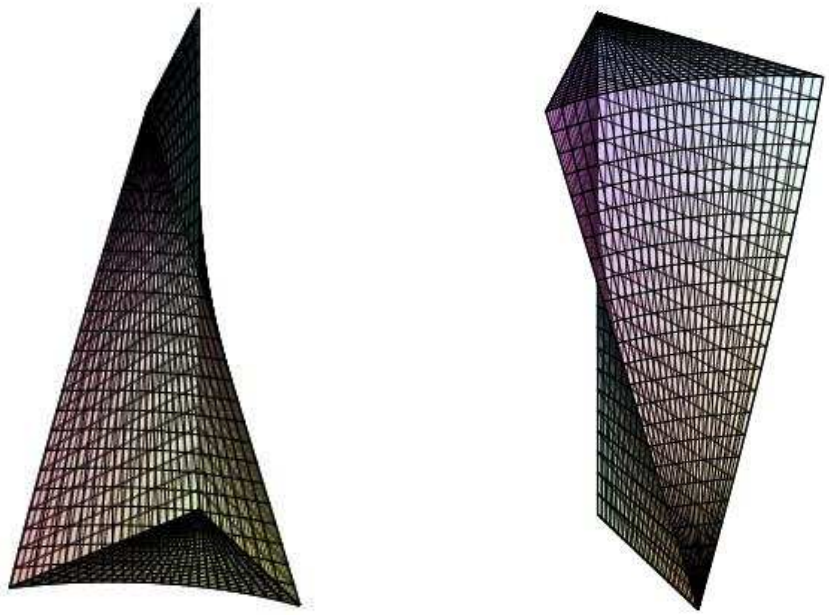

(a) $\mathbf{F}_7$ (b) $\mathbf{F}_8$

FIGURE 3.4: A realistic view of the two compact sides contained in $\mathcal{S}_0$.

(iii) The face $\mathcal{F}_2 = (z_0^+, z_0^-, z_2^-, z_2^+)$ of $\mathbf{F}_8$ is union of geodesics arcs with endpoints in edges $(z_0^+ z_0^-)$ and (z_2^+, z_2^-) on each slice. Therefore, its points are parameterized by

$$0 \leq r \leq \frac{1}{\sqrt{3}}, \quad \alpha = \frac{\pi}{6} - \frac{\theta}{2} \quad \text{and} \quad -\frac{\pi}{6} \leq \theta \leq \frac{\pi}{6}.$$

We remark the projection of $\mathcal{F}_2$ on the Heisenberg group is the same as the face $(\hat{z}_0^+, \hat{z}_0^-, \hat{z}_2^-, \hat{z}_2^+)$ of the prism in Figure 3.2, which corresponds to $\arg(z) = \pi/6$.

(iv) The face $\mathcal{F}_3 = (z_0^-, z_1^-, z_2^-)$ of $\mathbf{F}_7$ is its intersection with the bisector $T^{-1}(\mathcal{S}_0)$ given by $\theta = \pi/6$. Therefore, its points are parameterized by $-\pi/4 \leq \alpha \leq \pi/12$ and

$$0 \leq r \leq \cos\left(\alpha + \frac{\pi}{12}\right) - \sqrt{\frac{1}{3} - \sin^2\left(\alpha + \frac{\pi}{12}\right)}.$$

(v) The face $\mathcal{F}_4 = (z_0^+, z_1^+, z_2^+)$ of $\mathbf{F}_8$ is its intersection with the bisector $T(\mathcal{S}_0)$ given by $\theta = -\pi/6$. Therefore, its points are parameterized by $-\pi/12 \leq \alpha \leq \pi/4$ and

$$0 \leq r \leq \cos\left(\alpha - \frac{\pi}{12}\right) - \sqrt{\frac{1}{3} - \sin^2\left(\alpha - \frac{\pi}{12}\right)}.$$

(vi) The face $\mathcal{F}_5 = (z_1^+, z_1^-, z_2^-)$ of $\mathbf{F}_7$ is its intersection with the bisector $S^{-1}(\mathcal{S}_0)$ given by $-\pi/6 \leq \theta \leq \pi/6$, $-\theta/2 - \pi/6 \leq \alpha \leq \theta/2$ and

$$r = \frac{1}{\sqrt{3}}\left[2\cos\left(\frac{\theta}{2} + \frac{\pi}{12}\right)\cos\left(\alpha + \frac{\pi}{12}\right) - \sqrt{1 - 4\cos^2\left(\frac{\theta}{2} + \frac{\pi}{12}\right)\sin^2\left(\alpha + \frac{\pi}{12}\right)}\right].$$

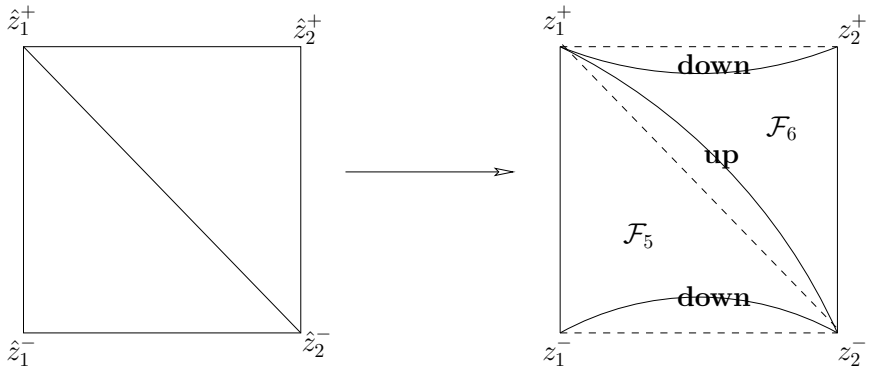

FIGURE 3.5: The modifications on the faces $\mathcal{F}_5$ and $\mathcal{F}_6$: top view.

(vii) The face $\mathcal{F}_6 = (z_1^+, z_2^-, z_2^+)$ of $\mathbf{F}_8$ is its intersection with the bisector $S(\mathcal{S}_0)$ given by $-\pi/6 \leq \theta \leq \pi/6$, $\theta/2 \leq \alpha \leq \pi/6 - \theta/2$ and

$$r = \frac{1}{\sqrt{3}}\left[2\cos\left(\frac{\theta}{2} - \frac{\pi}{12}\right)\cos\left(\alpha - \frac{\pi}{12}\right) - \sqrt{1 - 4\cos^2\left(\frac{\theta}{2} - \frac{\pi}{12}\right)\sin^2\left(\alpha - \frac{\pi}{12}\right)}\right].$$

We remark that the major modifications for the fundamental domain of $(G_2)_\infty$ occurred in the faces $\mathcal{F}_5$ and $\mathcal{F}_6$, see Figure 3.5.

3.3.5 The basic prism

We now are ready to construct the basic prism $\mathbf{P}_0$. In the previous section, we have constructed a fundamental domain for $(G_2)_\infty$. Thus a fundamental domain for G_2 is the intersection of the outside of the isometric sphere $\mathcal{S}_0$ of I_1 with the fundamental domain of $(G_2)_\infty$ we have already constructed. More precisely, the fundamental domain for G_2 is the geodesic cone over the interior of the basic prism to the cone point ∞.

In order to make the boundary of our prism lie outside any other isometric sphere, we should make suitable modifications to the fundamental domain of $(G_2)_\infty$. The modifications consist of using the intersection of $\mathcal{S}_0$ and its neighboring isometric spheres stated in Figure 3.5. The vertices of the fundamental domain are the same as those for the intersection of $\mathcal{S}_0$ with the prism we have already constructed for $(G_2)_\infty$, that is also the intersection of three neighboring bisectors with $\mathcal{S}_0$, listed in Section 3.3.2. There are some geodesic edges, one of whose is contained in the spine of isometric sphere $\mathcal{S}_0$, the others are each contained in one of two slices of bisector $\mathcal{S}_0$. Some generic edges are the intersection of three bisectors constructed in Section 3.3.3.

The two dimensional faces containing q_∞ are foliated by geodesics starting at the ideal point q_∞ and arriving at the corresponding edges. To determine the remaining compact faces and sides, we observe that all the finite edges are contained in the isometric sphere $\mathcal{S}_0$. Two of the faces are contained in complex lines, two of the faces are foliated by a family of geodesic arcs with endpoints at two edges, and the two remaining faces are defined as intersections of $\mathcal{S}_0$ with appropriate images of $\mathcal{S}_0$ under elements of $(G_2)_\infty$.

The two compact sides are contained in $\mathcal{S}_0$. The other six sides are cones based at the faces of the prism with the cone point the ideal vertex q_∞, all of which are listed in Section 3.3.4.

We give the definition of the basic prism $\mathbf{P}_0$.

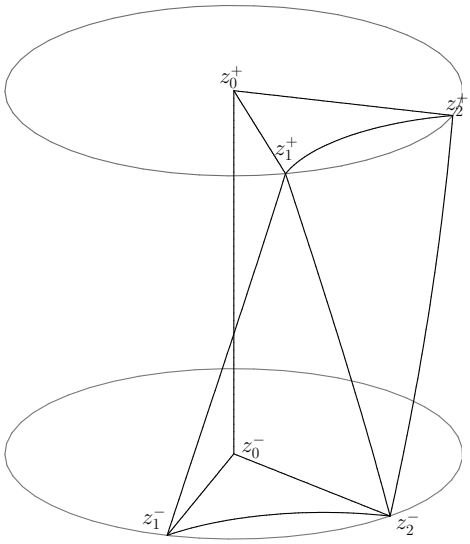

(a) 1-skeleton

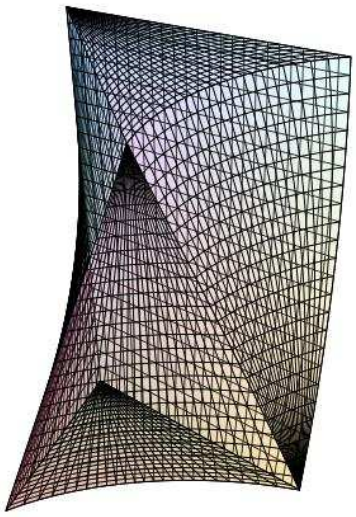

(b) 3-skeleton

FIGURE 3.6: A realistic view of the basic prism $\mathbf{P_0}$ inside the isometric sphere $\mathcal{S}_0$.

Definition 3.3.10. *In geographical coordinates, the prism $\boldsymbol{P}_0$ consists of those points of $\mathcal{S}_0$ for which $-\pi/6 \leq \theta \leq \pi/6$,*

$$0 \leq r \leq \begin{cases} \rho_1(\theta,\alpha) & \text{for } -\theta/2 - \pi/6 \leq \alpha \leq \theta/2, \\ \rho_2(\theta,\alpha) & \text{for } \theta/2 \leq \alpha \leq \pi/6 - \theta/2, \end{cases}$$

where $\rho_1(\theta,\alpha)$ and $\rho_2(\theta,\alpha)$ are defined as before.

Following from the Definitions 3.3.9 and 3.3.10, we see clearly that the basic prism $\mathbf{P}_0$ is the union of two compact sides $\mathbf{F}_7$ and $\mathbf{F}_8$. (Compare with the standard fundamental domain for $PSL(2,\mathbb{Z})$, that is a ideal geodesic triangle whose boundary consists of two vertical lines and an arc of Euclidean circle with radius 1 centered at origin. This arc is only one compact side of the fundamental domain of $PSL(2,\mathbb{Z})$ with its side pairing $z \mapsto -1/z$). The boundary of the prism are all the faces of the two compact sides except for the common face $\mathcal{F}'$ that is in the interior of $\mathbf{P}_0$. The schematic view is given in Figure 3.3 and a realistic view is given in Figure 3.6.

3.4 The side pairing maps

In the previous section we have constructed two compact sides $\mathbf{F}_7$ and $\mathbf{F}_8$ of the fundamental domain. The other sides are cones from the faces of our prism to the point q_∞ defined in Section 3.4.2. A side pairing map is an element of $PU(2,1)$ that sends one of these sides to another (possibly the same). In this section, we will describe all the side pairing maps in G_2.

3.4.1 Compact side pairing map

We consider the map I_1

$$\begin{bmatrix} 0 & 0 & i/\sqrt{3} \\ 0 & -\omega & 0 \\ i\sqrt{3} & 0 & 0 \end{bmatrix}$$

acting on $\mathcal{S}_0$ given by

$$I_1 : (r,\theta,\alpha) \longrightarrow (r,-\theta,\alpha+\pi/6).$$

By definition, we know that the compact side $\mathbf{F}_7$ is a region in $\mathcal{S}_0$ bounded by four faces $\mathcal{F}_1$, $\mathcal{F}'$, $\mathcal{F}_3$, $\mathcal{F}_5$ and the compact side $\mathbf{F}_8$ is a region in $\mathcal{S}_0$ bounded by four faces $\mathcal{F}'$, $\mathcal{F}_2$, $\mathcal{F}_4$, $\mathcal{F}_6$. Observe that the map

$$I_1 : (r,\theta,\alpha) \longrightarrow (r,-\theta,\alpha+\pi/6), \qquad I_1^2 = R : (r,\theta,\alpha) \longrightarrow (r,\theta,\alpha+\pi/3).$$

We can verify that

$$\mathcal{F}' = I_1(\mathcal{F}_1), \quad \mathcal{F}_4 = I_1(\mathcal{F}_3),$$

$$\mathcal{F}_6 = I_1(\mathcal{F}_5), \quad \mathcal{F}_2 = R(\mathcal{F}_1) = I_1^2(\mathcal{F}_1) = I_1(\mathcal{F}').$$

For example, we take a point (r,θ,α) of $\mathcal{F}_1$, that is satisfied the set of inequalities

$$0 \leq r \leq \frac{1}{\sqrt{3}}, \quad \alpha = -\frac{\theta}{2} - \frac{\pi}{6} \quad \text{and} \quad -\frac{\pi}{6} \leq \theta \leq \frac{\pi}{6}.$$

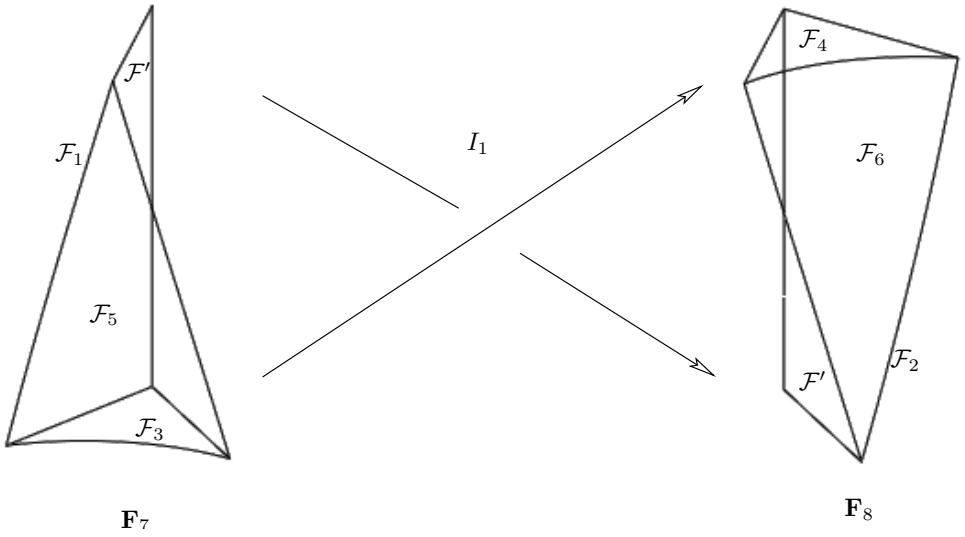

FIGURE 3.7: Two compact sides in geographical coordinates (r, θ, α) inside the isometric sphere $\mathcal{S}_0$ and its side pairing I_1 maps $\mathbf{F}_7$ to $\mathbf{F}_8$ upside down and with a rotation.

It is clearly that the point $I_1(r, \theta, \alpha)$ satisfies the equations

$$0 \leq r \leq \frac{1}{\sqrt{3}}, \quad \alpha = \frac{\theta}{2} \quad \text{and} \quad -\frac{\pi}{6} \leq \theta \leq \frac{\pi}{6},$$

that is, the point $I_1(r, \theta, \alpha)$ lies on the face $\mathcal{F}'$. Thus we can obtain $\mathbf{F}_8 = I_1(\mathbf{F}_7)$, namely, I_1 is the side pairing map from $\mathbf{F}_7$ to $\mathbf{F}_8$. The realistic view of these two compact sides and its side pairing is given by Figure 3.7.

3.4.2 Noncompact sides and side pairing maps

As the action of elements of $(G_2)_\infty$ preserves each horosphere, then we can give a natural extension of faces of the prism $\mathbf{P}_0$. We define two pyramids $\mathbf{F}_1, \mathbf{F}_2$ and four tetrahedra $\mathbf{F}_3, \mathbf{F}_4, \mathbf{F}_5, \mathbf{F}_6$. Each of these is the geodesic cone from q_∞ over the union of faces $\mathcal{F}_1, \mathcal{F}_2, \mathcal{F}_3, \mathcal{F}_4, \mathcal{F}_5$ and $\mathcal{F}_6$ of $\mathbf{P}_0$. To be precise, the pyramid $\mathbf{F}_1$ is defined to be the union of geodesic arcs based at the face $\mathcal{F}_1$ with cone point q_∞ and it is likewise for others. By constructions, the intersection of $\mathbf{P}_0$ with each of the pyramids $\mathbf{F}_1, \mathbf{F}_2$ and tetrahedra $\mathbf{F}_3, \mathbf{F}_4, \mathbf{F}_5, \mathbf{F}_6$ is nothing other than the corresponding face of $\mathbf{P}_0$.

We define the 4-dimensional polyhedron $\mathbf{D}$ to be the geodesic cone pointing to q_∞ over the interior of $\mathbf{P}_0$. Furthermore, $\mathbf{D}$ has eight three-dimensional sides, namely $\mathbf{F}_1$, $\mathbf{F}_2$, $\mathbf{F}_3$, $\mathbf{F}_4$, $\mathbf{F}_5$, $\mathbf{F}_6$, $\mathbf{F}_7$, $\mathbf{F}_8$. Later we will show $\mathbf{D}$ is a fundamental domain for G_2.

This enables us to give the following proposition.

Proposition 3.4.1. *$R^{-1}(\boldsymbol{D}) \cap \boldsymbol{D} = \mathbf{F}_1$, and R maps $\mathbf{F}_1$ to $\mathbf{F}_2$; $T^{-1}(\boldsymbol{D}) \cap \mathbf{D} = \mathbf{F}_3$, and T maps $\mathbf{F}_3$ to $\mathbf{F}_4$, likewise, $S^{-1}(\mathbf{D}) \cap \mathbf{D} = \mathbf{F}_5$, S maps $\mathbf{F}_5$ to $\mathbf{F}_6$.*

Proof. By construction these sides are corresponding to associated faces of $\mathbf{P}_0$, and so this directly follows from the matrices R, S and T in Proposition 3.2.2. □

We now have already described all the side pairing maps. In what follows, we summarize the side pairing maps in terms of their action on the vertices.

$$\begin{aligned}
R &: (\infty, z_0^+, z_0^-, z_1^-, z_1^+) \longmapsto (\infty, z_0^+, z_0^-, z_2^-, z_2^+),\\
S &: (\infty, z_1^+, z_1^-, z_2^-) \longmapsto (\infty, z_2^+, z_2^-, z_1^+),\\
T &: (\infty, z_0^-, z_1^-, z_2^-) \longmapsto (\infty, z_0^+, z_1^+, z_2^+),\\
I_1 &: (z_0^+, z_0^-, z_1^+, z_1^-, z_2^-) \longmapsto (z_0^-, z_0^+, z_2^-, z_1^+, z_2^+).
\end{aligned}$$

3.4.3 The face cycles

In this section we focus on the 2-dimensional faces of $\mathbf{D}$. These faces may be contained in complex lines or in Lagrangian planes. In such cases they are totally geodesic. Otherwise the face is not totally geodesic and we refer to it as generic. We will describe all the 2-dimensional faces and find the associated face cycles and cycle transformations, which will turn out to give a presentation after we check that hypotheses of the Poincaré's polyhedron theorem are satisfied.

Faces in complex lines

Observe that the faces $\mathcal{F}_3$ and $\mathcal{F}_4$ are each contained in a complex line, that is, a slice of $\mathcal{S}_0$. These two complex lines are paired by T and each is preserved by R. Moreover, one face is the image of the other under T or T^{-1}. In order to obtain cycle transformation we should find other side pairings for these two faces. We know these two faces are each contained in one of compact sides $\mathbf{F}_7$ and $\mathbf{F}_8$ and they are the associated to side pairing map I_1. Therefore, this cycle can be described as the following table, which each column has the vertices of each face and the generator in the fist row indicates that this column is the image of the previous one under this map.

$$\begin{array}{ccccc}
 & I_1 & & T^{-1} & \\
z_0^- & \longmapsto & z_0^+ & \longmapsto & z_0^- \\
z_1^- & \longmapsto & z_1^+ & \longmapsto & z_1^- \\
z_2^- & \longmapsto & z_2^+ & \longmapsto & z_2^-
\end{array}$$

The face $\mathcal{F}_3$ is fixed by $T^{-1}I_1$, which is a complex reflection of order 3. Therefore the cycle relation is $(T^{-1}I_1)^3 = I$.

The generic triangular faces

The faces $\mathcal{F}_5, \mathcal{F}_6$ with vertices the ordered triple $(z_1^+, z_1^-, z_2^-), (z_2^+, z_2^-, z_1^+)$ respectively are neither contained in complex line nor in Lagrangian planes. The map $S^{-1}I_1$ maps $\mathcal{F}_5$ to itself but acts on this face as a rotation of order 3, which is a regular elliptic element. They form a face cycle as described in the following table

$$\begin{array}{ccccccccccccc}
 & I_1 & & S^{-1} & & I_1 & & S^{-1} & & I_1 & & S^{-1} & \\
z_1^+ & \longmapsto & z_2^- & \longmapsto & z_1^- & \longmapsto & z_1^+ & \longmapsto & z_2^- & \longmapsto & z_2^+ & \longmapsto & z_1^+ \\
z_1^- & \longmapsto & z_1^+ & \longmapsto & z_2^- & \longmapsto & z_2^+ & \longmapsto & z_1^+ & \longmapsto & z_2^- & \longmapsto & z_1^- \\
z_2^- & \longmapsto & z_2^+ & \longmapsto & z_1^+ & \longmapsto & z_2^- & \longmapsto & z_1^- & \longmapsto & z_1^+ & \longmapsto & z_2^-
\end{array}$$

The associated face cycle transformation is $(S^{-1}I_1)^3$.

The generic quadrilateral faces

The faces $\mathcal{F}_1, \mathcal{F}', \mathcal{F}_2$ with vertices the ordered quadruples respectively $(z_0^+, z_1^+, z_1^-, z_0^-)$, $(z_0^-, z_2^-, z_1^+, z_0^+)$, $(z_0^+, z_2^+, z_2^-, z_0^-)$ are generic faces that form a single face cycle. This is described in the following table

$$\begin{array}{cccccccc} & I_1 & & I_1 & & R^{-1} & \\ z_0^+ & \longmapsto & z_0^- & \longmapsto & z_0^+ & \longmapsto & z_0^+ \\ z_1^+ & \longmapsto & z_2^- & \longmapsto & z_2^+ & \longmapsto & z_1^+ \\ z_1^- & \longmapsto & z_1^+ & \longmapsto & z_2^- & \longmapsto & z_1^- \\ z_0^- & \longmapsto & z_0^+ & \longmapsto & z_0^- & \longmapsto & z_0^- \end{array}$$

The associated cycle transformation is $R^{-1}I_1^2$.

The generic infinite faces

We have already seen the infinite faces and the associated face cycles, which correspond to edges and edge cycles we considered when we analyzed $(G_2)_\infty$. We now list them again.

There are two face cycles involving R associated to geodesic faces:

$$\begin{array}{ccccc} & R & \\ q_\infty & \longmapsto & q_\infty \\ z_0^+ & \longmapsto & z_0^+ \\ z_0^- & \longmapsto & z_0^- \end{array} \qquad \begin{array}{ccccccccc} & R & & T & & R^{-1} & & T^{-1} & \\ q_\infty & \longmapsto & q_\infty & \longmapsto & q_\infty & \longmapsto & q_\infty & \longmapsto & q_\infty \\ z_0^- & \longmapsto & z_0^- & \longmapsto & z_0^+ & \longmapsto & z_0^+ & \longmapsto & z_0^- \\ z_1^- & \longmapsto & z_2^- & \longmapsto & z_2^+ & \longmapsto & z_1^+ & \longmapsto & z_1^- \end{array}$$

The face cycles transformations are R and $T^{-1}R^{-1}TR$ respectively, which give rise to $R^6 = I$ and the latter may be rewritten as $[T, R] = I$.

There are another two face cycles involving S associated to generic faces:

$$\begin{array}{ccccccc} & S & & R^{-1} & \\ q_\infty & \longmapsto & q_\infty & \longmapsto & q_\infty \\ z_1^+ & \longmapsto & z_2^+ & \longmapsto & z_1^+ \\ z_1^- & \longmapsto & z_2^- & \longmapsto & z_1^- \end{array} \qquad \begin{array}{ccccccccc} & S & & S & & T^{-1} & \\ q_\infty & \longmapsto & q_\infty & \longmapsto & q_\infty & \longmapsto & q_\infty \\ z_1^- & \longmapsto & z_2^- & \longmapsto & z_1^+ & \longmapsto & z_1^- \\ z_2^- & \longmapsto & z_1^+ & \longmapsto & z_2^+ & \longmapsto & z_2^- \end{array}$$

The associated cycles are $R^{-1}S$ and $T^{-1}S^2$ respectively. These give the cycle relation $(R^{-1}S) = I$ and $T = S^2$.

3.5 The main theorems

In this section we prove that the 4-dimensional polyhedron **D** constructed as above is indeed a fundamental domain for G_2 and give a presentation for the group G_2.

3.5.1 D is a fundamental domain

In this subsection, we use Poincaré's polyhedron theorem to conclude **D** is a fundamental domain for G_2. The techniques are the same as [FP06] and [FFP10]. We just apply these arguments on this polyhedron **D**.

Theorem 3.5.1. *The polyhedron **D** is a fundamental domain for G_2.*

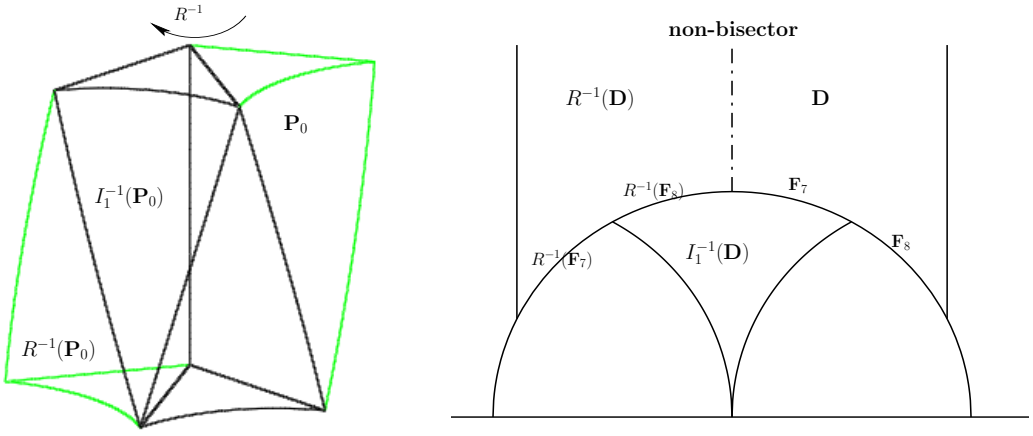

(a) 3-dimensional view

(b) 2-dimensional view

FIGURE 3.8: The images of $\mathbf{D}$ cover a neighborhood of the face $\mathcal{F}_1$.

Proof. We have given $\mathbf{D}$ the structure of a prism with side pairing maps. For each two-dimensional face of $\mathbf{D}$, we have found all the face cycles given by the side-pairing maps. In what follows, we want to verify that the images of $\mathbf{D}$ cover a neighborhood of the interior of each two-dimensional face.

The faces containing q_∞ are cones over its edges of $\mathbf{P}_0$. As the infinite faces are sent to other infinite faces by maps in $(G_2)_\infty$, then the face cycles from faces containing q_∞ are corresponding to edge cycles from $\mathbf{P}_0$ that are listed in Section 3.4.3. Therefore, the images of $\mathbf{D}$ under $(G_2)_\infty$ cover any horoball not intersecting $\mathcal{S}_0$ from the construction of the fundamental domain for $(G_2)_\infty$.

For all the compact faces, we need only take one face in each face cycle in order to verify the tessellation around the associated face. Now consider the face $\mathcal{F}_1$ with vertices the ordered quadruple $(z_0^+, z_1^+, z_1^-, z_0^-)$. The face cycle is

$$(z_0^+, z_1^+, z_1^-, z_0^-) \xrightarrow{I_1} (z_0^-, z_2^-, z_1^+, z_0^+) \xrightarrow{I_1} (z_0^+, z_2^+, z_2^-, z_0^-) \xrightarrow{R^{-1}} (z_0^+, z_1^+, z_1^-, z_0^-).$$

Therefore, $R^{-1}I_1^2$ is the identity on $\mathcal{F}_1$, that is also the identity in G_2. We want to show that $\mathbf{D}$, $I_1^{-1}(\mathbf{D})$, $I_1^{-2}(\mathbf{D}) = R^{-1}(\mathbf{D})$ cover a neighborhood of $\mathcal{F}_1$. In fact, the map R is a rotation of $\mathcal{S}_0$ about its spine and preserves $\mathcal{S}_0$. Therefore, $R^{-1}(\mathbf{P}_0)$ is also contained in $\mathcal{S}_0$. The image of $\mathbf{D}$ under R^{-1} is the geodesic cone of $R^{-1}(\mathbf{P}_0)$. Hence $\mathbf{D} \cup R^{-1}(\mathbf{D})$ cover that part of a neighborhood of $\mathcal{F}_1$ exterior to $\mathcal{S}_0$. Observe that the face $\mathcal{F}_1$ is contained in $I_1^{-1}(\mathbf{F}_8) = \mathbf{F}_7$ and $I_1^{-1}(\mathbf{F}_7) = I_1^{-2}(\mathbf{F}_8) = R^{-1}(\mathbf{F}_8)$, in other words, $I_1^{-1}(\mathbf{P}_0)$ has a common side with each of $\mathbf{P}_0$ and $R^{-1}(\mathbf{P}_0)$, namely, $\mathbf{P}_0 \cap I_1^{-1}(\mathbf{P}_0) = \mathbf{F}_7$ and $R^{-1}(\mathbf{P}_0) \cap I_1^{-1}(\mathbf{P}_0) = R^{-1}(\mathbf{F}_8)$. Moreover the maps I_1 swaps the exterior and the interior of $\mathcal{S}_0$. Thus we conclude that $\mathbf{D} \cup I_1^{-1}(\mathbf{D}) \cup R^{-1}(\mathbf{D})$ covers a neighborhood of $\mathcal{F}_1$, see Figure 3.8 for a schematic view.

Next we consider the face $\mathcal{F}_3$ with vertices the ordered triples (z_0^-, z_1^-, z_2^-). The face cycles are

$$(z_0^-, z_1^-, z_2^-) \xrightarrow{I_1} (z_0^+, z_1^+, z_2^+) \xrightarrow{T^{-1}} (z_0^-, z_1^-, z_2^-).$$

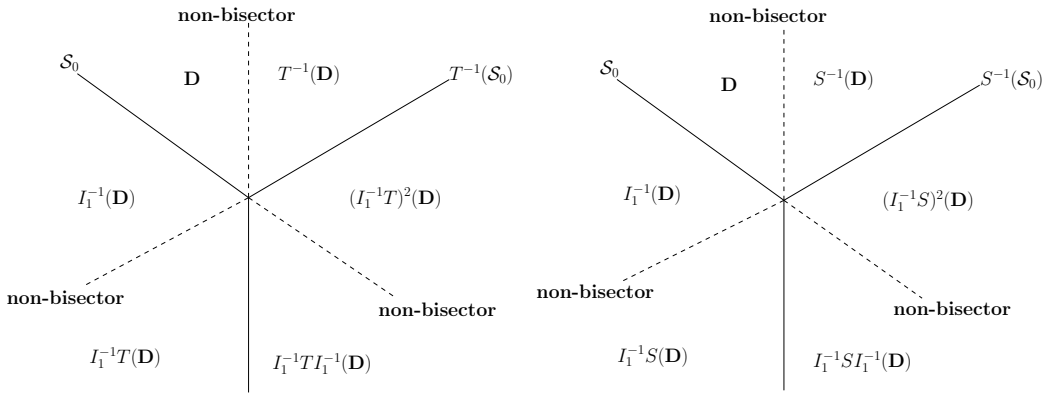

(a) The neighborhood of $\mathcal{F}_3$ (b) The neighborhood of $\mathcal{F}_5$

FIGURE 3.9: The images of $\mathbf{D}$ cover a neighborhood of the faces $\mathcal{F}_3$ and $\mathcal{F}_5$.

Therefore $T^{-1}I_1$ is the identity on $\mathcal{F}_3$ and a rotation about complex line containing (z_0^-, z_1^-, z_2^-). In fact, we can easily verify $(T^{-1}I_1)^3$ is identity in G_2. We will show that a neighborhoods of the face $\mathcal{F}_3$ is tessellated by some images of $\mathbf{D}$. To see this, first observe that T^{-1} is a vertical translation in the Heiseinberg group $\mathcal{N}$, therefore, $\mathbf{D} \cup T^{-1}(\mathbf{D})$ cover a neighborhood of $\mathcal{F}_3$ exterior to two isometric spheres $\mathcal{S}_0$ and $T^{-1}(\mathcal{S}_0)$. The result will be completed by a similar argument ([FFP10], Section 7.8). This argument may be applied to the faces that are in the intersection of two distinct isometric spheres of the Ford domain. This also shows a neighborhood of $\mathcal{F}_5$ is covering by some images of $\mathbf{D}$ since the face $\mathcal{F}_5$ is in the intersection of two isometric spheres of I_1 and $S^{-1}I_1S$.

From the point of view of geometry, we state that the face $\mathcal{F}_3$ is covered by $\mathbf{D}$, $I_1^{-1}(\mathbf{D})$, $I_1^{-1}T(\mathbf{D})$, $I_1^{-1}TI_1^{-1}(\mathbf{D})$, $(I_1^{-1}T)^2(\mathbf{D})$ and $(I_1^{-1}T)^2I_1^{-1}(\mathbf{D}) = T^{-1}(\mathbf{D})$ and the face $\mathcal{F}_5$ is tessellated by $\mathbf{D}$, $I_1^{-1}(\mathbf{D})$, $I_1^{-1}S(\mathbf{D})$, $I_1^{-1}SI_1^{-1}(\mathbf{D})$, $(I_1^{-1}S)^2(\mathbf{D})$ and $(I_1^{-1}S)^2I_1^{-1}(\mathbf{D}) = S^{-1}(\mathbf{D})$ by the same argument as above. We draw two-dimensional pictures to show more clearly, see Figure 3.9.

Notice that there is a difference between the two cases, that is not apparent from the two dimensional picture. Namely, the map $T^{-1}I_1$ is a complex reflection of order 3 and fixes each point of the face $\mathcal{F}_1$, whereas $S^{-1}I_1$ is a regular elliptic of order 3 and acts on the face $\mathcal{F}_5$ as a rotation.

By Poincaré's polyhedron theorem, we conclude that $\mathbf{D}$ is a fundamental domain for the group generated by the side pairing maps and the presentation is given by the cycle relations. Recall that G_2 was shown to be generated by R, S, T, I_1 in Proposition 3.2.5, which completes the proof. □

3.5.2 A presentation for G_2

In this section, we also use Poincaré's polyhedron theorem on $\mathbf{D}$ to derive a presentation for G_2. We know the generators of G_2 are side pairing maps for $\mathbf{D}$ given in Section 3.4.2.

For each two-dimensional face of $\mathbf{D}$, we have already found all the cycles given by the side-pairing maps listed in Section 3.4.3. Thus the stabilizer of infinity $(G_2)_\infty$ has the

following presentation

$$(G_2)_\infty = \langle R, S, T |\ R^6 = (R^{-1}S)^3 = [R,T] = S^2T^{-1} = identity \rangle.$$

For the compact faces, we have given the cycles in Section 3.4.3. Therefore, we have obtained the additional relations

$$(T^{-1}I_1)^3 = (S^{-1}I_1)^3 = R^{-1}I_1^2 = identity.$$

Thus a presentation for G_2 is given by

$$\langle R, S, T, I_1 |\ R^6 = (R^{-1}S)^3 = [R,T] = S^2T^{-1} = (T^{-1}I_1)^3 = (S^{-1}I_1)^3 = R^{-1}I_1^2 = id \rangle.$$

We want to give a briefer presentation by eliminating several generators. Suppose that $A_2 = T^{-1}I_1$ and $A_3 = S^{-1}I_1$, then we can get the relations $S = A_3A_2^{-1}$, $R = I_1^2 = (A_3A_2^{-1}A_3)^2$ which can be used to eliminate the generators R, S, T and I_1. From these relations we obtain the following theorem:

Theorem 3.5.2. *The maps $A_2 = T^{-1}I_1$ and $A_3 = S^{-1}I_1$ generate G_2. Moreover, a presentation on these generators is*

$$\langle A_2, A_3 |\ A_2^3 = A_3^3 = (A_3A_2^{-1}A_3)^{12} = [(A_3A_2^{-1}A_3)^2, (A_3A_2^{-1})^2] = identity \rangle.$$

Proof. We begin by showing that the relations involving A_2 and A_3 follow from the relations involving R, S, T and I_1. First, the relations $A_2^3 = A_3^3 = 1$ follow directly from the definition of A_2 and A_3. Secondly, observe that the relations

$$A_3A_2^{-1}A_3 = S^{-1}I_1I_1^{-1}TS^{-1}I_1 = I_1$$

and

$$A_3A_2^{-1} = S^{-1}I_1I_1^{-1}T = S, \quad T = S^2 = (A_3A_2^{-1})^2.$$

Thus $R = I_1^2$, $R^6 = 1$ and $[R,T]$=1 imply that

$$(A_3A_2^{-1}A_3)^{12} = [(A_3A_2^{-1}A_3)^2, (A_3A_2^{-1})^2] = 1.$$

Using $R = (A_3A_2^{-1}A_3)^2, S = A_3A_2^{-1}$, we obtain

$$I_1 = SA_3 = A_3A_2^{-1}A_3$$

and

$$T = I_1A_2^{-1} = A_3A_2^{-1}A_3A_2^{-1} = (A_3A_2^{-1})^2,$$

Hence, $\langle R, S, T, I_1 \rangle = \langle A_2, A_3 \rangle$.

Finally, we show that the relations involving R, S, T and I_1 are a consequence of those involving A_2, A_3. First, it is obvious that

$$(T^{-1}I_1)^3 = A_2^3 = 1, \quad (S^{-1}I_1)^3 = A_3^3 = 1, \quad R^6 = (A_3A_2^{-1}A_3)^{12} = 1,$$

and

$$R = (A_3A_2^{-1}A_3)^2 = I_1^2, \quad T = (A_3A_2^{-1})^2 = S^2, \quad [R,T] = [(A_3A_2^{-1}A_3)^2, (A_3A_2^{-1})^2] = 1.$$

Finally,

$$\begin{aligned}
(R^{-1}S)^3 &= [(A_3A_2^{-1}A_3)^{-2}A_3A_2^{-1}]^3 \\
&= (A_3^{-1}A_2A_3^{-1}A_2^{-1}A_2A_3^{-1}A_2A_2^{-1})^3 \\
&= (A_3^{-1}A_2A_3)^3 \\
&= A_3^{-1}A_2^3A_3 \\
&= 1.
\end{aligned}$$

This completes the proof. □

3.5.3 The volume of the orbifold $\mathbf{H}^2_{\mathbb{C}}/G_2$

We calculate the volume of $\mathbf{H}^2_{\mathbb{C}}/G_2$ using the complex hyperbolic Gauss-Bonnet formula. The similar case for Gauss-Picard group has been done, see [FFP10]. We state the Gauss-Bonnet theorem for our convenience.

$$\mathrm{Vol}(M) = \frac{8\pi^2}{3}\chi(M), \qquad \chi(M) = e_0 - e_1 + e_2 - e_3 + e_4,$$

where e_i is the numbers of i-cells weighted by the order of the stabilizers.

The volume of complex hyperbolic 2-orbifold $\mathbf{H}^2_{\mathbb{C}}/G_2$ was calculated firstly by John Parker [Par98] as $\pi^2/27$. Note that Stover [Sto10] states that there are exactly two non-compact arithmetic complex hyperbolic 2-orbifold of minimal volume $\pi^2/27$, whose fundamental groups are $PU(2,1;\mathbb{Z}[\omega])$ and its sister G_2. Observe, however, that [Par98] also uses the Gauss-Bonnet theorem to calculate the volume. From the Table 1 on pages 228 and 229 of [Hol80], Holzapfel shows that $\chi(\mathbf{H}^2_{\mathbb{C}}/SU(2,1;\mathbb{Z}[\omega])) = 1/24$, which implies that $\chi(\mathbf{H}^2_{\mathbb{C}}/PU(2,1;\mathbb{Z}[\omega])) = 1/72$. This is also shows the Euler characteristic of $\mathbf{H}^2_{\mathbb{C}}/G_2$ is $1/72$ by the fact that the groups $PU(2,1;\mathbb{Z}[\omega]))$ and G_2 have a common subgroup of index 4.

By the combinatorics of $\mathbf{D}$, we also show the volume of the orbifold $\mathbf{H}^2_{\mathbb{C}}/G_2$.

Proposition 3.5.3. *The volume of the orbifold $\boldsymbol{H}^2_{\mathbb{C}}/G_2$ is $\pi^2/27$.*

Proof. According to the Gauss-Bonnet theorem, we need only show the Euler characteristic of $\mathbf{H}^2_{\mathbb{C}}/G_2$ is $1/72$. It suffices to find the stabilizer of i-dimensional faces of $\mathbf{D}$ and calculate their order.

- Vertices:

Cycle	Stabilizer	Order
z_0^+, z_0^-	$\langle T^{-1}I_1, R\rangle$	18
$z_1^+, z_1^-, z_2^+, z_2^-$	$\langle I_1T^{-1}, S^{-1}R\rangle$	24

  The orders of the stabilizers are found as follows. Since $R = I_1^2$ and $[R,T] = I$, $T^{-1}I_1$ and R commute. Therefore, the group $\langle T^{-1}I_1, R\rangle$ is the product of two cyclic groups $\langle T^{-1}I_1\rangle$ and $\langle R\rangle$, and then it has order 18 since $(T^{-1}I_1)^3 = I$ and R has order 6. Next, it is easy to check that $(I_1T^{-1})(S^{-1}R)^{-1}$ has order 4, and that its square is in the center of $\langle I_1T^{-1}, S^{-1}R\rangle$. Therefore, $\langle I_1T^{-1}, S^{-1}R\rangle$ is a degree 2 extension of an (orientation preserving) $(2,3,3)$ triangle group (that is a tetrahedral group) and so it has order $2 \times 12 = 24$ (Compare with the Proposition 5.1 of [Par09]).

  We conclude that

$$e_0 = \frac{1}{18} + \frac{1}{24} = \frac{7}{72}.$$

- Edges:

Cycle	Stabilizer	Order
(z_0^+, z_0^-)	$\langle I_1 \rangle$	12
$(z_0^+, z_1^+), (z_0^+, z_2^+), (z_0^-, z_1^-), (z_0^-, z_2^-)$	$\langle T^{-1} I_1 \rangle$	3
$(z_1^+, z_1^-), (z_2^+, z_2^-), (z_1^+, z_2^+), (z_1^+, z_2^-), (z_1^-, z_2^-)$	$\langle R^{-1} S \rangle$	3
$(z_0^+, \infty), (z_0^-, \infty)$	$\langle R \rangle$	6
$(z_1^+, \infty), (z_1^-, \infty), (z_2^+, \infty), (z_2^-, \infty)$	$\langle R^{-1} S \rangle$	3

These stabilizers are all cyclic groups and so their orders are the same as those generators, seen in the previous section.

We conclude that

$$e_1 = \frac{1}{12} + \frac{1}{3} + \frac{1}{3} + \frac{1}{6} + \frac{1}{3} = \frac{5}{4}.$$

- 2-faces:

Cycle	Stabilizer	Order
$(z_0^+, z_1^+, z_2^+), (z_0^-, z_1^-, z_2^-)$	$\langle T^{-1} I_1 \rangle$	3
$(z_1^+, z_1^-, z_2^-), (z_2^+, z_2^-, z_1^+)$	$\langle S^{-1} I_1 \rangle$	3
$(z_0^+, z_0^-, z_1^-, z_1^+), (z_0^+, z_1^+, z_2^-, z_0^-), (z_0^+, z_0^-, z_2^-, z_2^+)$	$\langle Id \rangle$	1
(z_0^+, z_0^-, ∞)	$\langle R \rangle$	6
$(z_1^+, z_1^-, \infty), (z_2^+, z_2^-, \infty)$	$\langle R^{-1} S \rangle$	3
$(z_1^+, z_2^+, \infty), (z_1^+, z_2^-, \infty), (z_1^-, z_2^-, \infty)$	$\langle Id \rangle$	1
$(z_0^+, z_1^+, \infty), (z_0^+, z_2^+, \infty), (z_0^-, z_1^-, \infty), (z_0^-, z_2^-, \infty)$	$\langle Id \rangle$	1

These stabilizers are also cyclic and so their orders are obvious. We conclude that

$$e_2 = \frac{1}{3} + \frac{1}{3} + 1 + \frac{1}{6} + \frac{1}{3} + 1 + 1 = \frac{25}{6}.$$

- 3-faces:

Cycle	Stabilizer	Order
$(\infty, z_0^+, z_1^+, z_2^+), (\infty, z_0^-, z_1^-, z_2^-)$	$\langle Id \rangle$	1
$(\infty, z_1^+, z_1^-, z_2^-), (\infty, z_2^+, z_2^-, z_1^+)$	$\langle Id \rangle$	1
$(\infty, z_0^+, z_0^-, z_1^-, z_1^+), (\infty, z_0^+, z_0^-, z_2^-, z_2^+)$	$\langle Id \rangle$	1
$(z_0^+, z_1^+, z_0^-, z_1^-, z_2^-), (z_0^-, z_2^-, z_0^+, z_1^+, z_2^+)$	$\langle Id \rangle$	1

We conclude that

$$e_3 = 4.$$

- Finally $e_4 = 1$.

We compute now the orbifold Euler number to be

$$\chi(M) = e_0 - e_1 + e_2 - e_3 + e_4 = \frac{7}{72} - \frac{5}{4} + \frac{25}{6} - 4 + 1 = \frac{1}{72}.$$

□

3.5.4 Relation with Mostow's group

In his notation of [Mos80], Mostow considered a family of complex reflection groups with the angle $2\pi/p$ where p is one of $3, 4, 5$. He described these groups by a Coxetor diagram and a phase shift $\phi = \exp(\pi it/3)$ where $t = 1/p + 2/k - 1/2$ and k is an integer, showed the existence of non-arithmetic lattices in $PU(2,1)$ by the construction of an explicit fundamental domain of the groups for certain values of k and gave a presentation for each of these groups. Parker in the survey paper [Par09], defined again the Mostow's groups. In that case, he allows $p = 6$ and divides into two types of them. More precisely, Mostow's groups of the first type are the complex reflection groups where $1/p + 1/k \geq 1/2, p \leq 6$ and those of the second type are the groups where $1/p+1/k < 1/2, p \leq 6$. The Eisenstein-Picard modular group admits a presentation of a similar type, which is a Mostow's group of the first type with $p = 6$ and $k = 2$; (see [Par09] and Corollary 5.13 of [FP06]). For the sister of Eisenstein-Picard modular group, we show that it is a Mostow's group of the first kind with $p = 3$ and $k = 6$.

As in Theorem 3.5.2, if preserving the generator R, we may rewrite this presentation as

$$G_2 = \langle A_2, A_3, R|\ A_2^3 = A_3^3 = R^6 = [R, (A_3A_2^{-1})^2] = 1, R = (A_3A_2^{-1}A_3)^2\rangle.$$

Using the notation of [Par09], we state a Mostow's group of the first type with $p = 3$ and $k = 6$ as follows

$$\Gamma = \langle J, R_1, A_1|\ J^3 = R_1^3 = A_1^6 = 1, A_1 = (JR_1^{-1}J)^2, A_1R_1 = R_1A_1\rangle.$$

We make a explicit connection between the group G_2 and Γ in the following proposition.

Proposition 3.5.4. *There is a isomorphism φ from G_2 to Γ given by $\varphi(A_3) = J, \varphi(A_2) = R_1$ and $\varphi(R) = A_1$.*

Proof. First, observe that the orders of generators of G_2 and Γ are the same if giving a homomorphism satisfies with $\varphi(A_3) = J, \varphi(A_2) = R_1$ and $\varphi(R) = A_1$. So it need only to show other relations of G_2 and Γ are equivalent.

In fact,

$$A_1 = \varphi(R) = \varphi((A_3A_2^{-1}A_3)^2) = (\varphi(A_3)\varphi(A_2)^{-1}\varphi(A_3))^2 = (JR_1^{-1}J)^2$$

and $[R, (A_3A_2^{-1})^2] = 1$ yields $A_1(JR_1^{-1})^2A_1^{-1}(JR_1^{-1})^{-2} = 1$. Moreover,

$$\begin{aligned} 1 &= (JR_1^{-1})^{-2}A_1(JR_1^{-1})^2A_1^{-1} \\ &= R_1(J^{-1}R_1J^{-1})A_1(JR_1^{-1}J)R_1^{-1}A_1^{-1} \\ &= R_1A_1R_1^{-1}A_1^{-1} \end{aligned}$$

following from $A_1 = (JR_1^{-1}J)^2$, that is, $A_1R_1 = R_1A_1$. Obviously, the above steps are reversible, this complete the proof. □

Remark 3.5.5. For the general case of Mostow's groups of the first type with the values of p, k, the orbifold Euler characteristic has been calculated in [Sau90, Par09], that is,

$$\chi(\mathbf{H}^2_{\mathbb{C}}/\Gamma) = \frac{1}{2}\left[2\left(\frac{1}{2} - \frac{1}{p}\right) - \frac{1}{k}\right]^2.$$

Therefore, we can show again the Euler characteristic

$$\chi(M) = \chi(\mathbf{H}^2_{\mathbb{C}}/G_2) = \chi(\mathbf{H}^2_{\mathbb{C}}/\Gamma) = \frac{1}{72}$$

for $p = 3$ and $k = 6$ following from the Proposition 3.5.4.

Chapter 4

The Euclidean Picard modular lattices

This chapter has been accepted for publication in *Transactions of the American Mathematical Society.*

4.1 Introduction

Let $\mathcal{K} = \mathbb{Q}(\sqrt{-d})$ be a quadratic imaginary number field. Let $\mathcal{O}_d$ be the ring of algebraic integers of $\mathcal{K}$. The Bianchi groups $PSL_2(\mathcal{O}_d)$ are the simplest arithmetically defined discrete groups. In number theory they have been used to study the zeta-functions of binary Hermitian forms over the rings $\mathcal{O}_d$. As isometry groups acting on the half-upper space, they are of interest in the theory of Kleinian groups and the related theory of hyperbolic orbifolds. Bianchi groups can be considered as the natural algebraic generalization of the classical modular group $PSL_2(\mathbb{Z})$. A good general reference for the Bianchi groups and their relation to the modular group is [Fin89]. Likewise, *Picard modular groups* $PU(2,1;\mathcal{O}_d)$ is a natural generalization of the Bianchi groups. These groups have attracted a great deal of attention both for their intrinsic interest as discrete groups (see Holzapfel's book [Hol98]) and also for their applications in complex hyperbolic geometry (as holomorphic automorphism subgroups).

A general method to determine finite presentations for each of the Bianchi group $PSL_2(\mathcal{O}_d)$ was developed by Swan [Swa71] based on geometrical work of Bianchi, while a separate purely algebraic method was given by Cohn [Coh68]. The purpose of this chapter is to give a description of generators for certain Picard modular groups $PU(2,1;\mathcal{O}_d)$ where the ring $\mathcal{O}_d$ is Euclidean except for $d = 1, 3$ (these two exceptional cases have been studied in many aspects). Among the quadratic imaginary number rings $\mathcal{O}_d$ only $\mathcal{O}_1, \mathcal{O}_2, \mathcal{O}_3, \mathcal{O}_7, \mathcal{O}_{11}$ have a Euclidean algorithm, see [STa79], although there is a larger finite collection of $\mathcal{O}_d$'s ($d = 1$, 2, 3, 7, 11, 19, 43, 67, 163, see [Zin79]) which have class number one. For these values of d the orbifold $\mathbf{H}^2_{\mathbb{C}}/PU(2,1;\mathcal{O}_d)$ has only one cusp.

The main idea (inspired by the work in [FP06, FFP10, Zh11]), is to begin by finding suitable generators of the stabilizer of infinity of $PU(2,1;\mathcal{O}_d)$ and then construct a fundamental domain for the stabilizer acting on the boundary of complex hyperbolic space $\partial\mathbf{H}^2_{\mathbb{C}}$. The generators of the groups in ([FP06], [FFP10], [Zh11]) are easy to obtain since the fundamental domain constructed lies completely inside the boundary of the largest isometric sphere centered at origin. The real difficulty for the Picard modular groups studied here is to determine more isometric spheres such that the region that is the intersection of the exteriors of these isometric spheres and the fundamental domain for the stabilizer of the point at infinity we construct later has only one cusp. Again this reflects the underlying number theory; $\mathcal{O}_1$ and $\mathcal{O}_3$ have non-trivial units while the other three do not. A simple algorithm to decompose any transformation in the Picard group $PU(2,1;\mathcal{O}_1)$ as a product of the generators was given in [FFLP11], it would be interesting to extend their method to other Picard modular groups. However, it would also be important to find the generators in a geometric way. This will provide more important information for future research on the construction of an explicit fundamental domain for each of the Picard modular groups.

4.2 On the structure of the stabilizer

In this section we will obtain the generators and a presentation of the stabilizer of the point at infinity by analysis of the fundamental domain in the Heisenberg group.

Let $\mathcal{O}_d$ be the ring of integers in the quadratic imaginary number field $\mathbb{Q}(i\sqrt{d})$, where d is a positive square-free integer. If $d \equiv 1, 2 \ (mod\ 4)$, then $\mathcal{O}_d = \mathbb{Z}[i\sqrt{d}]$ and if $d \equiv 3 \ (mod\ 4)$, then $\mathcal{O}_d = \mathbb{Z}[\omega_d]$, where $\omega_d = (1 + i\sqrt{d})/2$. The group $\Gamma_d = PU(2, 1; \mathcal{O}_d)$ is called *Euclidean Picard modular group* if the ring $\mathcal{O}_d$ is Euclidean, namely, only the rings $\mathcal{O}_1, \mathcal{O}_2, \mathcal{O}_3, \mathcal{O}_7, \mathcal{O}_{11}$. Further relative to amalgamation property, these five groups can be subclassified into three groupings $\{\Gamma_1\}$, $\{\Gamma_3\}$, $\{\Gamma_2, \Gamma_7, \Gamma_{11}\}$. Since two classes $\{\Gamma_1\}, \{\Gamma_3\}$ (*c.f.* [FP06], [FFP10]) have been studied in detail, we mainly describe the remaining class $\{\Gamma_2, \Gamma_7, \Gamma_{11}\}$.

4.2.1 The stabilizer of q_∞

First we want to analyze $(\Gamma_d)_\infty$ with $d = 2, 7, 11$, the stabilizer of q_∞. Every element of $(\Gamma_d)_\infty$ is upper triangular and its diagonal entries are units in $\mathcal{O}_d$. Recall that the units of $\mathcal{O}_1$ are $\pm 1, \pm i$, they are $\pm 1, \pm\omega, \pm\omega^2$ for $\mathcal{O}_3$ and they are ± 1 for others. Therefore $(\Gamma_d)_\infty$ contains no dilations and so is a subgroup of $Isom(\mathcal{N})$ and fits into the exact sequence as

$$0 \longrightarrow \mathbb{R} \cap (\Gamma_d)_\infty \longrightarrow (\Gamma_d)_\infty \xrightarrow{\Pi_*} \Pi_*((\Gamma_d)_\infty) \longrightarrow 1.$$

We can write the isometry group of the integer lattice as

$$Isom(\mathcal{O}_d) = \left\{ \begin{bmatrix} \alpha & \beta \\ 0 & 1 \end{bmatrix} : \alpha, \beta \in \mathcal{O}_d, \alpha \text{ is a unit} \right\}.$$

We now find the image and kernel in this exact sequence.

Proposition 4.2.1. *The stabilizer $(\Gamma_d)_\infty$ of q_∞ in Γ_d satisfies*

$$0 \longrightarrow 2\sqrt{d}\mathbb{Z} \longrightarrow (\Gamma_d)_\infty \xrightarrow{\Pi_*} \Delta \longrightarrow 1,$$

where $\Delta \subset Isom(\mathcal{O}_d)$ is of index 2 if $d \equiv 2(mod\ 4)$ and $\Delta = Isom(\mathcal{O}_d)$ if $d \equiv 3(mod\ 4)$.

Proof. Although we only consider the cases $d = 2, 7, 11$, the ring $\mathcal{O}_2$ represents those for the values of d with $d \equiv 2(mod\ 4)$ and the rings $\mathcal{O}_7, \mathcal{O}_{11}$ represent those of the values $d \equiv 3(mod\ 4)$, the remaining case is the same as $\mathcal{O}_1$ which has been done in [FFP10]. Observe that $Isom(\mathcal{O}_d)$ is generated by the subgroup of translations

$$\left\{ \hat{T}_\beta = \begin{bmatrix} 1 & \beta \\ 0 & 1 \end{bmatrix} : \beta \in \mathcal{O}_d \right\}$$

and the finite subgroup of order two

$$\left\{ \hat{R}_\alpha = \begin{bmatrix} \alpha & 0 \\ 0 & 1 \end{bmatrix} : \alpha \in \mathcal{O}_d, \alpha \text{ is a unit} \right\}.$$

Then, to understand $\Delta \subset Isom(\mathcal{O}_d)$, it suffices to determine which translations can be lifted. We divide into two cases to complete the proof.

(i) **The case $\mathcal{O}_d$ with $d \equiv 2(mod\ 4)$**

Suppose that $\beta \in \mathcal{O}_d = \mathbb{Z}[i\sqrt{d}]$ and consider the translation $\hat{T}_\beta$ by β in $\mathbb{Z}[i\sqrt{d}]$ given above. The preimage of $\hat{T}_\beta$ under Π_* has the form

$$T_{\beta,t} = \begin{bmatrix} 1 & -\overline{\beta} & \frac{-|\beta|^2 + it}{2} \\ 0 & 1 & \beta \\ 0 & 0 & 1 \end{bmatrix}.$$

This map is in $PU(2,1;\mathbb{Z}[i\sqrt{d}])$ if and only if $|\beta|^2$ is an even integer and $t \in 2\sqrt{d}\mathbb{Z}$. Writing $\beta = m + i\sqrt{d}n$ for $m, n \in \mathbb{Z}$, then we can obtain $m \equiv 0 \ (mod\ 2)$ from the conditions $|\beta|^2 = m^2 + dn^2 \in 2\mathbb{Z}$ and $d \equiv 2(mod\ 4)$. Therefore, we conclude that $\Delta \subset Isom(\mathbb{Z}[i\sqrt{d}])$ is of index 2. Also, the kernel of Π_* is generated by

$$\begin{bmatrix} 1 & 0 & i\sqrt{d} \\ 0 & 1 & 0 \\ 0 & 0 & 1 \end{bmatrix},$$

which is a vertical translation of $(0, 2\sqrt{2})$.

(ii) **The case $\mathcal{O}_d$ with $d \equiv 3(mod\ 4)$**

Suppose that $\beta = m + n\frac{1+i\sqrt{d}}{2} \in \mathcal{O}_d$ with $m, n \in \mathbb{Z}$ for $d \equiv 3(mod\ 4)$. By the same argument of (i), it only suffices to determine m, n such that $|\beta|^2$ is an integer. For $d \equiv 3(mod\ 4)$, it is easy to show that $|\beta|^2 = m^2 + mn + n^2(d+1)/4 \in \mathbb{Z}$ for any $m, n \in \mathbb{Z}$, which implies that $\Delta = Isom(\mathcal{O}_d)$. Obviously, the kernel of Π_* is generated by a vertical translation of $(0, 2\sqrt{d})$.

□

4.2.2 Fundamental domains for the stabilizer

As the first step towards the construction of a fundamental domain for the action of $(\Gamma_d)_\infty$ on the Heisenberg group $\mathcal{N}$ for $d = 2, 7, 11$, we shall find the suitable generators of $Isom(\mathcal{O}_d)$ to construct a fundamental domain in $\mathbb{C}$. This was already done by Feustel and Hozapfel in [Feu84, FH83], we state it again for the convenience for the reader.

In the proof of Proposition 4.2.1 we saw that $\Delta = \Pi_*((\Gamma_2)_\infty)$ is a subgroup of index 2 in $Isom(\mathcal{O}_2)$ consisting of elements of $\mathrm{GL}(2, \mathcal{O}_2)$ of the form

$$\left\{ \begin{bmatrix} (-1)^j & m + i\sqrt{2}n \\ 0 & 1 \end{bmatrix} : j = 0, 1, m, n \in \mathbb{Z}, m \equiv 0(mod\ 2) \right\}.$$

A fundamental domain for this group is the triangle in $\mathbb{C}$ with vertices at $-1 + \sqrt{2}i/2$ and $1 \pm \sqrt{2}i/2$; see (a) in Figure 4.1. Side paring maps are given by

$$r_1^{(2)} = \begin{bmatrix} -1 & 0 \\ 0 & 1 \end{bmatrix},\ r_2^{(2)} = \begin{bmatrix} -1 & 2 \\ 0 & 1 \end{bmatrix},\ r_3^{(2)} = \begin{bmatrix} -1 & \sqrt{2}i \\ 0 & 1 \end{bmatrix}.$$

The first of these is a rotation of order 2 fixing origin, the second is a rotation of order 2 fixing 1 and the third is a rotation of order 2 fixing $\sqrt{2}i/2$. Indeed every element of $\Delta = GL(2, \mathcal{O}_2)$ is generated by $r_1^{(2)}, r_2^{(2)}, r_3^{(2)}$ as follows

$$\begin{aligned} \begin{bmatrix} (-1)^j & 2m + \sqrt{2}ni \\ 0 & 1 \end{bmatrix} &= \begin{bmatrix} 1 & 2 \\ 0 & 1 \end{bmatrix}^m \begin{bmatrix} 1 & \sqrt{2}i \\ 0 & 1 \end{bmatrix}^n \begin{bmatrix} -1 & 0 \\ 0 & 1 \end{bmatrix}^j \\ &= \left(r_2^{(2)} r_1^{(2)}\right)^m \left(r_3^{(2)} r_1^{(2)}\right)^n \left(r_1^{(2)}\right)^j. \end{aligned}$$

As the same argument, a fundamental domain for $Isom(\mathcal{O}_d)$ with $d = 7$ or 11 is the triangle in $\mathbb{C}$ with vertices at $(-1 + i\sqrt{d})/4$, $(1 - i\sqrt{d})/4$ and $(3 + i\sqrt{d})/4$; see (b) in Figure 4.1. Side paring maps are given by

$$r_1^{(d)} = \begin{bmatrix} -1 & 0 \\ 0 & 1 \end{bmatrix},\ r_2^{(d)} = \begin{bmatrix} -1 & 1 \\ 0 & 1 \end{bmatrix},\ r_3^{(d)} = \begin{bmatrix} -1 & (1 + i\sqrt{d})/2 \\ 0 & 1 \end{bmatrix}.$$

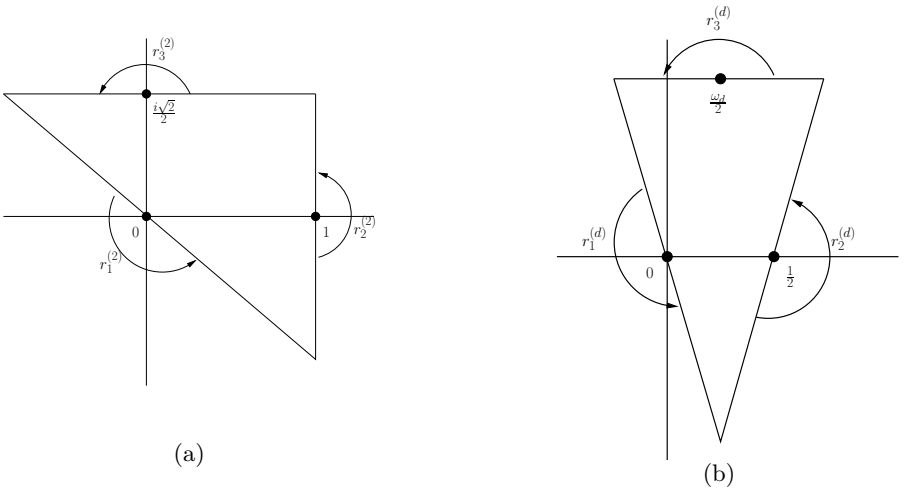

FIGURE 4.1: (a) Fundamental domain for a subgroup Δ of $Isom(\mathcal{O}_2)$ with index 2. (b) Fundamental domain for $Isom(\mathcal{O}_d)$ with $d = 7, 11$. This is also valid for all the values of d with $d \equiv 3(mod\ 4)$.

All these maps are rotations by π fixing $0, 1/2$ and $(1 + i\sqrt{d})/4$ respectively.

In order to produce a fundamental domain for $(\Gamma_d)_\infty$ we look at all the preimages of the triangle (that is a fundamental domain of $\Pi_*((\Gamma_d)_\infty)$) under vertical projection Π and we intersect this with a fundamental domain for $\ker(\Pi_*)$. The inverse of image of the triangle under Π is an infinite prism. The kernel of Π_* is the infinite cyclic group generated by T, the vertical translation by $(0, 2\sqrt{d})$. We give the generators and geometric presentations for the isotropy subgroups $(\Gamma_d)_\infty$ by analysis of the combinatorics of the fundamental domain in the Heisenberg group and compare on presentations with those given by Dekimpe [Dek96].

Proposition 4.2.2. $(\Gamma_2)_\infty$ *is generated by*

$$R_1^{(2)} = \begin{bmatrix} 1 & 0 & 0 \\ 0 & -1 & 0 \\ 0 & 0 & 1 \end{bmatrix}, \quad R_2^{(2)} = \begin{bmatrix} 1 & 2 & -2 \\ 0 & -1 & 2 \\ 0 & 0 & 1 \end{bmatrix},$$

$$R_3^{(2)} = \begin{bmatrix} 1 & -i\sqrt{2} & -1 \\ 0 & -1 & i\sqrt{2} \\ 0 & 0 & 1 \end{bmatrix} \quad \textit{and} \quad T^{(2)} = \begin{bmatrix} 1 & 0 & i\sqrt{2} \\ 0 & 1 & 0 \\ 0 & 0 & 1 \end{bmatrix}.$$

A presentation is given by

$$(\Gamma_2)_\infty = \langle R_j^{(2)}, T^{(2)} | {R_j^{(2)}}^2 = [T^{(2)}, R_j^{(2)}] = \left(T^{(2)^2} R_1^{(2)} R_3^{(2)} R_2^{(2)}\right)^2 = Id \rangle.$$

Proof. Those matrices are constructed by lifting generators of the subgroup $\Delta \subset Isom(\mathcal{O}_2)$ with index 2 and also $T^{(2)}$ is a generator of the kernel of the map Π_*. A fundamental domain can be constructed with side pairings as Figure 4.2, where the vertices of the prism are $v_3^+ = (-1+\sqrt{2}i/2, \sqrt{2})$, $v_2^+ = (1+\sqrt{2}i/2, \sqrt{2})$, $v_1^+ = (1-\sqrt{2}i/2, \sqrt{2})$ for the upper cap of the prism and $v_3^- = (-1 + \sqrt{2}i/2, -\sqrt{2})$, $v_2^- = (1 + \sqrt{2}i/2, -\sqrt{2})$, $v_1^- = (1 - \sqrt{2}i/2, -\sqrt{2})$ for the base. In particular, the points $v_4^\pm$, $v_5^\pm$, $v_6^\pm$ are the middle points of the edges $(v_1^\pm, v_2^\pm)$, $(v_2^\pm, v_3^\pm)$ and $(v_3^\pm, v_1^\pm)$, respectively.

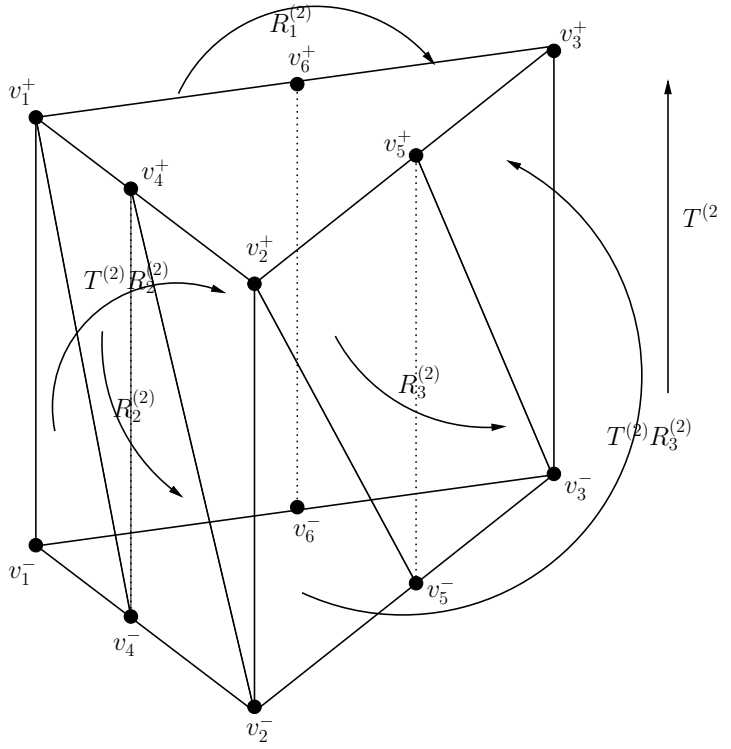

FIGURE 4.2: A fundamental domain $\mathbf{P}_2$ for $(\Gamma_2)_\infty$ in the Heisenberg group: the map $R_1^{(2)}$ rotates through π about $z = 0$, the map $R_2^{(2)}$ is a Heisenberg rotation through π about $z = 1$ and the map $R_3^{(2)}$ is a Heisenberg rotation through π about $z = \sqrt{2}i/2$.

The actions of side-pairing maps on $\mathcal{N}$ are given by

$$\begin{aligned}
R_1^{(2)}(z,t) &= (-z,t),\\
R_2^{(2)}(z,t) &= (-z+2, t+4\Im(z)),\\
R_3^{(2)}(z,t) &= (-z+i\sqrt{2}, t-2\sqrt{2}\Re(z)),\\
T^{(2)}(z,t) &= (z, t+2\sqrt{2}).
\end{aligned}$$

We describe the side pairing in terms of the action on the vertices:

$$\begin{aligned}
R_1^{(2)} &: (v_6^+, v_1^+, v_1^-, v_6^-) \longrightarrow (v_6^+, v_3^+, v_3^-, v_6^-),\\
R_2^{(2)} &: (v_1^+, v_4^+, v_4^-) \longrightarrow (v_2^-, v_4^+, v_4^-),\\
T^{(2)}R_2^{(2)} &: (v_1^+, v_1^-, v_4^-) \longrightarrow (v_2^+, v_2^-, v_4^+),\\
R_3^{(2)} &: (v_2^+, v_5^+, v_5^-) \longrightarrow (v_3^-, v_5^+, v_5^-),\\
T^{(2)}R_3^{(2)} &: (v_2^+, v_2^-, v_5^-) \longrightarrow (v_3^+, v_3^+, v_5^+),\\
T^{(2)} &: (v_1^-, v_4^-, v_2^-, v_5^-, v_3^-, v_6^-) \longrightarrow (v_1^+, v_4^+, v_2^+, v_5^+, v_3^+, v_6^+).
\end{aligned}$$

The presentation can be obtained following from the edge cycles of the fundamental domain.

Writting $\alpha = R_1^{(2)}$, $a = R_1^{(2)}R_2^{(2)}$, $b = R_1^{(2)}R_3^{(2)}$ and $c = T^{(2)}$, then it is easy to see that this presentation is equivalent to the presentation of the almost-crystallographic group of type $Q = p2$ given in the page 160 of [Dek96] with $k_1 = 4$ and $k_2 = k_3 = k_4 = 0$. □

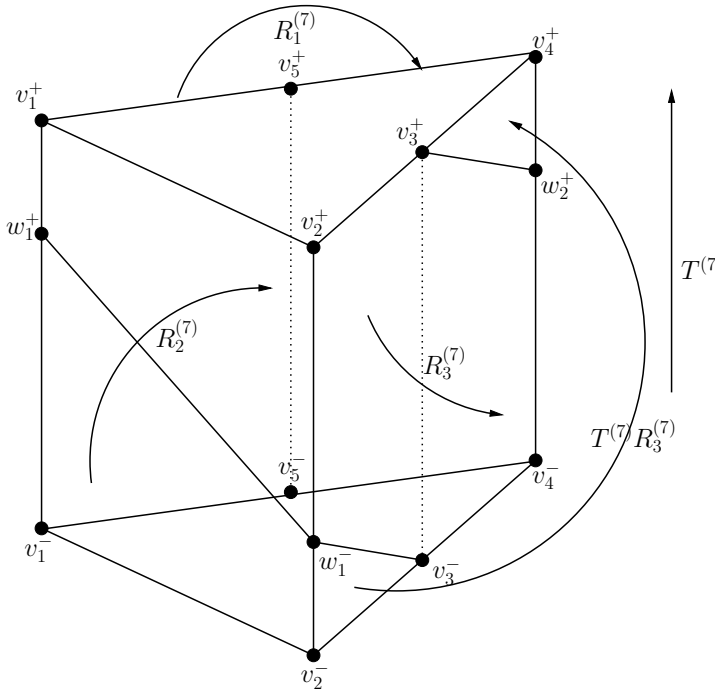

FIGURE 4.3: A fundamental domain $\mathbf{P}_7$ for $(\Gamma_7)_\infty$ in the Heisenberg group: the map $R_1^{(7)}$ rotates through π about $z = 0$, the action of parabolic $R_2^{(7)}$ is a Heisenberg rotation through π about $z = 1/2$ followed by an upward vertical translation by $\sqrt{7}$ and the map $R_3^{(7)}$ is a Heisenberg rotation through π about $z = (1 + i\sqrt{7})/4$.

Proposition 4.2.3. $(\Gamma_7)_\infty$ *is generated by*

$$R_1^{(7)} = \begin{bmatrix} 1 & 0 & 0 \\ 0 & -1 & 0 \\ 0 & 0 & 1 \end{bmatrix}, \quad R_2^{(7)} = \begin{bmatrix} 1 & 1 & -\overline{\omega}_7 \\ 0 & -1 & 1 \\ 0 & 0 & 1 \end{bmatrix},$$

$$R_3^{(7)} = \begin{bmatrix} 1 & \overline{\omega}_7 & -1 \\ 0 & -1 & \omega_7 \\ 0 & 0 & 1 \end{bmatrix} \quad \textit{and} \quad T^{(7)} = \begin{bmatrix} 1 & 0 & i\sqrt{7} \\ 0 & 1 & 0 \\ 0 & 0 & 1 \end{bmatrix}.$$

A presentation is given by

$$(\Gamma_7)_\infty = \langle R_j^{(7)}, T^{(7)} | {R_1^{(7)}}^2 = {R_3^{(7)}}^2 = [T^{(7)}, R_1^{(7)}] = [T^{(7)}, R_3^{(7)}] = T^{(7)} {R_2^{(7)}}^{-2} = \left(R_1^{(7)} R_3^{(7)} R_2^{(7)}\right)^2 = Id \rangle.$$

Proof. Those matrices are constructed by lifting generators of $Isom(\mathcal{O}_7)$ and also $T^{(7)}$ is a generator of the kernel of the map Π_*. A fundamental domain can be constructed with side pairings as Figure 4.3, where the vertices of the prism are $v_1^+ = ((1 - i\sqrt{7})/4, \sqrt{7})$, $v_2^+ = ((3+i\sqrt{7})/4, \sqrt{7})$, $v_4^+ = ((-1+i\sqrt{7})/4, \sqrt{7})$ for the upper cap of the prism and $v_1^- = ((1-i\sqrt{7})/4, -\sqrt{7})$, $v_2^- = ((3+i\sqrt{7})/4, -\sqrt{7})$, $v_4^- = ((-1+i\sqrt{7})/4, -\sqrt{7})$ for the base. The points $v_3^\pm$ and $v_5^\pm$ are the middle points of the edges $(v_2^\pm, v_4^\pm)$ and $(v_4^\pm, v_1^\pm)$. In particular, we introduce more three points $w_1^+ = ((1 - i\sqrt{7})/4, \sqrt{7}/2)$, $w_2^- = ((3 + i\sqrt{7})/4, -\sqrt{7}/2)$

and $w_3^+ = ((-1+i\sqrt{7})/4, \sqrt{7}/2)$. The actions of side-pairing maps on $\mathcal{N}$ are given by

$$\begin{aligned} R_1^{(7)}(z,t) &= (-z,t),\\ R_2^{(7)}(z,t) &= (-z+1, t+2\Im(z)+\sqrt{7}),\\ R_3^{(7)}(z,t) &= (-z+\omega_7, t+2\Im(\overline{\omega}_7 z)),\\ T^{(7)}(z,t) &= (z, t+2\sqrt{7}). \end{aligned}$$

We describe the side pairing in terms of the action on the vertices:

$$\begin{aligned} R_1^{(7)} &: (v_5^+, v_1^+, v_1^-, v_5^-) \longrightarrow (v_5^+, v_4^+, v_4^-, v_5^-),\\ R_2^{(7)} &: (v_1^-, v_2^-, w_1^-, w_1^+) \longrightarrow (w_1^-, w_1^+, v_1^+, v_2^+),\\ R_3^{(7)} &: (v_2^+, w_1^-, v_3^-, v_3^+) \longrightarrow (w_2^+, v_4^-, v_3^-, v_3^+),\\ T^{(7)}R_3^{(7)} &: (w_1^-, v_2^-, v_3^-) \longrightarrow (v_4^+, w_2^+, v_3^+),\\ T^{(7)} &: (v_1^-, v_2^-, v_3^-, v_4^-, v_5^-) \longrightarrow (v_1^+, v_2^+, v_3^+, v_4^+, v_5^+). \end{aligned}$$

The presentation can be obtained following from the edge cycles of the fundamental domain.

Writting $\alpha = R_1^{(7)}$, $a = R_1^{(7)}R_2^{(7)}$, $b = R_1^{(7)}R_3^{(7)}$ and $c = T^{(7)}$, then it is easy to see that this presentation is equivalent to the presentation of the almost-crystallographic group of type $Q = p2$ given in the page 160 of [Dek96] with $k_1 = k_2 = 1$ and $k_3 = k_4 = 0$. □

Proposition 4.2.4. $(\Gamma_{11})_\infty$ *is generated by*

$$R_1^{(11)} = \begin{bmatrix} 1 & 0 & 0\\ 0 & -1 & 0\\ 0 & 0 & 1 \end{bmatrix}, \quad R_2^{(11)} = \begin{bmatrix} 1 & 1 & -\overline{\omega}_{11}\\ 0 & -1 & 1\\ 0 & 0 & 1 \end{bmatrix},$$

$$R_3^{(11)} = \begin{bmatrix} 1 & \overline{\omega}_{11} & -1-\overline{\omega}_{11}\\ 0 & -1 & \omega_{11}\\ 0 & 0 & 1 \end{bmatrix} \quad \textit{and} \quad T^{(11)} = \begin{bmatrix} 1 & 0 & i\sqrt{11}\\ 0 & 1 & 0\\ 0 & 0 & 1 \end{bmatrix}.$$

A presentation is given by

$$\begin{aligned} (\Gamma_{11})_\infty = \langle R_j^{(11)}, T^{(11)} | {R_1^{(11)}}^2 = [T^{(11)}, R_1^{(11)}] = T^{(11)}{R_2^{(11)}}^{-2}\\ = T^{(11)}{R_3^{(11)}}^{-2} = T^{(11)}\left(R_1^{(11)}R_3^{(11)}R_2^{(11)}\right)^{-2} = Id\rangle. \end{aligned}$$

Proof. Those matrices are constructed by lifting generators of $Isom(\mathcal{O}_{11})$ and also $T^{(11)}$ is a generator of the kernel of the map Π_*. A fundamental domain can be constructed with side pairings as Figure 4.4, where the vertices of the prism are $v_1^+ = ((1-i\sqrt{11})/4, \sqrt{11})$, $v_2^+ = ((3+i\sqrt{11})/4, 3\sqrt{11}/2)$, $v_3^+ = ((-1+i\sqrt{11})/4, 2\sqrt{11})$ for the upper cap of the prism and $v_1^- = ((1-i\sqrt{11})/4, -\sqrt{11})$, $v_2^- = ((3+i\sqrt{11})/4, -\sqrt{11}/2)$, $v_3^- = ((-1+i\sqrt{11})/4, 0)$ for the base. The points $v_0^\pm$ are the middle points of the edges $(v_1^\pm, v_3^\pm)$. In particular, we introduce more three points $w_1 = ((1-i\sqrt{11})/4, 0)$, $w_2 = ((3+i\sqrt{11})/4, \sqrt{11}/2)$ and $w_3 = ((-1+i\sqrt{11})/4, \sqrt{11})$. The actions of side-pairing maps on $\mathcal{N}$ are given by

$$\begin{aligned} R_1^{(11)}(z,t) &= (-z,t),\\ R_2^{(11)}(z,t) &= (-z+1, t+2\Im(z)+\sqrt{11}),\\ R_3^{(11)}(z,t) &= (-z+\omega_{11}, t+2\Im(\overline{\omega}_{11} z)+\sqrt{11}),\\ T^{(11)}(z,t) &= (z, t+2\sqrt{11}). \end{aligned}$$

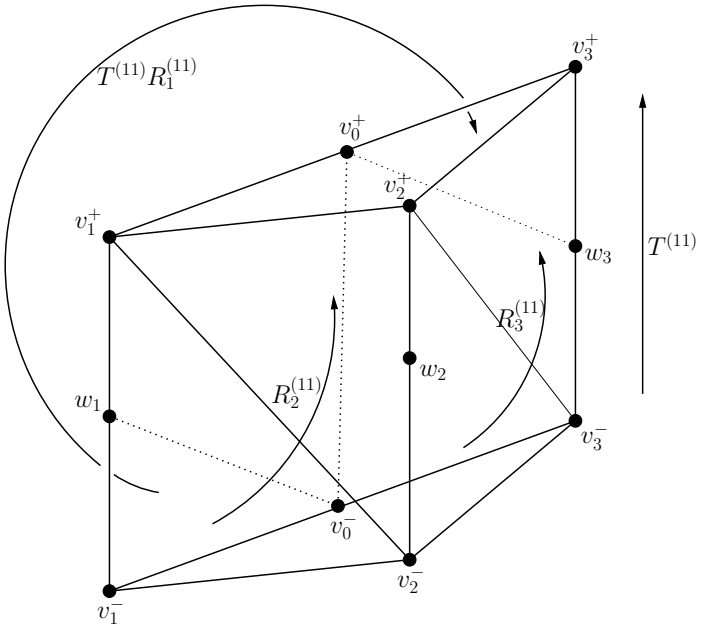

FIGURE 4.4: A fundamental domain $\mathbf{P}_{11}$ for $(\Gamma_{11})_\infty$ in the Heisenberg group: the map $R_1^{(11)}$ rotates through π about $z = 0$, the action of parabolic $R_2^{(11)}$ is a screw Heisenberg rotation through π about $z = 1/2$ followed by an upward vertical translation by $\sqrt{11}$ and the map $R_3^{(11)}$ is a screw Heisenberg rotation through π about $z = (1 + i\sqrt{11})/4$ followed by an upward vertical translation by $\sqrt{11}$.

We describe the side pairing in terms of the action on the vertices:

$$\begin{aligned}
R_1^{(11)} &: (v_0^+, v_1^+, w_1, v_0^-) \longrightarrow (v_0^+, w_3, v_3^-, v_0^-),\\
T^{(11)}R_1^{(11)} &: (w_1, v_1^-, v_0^-) \longrightarrow (v_3^+, w_3, v_0^+),\\
R_2^{(11)} &: (v_1^+, w_1, v_1^-, v_2^-) \longrightarrow (v_2^+, w_2, v_2^-, v_1^+),\\
R_3^{(11)} &: (v_2^+, w_2, v_2^-, v_3^-) \longrightarrow (v_3^+, w_3, v_3^-, v_2^+),\\
T^{(11)} &: (v_0^-, v_1^-, v_2^-, v_3^-) \longrightarrow (v_0^+, v_1^+, v_2^+, v_3^+).
\end{aligned}$$

The presentation can be obtained following from the edge cycles of the fundamental domain.

Writting $\alpha = R_1^{(11)}$, $a = R_1^{(11)}R_2^{(11)}$, $b = R_1^{(11)}R_3^{(11)}$ and $c = T^{(11)}$, then it is easy to see that this presentation is equivalent to the presentation of the almost-crystallographic group of type $Q = p2$ given in the page 160 of [Dek96] with $k_1 = k_4 = 0$ and $k_2 = k_3 = 0$. □

4.3 Statement of the results

In this section, we introduce the method used in ([FP06], [FFP10] and [Zh11]) to determine the generators of the Euclidean Picard modular groups and then state our results.

Recall the map

$$I_0 = \begin{bmatrix} 0 & 0 & 1 \\ 0 & -1 & 0 \\ 1 & 0 & 0 \end{bmatrix}$$

defined in the Section 2.2. We consider the isometric sphere $\mathcal{B}_0$ of I_0 given by (2.2), which is a Cygan sphere centred at $o = (0, 0, 0)$ with radius $\sqrt{2}$. Observe that I_0 maps $\mathcal{B}_0$ to itself and swaps the inside and the outside of $\mathcal{B}_0$. Given an element of Γ_d of the form (2.4), we know that the radius of its isometric sphere is $\sqrt{2/|g|}$. For each case $\mathcal{O}_d$, the radius of isometric sphere is not greater than $\sqrt{2}$ since the absolute of g is not smaller than 1 for $g \in \mathcal{O}_d$. We show that the largest isometric spheres are all images of $\mathcal{B}_0$ under the elements in $(\Gamma_d)_\infty$.

Proposition 4.3.1. *An isometric sphere has the largest radius if and only if it is the image of $\mathcal{B}_0$ under an element in $(\Gamma_d)_\infty$.*

Proof. Obviously, the image of $\mathcal{B}_0$ under an element in $(\Gamma_d)_\infty$ has the same radius $\sqrt{2}$. Conversely, given an element G of the form (2.4) such that $G(q_\infty) \neq q_\infty$, then the isometric sphere of G has the largest radius only if $g = 1$. So the center of the isometric sphere of G in horospherical coordinates is $G^{-1}(\infty) = (\overline{h}, 2\Im(j), 0)$. Since $\overline{h}$ and $2\Im(\overline{j}) \in \mathcal{O}_d$, we can take a Heisenberg translation $T \in (\Gamma_d)_\infty$ mapping the origin to $(\overline{h}, 2\Im(\overline{j}))$. Writing $T' = GTI_0$, we know that T' fixes ∞. We conclude explicitly that the isometric sphere of G is

$$\left\{ \mathbf{z} \in \mathbf{H}^2_{\mathbb{C}} : |\langle \mathbf{z}, q_\infty \rangle| = |\langle \mathbf{z}, G^{-1}(q_\infty) \rangle| = |\langle \mathbf{z}, TI_0(q_\infty) \rangle| \right\},$$

which is the image of $\mathcal{B}_0$ under T. □

Our method is based on the special feature that the orbifold $\mathbf{H}^2_{\mathbb{C}}/\Gamma_d$ has only one cusp for $d = 2, 7, 11$. For these types of orbifolds, one would like to construct a fundamental domain using the Ford domain (that is the intersection of the exteriors of isometric spheres of all elements not fixing infinity), namely, the intersection of the Ford domain and a fundamental domain for the stabilizer of infinity. The Ford domain is canonical, but we can choose a fundamental domain for the stabilizer freely. In the previous section, we found suitable generators of the stabilizer and constructed a fundamental domain for the stabilizer in the Heisenberg group. We will show that adjoining I_0 to $(\Gamma_d)_\infty$ gives the Euclidean Picard modular groups Γ_d. The basic idea of the proof is analogous to Theorem 3.5 of [FP06].

- Find a sufficient many of isometric spheres such that the union of the interior of the boundary of these isometric spheres in the Heisenberg group covers each of the prisms we constructed in the previous section. The problem of determining the isometric spheres, as the key point, will be shown in the next section.

- From the first step, there is a fundamental domain for $\langle R_1^{(d)}, R_2^{(d)}, R_3^{(d)}, T^{(d)}, I_0 \rangle$ contained in the region that is obtained from the intersection of the exteriors of a finite many isometric spheres found in the above step with the fundamental domain for the stabilizer of infinity. It is obviously that this region is not exactly a fundamental domain since the isometric spheres which we found are sufficiently but not necessarily to cover the prism. However, this region has only one cusp; see Figure 4.5.

- Clearly, it follows that $\langle R_1^{(d)}, R_2^{(d)}, R_3^{(d)}, T^{(d)}, I_0 \rangle$ has only one cusp q_∞. Since the group $\langle R_1^{(d)}, R_2^{(d)}, R_3^{(d)}, T^{(d)}, I_0 \rangle$ is a subgroup of Γ_d and both groups have cofinite

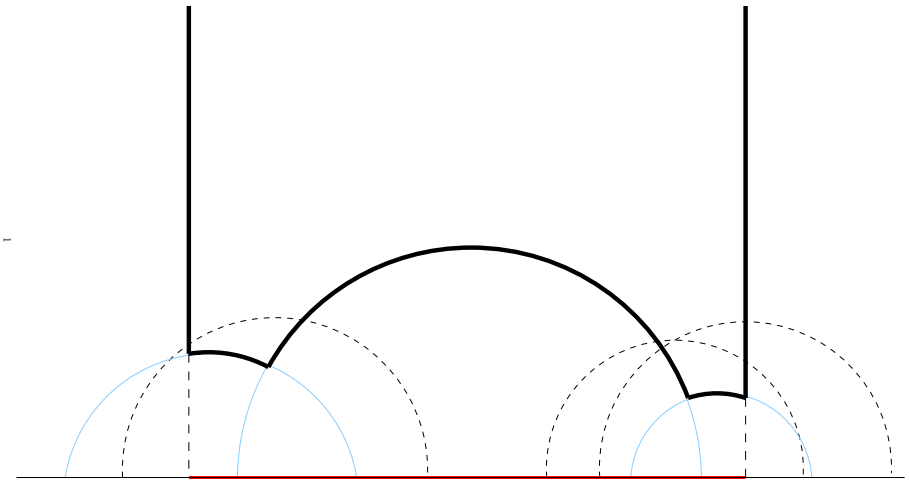

FIGURE 4.5: A schematic view in 2-dimension. The red line indicates a fundamental domain for the cusp group in the Heisenberg group. The region bounded by the bold lines (arcs) contains a fundamental domain for $\langle R_1^{(d)}, R_2^{(d)}, R_3^{(d)}, T^{(d)}, I_0\rangle$. The half-circles drawn by the dotted line are other possible isometric spheres intersecting with the fundamental domain for the cusp group.

volume, $\langle R_1^{(d)}, R_2^{(d)}, R_3^{(d)}, T^{(d)}, I_0\rangle$ must have finite index. Therefore, the fact that both groups have the same stabilizer of q_∞ implies they are the same.

After we check the determination of isometric spheres, we obtain the main results as follows.

Theorem 4.3.2. *Let $\mathcal{K} = \mathbb{Q}(\sqrt{-2})$ and let $\mathcal{O}_2 = \mathbb{Z}[i\sqrt{2}]$. Then the group $PU(2,1,\mathcal{O}_2)$ is generated by the elements*

$$I_0 = \begin{bmatrix} 0 & 0 & 1 \\ 0 & -1 & 0 \\ 1 & 0 & 0 \end{bmatrix}, R_1^{(2)} = \begin{bmatrix} 1 & 0 & 0 \\ 0 & -1 & 0 \\ 0 & 0 & 1 \end{bmatrix}, R_2^{(2)} = \begin{bmatrix} 1 & 2 & -2 \\ 0 & -1 & 2 \\ 0 & 0 & 1 \end{bmatrix},$$

$$R_3^{(2)} = \begin{bmatrix} 1 & -i\sqrt{2} & -1 \\ 0 & -1 & i\sqrt{2} \\ 0 & 0 & 1 \end{bmatrix} \quad \textit{and} \quad T^{(2)} = \begin{bmatrix} 1 & 0 & i\sqrt{2} \\ 0 & 1 & 0 \\ 0 & 0 & 1 \end{bmatrix}.$$

Theorem 4.3.3. *Let $\mathcal{K} = \mathbb{Q}(\sqrt{-7})$ and let $\mathcal{O}_7 = \mathbb{Z}[\omega_7]$, where $\omega_7 = \frac{1}{2}(1 + i\sqrt{7})$, be the ring of integers of $\mathcal{K}$. Then the group $PU(2,1,\mathcal{O}_7)$ is generated by the elements*

$$I_0 = \begin{bmatrix} 0 & 0 & 1 \\ 0 & -1 & 0 \\ 1 & 0 & 0 \end{bmatrix}, R_1^{(7)} = \begin{bmatrix} 1 & 0 & 0 \\ 0 & -1 & 0 \\ 0 & 0 & 1 \end{bmatrix}, R_2^{(7)} = \begin{bmatrix} 1 & 1 & -\overline{\omega}_7 \\ 0 & -1 & 1 \\ 0 & 0 & 1 \end{bmatrix},$$

$$R_3^{(7)} = \begin{bmatrix} 1 & \overline{\omega}_7 & -1 \\ 0 & -1 & \omega_7 \\ 0 & 0 & 1 \end{bmatrix} \quad \textit{and} \quad T^{(7)} = \begin{bmatrix} 1 & 0 & i\sqrt{7} \\ 0 & 1 & 0 \\ 0 & 0 & 1 \end{bmatrix}.$$

Theorem 4.3.4. *Let $\mathcal{K} = \mathbb{Q}(\sqrt{-11})$ and let $\mathcal{O}_{11} = \mathbb{Z}[\omega_{11}]$, where $\omega_{11} = \frac{1}{2}(1 + i\sqrt{11})$, be the ring of integers of $\mathcal{K}$. Then the group $PU(2, 1, \mathcal{O}_{11})$ is generated by the elements*

$$I_0 = \begin{bmatrix} 0 & 0 & 1 \\ 0 & -1 & 0 \\ 1 & 0 & 0 \end{bmatrix}, R_1^{(11)} = \begin{bmatrix} 1 & 0 & 0 \\ 0 & -1 & 0 \\ 0 & 0 & 1 \end{bmatrix}, R_2^{(11)} = \begin{bmatrix} 1 & 1 & -\overline{\omega}_{11} \\ 0 & -1 & 1 \\ 0 & 0 & 1 \end{bmatrix},$$

$$R_3^{(11)} = \begin{bmatrix} 1 & \overline{\omega}_{11} & -1 - \overline{\omega}_{11} \\ 0 & -1 & \omega_{11} \\ 0 & 0 & 1 \end{bmatrix} \quad \text{and} \quad T^{(11)} = \begin{bmatrix} 1 & 0 & i\sqrt{11} \\ 0 & 1 & 0 \\ 0 & 0 & 1 \end{bmatrix}.$$

Remark 4.3.5. For other values of d such that $\mathcal{O}_d$ has class number one, namely $d = 19$, $43, 67, 163$, we can construct the same type of fundamental domain for $(\Gamma_d)_\infty$ in the Heisenberg group as $(\Gamma_{11})_\infty$. All generators as the above types lie in $PU(2, 1; \mathcal{O}_d)$, but we don't know whether adjoining the element I_0 to $(\Gamma_d)_\infty$ generates the full group $PU(2, 1; \mathcal{O}_d)$. Furthermore, the method of [FFLP11] could not be extended to non-Euclidean Picard modular groups.

4.4 Determination of the isometric spheres

Recall that the Cygan sphere $\mathcal{B}_0$ is the isometric sphere of I_0. The boundary of $\mathcal{B}_0$ is a *spinal sphere* denoted by $\mathcal{S}_0$ (this is not the same as the one in Chapter 3) in the Heisenberg group, which is defined by

$$\mathcal{S}_0 = \left\{(z, t) : \left||z|^2 + it\right| = 2\right\}. \tag{4.1}$$

Indeed we only need to consider the boundaries of isometric spheres in the Heisenberg group because two isometric spheres have a non-empty interior intersection if and only if their boundaries have a non-empty interior intersection.

4.4.1 The case $\mathcal{O}_2$

In the cases of $PU(2, 1; \mathcal{O}_1)$ and $PU(2, 1; \mathcal{O}_3)$, all the vertices of the fundamental domain for the stabilizer of q_∞ acting on $\partial\mathbf{H}^2_{\mathbb{C}}$ lie inside $\mathcal{S}_0$. For the group $PU(2, 1; \mathcal{O}_2)$, it is not hard to show that six vertices of the prism $\mathbf{P}_2$ lie outside $\mathcal{S}_0$. Therefore we need to find more isometric spheres whose boundaries together with $\mathcal{S}_0$ contain the prism $\mathbf{P}_2$.

We consider the map

$$I_0 R_2^{(2)} I_0 = \begin{bmatrix} 1 & 0 & 0 \\ -2 & -1 & 0 \\ -2 & -2 & 1 \end{bmatrix},$$

whose isometric sphere which we denote by $\mathcal{B}_1$ is a Cygan sphere centered at the point $(1, 0, 0)$ (in horospherical coordinates) with radius 1. The boundary of $\mathcal{B}_1$ is given by

$$\mathcal{S}_1 = \left\{(z, t) : \left||z - 1|^2 + it + 2i\Im(z)\right| = 1\right\}. \tag{4.2}$$

Minimizing the number of spinal spheres by the symmetry of $R_1^{(2)}$, it suffices to consider $\mathcal{S}_0$ and several images of $\mathcal{S}_1$ under some suitable elements in $(\Gamma_2)_\infty$. In Heisenberg

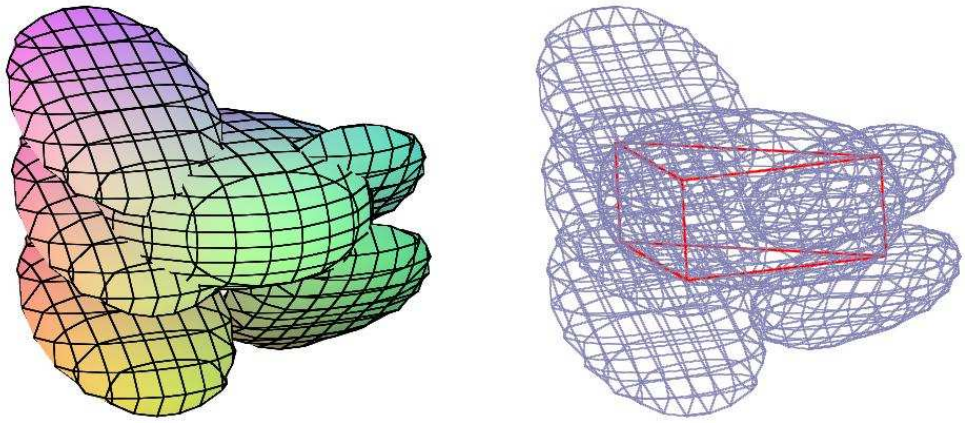

(a) (b)

FIGURE 4.6: (a) The shading view of neighboring spinal spheres containing the fundamental domain for $(\Gamma_2)_\infty$. (b) Another view for these spinal spheres.

coordinates these are given by

$$\begin{aligned}
T^{(2)}(\mathcal{S}_1) &= \left\{(z,t) : \left||z-1|^2 + it - 2i\sqrt{2} + 2i\Im(z)\right| = 1\right\},\\
T^{(2)^{-1}}(\mathcal{S}_1) &= \left\{(z,t) : \left||z-1|^2 + it + 2i\sqrt{2} + 2i\Im(z)\right| = 1\right\},\\
R_1^{(2)}(\mathcal{S}_1) &= \left\{(z,t) : \left||z+1|^2 + it - 2i\Im(z)\right| = 1\right\},\\
T^{(2)^{-1}}R_1^{(2)}(\mathcal{S}_1) &= \left\{(z,t) : \left||z+1|^2 + it + 2i\sqrt{2} - 2i\Im(z)\right| = 1\right\}.
\end{aligned}$$

We claim that the prism $\mathbf{P}_2$ lies inside the union of $\mathcal{S}_0$ and these images of $\mathcal{S}_1$, see Figure 4.6 for viewing these spinal spheres.

Proposition 4.4.1. *The prism $\mathbf{P}_2$ is contained in the union of the interiors of the spinal spheres $\mathcal{S}_0$, $\mathcal{S}_1$, $T^{(2)}(\mathcal{S}_1)$, $T^{(2)^{-1}}(\mathcal{S}_1)$, $R_1^{(2)}(\mathcal{S}_1)$ and $T^{(2)^{-1}}R_1^{(2)}(\mathcal{S}_1)$.*

Proof. It suffices to show there exist three points $(v_1^+)^{(j)}$ $(j = 1,2,3)$ on the edges (v_1^+, v_1^-), (v_1^+, v_2^+) and (v_1^+, v_3^+) which lie in the intersection of the interiors of $\mathcal{S}_0$ and $\mathcal{S}_1$ such that the tetrahedron $\mathbb{T}(v_1^+)$ with vertices v_1^+, $(v_1^+)^{(1)}$, $(v_1^+)^{(2)}$, $(v_1^+)^{(3)}$ lies inside $\mathcal{S}_1$. By the same argument, we can also obtain five other tetrahedra $\mathbb{T}(v_2^+)$, $\mathbb{T}(v_3^+)$, $\mathbb{T}(v_1^-)$, $\mathbb{T}(v_2^-)$, $\mathbb{T}(v_3^-)$ with apex v_2^+, v_3^+, v_1^-, v_2^-, v_3^- respectively such that $\mathbb{T}(v_2^+) \in Int(T^{(2)}(\mathcal{S}_1))$, $\mathbb{T}(v_3^+) \in Int(R_1^{(2)}(\mathcal{S}_1))$, $\mathbb{T}(v_1^-) \in Int(T^{(2)^{-1}}(\mathcal{S}_1))$, $\mathbb{T}(v_2^-) \in Int(\mathcal{S}_1)$ and $\mathbb{T}(v_3^-) \in Int(T^{(2)^{-1}}R_1^{(2)}(\mathcal{S}_1))$. Moreover, the core part obtained by cutting off six the tetrahedra from the prism lies inside $\mathcal{S}_0$.

We shall prove the existence of the tetrahedron $\mathbb{T}(v_1^+)$ and the others follow similarly. The edge joining v_1^+ and v_1^- is contained in the complex line $z = 1 - \sqrt{2}i/2$ which is given by points with Heisenberg coordinates

$$z = 1 - \sqrt{2}i/2, \quad -\sqrt{2} \le t \le \sqrt{2}.$$

The edge joining v_1^+ and v_2^+ is given by points with Heisenberg coordinates

$$\Re(z) = 1, \quad -\sqrt{2}/2 \le \Im(z) \le \sqrt{2}/2, \quad t = \sqrt{2}.$$

The edge joining v_1^+ and v_3^+ is given by points with Heisenberg coordinates

$$\Re(z) = -\sqrt{2}\Im(z), \quad t = \sqrt{2}.$$

From the equations (4.1) and (4.2), the points on the edge (v_1^+, v_1^-) lie in the intersection of the interiors of $\mathcal{S}_0$ and $\mathcal{S}_1$ if and only if

$$|3/2 + it| < 2 \quad \text{and} \quad \left|1/2 - (t - \sqrt{2})i\right| < 1. \tag{4.3}$$

By easy calculations, the inequalities (4.3) are equivalent to

$$\sqrt{2} - \sqrt{3}/2 < t < \sqrt{7}/2.$$

Using the same argument as above, we obtain that the points on the edge (v_1^+, v_2^+) lie in the intersection of the interiors of $\mathcal{S}_0$ and $\mathcal{S}_1$ if and only if $\Re(z) = 1$ and $-\sqrt{\sqrt{2}-1} < \Im(z) < \delta_1$, where $\delta_1 \approx -0.208$ is the largest real root of the equation $x^4+4x^2+4\sqrt{2}x+1 = 0$. The points on the edge (v_1^+, v_3^+) lie in the intersection of the interiors of $\mathcal{S}_0$ and $\mathcal{S}_1$ if and only if $\Re(z) = -\sqrt{2}\Im(z)$ and $-2^{1/4}/\sqrt{3} < \Im(z) < \delta_2$, where $\delta_2 \approx -0.264$ is the largest real root of the equation $9x^4 + 12\sqrt{2}x^3 + 18x^2 + 8\sqrt{2}x + 2 = 0$.

In term of these, we choose three points as $(v_1^+)^{(1)} = (1-\sqrt{2}i/2, 1)$ on the edge (v_1^+, v_1^-), $(v_1^+)^{(2)} = (1 - i/2, \sqrt{2})$ on the edge (v_1^+, v_2^+) and $(v_1^+)^{(3)} = (\sqrt{2}/2 - i/2, \sqrt{2})$ on the edge (v_1^+, v_3^+), which are inside the intersection of the interiors of $\mathcal{S}_0$ and $\mathcal{S}_1$. Since the vertex v_1^+ lies inside $\mathcal{S}_1$, the tetrahedron $\mathbb{T}(v_1^+)$ with the vertices v_1^+, $(v_1^+)^{(1)}$, $(v_1^+)^{(2)}$, $(v_1^+)^{(3)}$ lies inside $\mathcal{S}_1$ by Lemma 1.4.7. □

4.4.2 The case $\mathcal{O}_7$

In this case, the distance between the top and base of the fundamental domain for the stabilizer $(\Gamma_7)_\infty$ is greater than the diameter of $\mathcal{S}_0$, which implies that the prism $\mathbf{P}_7$ can not be contained inside $\mathcal{S}_0$ completely. Due to increasing the length of Heisenberg translations, only the images of $\mathcal{S}_0$ under the elements in $(\Gamma_7)_\infty$ could not cover the whole prism. We show that there are also isometric spheres with Cygan radius smaller than $\sqrt{2}$ whose centers are near to the origin.

Therefore we consider the map

$$Q = I_0 R_2^{(7)} I_0 = \begin{bmatrix} 1 & 0 & 0 \\ 1 & 1 & 0 \\ \overline{\omega}_7 & 1 & 1 \end{bmatrix}.$$

Consider the isometric spheres of Q and Q^{-1}, which we denote by $\mathcal{B}_2$ and $\mathcal{B}_3$, respectively. The center of $\mathcal{B}_2$ is $Q^{-1}(\infty)$, which is the point with horospherical coordinates $(1/4 + i\sqrt{7}/4, \sqrt{7}/2, 0)$ and the center of $\mathcal{B}_3$, is $Q(\infty)$ which has horospherical coordinates $(1/4 - i\sqrt{7}/4, \sqrt{7}/2, 0)$. Both these isometric spheres have Cygan radius $\sqrt{2/|\omega_7|} = 2^{1/4}$. The boundaries of these isometric spheres $\mathcal{B}_2$ and $\mathcal{B}_3$ are in Heisenberg coordinates given by

$$\mathcal{S}_2 = \left\{(z,t) : \left||z - \omega_7/2|^2 + it + i\sqrt{7}/2 + i\Im(\overline{\omega}_7 z)\right| = \sqrt{2}\right\}, \tag{4.4}$$

$$\mathcal{S}_3 = \left\{(z,t) : \left||z - \overline{\omega}_7/2|^2 + it - i\sqrt{7}/2 + i\Im(\omega_7 z)\right| = \sqrt{2}\right\}. \tag{4.5}$$

In order to cover the prim $\mathbf{P}_7$ by the spinal spheres, we use the symmetry property of $R_1^{(7)}$. It suffices to consider $\mathcal{S}_0, \mathcal{S}_2$ and the images of $\mathcal{S}_0$ and $\mathcal{S}_3$ under suitable elements in

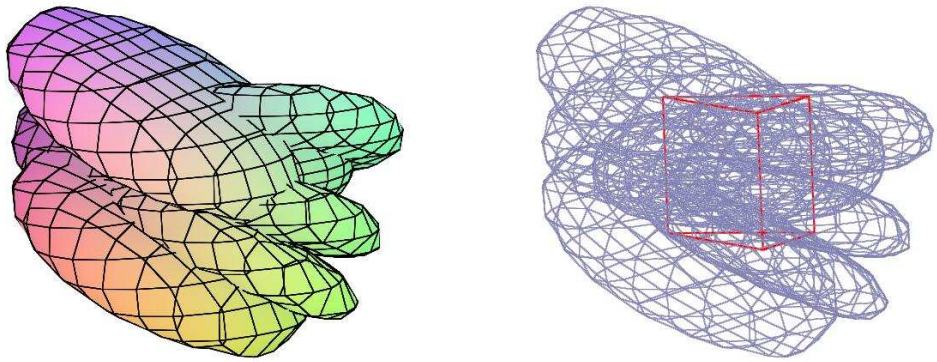

(a) (b)

FIGURE 4.7: (a) The shading view of neighboring spinal spheres containing the fundamental domain for $(\Gamma_7)_\infty$. (b) Another view for these spinal spheres.

$(\Gamma_7)_\infty$. These spinal spheres are points with Heisenberg coordinates given by

$$\begin{aligned}
R_2^{(7)}(\mathcal{S}_0) &= \left\{(z,t) : \left||z-1|^2 + it - i\sqrt{7} + 2i\Im(z)\right| = 4\right\},\\
R_2^{(7)^{-1}}(\mathcal{S}_0) &= \left\{(z,t) : \left||z-1|^2 + it + i\sqrt{7} + 2i\Im(z)\right| = 4\right\},\\
R_2^{(7)^{-1}}(\mathcal{S}_3) &= \left\{(z,t) : \left||z-(1+\omega_7)/2|^2 + it + i\sqrt{7} + i\Im((1+\overline{\omega}_7))\right| = \sqrt{2}\right\},\\
R_3^{(7)}R_2^{(7)}(\mathcal{S}_3) &= \left\{(z,t) : \left||\zeta+\overline{\omega}_7/2|^2 + it - i\sqrt{7}/2 - i\Im(\omega_7 z)\right| = \sqrt{2}\right\},\\
R_1^{(7)}R_3^{(7)}R_2^{(7)}(\mathcal{S}_3) &= \left\{(z,t) : \left||z-\overline{\omega}_7/2|^2 + it - i\sqrt{7}/2 + i\Im(\omega_7 z)\right| = \sqrt{2}\right\}.
\end{aligned}$$

We claim that the prism $\mathbf{P}_7$ lies inside the union of $\mathcal{S}_0$, $\mathcal{S}_2$ and these images $R_2^{(7)}(\mathcal{S}_0)$, $R_2^{(7)^{-1}}(\mathcal{S}_0)$, $R_2^{(7)^{-1}}(\mathcal{S}_3)$, $R_3^{(7)}R_2^{(7)}(\mathcal{S}_3)$, $R_1^{(7)}R_3^{(7)}R_2^{(7)}(\mathcal{S}_3)$, see Figure 4.7 for viewing these spinal spheres.

Proposition 4.4.2. *The prism* $\mathbf{P}_7$ *is contained in the union of the interiors of the spinal spheres* $\mathcal{S}_0$, $\mathcal{S}_2$, $R_2^{(7)}(\mathcal{S}_0)$, $R_2^{(7)^{-1}}(\mathcal{S}_0)$, $R_2^{(7)^{-1}}(\mathcal{S}_3)$, $R_3^{(7)}R_2^{(7)}(\mathcal{S}_3)$ *and* $R_1^{(7)}R_3^{(7)}R_2^{(7)}(\mathcal{S}_3)$.

Proof. It suffices to show that the prism $\mathbf{P}_7$ can be decomposed into several pieces as polyhedra such that each polyhedron lies inside a spinal sphere which is described in the proposition and the common face of two adjacent polyhedra lie in the intersection of the interior of two spinal spheres which contain these two polyhedra.

We need to add sixteen points on the faces of the prism $\mathbf{P}_7$ in order to decompose the prim into seven polyhedra. These points are given, in Heisenberg coordinates, by

$$\begin{aligned}
p_1 &= (1/4 - i\sqrt{7}/4, 3/2), & p_2 &= (0.11 - i11\sqrt{7}/100, 1.44 + \sqrt{7}/50),\\
p_3 &= (1/2, 8/5), & p_4 &= (-1/10 + i\sqrt{7}/10, \sqrt{7}),\\
p_5 &= (-1/10 + i\sqrt{7}/10, \sqrt{7}/2), & p_6 &= (3/4 + i\sqrt{7}/4, 1.7),\\
p_7 &= (-1/4 + i\sqrt{7}/4, 1), & p_8 &= (1/4 - i\sqrt{7}/4, -1),\\
p_9 &= (1/60 - i\sqrt{7}/60, -2\sqrt{7}/3), & p_{10} &= (-1/20 + i\sqrt{7}/20, -\sqrt{7}),\\
p_{11} &= (3/5 + i\sqrt{7}/10, -2\sqrt{7}/3), & p_{12} &= (7/10 + i\sqrt{7}/5, -\sqrt{7}),\\
p_{13} &= (3/4 + i\sqrt{7}/4, -2\sqrt{7}/3), & p_{14} &= (5/12 + i\sqrt{7}/4, -2\sqrt{7}/3),\\
p_{15} &= (1/4 + i\sqrt{7}/4, -\sqrt{7}), & p_{16} &= (-1/4 + i\sqrt{7}/4, -1).
\end{aligned}$$

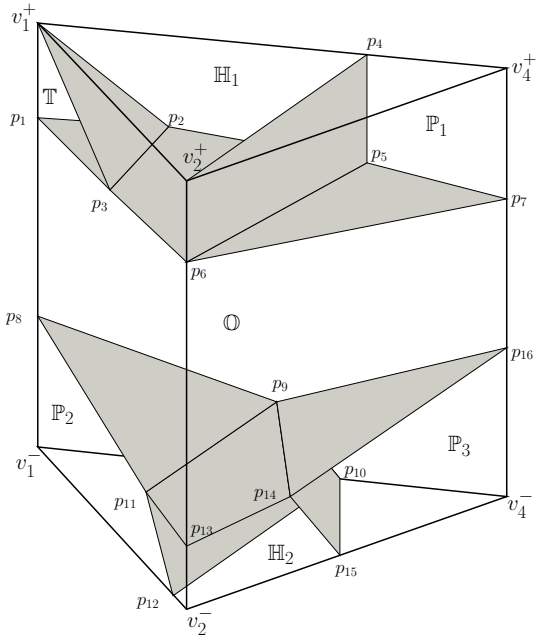

FIGURE 4.8: The decomposition of the prism $\mathbf{P}_7$ into the pieces of polyhedra.

We describe these polyhedra as follows:

- The tetrahedron $\mathbb{T}$ with the vertices v_1^+, p_1, p_2, p_3;
- The hexahedron $\mathbb{H}_1$ with the vertices v_1^+, v_2^+, p_2, p_3, p_4, p_5, p_6;
- The pentahedron $\mathbb{P}_1$ with the vertices v_2^+, p_4, p_5, p_6, v_4^+, p_7;
- The pentahedron $\mathbb{P}_2$ with the vertices v_1^-, p_8, p_9, p_{10}, p_{11}, p_{12};
- The hexahedron $\mathbb{H}_2$ with the vertices p_9, p_{10}, p_{11}, p_{12}, p_{13}, v_2^-, p_{14}, p_{15};
- The pentahedron $\mathbb{P}_3$ with the vertices p_9, p_{10}, p_{14}, p_{15}, p_{16}, v_4^+;
- The octahedron $\mathbb{O}$ with the vertices p_1, p_2, p_3, p_5, p_6, p_7, p_8, p_9, p_{11}, p_{13}, p_{14}, p_{16}.

Note that the face (p_1, p_2, p_3) of $\mathbb{T}$ and the face (p_2, p_3, p_5, p_6) of $\mathbb{H}_1$ are on the face (p_1, p_5, p_6) of $\mathbb{O}$; the common face (v_2^+, p_4, p_5, p_6) of $\mathbb{H}_1$ and $\mathbb{P}_1$ is a vertical plane; the face $(p_9, p_{11}, p_{13}, p_{14})$ of $\mathbb{H}_2$ is parallel to the base of the prism. Furthermore, the faces $(p_9, p_{10}, p_{11}, p_{12})$ and $(p_9, p_{10}, p_{14}, p_{15})$ are the trapeziums since the edge (p_9, p_{11}) is parallel to (p_{10}, p_{12}) and the edge (p_9, p_{14}) is parallel to (p_{10}, p_{15}).

By examining the location of the points and applying Lemma 1.4.7, we conclude that the tetrahedron $\mathbb{T}$ is inside the spinal sphere $R_1^{(7)} R_3^{(7)} R_2^{(7)}(\mathcal{S}_3)$; the hexahedron $\mathbb{H}_1$ is contained inside the spinal sphere $R_2^{(7)}(\mathcal{S}_0)$; the pentahedron $\mathbb{P}_1$ is inside $R_3^{(7)} R_2^{(7)}(\mathcal{S}_3)$; the pentahedron $\mathbb{P}_2$ is contained inside ${R_2^{(7)}}^{-1}(\mathcal{S}_0)$; the hexahedron $\mathbb{H}_2$ is contained inside ${R_2^{(7)}}^{-1}(\mathcal{S}_3)$; the pentahedron $\mathbb{P}_3$ is inside $\mathcal{S}_2$; the remaining octahedron $\mathbb{O}$ is inside $\mathcal{S}_0$; see Figure 4.8 for viewing the polyhedral decomposition of the prism. □

4.4.3 The case $\mathcal{O}_{11}$

In this case, we again know that the fundamental domain for the stabilizer $(\Gamma_{11})_\infty$ cannot be inside $\mathcal{S}_0$ completely. The radius of spinal spheres other than the largest are so small that these spinal spheres do not contribute much to covering the prism $\mathbf{P}_{11}$. Due to the different shape of the prism $\mathbf{P}_{11}$ with the case $\mathcal{O}_7$, we only need to consider the largest spinal spheres which are the images of $\mathcal{S}_0$ under the elements of $(\Gamma_{11})_\infty$. In order to determine a union of the spinal spheres which covers the prism $\mathbf{P}_{11}$, we minimize their number by the symmetry of $R_1^{(11)}$. It suffices to consider $\mathcal{S}_0$ and the images of $\mathcal{S}_0$ under suitable elements in $(\Gamma_{11})_\infty$. In Heisenberg coordinates they are given by

$$\begin{aligned}
T^{(11)}(\mathcal{S}_0) &= \left\{(z,t) : \left||z|^2 + it - 2i\sqrt{11} + 2i\Im(z)\right| = 4\right\},\\
R_2^{(11)}(\mathcal{S}_0) &= \left\{(z,t) : \left||z-1|^2 + it - i\sqrt{11} + 2i\Im(z)\right| = 4\right\},\\
R_1^{(11)}R_2^{(11)}(\mathcal{S}_0) &= \left\{(z,t) : \left||z+1|^2 + it - i\sqrt{11} - 2i\Im(z)\right| = 4\right\},\\
{R_2^{(11)}}^{-1}(\mathcal{S}_0) &= \left\{(z,t) : \left||z-1|^2 + it + i\sqrt{11} + 2i\Im(z)\right| = 4\right\},\\
R_3^{(11)}(\mathcal{S}_0) &= \left\{(z,t) : \left||z-\omega_{11}|^2 + it - i\sqrt{11} - 2i\Im(\overline{\omega}_{11}z)\right| = 4\right\},\\
{R_3^{(11)}}^{-1}(\mathcal{S}_0) &= \left\{(z,t) : \left||z-\omega_{11}|^2 + it + i\sqrt{11} - 2i\Im(\overline{\omega}_{11}z)\right| = 4\right\},\\
R_3^{(11)}R_2^{(11)}(\mathcal{S}_0) &= \left\{(z,t) : \left||z+\overline{\omega}_{11}|^2 + it - i\sqrt{11} - 2i\Im(\omega_{11}z)\right| = 4\right\},\\
R_1^{(11)}R_3^{(11)}R_2^{(11)}(\mathcal{S}_0) &= \left\{(z,t) : \left||z-\overline{\omega}_{11}|^2 + it - i\sqrt{11} + 2i\Im(\omega_{11}z)\right| = 4\right\},\\
R_1^{(11)}{R_3^{(11)}}^{-1}R_2^{(11)}(\mathcal{S}_0) &= \left\{(z,t) : \left||z-\overline{\omega}_{11}|^2 + it + i\sqrt{11} + 2i\Im(\omega_{11}z)\right| = 4\right\}.
\end{aligned}$$

Definition 4.4.3. *Let X be a closed polygonal chain (not necessarily in a plane) in 3-dimensional space, then a topological disc defined by the cone over X with apex v is called a **cone-polygon**, denoted by $\mathscr{D}_v(X)$.*

Note that a polygon in traditional sense can be interpreted as a cone-polygon, in that case, the boundary of cone-polygon and the apex lie in the same plane and moreover the apex is in the interior of the boundary. We claim that the prism $\mathbf{P}_{11}$ lies inside the union of $\mathcal{S}_0$ and its images as above, see Figure 4.9 for viewing these spinal spheres.

Proposition 4.4.4. *The prism $\mathbf{P}_{11}$ is contained in the union of the interiors of the spinal spheres $\mathcal{S}_0$, $T^{(11)}(\mathcal{S}_0)$, $R_2^{(11)}(\mathcal{S}_0)$, ${R_2^{(11)}}^{-1}(\mathcal{S}_0)$, $R_3^{(11)}(\mathcal{S}_0)$, ${R_3^{(11)}}^{-1}(\mathcal{S}_0)$, $R_3^{(11)}R_2^{(11)}(\mathcal{S}_0)$, $R_1^{(11)}R_2^{(11)}(\mathcal{S}_0)$, $R_1^{(11)}{R_3^{(11)}}^{-1}R_2^{(11)}(\mathcal{S}_0)$ and $R_1^{(11)}R_3^{(11)}R_2^{(11)}(\mathcal{S}_0)$*

Proof. Using the same argument as Proposition 4.4.2, we want to decompose the prism $\mathbf{P}_{11}$ into several polyhedral cells. The difference is the complicated intersection of the spinal spheres, which makes it difficult to decompose into several polyhedral cells, each of which is contained in one spinal sphere. Observe that a union of interiors of several spinal spheres is a star-convex set if they have a non-empty interior intersection. We shall show that the collection of these spinal spheres can be separated into several parts such that each part contains certain polyhedral cell. All these polyhedral cells are defined by the cone-polygon as its boundary.

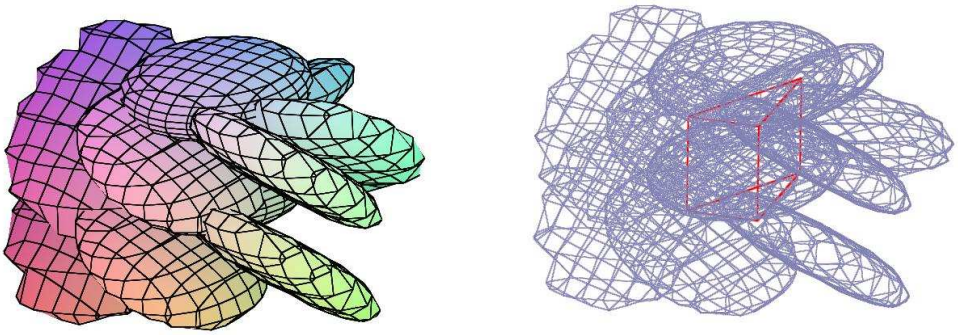

(a) (b)

FIGURE 4.9: (a) The shading view of neighboring spinal spheres containing the fundamental domain for $(\Gamma_{11})_\infty$. (b) Another view for these spinal spheres.

We first define a tetrahedron $\mathfrak{T}$ with vertices v_1^-, q_1, q_2, q_3, where

$$\begin{aligned} q_1 &= \left(1/4 - i\sqrt{11}/4, -2\sqrt{11}/3\right), \\ q_2 &= \left(3/20 - 3i\sqrt{11}/20, -4\sqrt{11}/5\right), \\ q_3 &= \left(7/20 - 3i\sqrt{11}/20, -9\sqrt{11}/10\right). \end{aligned}$$

Observe that the points q_1, q_2, q_3 lie on the edges (v_1^+, v_1^-), (v_1^-, v_3^-) and (v_1^-, v_2^-), respectively. By Lemma 1.4.7 and simple calculations show that the tetrahedron $\mathfrak{T}$ is contained inside $R_1^{(11)} {R_3^{(11)}}^{-1} R_2^{(11)}(\mathcal{S}_0)$.

Next, we define a hexahedron $\mathfrak{H}_1$ with vertices $q_1, q_2, q_3, q_4, q_5, q_6, q_7, v_0^+$ and another hexahedron $\mathfrak{H}_2$ with vertices $v_2^-, q_5, q_6, q_7, q_8, q_9$, where

$$\begin{aligned} q_4 &= \left(1/4 - i\sqrt{11}/4, -1/2\right), & q_5 &= \left(0.42 + 0.26i, -0.71\sqrt{11} + 0.39\right), \\ q_6 &= \left(0.6 + i\sqrt{11}/10, -0.65\sqrt{11}\right), & q_7 &= \left(0.58 + 2i\sqrt{11}/25, -1.92\right), \\ q_8 &= \left(3/4 + i\sqrt{11}/4, 0\right), & q_9 &= (0.55 + i\sqrt{11}/4, -2\sqrt{11}/5). \end{aligned}$$

Observe that the points q_4, q_6, q_8, q_9 lie on the edges (v_1^+, v_1^-), (v_1^-, v_2^-), (v_2^+, v_2^-) and (v_2^-, v_3^-), respectively. The points q_5 lies on the interior of the base of the prism $\mathbf{P}_{11}$ and the point q_7 lies on the interior of the face $(v_1^+, v_1^-, v_2^-, v_2^+)$. Then we know that the hexahedron $\mathfrak{H}_1$ has the faces (q_1, q_2, q_3), (q_4, q_5, v_0^-), (q_4, q_5, q_7), (q_5, q_6, q_7), (q_1, q_2, v_0^+, q_4) and $(q_1, q_3, q_6, q_7, q_4)$ and the hexahedron $\mathfrak{H}_2$ has the faces (q_5, q_6, q_7), (q_5, q_7, q_8), (v_2^-, q_8, q_9), (q_5, q_8, q_9), (q_6, q_7, q_8, v_2^-), (q_5, q_6, v_2^-, q_9). By examining the location of these points and Lemma 1.4.7, we conclude that the hexahedron $\mathfrak{H}_1$ is contained inside ${R_2^{(11)}}^{-1}(\mathcal{S}_0)$ and the hexahedron $\mathfrak{H}_2$ is lied inside ${R_3^{(11)}}^{-1}(\mathcal{S}_0)$.

We focus on describing other polyhedral cells in the decomposition of the prism $\mathbf{P}_{11}$. Let $\mathscr{U}_1$ denote the union of $R_2^{(11)}(\mathcal{S}_0)$, $R_1^{(11)}R_2^{(11)}(\mathcal{S}_0)$ and $R_1^{(11)}R_3^{(11)}R_2^{(11)}(\mathcal{S}_0)$. We verify that $q_{10} = (0.2 - 0.4i, 2.4)$ is in the intersection of the interiors of these three spinal spheres, which implies that $\mathscr{U}_1$ is a star-convex set about q_{11}. Analogously, we know $\mathscr{U}_2$, denoted by the union of $T^{(11)}(\mathcal{S}_0)$, $R_3^{(11)}(\mathcal{S}_0)$, $R_1^{(11)}R_2^{(11)}(\mathcal{S}_0)$ and $R_3^{(11)}R_2^{(11)}(\mathcal{S}_0)$, is a star-convex set about $q_{11} = (0.18 + 0.72i, 4.8)$. This can be verified by examining the location of q_{12} which is in the intersection of the interiors of these four spinal spheres. We need to add

the following points on the faces of the prism $\mathbf{P}_{11}$, each of which is in the intersection of the interiors of at least two spinal spheres.

$$\begin{array}{ll}
q_{12} = (1/4 - i\sqrt{11}/4, \sqrt{11}/2), & q_{13} = (0.21 - 0.21i\sqrt{11}, \sqrt{11}/2), \\
q_{14} = (0, \sqrt{11}/2), & q_{15} = (-0.21 + 0.21i\sqrt{11}, \sqrt{11}/2), \\
q_{16} = (i\sqrt{11}/4, 1), & q_{17} = (3/4 + i\sqrt{11}/4, 1), \\
q_{18} = (0.42 - 2i\sqrt{11}/25, 1.95), & q_{19} = (3/4 + i\sqrt{11}/4, \sqrt{11}), \\
q_{20} = (0.6 + i\sqrt{11}/10, 27\sqrt{11}/20), & q_{21} = (0.42 + 0.26i, 1.29\sqrt{11} + 0.39), \\
q_{22} = (-1.4 + 1.4i\sqrt{11}, 4\sqrt{11}/5), & q_{23} = (-1/4 + i\sqrt{11}/4, \sqrt{11}/2).
\end{array}$$

Observe that the points q_{12}, q_{20}, q_{23} lie on the edges (v_1^+, v_1^-), (v_1^+, v_2^+) and (v_3^+, v_3^-) respectively and the points q_{17}, q_{19} lie on the edge (v_2^+, v_2^-). Moreover, the points q_{13}, q_{14}, q_{15}, q_{22} lie on the interior of the face $(v_1^+, v_1^-, v_3^-, v_3^+)$, the point q_{16} lies on the interior of the face $(v_2^+, v_2^-, v_3^-, v_3^+)$, the point q_{18} lies on the interior of the face $(v_1^+, v_1^-, v_2^-, v_2^+)$ and the points q_{21} lies on the interior of the top (v_1^+, v_2^+, v_3^+). We need to add other three points in the interior of the prism $\mathbf{P}_{11}$ which are used to define the cone-polygon,

$$\begin{array}{l}
q_{24} = (-0.16 + 0.74i, 1.4), \\
q_{25} = (0.328 - 0.28i, 1.99), \\
q_{26} = (0.325 + 0.29i, 4.652).
\end{array}$$

We verify the location of all these points as follows:

- The point q_{12} is in the intersection of the interiors of $\mathcal{S}_0$ and $R_1^{(11)}R_3^{(11)}R_2^{(11)}(\mathcal{S}_0)$;
- The point q_{13} is in the intersection of the interiors of $\mathcal{S}_0$, $R_1^{(11)}R_3^{(11)}R_2^{(11)}(\mathcal{S}_0)$ and $R_1^{(11)}R_2^{(11)}(\mathcal{S}_0)$;
- The point q_{12} is in the intersection of the interiors of $\mathcal{S}_0$ and $R_1^{(11)}R_3^{(11)}R_2^{(11)}(\mathcal{S}_0)$;
- The point q_{13} is in the intersection of the interiors of $\mathcal{S}_0$, $R_1^{(11)}R_3^{(11)}R_2^{(11)}(\mathcal{S}_0)$ and $R_1^{(11)}R_2^{(11)}(\mathcal{S}_0)$;
- The point q_{14} is in the intersection of the interiors of $\mathcal{S}_0$, $R_2^{(11)}(\mathcal{S}_0)$ and $R_1^{(11)}R_2^{(11)}(\mathcal{S}_0)$;
- The point q_{15} is in the intersection of the interiors of $\mathcal{S}_0$, $R_2^{(11)}(\mathcal{S}_0)$, $R_3^{(11)}(\mathcal{S}_0)$ and $R_3^{(11)}R_2^{(11)}(\mathcal{S}_0)$;
- The points q_{16}, q_{19}, q_{20} are in the intersection of the interiors of $R_2^{(11)}(\mathcal{S}_0)$ and $R_3^{(11)}(\mathcal{S}_0)$;
- The point q_{17} is in the intersection of the interiors of $\mathcal{S}_0$ and $R_2^{(11)}(\mathcal{S}_0)$;
- The point q_{18} is in the intersection of the interiors of $\mathcal{S}_0$, $R_1^{(11)}R_3^{(11)}R_2^{(11)}(\mathcal{S}_0)$ and $R_2^{(11)}(\mathcal{S}_0)$;
- The point q_{21} is in the intersection of the interiors of $T^{(11)}(\mathcal{S}_0)$, $R_2^{(11)}(\mathcal{S}_0)$ and $R_3^{(11)}(\mathcal{S}_0)$;
- The point q_{22} is in the intersection of the interiors of $R_1^{(11)}R_2^{(11)}(\mathcal{S}_0)$, $R_2^{(11)}(\mathcal{S}_0)$ and $R_3^{(11)}(\mathcal{S}_0)$;
- The point v_0^+ is in the intersection of the interiors of $R_1^{(11)}R_2^{(11)}(\mathcal{S}_0)$ and $T^{(11)}(\mathcal{S}_0)$, $R_2^{(11)}(\mathcal{S}_0)$;

- The point q_{23} is in the intersection of the interiors of $\mathcal{S}_0$, $R_3^{(11)}(\mathcal{S}_0)$ and $R_3^{(11)}R_2^{(11)}(\mathcal{S}_0)$;
- The point q_{24} is in the intersection of the interiors of $\mathcal{S}_0$, $R_2^{(11)}(\mathcal{S}_0)$, $R_3^{(11)}(\mathcal{S}_0)$ and $R_3^{(11)}R_2^{(11)}(\mathcal{S}_0)$;
- The point q_{25} is in the intersection of the interiors of $\mathcal{S}_0$, $R_2^{(11)}(\mathcal{S}_0)$, $R_1^{(11)}R_2^{(11)}(\mathcal{S}_0)$ and $R_1^{(11)}R_3^{(11)}R_2^{(11)}(\mathcal{S}_0)$;
- The point q_{26} is in the intersection of the interiors of $T^{(11)}(\mathcal{S}_0)$, $R_2^{(11)}(\mathcal{S}_0)$, $R_3^{(11)}(\mathcal{S}_0)$ and $R_1^{(11)}R_2^{(11)}(\mathcal{S}_0)$.

In terms of these, we denote by X_1 a closed polygonal chain joining in order with the points p_{12}, p_{13}, p_{14}, p_{15}, p_{16}, p_{17}, p_{18} and denote by X_2 a closed polygonal chain joining in order with the points p_{16}, p_{19}, p_{20}, p_{21}, v_0^+, p_{22}, p_{24}. So then we can define two cone-polygons $\mathscr{D}_{q_{25}}(X_1)$ and $\mathscr{D}_{q_{26}}(X_2)$. By examining the locations of these points, we show that $\mathscr{D}_{q_{25}}(X_1)$ is in the intersection of the interiors of $\mathcal{S}_0$, $\mathcal{U}_1$ and $\mathscr{D}_{q_{26}}(X_2)$ is in the intersection of the interiors of $R_2^{(11)}(\mathcal{S}_0)$ and $T^{(11)}(\mathcal{S}_0)$, $R_1^{(11)}R_2^{(11)}(\mathcal{S}_0)$, $R_3^{(11)}(\mathcal{S}_0)$, namely, the intersection of the interiors of $\mathscr{U}_1$ and $\mathscr{U}_2$. The remaining faces can be easily verified which are contained inside $\mathcal{S}_0, \mathscr{U}_1$ or $\mathscr{U}_2$.

Finally, we define three polyhedral cells as follows:

(i) The polyhedral cell $\mathfrak{P}_1$ is defined by its boundary as the faces $\mathscr{D}_{q_{25}}(X_1)$, $\mathscr{D}_{q_{26}}(X_2)$, $(v_1^+, q_{20}, q_{21}, v_0^+)$, $(v_1^+, q_{12}, q_{18}, q_{17}, q_{19}, q_{20})$ and $(v_1^+, q_{12}, q_{13}, q_{14}, q_{15}, q_{22}, v_0^+)$;

(ii) The polyhedral cell $\mathfrak{P}_2$ is defined by the faces $\mathscr{D}_{q_{26}}(X_2)$, (q_{23}, q_{16}, q_{24}), (q_{15}, q_{23}, q_{24}), $(v_1^+, q_{20}, q_{21}, v_0^+)$, $(v_1^+, q_{12}, q_{18}, q_{17}, q_{19}, q_{20})$ and $(v_1^+, q_{12}, q_{13}, q_{14}, q_{15}, q_{22}, v_0^+)$ as its boundary;

(iii) The polyhedral cell $\mathfrak{P}_3$ is defined by the faces $\mathscr{D}_{q_{25}}(X_1)$, (q_4, q_5, q_7), (q_5, q_7, q_8), (q_4, q_5, v_0^-), (v_3^-, v_0^-, q_5, q_9), $(q_8, q_9, v_3^-, q_{23}, q_{16}, q_{17})$, (q_{15}, q_{23}, q_{24}), $(q_4, q_7, q_8, q_{17}, q_{18}, q_{12})$, (q_{23}, q_{16}, q_{24}) and $(q_{12}, q_{13}, q_{14}, q_{15}, q_{23}, v_3^-, v_0^-, q_4)$ as its boundary.

By Lemma 1.4.7 and the properties of star-convex of $\mathscr{U}_1$ and $\mathscr{U}_2$, we conclude that the polyhedral cell $\mathfrak{P}_1$ contained inside $\mathscr{U}_1$; the polyhedral cell $\mathfrak{P}_2$ contained inside $\mathscr{U}_2$; the polyhedral cell $\mathfrak{P}_3$ is contained inside $\mathcal{S}_0$. This completes the proof. □

Chapter 5

New construction of fundamental domains for certain Mostow groups

5.1 Introduction

In [Mos80] Mostow used the construction of fundamental domain to show that certain subgroups of $PU(2,1)$ are lattices. More recently, there has been a renewed interest in construction of fundamental domain (see [DFP05, FP06, FFP10, Par06, Zh11]. In particular, Deraux, Falbel and Paupert gave a new construction of fundamental domains for some of the groups considered by Mostow in [Mos80]. In this chapter we give another construction for the same groups. Our construction generalizes the fundamental domain we gave for the sister of the Eisenstein-Picard modular group. This generalization is in the same spirit as the construction of fundamental domains for Livné's groups given by Parker [Par06] which generalizes the construction of the domain for the Eisenstein-Picard modular group given in [FP06].

Mostow groups are generated by three complex reflections R_1, R_2, R_3 each of order $p = 3, 4, 5$. The complex lines fixed by three reflections are permuted by a map J of order 3, equivalently, $JR_iJ^{-1} = R_{i+1}$ (indices taken cyclically). So $\langle R_1, R_2, R_3\rangle$ is a normal subgroup of $\langle R_1, J\rangle$ with index 3 (or 1). Moreover, the complex reflection R_i satisfies the braid relation $R_iR_jR_i = R_jR_iR_j$. Such groups are determined up to conjugation by a real parameter, which Mostow calls a *phase shift*, and denoted by φ. These groups have the property that $A_i = (JR_i^{-1}J)^2$ is also a complex reflection and there is a one to one correspondence between the phase shift parameter φ and the angle of this reflection A_i. In order for $\langle R_1, J\rangle$ to be discrete, the complex reflection A_i should have finite order and we take this order to be k. Following Parker [Par09], we use p and k rather than φ to specify the group $\langle R_1, J\rangle$.

In this chapter we mainly restrict our attention to the case $p = 3$. When $p = 3$ the values of k that lead to a lattice are exactly those for which there is an integer l so that $1/k + 1/l = 1/6$ (see also the table of [Par09], page 27). In [Zh11] we constructed a fundamental domain for the case $k = 6$ and while we consider the case $k \geq 7$ here and we construct a fundamental domain whose shape is based on the shape of the domain in [Zh11]. The main difference is that the vertex of ∞ is replaced with a triangle in a complex line and we need to be careful when constructing geodesic cones to point this triangle. Our construction is inspired by the construction of Parker [Par06] where $p \geq 7$ and $k = 2$. The fundamental domains Parker constructed are a generalization of the construction for $p = 6, k = 2$ given in [FP06]. Again the main difference is that the vertex of ∞ is replaced with a triangle in a complex line.

Our fundamental polyhedron is a 4-dimensional domain, which is well defined by its boundary (the union of 3-cells is homeomorphic to S^3). Analogous to [Par06], the basic construction is to take a complex line L_0 instead of ∞ fixed by $\Gamma_0 \subset \Gamma$ (assume that Γ is the group we consider) and the intersection of a fundamental domain for Γ_0 and a Dirichlet type domain for Γ/Γ_0 (suppose that L_0 does not intersect any of its images under Γ/Γ_0). We adopt, in this chapter, the notions of polyhedron that the 3-dimensional $(2, 1, 0$-dimensional) skeletons of polyhedron are called the *sides* (*faces*, *edges* and *vertices*) respectively. The vertices of our polyhedron are the intersection of two complex lines. Many, but not all, edges are geodesic arcs. Most of the sides are contained in bisectors. Only two sides not contained in bisectors will be constructed; they are the foliated by the geodesic 2-dimensional cones (each of pieces called a *sheet* in what follows). Each of the faces is either contained in totally geodesic submanifolds or contained in a Giraud disc or a foliation of geodesics. Consider the group generated by the side pairings of our polyhedron, we use the appropriate version of the Poincaré's polyhedron theorem to show that our polyhedron is a fundamental domain and give a presentation for this group.

5.2 Description of the group

We consider the complex hyperbolic triangle group generated by three complex reflections R_1, R_2, R_3 of order p with the property that there is an element J of order 3 so that

$$J^3 = I, \quad R_2 = JR_1J^{-1}, \quad R_3 = JR_2J^{-1} = J^{-1}R_1J. \tag{5.1}$$

We call $\langle R_1, R_2, R_3\rangle$ an *equilateral triangle group* if satisfy the condition (5.1). For more details on complex hyperbolic triangle groups, we refer to [PPa09] as a general reference.

5.2.1 The group Γ_k

Consider an equilateral complex hyperbolic triangle group defined as (5.1), up to conjugation, equilateral complex triangle group may be parameterized by $\tau = \mathrm{tr}(R_1J)$ (see [PPa09]). For the stake of simplicity, we denote by $u = e^{2i\pi/3p}$. Using their normalization of [PPa09], we may take the Hermitian form H to be

$$H = \begin{bmatrix} 2-u^3-\overline{u}^3 & (\overline{u}^2-u)\tau & (u^2-\overline{u})\overline{\tau} \\ (u^2-\overline{u})\overline{\tau} & 2-u^3-\overline{u}^3 & (\overline{u}^2-u)\tau \\ (\overline{u}^2-u)\tau & (u^2-\overline{u})\overline{\tau} & 2-u^3-\overline{u}^3 \end{bmatrix}. \tag{5.2}$$

This leads to the following matrices in $SU(H)$ for R_1, R_2, R_3 and J:

$$R_1 = \begin{bmatrix} u^2 & \tau & -u\overline{\tau} \\ 0 & \overline{u} & 0 \\ 0 & 0 & \overline{u} \end{bmatrix}, \qquad R_2 = \begin{bmatrix} \overline{u} & 0 & 0 \\ -u\overline{\tau} & u^2 & \tau \\ 0 & 0 & \overline{u} \end{bmatrix},$$
$$R_3 = \begin{bmatrix} \overline{u} & 0 & 0 \\ 0 & \overline{u} & 0 \\ \tau & -u\overline{\tau} & u^2 \end{bmatrix}, \qquad J = \begin{bmatrix} 0 & 0 & 1 \\ 1 & 0 & 0 \\ 0 & 1 & 0 \end{bmatrix}.$$

As shown in [Par09] that $|\tau| = 1$ is equivalent to Mostow's condition that the generators R_j and R_k satisfy the braid relation $R_jR_kR_j = R_kR_jR_k$ for $j \neq k$. Furthermore, following Sauter [Sau90] we define $A_j = (JR_j^{-1}J)^2$ for $j = 1, 2, 3$, then A_j is a complex reflection or a pure Heisenberg translation.

We focus on our attention to consider the group generated by three complex reflections of order 3 and so $u^3 = e^{2i\pi/3}$ is a cube root of unity. We follow Parker and Paupert's expressions and write $\tau = -e^{-2i\pi/3k}$, and denote the corresponding group by Γ_k. Following the notation of [Zh11], we give the geometrical generators as $R = (JR_1^{-1}J)^2$, $S = JR_1^{-1}$, $T = (JR_1^{-1})^2$ and $I_1 = JR_1^{-1}J$ and so the group Γ_k may be rewritten as $\langle R, S, T, I_1\rangle$. Our main result is to construct a fundamental domain of Γ_k acting on the complex hyperbolic space and obtain a geometrical presentation for the group Γ_k.

5.2.2 The stabilizer of complex line

In this section we shall explore the isotropy subgroup of complex line in Γ_k, which gives rise to the suitable values of k we need. As described in [Zh11], the subgroup $\langle R, S, T\rangle$ is conjugate to the stabilizer of infinity. It is natural to consider the subgroup $\langle R, S, T\rangle$ of Γ_k and calculate the common eigenvector $\mathbf{n}$ of R, S and T.

Following the definitions, we see easily that $T = S^2$, which can simplify the group $\langle R, S, T\rangle$ to $\langle R, S\rangle = \langle R^{-1}S, S\rangle = \langle R_3, JR_1^{-1}\rangle$. It suffices to find a common eigenvector of R_3 and JR_1^{-1}. As the matrix of $SU(H)$,

$$R_3 = \begin{bmatrix} \overline{u} & 0 & 0 \\ 0 & \overline{u} & 0 \\ \tau & -u\overline{\tau} & u^2 \end{bmatrix}, \quad JR_1^{-1} = \begin{bmatrix} 0 & 0 & u \\ \overline{u}^2 & -\overline{u}\tau & \overline{\tau} \\ 0 & u & 0 \end{bmatrix}.$$

By simply calculations, it is easy to see that the common eigenvector of R_3 and JR_1^{-1} in $\mathbb{C}^{2,1}$ is

$$\mathbf{n} = \begin{bmatrix} u^2\overline{\tau} \\ \overline{u}^2\tau \\ -1 \end{bmatrix}.$$

Moreover, T is a complex reflection on the complex line with polar vector $\mathbf{n}$, that is the eigenvector corresponding to non-repeated eigenvalue of T.

Using the Hermitian form (5.2), the following calculations enable us to know whether the eigenvector $\mathbf{n}$ is a negative, null or positive vector in $\mathbb{C}^{2,1}$.

$$\begin{aligned} \langle \mathbf{n}, \mathbf{n}\rangle &= \begin{bmatrix} \overline{u}^2\tau & u^2\overline{\tau} & -1 \end{bmatrix} H \begin{bmatrix} u^2\overline{\tau} \\ \overline{u}^2\tau \\ -1 \end{bmatrix} \\ &= 1 - u^3 + \overline{u}^6\tau^3 - \overline{u}^3\tau^3 + u^6\overline{\tau}^3 - u^3\overline{\tau}^3 + 1 - \overline{u}^3 \\ &= 2 - u^3 - \overline{u}^3 + (u^3 - \overline{u}^3)\tau^3 + (\overline{u}^3 - u^3)\overline{\tau}^3 \\ &= 3 + 2i\sin(2\pi/3)(\tau^3 - \overline{\tau}^3) \\ &= 3 - 2\sqrt{3}\sin(2\pi/k). \end{aligned}$$

This becomes

$$\begin{aligned} \langle \mathbf{n}, \mathbf{n}\rangle > 0 &\Leftrightarrow k > 6, \\ \langle \mathbf{n}, \mathbf{n}\rangle = 0 &\Leftrightarrow k = 6, \\ \langle \mathbf{n}, \mathbf{n}\rangle < 0 &\Leftrightarrow k < 6. \end{aligned}$$

For $k > 6$, in other words, $\mathbf{n}$ is a positive vector in $\mathbb{C}^{2,1}$, then it is polar vector to a complex line as required. When $k = 6$ the eigenvector $\mathbf{n}$ turns into a null vector. Thus as $\mathbf{n}$ tends to the null we must also have the complex line with polar vector $\mathbf{n}$ degenerating to a point on the boundary of complex hyperbolic space as well. This limiting configuration corresponds to the cusp of lattice, which is isomorphic to the sister of Eisenstein-Picard modular group treated in [Zh11].

5.2.3 New normalization of Γ_k

Using the Hermitian form (5.2), calculations in complex hyperbolic space have a tendency to become extremely complicated, which means that explicit constructions are rather difficult to obtain. We have to make a good choice of coordinates in order to give simple, explicit geometrical arguments on Γ_k. In what follows we choose the first Hermitian matrix

$$H_1 = \begin{bmatrix} 1 & 0 & 0 \\ 0 & 1 & 0 \\ 0 & 0 & -1 \end{bmatrix}.$$

The corresponding Hermitian form in complex vector space $\mathbb{C}^{2,1}$ is defined by

$$\langle z, w\rangle = z_1\overline{w}_1 + z_2\overline{w}_2 - z_3\overline{w}_3,$$

where z and w are the column vectors $[z_1, z_2, z_3]^t$ and $[w_1, w_2, w_3]^t$ respectively. Thus we obtain in non-homogeneous coordinates the complex ball

$$\mathbf{H}^2_{\mathbb{C}} = \{(z_1, z_2) \in \mathbb{C}^2 : |z_1|^2 + |z_2|^2 < 1\}.$$

The key point of our normalization is based on the geometrical observation of two complex lines fixed by T and R respectively. Following from the braid relation, it is easy to know that R commutes with T. Thus two complex lines fixed by T and R are orthogonal, denoted by $\mathcal{C}_1$ and $\mathcal{C}_2$ respectively. We choose a new coordinate system of the complex ball, which makes $\mathcal{C}_1$ and $\mathcal{C}_2$ to be the z_1-axis and z_2-axis, specifically

$$\mathcal{C}_1 = \{(z_1, 0) \in \mathbb{C}^2 : |z_1| < 1\}, \tag{5.3}$$
$$\mathcal{C}_2 = \{(0, z_2) \in \mathbb{C}^2 : |z_2| < 1\}. \tag{5.4}$$

We now start to normalize the generators of Γ_k in the new system of coordinates. Before normalizing, we need to introduce two angle parameters, denoted by $\phi_1 = \pi/k$ and $\phi_2 = \pi/6 - \pi/k$, which play an important role in the normalization of the group Γ_k. Also, we shall give several numbers related to ϕ_1 and ϕ_2 in order to simplify the expressions. For convenience, we remind the readers to keep these numbers in mind.

$$x_1 = \sqrt{\frac{\sin(\pi/6 - \phi_1)}{\sin(\pi/6 + \phi_1)}}, \qquad x_2 = \sqrt{\frac{\sin(\pi/6 - \phi_2)}{\sin(\pi/6 + \phi_2)}},$$
$$\mu = \sqrt{\frac{\tan(\phi_1/2)}{\tan(\pi/6 - \phi_1/2)}}, \qquad \lambda = \sqrt{\tan(\phi_1/2)\tan(\pi/6 - \phi_1/2)},$$
$$\rho = \sqrt{\frac{\sin(\pi/6 - \phi_1/2)}{\cos(\phi_1/2)\sin(\pi/6 + \phi_1)}}.$$

As the matrix of $SU(2,1)$, complex reflections R and T are given by

$$R = \begin{bmatrix} e^{4i\phi_1/3} & 0 & 0 \\ 0 & e^{-2i\phi_1/3} & 0 \\ 0 & 0 & e^{-2i\phi_1/3} \end{bmatrix},$$
$$T = \begin{bmatrix} e^{-2i\phi_2/3} & 0 & 0 \\ 0 & e^{4i\phi_2/3} & 0 \\ 0 & 0 & e^{-2i\phi_2/3} \end{bmatrix}. \tag{5.5}$$

We start to define the vertices of our polyhedron to be intersection of two complex lines. Basically, we consider two more complex lines fixed by R_1 and R_3, denoted by $\mathcal{L}_1$ and $\mathcal{L}_3$ respectively.

(i) The vertices on $\mathcal{L}_1$:

$$\mathbf{z}_1 = \mathcal{L}_1 \cap \mathcal{C}_2,\ \mathbf{z}_2 = \mathcal{L}_1 \cap \mathcal{L}_3, \quad \mathbf{z}_3 = \mathcal{L}_1 \cap R(\mathcal{L}_3);$$

(ii) The vertices on $T(\mathcal{L}_1)$:

$$\mathbf{z}_6 = T(\mathcal{L}_1) \cap \mathcal{C}_2,\ \mathbf{z}_4 = T(\mathcal{L}_1) \cap \mathcal{L}_3,\ \mathbf{z}_5 = T(\mathcal{L}_1) \cap R(\mathcal{L}_3);$$

(iii) The vertices on $\mathcal{C}_1$:

$$\mathbf{z}_7 = \mathcal{C}_1 \cap \mathcal{C}_2,\ \mathbf{z}_8 = \mathcal{C}_1 \cap \mathcal{L}_3,\ \mathbf{z}_9 = \mathcal{C}_1 \cap R(\mathcal{L}_3).$$

Proposition 5.2.1. *If $\mathbf{z}_j$ is defined as (i), (ii) and (iii) for $j = 1, 2, \cdots, 9$, then we have*

$$\begin{array}{lll} \mathbf{z}_3 = R(\mathbf{z}_2), & \mathbf{z}_5 = R(\mathbf{z}_4), & \mathbf{z}_9 = R(\mathbf{z}_8), \\ \mathbf{z}_6 = T(\mathbf{z}_1), & \mathbf{z}_4 = T(\mathbf{z}_2), & \mathbf{z}_5 = T(\mathbf{z}_3). \end{array}$$

Proof. The braid relations give rise to the properties that R commutes with R_1 and T commutes with R_3. As a consequence, we know that R commutes with TR_1T^{-1} and T commutes with RR_3R^{-1}. It follows that $\mathcal{C}_1$ is orthogonal to $\mathcal{L}_3, R(\mathcal{L}_3)$ and $\mathcal{C}_2$ is orthogonal to $\mathcal{L}_1, T(\mathcal{L}_1)$. We see clearly that R preserves $\mathcal{L}_1, T(\mathcal{L}_1), \mathcal{C}_1$ and T preserves $\mathcal{L}_3, R(\mathcal{L}_3), \mathcal{C}_2$. The result follows easily from the definitions. □

We now start with investigating the coordinates of complex lines of $\mathcal{L}_1$ and $\mathcal{L}_3$ by the symmetry map J. Consider the triangle with the vertices $\mathbf{z}_2$, $\mathbf{z}_3$, $\mathbf{z}_4$, first observe that J acts on the vertices with the property that $J(\mathbf{z}_j) = \mathbf{z}_{j+1}$ (with indices taken cyclically). To see this, it follows from $R_1(\mathbf{z}_2) = R_3(\mathbf{z}_2) = \mathbf{z}_2$ and $J^3 = 1$ that

$$\begin{aligned} J(\mathbf{z}_2) &= RR_3R_1(\mathbf{z}_2) = R(\mathbf{z}_2) = \mathbf{z}_3, \\ J(\mathbf{z}_4) &= JT(\mathbf{z}_2) = J^{-1}R_1^{-1}J(\mathbf{z}_2) = R_3^{-1}(\mathbf{z}_2) = \mathbf{z}_2, \\ J(\mathbf{z}_3) &= JR(\mathbf{z}_2) = J^{-1}R_1^{-1}R_3^{-1}(\mathbf{z}_2) = J^{-1}(\mathbf{z}_2) = \mathbf{z}_4. \end{aligned}$$

Thus, this is an equilateral triangle whose vertices as the vectors of $\mathbb{C}^{2,1}$ satisfy the following conditions

$$\langle \mathbf{z}_1, \mathbf{z}_1 \rangle = \langle \mathbf{z}_2, \mathbf{z}_2 \rangle = \langle \mathbf{z}_3, \mathbf{z}_3 \rangle, \quad |\langle \mathbf{z}_1, \mathbf{z}_2 \rangle| = |\langle \mathbf{z}_2, \mathbf{z}_3 \rangle| = |\langle \mathbf{z}_3, \mathbf{z}_1 \rangle|. \tag{5.6}$$

The condition (5.6) gives rise to the coordinates of complex lines $\mathcal{L}_1$ and $\mathcal{L}_3$, which are given by, in terms of non-homogeneous coordinates

$$\mathcal{L}_1 = \left\{ \left(z_1, x_2 e^{-i\phi_2} \right) \in \mathbb{C}^2 : |z_1| < \sqrt{1 - x_2^2} \right\}, \tag{5.7}$$

$$\mathcal{L}_3 = \left\{ \left(x_1 e^{-i\phi_1}, z_2 \right) \in \mathbb{C}^2 : |z_2| < \sqrt{1 - x_1^2} \right\}. \tag{5.8}$$

As the vectors of $\mathbb{C}^{2,1}$, these vertices are given by

$$\begin{array}{lll} \mathbf{z_1} = \begin{bmatrix} 0 \\ x_2 e^{-i\phi_2} \\ 1 \end{bmatrix}, & \mathbf{z_2} = \begin{bmatrix} x_1 e^{-i\phi_1} \\ x_2 e^{-i\phi_2} \\ 1 \end{bmatrix}, & \mathbf{z_3} = \begin{bmatrix} x_1 e^{i\phi_1} \\ x_2 e^{-i\phi_2} \\ 1 \end{bmatrix}, \\ \mathbf{z_4} = \begin{bmatrix} x_1 e^{-i\phi_1} \\ x_2 e^{i\phi_2} \\ 1 \end{bmatrix}, & \mathbf{z_5} = \begin{bmatrix} x_1 e^{i\phi_1} \\ x_2 e^{i\phi_2} \\ 1 \end{bmatrix}, & \mathbf{z_6} = \begin{bmatrix} 0 \\ x_2 e^{i\phi_2} \\ 1 \end{bmatrix}, \\ \mathbf{z_7} = \begin{bmatrix} 0 \\ 0 \\ 1 \end{bmatrix}, & \mathbf{z_8} = \begin{bmatrix} x_1 e^{-i\phi_1} \\ 0 \\ 1 \end{bmatrix}, & \mathbf{z_9} = \begin{bmatrix} x_1 e^{i\phi_1} \\ 0 \\ 1 \end{bmatrix}. \end{array} \tag{5.9}$$

Recall, (c.f. Proposition 1.3.6) given a vector v with $\langle v, v\rangle > 0$, complex reflection in the complex line with polar vector v is given by

$$R_{v,\zeta}(z) = z + (\zeta - 1)\frac{\langle z, v\rangle}{\langle v, v\rangle}v. \tag{5.10}$$

where ζ is a complex number of absolute value one.

Observe that the polar vectors to complex lines $\mathcal{L}_1$ and $\mathcal{L}_3$, denoted by $\mathbf{n}_1, \mathbf{n}_3$ respectively, are given by

$$\mathbf{n}_1 = \begin{bmatrix} 0 \\ 1 \\ x_2 e^{i\phi_2} \end{bmatrix}, \quad \mathbf{n}_3 = \begin{bmatrix} 1 \\ 0 \\ x_2 e^{i\phi_1} \end{bmatrix}.$$

Since R_1 and R_3 are complex reflections with order 3, we denote $\zeta = u^3 = e^{2i\pi/3}$ and then $\zeta - 1 = i\sqrt{3}e^{i\pi/3}$. Using the formula (5.10) together with the fact that $\langle \mathbf{n}_1, \mathbf{n}_1\rangle = 1 - x_2^2$ and $\langle \mathbf{n}_3, \mathbf{n}_3\rangle = 1 - x_1^2$, complex reflections R_1 and R_3 are given as the matrix of $SU(2,1)$ by

$$R_1 = \begin{bmatrix} \overline{u} & 0 & 0 \\ 0 & \frac{i(u^2+\overline{u})e^{-i\phi_2}}{2\sin\phi_2} & -\frac{i(u^2+\overline{u})\sqrt{1-4\sin^2\phi_2}e^{-i\phi_2}}{2\sin\phi_2} \\ 0 & \frac{i(u^2+\overline{u})\sqrt{1-4\sin^2\phi_2}e^{i\phi_2}}{2\sin\phi_2} & -\frac{i(u^2+\overline{u})e^{i\phi_2}}{2\sin\phi_2} \end{bmatrix},$$

$$R_3 = \begin{bmatrix} \frac{i(u^2+\overline{u})e^{-i\phi_1}}{2\sin\phi_1} & 0 & -\frac{i(u^2+\overline{u})\sqrt{1-4\sin^2\phi_1}e^{-i\phi_1}}{2\sin\phi_1} \\ 0 & \overline{u} & 0 \\ \frac{i(u^2+\overline{u})\sqrt{1-4\sin^2\phi_1}e^{i\phi_1}}{2\sin\phi_1} & 0 & -\frac{i(u^2+\overline{u})e^{i\phi_1}}{2\sin\phi_1} \end{bmatrix}.$$

The symmetry map J plays an important role in the construction which is obtained from $J = RR_3R_1$ that

$$J = e^{i(\phi_2-\phi_1+\pi)/3}\begin{bmatrix} \frac{e^{i\phi_1}}{2\sin\phi_1} & \frac{\sqrt{(1-4\sin^2\phi_1)(1-4\sin^2\phi_2)}}{4\sin\phi_1\sin\phi_2} & -\frac{\sqrt{1-4\sin^2\phi_1}}{4\sin\phi_1\sin\phi_2} \\ 0 & \frac{e^{-i\phi_2}}{2\sin\phi_2} & -\frac{\sqrt{1-4\sin^2\phi_2}e^{-i\phi_2}}{2\sin\phi_2} \\ \frac{\sqrt{1-4\sin^2\phi_1}e^{i\phi_1}}{2\sin\phi_1} & \frac{\sqrt{1-4\sin^2\phi_2}}{4\sin\phi_1\sin\phi_2} & -\frac{1}{4\sin\phi_1\sin\phi_2} \end{bmatrix}.$$

We now define, from the relations $S = JR_1^{-1}, I_1 = TR_1$, the remaining generators as follows

$$S = \frac{e^{-i\phi_2/3}}{2\sin\phi_1}\begin{bmatrix} 1 & 0 & -\sqrt{1-4\sin^2\phi_1} \\ 0 & -2\sin\phi_1 e^{i\phi_2} & 0 \\ \sqrt{1-4\sin^2\phi_1} & 0 & -1 \end{bmatrix}, \tag{5.11}$$

$$I_1 = \frac{e^{-i\phi_1/3}}{2\sin\phi_2}\begin{bmatrix} -2\sin\phi_2 e^{i\phi_1} & 0 & 0 \\ 0 & 1 & -\sqrt{1-4\sin^2\phi_2} \\ 0 & \sqrt{1-4\sin^2\phi_2} & -1 \end{bmatrix}. \tag{5.12}$$

5.3 A combinatorial polyhedron

In this section we construct a polyhedron $\mathbf{D}$ which we will prove later to be a fundamental domain for Γ_k in complex hyperbolic space. The polyhedron $\mathbf{D}$ is defined to be

4-dimensional domain bounded by the sides we construct in the Sections 5.3.2 and 5.3.3. Many (but not all) sides of **D** are contained in bisectors and the vertices are the same as defined in previous section. The main idea of construction is to happen on the sides that are not contained in bisectors, each of which is the foliation of the geodesic triangle cones over *Giraud disc*. To have a schematic view of the polyhedron, we refer the readers to see Figures 5.4 and 5.8.

5.3.1 Bisectors

In this section we review briefly the theory of bisectors and summarize some bisectors that contain four sides of our polyhedron.

Definition 5.3.1. *The standard bisector in the ball model is defined as*

$$\mathcal{B}_0 = \{(z_1, z_2) \in \mathbf{H}^2_{\mathbb{C}} : z_1 \in \mathbb{C}, \Im(z_2) = 0\}$$

in non-homogeneous coordinates, which is equidistant from $p = (0, i/2)$ *and* $q = (0, -i/2)$ *given in (2.1).*

We have given the *geographical coordinates* on the isometric spheres. Analogously, the standard bisector $\mathcal{B}_0$ (compare with [FP06]) is parameterized, in geographical coordinates, by

$$\left\{ \begin{bmatrix} re^{i\alpha} \\ s \\ 1 \end{bmatrix} : \alpha \in [-\pi/2, \pi/2), s \in [-1, 1], r \in \left[-\sqrt{1-s^2}, \sqrt{1-s^2}\right] \right\}. \tag{5.13}$$

The spine, slices and meridians of $\mathcal{B}_0$ are given in the next proposition in terms of geographical coordinates.

Proposition 5.3.2. *The standard bisector with geographical coordinates is given by (5.13). Furthermore,*

- *the spine of* $\mathcal{B}_0$ *is given by* $r = 0$*;*
- *the slices of* $\mathcal{B}_0$ *are given by* $s = s_0$ *for fixed* $s_0 \in [-1, 1]$*;*
- *the meridians of* $\mathcal{B}_0$ *are given by* $\alpha = \alpha_0$ *for fixed* $\alpha_0 \in [-\pi/2, \pi/2)$*.*

Four of the bisectors we use to construct the polyhedron **D** have a very simple description. These four bisectors come in two cospinal pairs, the complex spines being the coordinate axes. We now write down these bisectors and some of the points for (5.9) that are contained in the corresponding bisector.

Bisector	Definition	Vertices on spine	Other vertices
$\mathcal{B}_{78}$	$\arg(z_1) = -\phi_1$	$\mathbf{z}_7, \mathbf{z}_8$	$\mathbf{z}_1, \mathbf{z}_2, \mathbf{z}_4, \mathbf{z}_6$
$\mathcal{B}_{79}$	$\arg(z_1) = \phi_1$	$\mathbf{z}_7, \mathbf{z}_9$	$\mathbf{z}_1, \mathbf{z}_3, \mathbf{z}_5, \mathbf{z}_6$
$\mathcal{B}_{17}$	$\arg(z_2) = -\phi_2$	$\mathbf{z}_1, \mathbf{z}_7$	$\mathbf{z}_2, \mathbf{z}_3, \mathbf{z}_8, \mathbf{z}_9$
$\mathcal{B}_{67}$	$\arg(z_2) = \phi_2$	$\mathbf{z}_6, \mathbf{z}_7$	$\mathbf{z}_4, \mathbf{z}_5, \mathbf{z}_8, \mathbf{z}_9$

5.3.2 The core sides

In this section we define two core sides $\mathcal{S}_c$ and $\mathcal{S}'_c$ of the polyhedron $\mathbf{D}$ contained in a bisector $\mathcal{B}_c$, called the *core bisector*, which is the equidistant between two complex lines $\mathcal{C}_1$ and $I_1^{-1}(\mathcal{C}_1)$ as explained in Section 2.1 (compare [Zh11]). Also we call the *core prism* $\mathcal{P}_c$ in $\mathcal{B}_c$ which is made up of two sides $\mathcal{S}_c$ and $\mathcal{S}'_c$ as shown in Figure 5.4 for the schematic view. Furthermore, other sides of $\mathbf{D}$ come from the foliation of geodesics connecting with points on the faces of $\mathcal{P}_c$ and points of the top triangle. Four of these are contained in the bisectors given in the previous section. In the case of the sister G_2, noncompact sides of fundamental polyhedron arise from the limiting configuration that the top triangle converges to an ideal vertex. In other words, that is the geodesic cone over the faces of the core prism to the ideal point which is the cusp of lattice; see [Zh11].

The core bisector and its neighbors

Let $\mathbf{n}_0$ denote the polar vector to complex line $\mathcal{C}_1$ and denote $I_1^{-1}(\mathbf{n}_0)$ its image under by I_1^{-1}, these are

$$\mathbf{n}_0 = \begin{bmatrix} 0 \\ 1 \\ 0 \end{bmatrix}, \qquad I_1^{-1}(\mathbf{n}_0) = \frac{e^{i\phi_1/3}}{2\sin\phi_2} \begin{bmatrix} 0 \\ 1 \\ \sqrt{1-4\sin^2\phi_2} \end{bmatrix}.$$

It is clear that $\langle \mathbf{n}_0, \mathbf{n}_0 \rangle = \langle I_1^{-1}(\mathbf{n}_0), I_1^{-1}(\mathbf{n}_0) \rangle = 1$. We consider the bisector equidistant from $\mathbf{n}_0$ and $I_1^{-1}(\mathbf{n}_0)$ which is defined in non-homogeneous coordinates (c.f. (2.1)) by

$$\mathcal{B}_c = \left\{ (z_1, z_2) \in \mathbf{H}^2_{\mathbb{C}} : 2\sin\phi_2 |z_2| = |z_2 - \sqrt{1-4\sin^2\phi_2}| \right\}. \tag{5.14}$$

Moreover, the complex spine of $\mathcal{B}_c$ is exactly $\mathcal{C}_2$ that spanned by $\mathbf{n}_0$ and $I_1^{-1}(\mathbf{n}_0)$. Since both complex lines $\mathcal{L}_1$ and $T(\mathcal{L}_1)$ are orthogonal to complex spine $\mathcal{C}_2$, it follows that the spine of $\mathcal{B}_c$ pass through a pair of vertices $\mathbf{z}_1$ and $\mathbf{z}_6$ by the slice decomposition for bisector, see Figure 5.1.

We shall explore the spine of $\mathcal{B}_c$ in order to give the parametrization in terms of geographical coordinates (r, s, α). We use the coordinate system $(x, y) = (\mathrm{Re}(z), \mathrm{Im}(z))$ in $\mathbb{C}$, then the Poincaré disc turns out to be $\{(x, y) | x^2 + y^2 < 1\}$ and the spine σ :

$$\left(x - \frac{1}{\sqrt{1-4\sin^2\phi_2}} \right)^2 + y^2 = \frac{4\sin^2\phi_2}{1-4\sin^2\phi_2}. \tag{5.15}$$

This is a circle centered at $\left(\frac{1}{\sqrt{1-4\sin^2\phi_2}}, 0 \right)$ with the radius $\frac{2\sin\phi_2}{\sqrt{1-4\sin^2\phi_2}}$. The spine σ intersects with x-axis at the point $(\mu, 0)$. Then we apply a Möbius transformation ψ mapping $(\mu, 0)$ to the origin in the Poincaré's disc, i.e.

$$\psi(z) = \frac{z-\mu}{1-\mu z}.$$

The equation (5.15) becomes $|z+\mu| = |z-\mu|$ under the map ψ, i.e. y-axis. Taking a matrix C in $SU(2,1)$ as

$$C = \begin{bmatrix} e^{-i\pi/6} & 0 & 0 \\ 0 & e^{i\pi/3}/(1-\mu^2) & e^{-i\pi/6}\mu/(1-\mu^2) \\ 0 & e^{i\pi/3}\mu/(1-\mu^2) & e^{-i\pi/6}/(1-\mu^2) \end{bmatrix},$$

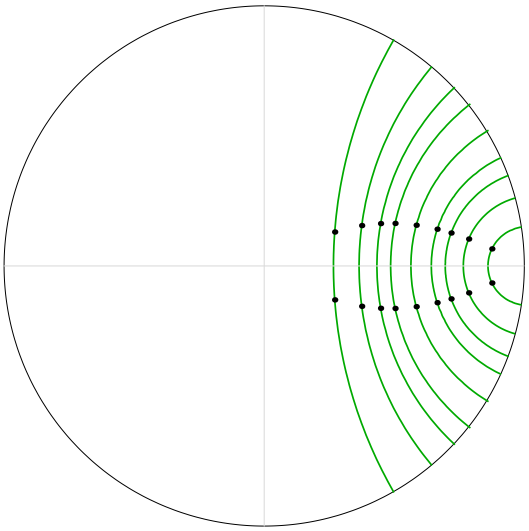

FIGURE 5.1: Configuration of the spines of bisector $\mathcal{B}_c$ and $\mathbf{z}_1, \mathbf{z}_6$ on the complex spine $\mathcal{C}_2$ for $k = 7, 8, 9, 10, 12, 15, 18, 24, 42$. Here the spine is close to the origin as k large.

then the matrix C maps the spine of standard bisector $\mathcal{B}_0$ to the spine of $\mathcal{B}_c$ and furthermore the geographical coordinates on $\mathcal{B}_c$ turns out to be obtained from $\mathcal{B}_0$. Therefore the core bisector $\mathcal{B}_c$ is given in terms of geographical coordinates (r, s, α) by

$$\left\{ \begin{bmatrix} \sqrt{1-\mu^2} r e^{i\alpha} \\ \mu + is \\ 1 + i\mu s \end{bmatrix} : \begin{array}{l} \alpha \in [-\pi/2, \pi/2), \quad s \in [-1, 1], \\ r \in \left[-\sqrt{1-s^2}, \sqrt{1-s^2}\right] \end{array} \right\}. \tag{5.16}$$

We start to define two sides $\mathcal{S}_c$ and $\mathcal{S}'_c$ in the geographical coordinates. As described in [FFP10], we will discuss the triangular face with the vertices $\mathbf{z}_2, \mathbf{z}_3, \mathbf{z}_4$ on the intersection $\mathcal{B}_c \cap S^{-1}(\mathcal{B}_c)$ in terms of two slice s-parameters. We give the details for this face on $\mathcal{B}_c \cap S^{-1}(\mathcal{B}_c)$ and others follow similarly.

Proposition 5.3.3. *The part of $\mathcal{B}_c \cap S^{-1}(\mathcal{B}_c)$ outside $T^{-1}(\mathcal{B}_c)$, $R^{-1}S(\mathcal{B}_c)$, $S(\mathcal{B}_c)$ forms a triangular face of fundamental polyhedron, see Figure 5.2. In terms of geographical coordinates (r_0, s_0, α_0) on $\mathcal{B}_c$ and (r_1, s_1, α_1) on $S^{-1}(\mathcal{B}_c)$ this face is given by*

$$-\lambda \leq s_0 \leq \lambda, \quad -\lambda \leq s_1 \leq \lambda, \quad -2\lambda \leq s_0 - s_1 \leq 0. \tag{5.17}$$

Moreover, the boundary of this triangle admits the following description in geographical coordinates.

(i) Points of $\mathcal{B}_c \cap S^{-1}(\mathcal{B}_c) \cap T^{-1}(\mathcal{B}_c)$ are given by $s_0 = -\lambda$.

(ii) Points of $\mathcal{B}_c \cap S^{-1}(\mathcal{B}_c) \cap S(\mathcal{B}_c)$ are given by $s_1 = \lambda$.

(iii) Points of $\mathcal{B}_c \cap S^{-1}(\mathcal{B}_c) \cap R^{-1}S(\mathcal{B}_c)$ are given by $s_0 - s_1 = 0$.

Similarly, we state the result on the intersection of $\mathcal{B}_c \cap S(\mathcal{B}_c)$.

FIGURE 5.2: A schematic picture of triangular face $\mathcal{F}_{234}$.The level sets of s_0 are dashed lines and the level sets of s_1 are dotted lines.

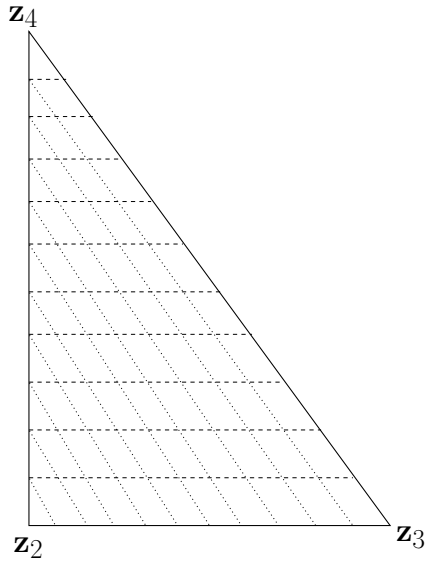

Proposition 5.3.4. *The part of $\mathcal{B}_c \cap S(\mathcal{B}_c)$ outside $T(\mathcal{B}_c)$, $RS^{-1}(\mathcal{B}_c)$, $S^{-1}(\mathcal{B}_c)$ forms a triangular face of fundamental polyhedron, see Figure 5.3. In terms of geographical coordinates (r_0, s_0, α_0) on $\mathcal{B}_c$ and (r_2, s_2, α_2) on $S(\mathcal{B}_c)$ this face is given by*

$$-\lambda \leq s_0 \leq \lambda, \quad -\lambda \leq s_2 \leq \lambda, \quad 0 \leq s_0 - s_2 \leq 2\lambda. \tag{5.18}$$

Moreover, the boundary of this triangle admits the following description in geographical coordinates.

(i) Points of $\mathcal{B}_c \cap S(\mathcal{B}_c) \cap T(\mathcal{B}_c)$ are given by $s_0 = \lambda$.

(ii) Points of $\mathcal{B}_c \cap S(\mathcal{B}_c) \cap S^{-1}(\mathcal{B}_c)$ are given by $s_2 = -\lambda$.

(iii) Points of $\mathcal{B}_c \cap S(\mathcal{B}_c) \cap RS^{-1}(\mathcal{B}_c)$ are given by $s_0 - s_2 = 0$.

Proof. The first item follows directly from Lemma 5.3.10. The map S sends $(r_0, s_0, \alpha_0) \in \mathcal{B}_c$ to $(r_2, s_2, \alpha_2) \in S(\mathcal{B}_c)$. Thus S sends the points on $\mathcal{B}_c \cap S^{-1}(\mathcal{B}_c) \cap T^{-1}(\mathcal{B}_c)$ given by $s_0 = -\lambda$ to the points on $\mathcal{B}_c \cap S(\mathcal{B}_c) \cap S^{-1}(\mathcal{B}_c)$ given by $s_2 = -\lambda$.

We will postpone (iii) part of the proof until to Corollary 5.3.9. □

We remark that none of the triple intersections (i) to (iii) in Propositions 5.3.3 and 5.3.4 is contained in a geodesic. Before we prove the Proposition 5.3.3, we need to explore the intersection $\mathcal{B}_c \cap S^{-1}(\mathcal{B}_c)$ in terms of two slices parameters s_0, s_1 and how intersects the neighboring bisectors $T^{-1}(\mathcal{B}_c)$, $R^{-1}S(\mathcal{B}_c)$ and $S(\mathcal{B}_c)$.

Proposition 5.3.5. *Consider the geographical coordinates (r_0, s_0, α_0) on $\mathcal{B}_c$ and (r_1, s_1, α_1) on $S^{-1}(\mathcal{B}_c)$. Points on $\mathcal{B}_c \cap S^{-1}(\mathcal{B}_c)$ may be uniquely expressed in terms of s_0 and s_1; see Figure 5.2. The range of these parameters is determined by the inequality*

$$\left| \frac{(1 + i\mu s_0)(\mu + is_1) - 2\sin\phi_1 e^{i\phi_2}(1 + i\mu s_1)(\mu + is_0)}{\sqrt{(1-\mu^2)(1 - 4\sin^2\phi_1)}(\mu + is_1)} \right| < \sqrt{1 - s_0^2}.$$

The other coordinates are given by

$$r_0e^{i\alpha_0} = \frac{(1+i\mu s_0)(\mu+is_1) - 2\sin\phi_1 e^{i\phi_2}(1+i\mu s_1)(\mu+is_0)}{\sqrt{(1-\mu^2)(1-4\sin^2\phi_1)}(\mu+is_1)} \tag{5.19}$$

$$r_1e^{i\alpha_1} = \frac{(1+i\mu s_1)(\mu+is_0) - 2\sin\phi_1 e^{-i\phi_2}(1+i\mu s_0)(\mu+is_1)}{\sqrt{(1-\mu^2)(1-4\sin^2\phi_1)}(\mu+is_0)} \tag{5.20}$$

Proof. In geographical coordinates, points of $\mathcal{B}_c \cap S^{-1}(\mathcal{B}_c)$ are given by

$$\begin{bmatrix} 1 & 0 & -\sqrt{1-4\sin^2\phi_1} \\ 0 & -2\sin\phi_1 e^{-i\phi_2} & 0 \\ \sqrt{1-4\sin^2\phi_1} & 0 & -1 \end{bmatrix} \begin{bmatrix} \sqrt{1-\mu^2}r_1e^{i\alpha_1} \\ \mu+is_1 \\ 1+i\mu s_1 \end{bmatrix}$$
$$= \begin{bmatrix} \sqrt{1-\mu^2}r_1e^{i\alpha_1} - \sqrt{1-4\sin^2\phi_1}(1+i\mu s_1) \\ -2\sin\phi_1 e^{-i\phi_2}(\mu+is_1) \\ \sqrt{1-4\sin^2\phi_1}\sqrt{1-\mu^2}r_1e^{i\alpha_1} - (1+i\mu s_1) \end{bmatrix} = \begin{bmatrix} \sqrt{1-\mu^2}r_0e^{i\alpha_0} \\ \mu+is_0 \\ 1+i\mu s_0 \end{bmatrix}$$

These points as the above expression are the same with homogeneous coordinates in $\mathbb{C}^{2,1}$. Hence

$$\frac{-2\sin\phi_1 e^{-i\phi_2}(\mu+is_1)}{\sqrt{1-4\sin^2\phi_1}\sqrt{1-\mu^2}r_1e^{i\alpha_1} - (1+i\mu s_1)} = \frac{\mu+is_0}{1+i\mu s_0}, \tag{5.21}$$

$$\frac{\sqrt{1-\mu^2}r_1e^{i\alpha_1} - \sqrt{1-4\sin^2\phi_1}(1+i\mu s_1)}{-2\sin\phi_1 e^{-i\phi_2}(\mu+is_1)} = \frac{\sqrt{1-\mu^2}r_0e^{i\alpha_0}}{\mu+is_0}. \tag{5.22}$$

Rearranging (5.21) gives

$$r_1e^{i\alpha_1} = \frac{(1+i\mu s_1)(\mu+is_0) - 2\sin\phi_1 e^{-i\phi_2}(1+i\mu s_0)(\mu+is_1)}{\sqrt{(1-\mu^2)(1-4\sin^2\phi_1)}(\mu+is_0)}.$$

To find $r_0e^{i\alpha_0}$ we just use this formula to substitute for $r_1e^{i\alpha_1}$ in (5.22).

In order to be in $\mathcal{B}_c$ we must have $r_0^2 < 1 - s_0^2$. Using (5.19) we can obtain the range of s_0, s_1 as required. □

Analogously, we describe $\mathcal{B}_c \cap S(\mathcal{B}_c)$ and $\mathcal{B}_c \cap R^{-1}S(\mathcal{B}_c)$.

Proposition 5.3.6. *Consider the geographical coordinates (r_0, s_0, α_0) on $\mathcal{B}_c$ and (r_2, s_2, α_2) on $S(\mathcal{B}_c)$. Points on $\mathcal{B}_c \cap S(\mathcal{B}_c)$ may be uniquely expressed in terms of s_0 and s_2. The range of these parameters is determined by the inequality*

$$\left| \frac{(1+i\mu s_0)(\mu+is_2) - 2\sin\phi_1 e^{-i\phi_2}(1+i\mu s_2)(\mu+is_0)}{\sqrt{(1-\mu^2)(1-4\sin^2\phi_1)}(\mu+is_2)} \right| < \sqrt{1-s_0^2}.$$

The other coordinates are given by

$$r_0e^{i\alpha_0} = \frac{(1+i\mu s_0)(\mu+is_2) - 2\sin\phi_1 e^{-i\phi_2}(1+i\mu s_2)(\mu+is_0)}{\sqrt{(1-\mu^2)(1-4\sin^2\phi_1)}(\mu+is_2)} \tag{5.23}$$

$$r_2e^{i\alpha_2} = \frac{(1+i\mu s_2)(\mu+is_0) - 2\sin\phi_1 e^{i\phi_2}(1+i\mu s_0)(\mu+is_2)}{\sqrt{(1-\mu^2)(1-4\sin^2\phi_1)}(\mu+is_0)} \tag{5.24}$$

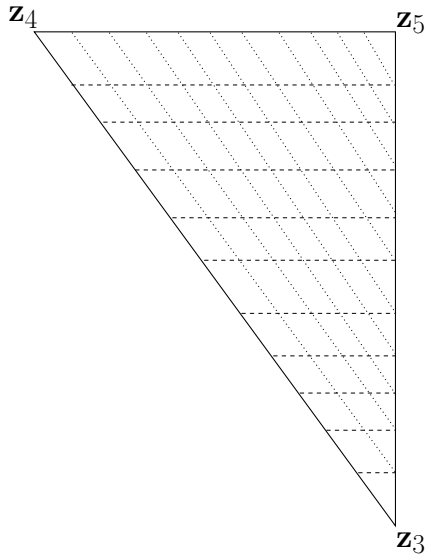

FIGURE 5.3: A schematic picture of triangular face $\mathcal{F}_{345}$. The level sets of s_0 are dashed lines and the level sets of s_2 are dotted lines.

Proposition 5.3.7. *Consider the geographical coordinates (r_0, s_0, α_0) on $\mathcal{B}_c$ and (r_3, s_3, α_3) on $R^{-1}S(\mathcal{B}_c)$. Points on $\mathcal{B}_c \cap R^{-1}S(\mathcal{B}_c)$ may be uniquely expressed in terms of s_0 and s_3. The range of these parameters is determined by the inequality*

$$\left| \frac{(1+i\mu s_0)(\mu+is_3) - 2\sin\phi_1 e^{-i\phi_2}(1+i\mu s_3)(\mu+is_0)}{\sqrt{(1-\mu^2)(1-4\sin^2\phi_1)}(\mu+is_3)} \right| < \sqrt{1-s_0^2}.$$

The other coordinates are given by

$$r_0 e^{i\alpha_0} = \frac{e^{-2i\phi_1}[(1+i\mu s_0)(\mu+is_3) - 2\sin\phi_1 e^{-i\phi_2}(1+i\mu s_3)(\mu+is_0)]}{\sqrt{(1-\mu^2)(1-4\sin^2\phi_1)}(\mu+is_3)} \tag{5.25}$$

$$r_3 e^{i\alpha_3} = \frac{(1+i\mu s_3)(\mu+is_0) - 2\sin\phi_1 e^{i\phi_2}(1+i\mu s_0)(\mu+is_3)}{\sqrt{(1-\mu^2)(1-4\sin^2\phi_1)}(\mu+is_0)} \tag{5.26}$$

Proof. In geographical coordinates, points of $\mathcal{B}_c \cap R^{-1}S(\mathcal{B}_c)$ are given by

$$\begin{bmatrix} u^2 e^{i\phi_2} & 0 & -u^2\sqrt{1-4\sin^2\phi_1}e^{i\phi_2} \\ 0 & 2\overline{u}\sin\phi_1 & 0 \\ -\overline{u}\sqrt{1-4\sin^2\phi_1}e^{-i\phi_2} & 0 & \overline{u}e^{-i\phi_2} \end{bmatrix} \begin{bmatrix} \sqrt{1-\mu^2}r_3 e^{i\alpha_3} \\ \mu+is_3 \\ 1+i\mu s_3 \end{bmatrix}$$
$$= \begin{bmatrix} e^{-2i\phi_1}[\sqrt{1-\mu^2}r_3 e^{i\alpha_3} - \sqrt{1-4\sin^2\phi_1}(1+i\mu s_3)] \\ -2\sin\phi_1 e^{i\phi_2}(\mu+is_3) \\ \sqrt{1-4\sin^2\phi_1}\sqrt{1-\mu^2}r_3 e^{i\alpha_3} - (1+i\mu s_1) \end{bmatrix} = \begin{bmatrix} \sqrt{1-\mu^2}r_0 e^{i\alpha_0} \\ \mu+is_0 \\ 1+i\mu s_0 \end{bmatrix}.$$

The result follows as before. □

Corollary 5.3.8. *In terms of geographical coordinates (r_1, s_1, α_1) on $S^{-1}(\mathcal{B}_c)$ and (r_2, s_2, α_2) on $S(\mathcal{B}_c)$, points of $\mathcal{B}_c \cap S^{-1}(\mathcal{B}_c) \cap S(\mathcal{B}_c)$ are given by $s_1 = \lambda$ or $s_2 = -\lambda$.*

Proof. Points of $\mathcal{B}_c \cap S^{-1}(\mathcal{B}_c) \cap S(\mathcal{B}_c)$ are given by

$$\begin{aligned} r_0 e^{i\alpha_0} &= \frac{(1+i\mu s_0)(\mu+is_1) - 2\sin\phi_1 e^{i\phi_2}(1+i\mu s_1)(\mu+is_0)}{\sqrt{(1-\mu^2)(1-4\sin^2\phi_1)}(\mu+is_1)} \\ &= \frac{(1+i\mu s_0)(\mu+is_2) - 2\sin\phi_1 e^{-i\phi_2}(1+i\mu s_2)(\mu+is_0)}{\sqrt{(1-\mu^2)(1-4\sin^2\phi_1)}(\mu+is_2)}. \end{aligned}$$

From this we find

$$e^{i\phi_2}[\mu(1-s_1s_2)+i(s_2+\mu s_1)] = e^{-i\phi_2}[\mu(1-s_1s_2)+i(s_1+\mu s_2)].$$

Hence $s_1+s_2=0$ and $s_1=\lambda$. □

Corollary 5.3.9. *In terms of geographical coordinates (r_0,s_0,α_0) on $\mathcal{B}_c$, (r_1,s_1,α_1) on $S^{-1}(\mathcal{B}_c)$ and (r_3,s_3,α_3) on $R^{-1}S(\mathcal{B}_c)$, points of $\mathcal{B}_c \cap S^{-1}(\mathcal{B}_c) \cap R^{-1}S(\mathcal{B}_c)$ are given by $s_0-s_1=0$ and $s_0-s_3=0$.*

Proof. Points of $\mathcal{B}_c \cap S^{-1}(\mathcal{B}_c) \cap R^{-1}S(\mathcal{B}_c)$ are given by

$$\begin{aligned} r_0 e^{i\alpha_0} &= \frac{(1+i\mu s_0)(\mu+is_1) - 2\sin\phi_1 e^{i\phi_2}(1+i\mu s_1)(\mu+is_0)}{\sqrt{(1-\mu^2)(1-4\sin^2\phi_1)}(\mu+is_1)} \\ &= \frac{e^{-2i\phi_1}[(1+i\mu s_0)(\mu+is_3) - 2\sin\phi_1 e^{-i\phi_2}(1+i\mu s_3)(\mu+is_0)]}{\sqrt{(1-\mu^2)(1-4\sin^2\phi_1)}(\mu+is_3)}. \end{aligned}$$

From this we find

$$\frac{e^{i\pi/6}(1+i\mu s_1)}{\mu+is_1} - \frac{e^{-i\pi/6}(1+i\mu s_3)}{\mu+is_3} = \frac{i(1+i\mu s_0)}{\mu+is_0}.$$

Comparing with the real and imaginary parts yields

$$\begin{aligned} \sqrt{3}\mu(s_1-s_3) + 2s_1s_3 &= s_0(s_1+s_3), \\ \sqrt{3}s_0(s_1-s_3) + 2\mu s_0 &= \mu(s_1+s_3). \end{aligned}$$

This simplifies to be a quadratic equation with respect to s_1 that

$$(\sqrt{3}s_0-\mu)s_1^2 + (2\mu s_0 + \sqrt{3}\mu^2 - \sqrt{3}s_0^2)s_1 - \mu s_0(\sqrt{3}\mu+s_0) = 0$$

whose solutions are $s_1=s_0$ and $s_1 = \frac{\mu(\sqrt{3}\mu+s_0)}{\mu-\sqrt{3}s_0} > \lambda$ which is impossible. Thus we obtain $s_0=s_1=s_3$. □

Proof of (iii) part of Proposition 5.3.4. Since the map R preserves the s_0-slices of $\mathcal{B}_c$ and sends $(r_3,s_3,\alpha_3) \in R^{-1}S(\mathcal{B}_c)$ to $(r_2,s_2,\alpha_2) \in S(\mathcal{B}_c)$, it follows that points of $\mathcal{B}_c \cap S^{-1}(\mathcal{B}_c) \cap R^{-1}S(\mathcal{B}_c)$ given by $s_0-s_3=0$ are sent by R to be points of $\mathcal{B}_c \cap S(\mathcal{B}_c) \cap RS^{-1}(\mathcal{B}_c)$ given by $s_0-s_2=0$ as required. □

We now investigate the intersection of $\mathcal{B}_c$ with its images under T and T^{-1}.

Lemma 5.3.10. *The bisectors $\mathcal{B}_c$ and $T^{-1}(\mathcal{B}_c)$ have a common slice which corresponding to $s_0=-\lambda$ in terms of geographical coordinates (r_0,s_0,α_0) on $\mathcal{B}_c$.*

Likewise, $\mathcal{B}_c$ and $T(\mathcal{B}_c)$ have a common slice $s_0=\lambda$ in geographical coordinates.

Proof. Points of $\mathcal{B}_c$ are given by $2\sin\phi_2|z_2| = |z_2 - \sqrt{1-4\sin^2\phi_2}|$ and points of $T^{-1}(\mathcal{B}_c)$ are given by $2\sin\phi_2|z_2| = |z_2 - \sqrt{1-4\sin^2\phi_2}e^{-2i\phi_2}|$. The common solution is $z_2 = x_2e^{-i\phi_2}$. In geographical coordinates this is

$$\frac{\mu + is_0}{1 + i\mu s_0} = x_2e^{-i\phi_2}$$

and $s_0 \in [-1, 1]$, we obtain that $s_0 = -\lambda$. □

The vertices

We have already seen the vertices $\mathbf{z}_i$ $(i = 1, 2, \cdots, 6)$ of $\mathbf{D}$ lying on two slices $\mathcal{L}_1$ and $T(\mathcal{L}_1)$ of $\mathcal{B}_c$. We now list them again as the intersection of $\mathcal{B}_c$ with images of $\mathcal{B}_c$ under suitable elements in the stabilizer of $\mathcal{C}_1$ and discuss their non-homogeneous coordinates and geographical coordinates.

(i) The vertices on the slice $\mathcal{L}_1 = \mathcal{B}_c \cap T^{-1}(\mathcal{B}_c)$ corresponding to $s = -\lambda$. Let $\mathbf{z}_1$ define the intersection of the spine of $\mathcal{B}_c$ with $\mathcal{L}_1$. The other vertices are given by

$$\mathbf{z}_2 = \mathcal{B}_c \cap T^{-1}(\mathcal{B}_c) \cap S^{-1}(\mathcal{B}_c) \cap R^{-1}S(\mathcal{B}_c),$$
$$\mathbf{z}_3 = \mathcal{B}_c \cap T^{-1}(\mathcal{B}_c) \cap S(\mathcal{B}_c) \cap RS^{-1}(\mathcal{B}_c).$$

(ii) The vertices on the slice $T(\mathcal{L}_1) = \mathcal{B}_c \cap T(\mathcal{B}_c)$ corresponding to $s = \lambda$. Let $\mathbf{z}_6$ define the intersection of the spine of $\mathcal{B}_c$ with $T(\mathcal{L}_1)$. The other vertices are given by

$$\mathbf{z}_4 = \mathcal{B}_c \cap T(\mathcal{B}_c) \cap S^{-1}(\mathcal{B}_c) \cap R^{-1}S(\mathcal{B}_c),$$
$$\mathbf{z}_5 = \mathcal{B}_c \cap T(\mathcal{B}_c) \cap S(\mathcal{B}_c) \cap RS^{-1}(\mathcal{B}_c).$$

In non-homogeneous coordinates and geographical coordinates of the vertices $\mathbf{z}_i$ are given by

	z_1	z_2	r	s	α
$\mathbf{z}_1$	0	$x_2e^{-i\phi_2}$	0	$-\lambda$	
$\mathbf{z}_2$	$x_1e^{-i\phi_1}$	$x_2e^{-i\phi_2}$	ρ	$-\lambda$	$-3\phi_1/2$
$\mathbf{z}_3$	$x_1e^{i\phi_1}$	$x_2e^{-i\phi_2}$	ρ	$-\lambda$	$\phi_1/2$
$\mathbf{z}_4$	$x_1e^{-i\phi_1}$	$x_2e^{i\phi_2}$	ρ	λ	$-\phi_1/2$
$\mathbf{z}_5$	$x_1e^{i\phi_1}$	$x_2e^{i\phi_2}$	ρ	λ	$3\phi_1/2$
$\mathbf{z}_6$	0	$x_2e^{i\phi_2}$	0	λ	

The edges

We now characterize the edges of the prism contained in the intersection of three bisectors. Let $\gamma_{jk} = \gamma_{kj}$ denote the edge of $\mathbf{D}$ with the vertices $\mathbf{z}_j$ and $\mathbf{z}_k$ as endpoints. Just half of the edges are contained in geodesic. We now list them in the following lemmas. Recall the number $\rho = \sqrt{\frac{\sin(\pi/6-\phi_1/2)}{\cos(\phi_1/2)\sin(\pi/6+\phi_1)}}$ for the reader as shown in Section 5.2.3.

Lemma 5.3.11. *(i) The edge γ_{16} is contained in the spine of $\mathcal{B}_c$;*

(ii) The edge γ_{12} is a geodesic arc, given in geographical coordinates by

$$0 \leq r_0 \leq \rho, \quad s_0 = -\lambda, \quad \alpha_0 = -\frac{3\phi_1}{2}.$$

(iii) The edge γ_{13} is a geodesic arc, given in geographical coordinates by

$$0 \leq r_0 \leq \rho, \quad s_0 = -\lambda, \quad \alpha_0 = \frac{\phi_1}{2}.$$

(iv) The edge γ_{46} is a geodesic arc, given in geographical coordinates by

$$0 \leq r_0 \leq \rho, \quad s_0 = \lambda, \quad \alpha_0 = -\frac{\phi_1}{2}.$$

(v) The edge γ_{56} is a geodesic arc, given in geographical coordinates by

$$0 \leq r_0 \leq \rho, \quad s_0 = \lambda, \quad \alpha_0 = \frac{3\phi_1}{2}.$$

Proof. Part (i) follows by construction. We now prove (ii) and the other parts follow similarly. The edge γ_{12} is defined to be the intersection of $\mathcal{B}_c \cap T^{-1}(\mathcal{B}_c) \cap \mathcal{B}_{78}$. It follows that the edge is contained in the slice of $\mathcal{B}_c$ with $s_0 = -\lambda$ by Lemma 5.3.10. Following the definition of $\mathcal{B}_{78}$, we see that $\arg(z_1) = \arg\left(\frac{e^{i\alpha_0}}{1-i\tan(\phi_1/2)}\right) = -\phi_1$ which implies that $\alpha_0 = -3\phi_1/2$. Therefore this edge is a geodesic arc since it is contained both a Lagrangian plane and a complex line. Moreover, we know that $r_0 = 0$ at $\mathbf{z}_1$ and $r_0 = \rho$ at $\mathbf{z}_2$. □

We describe the edges not contained in a geodesic arc.

Lemma 5.3.12. *(i) The edge γ_{24} is given the points (r_0, s_0, α_0) of $\mathcal{B}_c$ by*

$$r_0 e^{i\alpha_0} = \frac{2\sin\phi_2 e^{-i\phi_1}(1 + i\mu s_0)}{\sqrt{(1-\mu^2)(1-4\sin^2\phi_1)}}$$

where $s_0 \in [-\lambda, \lambda]$ and not contained in a geodesic.

(ii) The edge γ_{34} is given the points (r_0, s_0, α_0) of $\mathcal{B}_c$ by

$$r_0 e^{i\alpha_0} = \frac{2\sin\phi_2(1 - i\mu s_0)}{\sqrt{(1-\mu^2)(1-4\sin^2\phi_1)}}$$

where $s_0 \in [-\lambda, \lambda]$ and not contained in a geodesic.

(iii) The edge γ_{35} is given the points (r_0, s_0, α_0) of $\mathcal{B}_c$ by

$$r_0 e^{i\alpha_0} = \frac{2\sin\phi_2 e^{i\phi_1}(1 + i\mu s_0)}{\sqrt{(1-\mu^2)(1-4\sin^2\phi_1)}}$$

where $s_0 \in [-\lambda, \lambda]$ and not contained in a geodesic.

(iv) The edge γ_{23} is given by points (r_0, s_0, α_0) of $\mathcal{B}_c$ with $s_0 = -\lambda$ and

$$r_0 e^{i\alpha_0} = \frac{(1 - i\mu\lambda)(\mu + is_1) - 2\sin\phi_1 e^{i\phi_2}(1 + i\mu s_1)(\mu - i\lambda)}{\sqrt{(1-\mu^2)(1-4\sin^2\phi_1)}(\mu + is_1)}$$

where $s_1 \in [-\lambda, \lambda]$ and not contained in a geodesic.

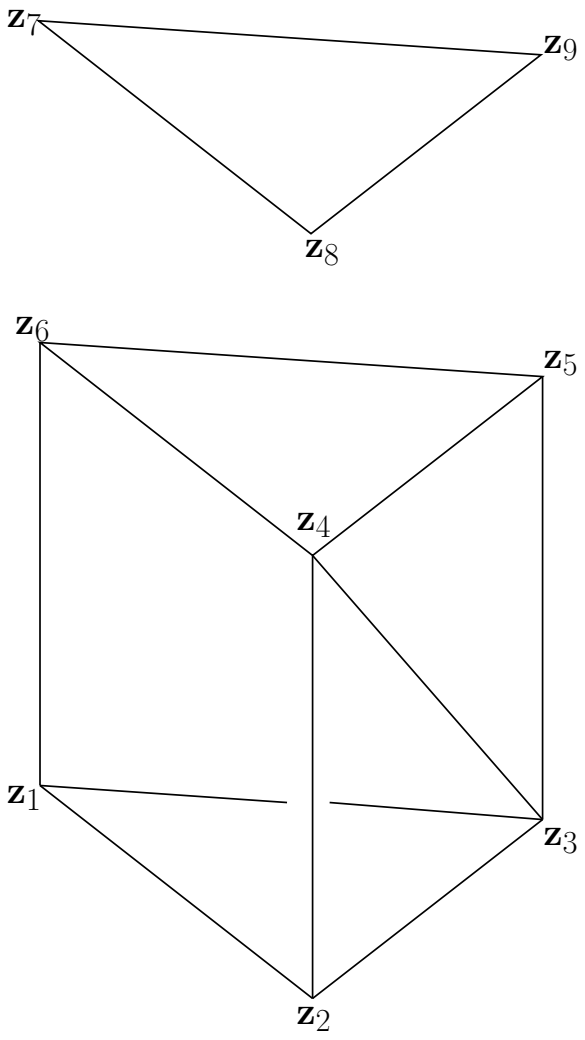

FIGURE 5.4: The schematic view of the core prism $\mathcal{P}_c$ contained in $\mathcal{B}_c$ and the geodesic triangle on the complex line $\mathcal{C}_1$.

(v) The edge γ_{45} is given by points (r_0, s_0, α_0) of $\mathcal{B}_c$ with $s_0 = \lambda$ and

$$r_0 e^{i\alpha_0} = \frac{(1+i\mu\lambda)(\mu+is_2) - 2\sin\phi_1 e^{-i\phi_2}(1+i\mu s_2)(\mu+i\lambda)}{\sqrt{(1-\mu^2)(1-4\sin^2\phi_1)}(\mu+is_2)}$$

where $s_2 \in [-\lambda, \lambda]$ and not contained in a geodesic.

Proof. We now prove (i) and the others follow similarly. This follows by substituting $s_1 = s_0$ in (5.19) and using the fact that $\mathbf{z}_2$ and $\mathbf{z}_4$ correspond to $s_0 = -\lambda$ and $s_0 = \lambda$ respectively. In particular, we see that neither s_0 nor α_0 is constant on this edge. This implies that this edge cannot be contained in a geodesic. □

The faces

In order to define the two sides $\mathcal{S}_c$ and $\mathcal{S}'_c$ contained in $\mathcal{B}_c$, it suffices to describe their faces. We denote them by $\mathcal{F}_{ijk}$ or $\mathcal{F}_{ijkl}$, where i, j, k and l are the indices of the vertices of the face. We repeat the previous result and summarize them again.

- Two $\mathbb{C}$-planar faces $\mathcal{F}_{123}$ and $\mathcal{F}_{456}$. The boundary of $\mathcal{F}_{123}$ is $\gamma_{12} \cup \gamma_{13} \cup \gamma_{23}$ and the boundary of $\mathcal{F}_{456}$ is $\gamma_{46} \cup \gamma_{56} \cup \gamma_{45}$.
- Two triangular faces $\mathcal{F}_{234}$ and $\mathcal{F}_{345}$ are contained in the intersections $\mathcal{B}_c \cap S^{-1}(\mathcal{B}_c)$ and $\mathcal{B}_c \cap S(\mathcal{B}_c)$ respectively. The boundary of $\mathcal{F}_{234}$ is $\gamma_{23} \cup \gamma_{34} \cup \gamma_{24}$ and the boundary of $\mathcal{F}_{345}$ is $\gamma_{34} \cup \gamma_{45} \cup \gamma_{35}$.
- Three quadrilateral faces $\mathcal{F}_{1246}, \mathcal{F}_{1346}$ and $\mathcal{F}_{1356}$ are foliated by geodesics. More precisely, given a fixed $s_0 \in [-\lambda, \lambda]$, the slice s_0 intersects with the face $\mathcal{F}_{1246}$ (resp. $\mathcal{F}_{1346}$ and $\mathcal{F}_{1356}$) to be a geodesic, one of whose endpoints is lying at γ_{16} and the other is lying at γ_{24} (resp. γ_{34} and γ_{35}). The boundary of $\mathcal{F}_{1246}$ is $\gamma_{12} \cup \gamma_{24} \cup \gamma_{46} \cap \gamma_{16}$, the boundary of $\mathcal{F}_{1346}$ is $\gamma_{13} \cup \gamma_{34} \cup \gamma_{46} \cap \gamma_{16}$ and the boundary of $\mathcal{F}_{1356}$ is $\gamma_{13} \cup \gamma_{35} \cup \gamma_{56} \cap \gamma_{16}$.

We remark that the faces $\mathcal{F}_{1246}$ and $\mathcal{F}_{1356}$ are contained in the intersection of $\mathcal{B}_c$ with $\mathcal{B}_{78}$ and $\mathcal{B}_{79}$ respectively. Since each geodesic as a foliation of $\mathcal{F}_{1246}$ (or $\mathcal{F}_{1356}$) is also lying in a meridian of $\mathcal{B}_{78}$ (or $\mathcal{B}_{79}$).

To this end, we give the definitions of two sides $\mathcal{S}_c$ and $\mathcal{S}'_c$. Note that the boundary of $\mathcal{S}_c$ is $\mathcal{F}_{1246} \cup \mathcal{F}_{1346} \cup \mathcal{F}_{123} \cup \mathcal{F}_{234}$ and the boundary of $\mathcal{S}'_c$ is $\mathcal{F}_{1346} \cup \mathcal{F}_{1356} \cup \mathcal{F}_{456} \cup \mathcal{F}_{345}$.

Definition 5.3.13. *The side $\mathcal{S}_c$ is made up of those points (r_0, s_0, α_0) of $\mathcal{B}_c$ with*

(i) $-\lambda \leq s_0 \leq \lambda$;

(ii) $\arctan(\mu s_0) - \phi_1 \leq \alpha_0 \leq -\arctan(\mu s_0)$;

(iii) (r_0, s_0, α_0) *is outside* $S^{-1}(\mathcal{B}_c)$.

We has shown that a point (r_0, s_0, α_0) in the intersection $\mathcal{B}_c \cap S^{-1}(\mathcal{B}_c)$ need to satisfy the formula (5.19). Compare with two sides of equality in (5.19), it follows that the ratio between the imaginary part and real part of the right side of (5.19) is equal to $\tan \alpha_0$, which makes s_1 out to be a function $f(s_0, \alpha_0)$ with respect to s_0 and α_0. Thus the condition (iii) can be written in terms of geographical coordinates as

$$r_0 \leq \left| \frac{(1 + i\mu s_0)(\mu + is_1) - 2\sin\phi_1 e^{i\phi_2}(1 + i\mu s_1)(\mu + is_0)}{\sqrt{(1-\mu^2)(1 - 4\sin^2\phi_1)}(\mu + is_1)} \right|$$

by replacing s_1 with $f(s_0, \alpha_0)$.

Definition 5.3.14. *The side $\mathcal{S}'_c$ is made up of those points (r_0, s_0, α_0) of $\mathcal{B}_c$ with*

(i) $-\lambda \leq s_0 \leq \lambda$;

(ii) $-\arctan(\mu s_0) \leq \alpha_0 \leq \arctan(\mu s_0) + \phi_1$;

(iii) (r_0, s_0, α_0) *is outside* $S(\mathcal{B}_c)$.

The condition (iii) is the same argument as (iii) of Definition 5.3.13 only if consider (5.23) in Proposition 5.3.6.

5.3.3 Sides of prism type

In this section we define four sides of the polyhedron **D**. These sides are contained in bisectors, denoted by $\mathcal{S}_{17}, \mathcal{S}_{67}, \mathcal{S}_{78}$ and $\mathcal{S}_{79}$ each of whose indices is the same as its corresponding bisector. A simple description of these sides is a triangular prism whose top and bottom faces are respectively contained in different slices of a bisector.

The sides $\mathcal{S}_{78}$ and $\mathcal{S}_{79}$

For these two sides, we only need to analyze the side $\mathcal{S}_{78}$ and the other follows similarly since $\mathcal{B}_{79} = R(\mathcal{B}_{78})$.

Recall, two vertices $\mathbf{z}_7$ and $\mathbf{z}_8$ lie on the spine of $\mathcal{B}_{78}$. We take the edge γ_{78} is a geodesic segment contained in the spine of $\mathcal{B}_{78}$. In terms of slice decomposition, the faces $\mathcal{F}_{167}$ and $\mathcal{F}_{248}$ are respectively contained in two of the slices of $\mathcal{B}_{78}$. In terms of meridian decomposition, the faces $\mathcal{F}_{1278}$ and $\mathcal{F}_{4678}$ are respectively contained in two of the meridians of $\mathcal{B}_{78}$. To see this, we verify that $\arg(\mathbf{z}_2) = -\phi_2$ for the vertices $\mathbf{z}_1, \mathbf{z}_2$ and $\arg(\mathbf{z}_2) = \phi_2$ for the vertices $\mathbf{z}_4, \mathbf{z}_6$ in (5.9).

We define the face $\mathcal{F}_{1246}$ to be the intersection of $\mathcal{B}_{78}$ and $\mathcal{B}_c$. More precise, a point (z_1, z_2) on the intersection of $\mathcal{B}_{78} \cap \mathcal{B}_c$ in non-homogeneous coordinates is given by

$$\arg(z_1) = -\phi_1, \quad 2\sin\phi_2|z_2| = |z_2 - \sqrt{1 - 4\sin^2\phi_2}|.$$

Furthermore, a point $\mathbf{z} = (z_1, z_2)$ of $\mathcal{B}_{78}$ lies outside of $\mathcal{B}_c$, (i.e. the distance between $\mathbf{z}$ and $I_1^{-1}(\mathcal{C}_1)$ is greater than the distance between $\mathbf{z}$ and $\mathcal{C}_1$) if and only if

$$\arg(z_1) = -\phi_1, \quad 2\sin\phi_2|z_2| < |z_2 - \sqrt{1 - 4\sin^2\phi_2}|.$$

From the above analysis, we give the following explicit definition of the sides $\mathcal{S}_{78}$ and $\mathcal{S}_{79}$.

Definition 5.3.15. *The side $\mathcal{S}_{78}$ is made up of those points (z_1, z_2) of $\mathcal{B}_{78}$ with*

$$\begin{gathered}\arg(z_1) = -\phi_1, \quad |z_1| \le x_1, \quad -\phi_2 \le \arg(z_2) \le \phi_2, \\ 2\sin\phi_2|z_2| \le |z_2 - \sqrt{1 - 4\sin^2\phi_2}|.\end{gathered}$$

Definition 5.3.16. *The side $\mathcal{S}_{79}$ is made up of those points (z_1, z_2) of $\mathcal{B}_{79}$ with*

$$\begin{gathered}\arg(z_1) = \phi_1, \quad |z_1| \le x_1, \quad -\phi_2 \le \arg(z_2) \le \phi_2, \\ 2\sin\phi_2|z_2| \le |z_2 - \sqrt{1 - 4\sin^2\phi_2}|.\end{gathered}$$

Remark 5.3.17. The face $\mathcal{F}_{1246}$ is foliated by geodesics each of which are the intersection of a meridian of $\mathcal{B}_{78}$ and a slice of $\mathcal{B}_c$. Points in the intersection is given by

$$\arg(z_2) = \arg\left(\frac{\mu + is}{1 + i\mu s}\right) = \text{const} \in [-\phi_2, \phi_2],$$

which is corresponding to a constant s_0.

The sides $\mathcal{S}_{17}$ and $\mathcal{S}_{67}$

Similarly, these two sides are respectively contained in cospinal and cotranchal bisectors whose common slice is $\mathcal{C}_1$ and common complex spine is $\mathcal{C}_2$.

We begin with defining the common face $\mathcal{F}_{789}$. Recall that the edges γ_{78} and γ_{79} are the geodesic segments contained in the spines of $\mathcal{B}_{78}$ and $\mathcal{B}_{79}$ respectively. We define the edge γ_{89} to be a geodesic segment connecting with $\mathbf{z}_8$ and $\mathbf{z}_9$. In order to see this, we apply S on the complex line $\mathcal{C}_1$. Recall, S preserves the complex line $\mathcal{C}_1$ and S^2 acts on $\mathcal{C}_1$ as identity. Using this, we see that the restriction of S to $\mathcal{C}_1$ is given by

$$S\big|_{\mathcal{C}_1}: \quad z \to \frac{z-\sqrt{1-4\sin^2\phi_1}}{\sqrt{1-4\sin^2\phi_1}z-1}, \quad |z|<1.$$

Since $S\big|_{\mathcal{C}_1}$ is of order 2, it preserves the geodesic passing through $\mathbf{z}_8$ and $\mathbf{z}_9$ and acts as a rotation of π at its fixed point $(\sqrt{\tan(\phi_2/2)/\tan(\pi/6-\phi_2/2)},0)$. From the above analysis, we define the face $\mathcal{F}_{789}$ to be a geodesic triangular face lying on the complex line $\mathcal{C}_1$, refer to Figure 5.5.

In order to define two sides $\mathcal{S}_{17}$ and $\mathcal{S}_{67}$, it remains to define two faces $\mathcal{F}_{2389}$ and $\mathcal{F}_{4589}$.

- We denote $\alpha=\arg(z_1)$ and so the meridians of $\mathcal{B}_{17}$ and $\mathcal{B}_{67}$ correspond to α being constant. We denote $[z,w]$ by the geodesic segment between z and w in $\mathbf{H}^2_{\mathbb{C}}$.
- Projecting a meridian α onto $\mathcal{C}_1$, it becomes a straight line passing through the origin with angle α.
- For each $\alpha\in[-\phi_1,\phi_1]$, we denote $\mathbf{p}_0^\alpha$ by the intersection of this straight line with the edge γ_{89}. Moreover, we denote by $\mathbf{p}_1^\alpha$ and $\mathbf{p}_2^\alpha$ by the intersection of the meridian α with the edges γ_{23} and γ_{45} respectively.

We now define the faces $\mathcal{F}_{2389}$ and $\mathcal{F}_{4589}$ as follows:

$$\mathcal{F}_{2389}=\bigcup_{\alpha\in[-\phi_1,\phi_1]}[\mathbf{p}_1^\alpha,\mathbf{p}_0^\alpha] \text{ and } \mathcal{F}_{4589}=\bigcup_{\alpha\in[-\phi_1,\phi_1]}[\mathbf{p}_2^\alpha,\mathbf{p}_0^\alpha].$$

The region $\{(z_1,z_2): -\phi_1\le\arg(z_1)\le\phi_1, \arg(z_2)=-\phi_2, |z_2|\le x_2\}$ enclosed by two different slices and meridians of $\mathcal{B}_{17}$ is called a *dihedral angle region*. From the geometric view of point, the face $\mathcal{F}_{2389}$ separates the dihedral angle region in $\mathcal{B}_{17}$ into two components. We are interested in the component containing the spine of $\mathcal{B}_{17}$, and we denote this component by $\mathfrak{C}_{17}$. Similarly, $\mathfrak{C}_{67}$ is the component of the dihedral angle region in $\mathcal{B}_{67}$ containing its spine.

Definition 5.3.18. *The side $\mathcal{S}_{17}$ is made up of those points (z_1,z_2) of $\mathcal{B}_{17}$ with*

$$-\phi_1\le\arg(z_1)\le\phi_1, \quad \arg(z_2)=-\phi_2, \quad |z_2|\le x_2$$

and (z_1,z_2) is lying in $\mathfrak{C}_{17}$.

Definition 5.3.19. *The side $\mathcal{S}_{67}$ is made up of those points (z_1,z_2) of $\mathcal{B}_{67}$ with*

$$-\phi_1\le\arg(z_1)\le\phi_1, \quad \arg(z_2)=\phi_2, \quad |z_2|\le x_2$$

and (z_1,z_2) is lying in $\mathfrak{C}_{67}$.

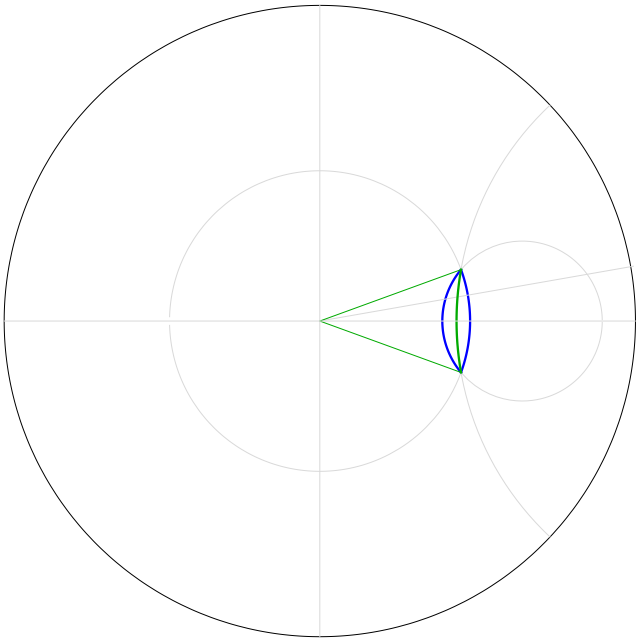

FIGURE 5.5: The triangle drawn by green line indicates the face $\mathcal{F}_{789}$. Orthogonal projection of the edges γ_{23} and γ_{45} onto $\mathcal{C}_1$ is the blue arc of circle lying inside $\mathcal{F}_{789}$ and another blue arc indicates the projection of γ_{34}.

5.3.4 Sides of wedge type

We define, in this section, two special sides $\mathcal{S}_g$ and $\mathcal{S}'_g$ which are not contained in bisectors. These sides are foliated by 2-dimensional cones over *Giraud disc*.

Projection of the faces $\mathcal{F}_{234}$ and $\mathcal{F}_{345}$

Recall that orthogonal projection of the faces $\mathcal{F}_{234}$ and $\mathcal{F}_{345}$ onto $\mathcal{C}_1$ is a leaf-shaped region bounded by two blue arcs in Figure 5.5. The edge γ_{89} separates the leaf-shaped region into two parts, denoted by A and B; see Figure 5.6.

For $\alpha \in [-\phi_1, \phi_1]$, we denote l_α by the intersection of a straight line of angle α passing through the origin with A. Clearly, A is foliated by the straight segments l_α for $\alpha \in [-\phi_1, \phi_1]$. Furthermore, the straight segment reduces to $\mathbf{z}_9$ for $\alpha = \phi_1$ or $\mathbf{z}_8$ for $\alpha = -\phi_1$. Since S is of order 2 by acting on $\mathcal{C}_1$, S maps A to B (or B to A). It follows that B can be foliated by the geodesic arcs $l'_\alpha = S(l_{-\alpha})$ for $\alpha \in [-\phi_1, \phi_1]$. From Lemma 5.3.20, we see that l_α and l'_α have the same common endpoint $\mathbf{p}_0^\alpha$. Thus the connected curves $l_\alpha \cup l'_\alpha$ are leaves of a foliation of the leaf-shaped region $A \cup B$ for $\alpha \in [-\phi_1, \phi_1]$.

Lemma 5.3.20. *For $\alpha \in [-\phi_1, \phi_1]$, then $S|_{\mathcal{C}_1}(\mathbf{p}_0^{-\alpha}) = \mathbf{p}_0^\alpha$.*

Proof. Using the z-coordinate in $\mathcal{C}_1$, the edge γ_{89} is a geodesic which can be written by

$$\left| z - \frac{1}{\sqrt{1 - 4\sin^2\phi_1}} \right| = \frac{2\sin\phi_1}{\sqrt{1 - 4\sin^2\phi_1}}$$

with $|z| < 1$. Then the point $\mathbf{p}_0^{-\alpha} = re^{-i\alpha}$ on the edge γ_{89} may satisfy

$$r^2 - \frac{2r\cos\alpha}{\sqrt{1 - 4\sin^2\phi_1}} + 1 = 0. \tag{5.27}$$

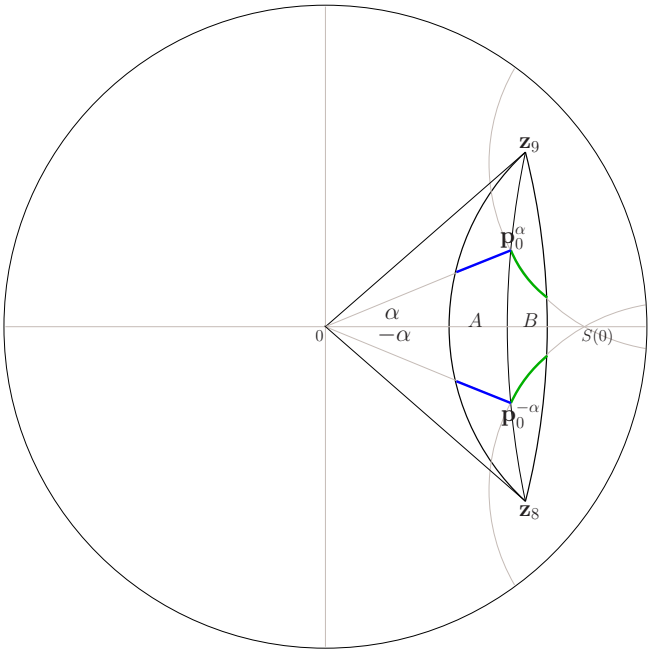

FIGURE 5.6: The leaf-shaped region is separated by γ_{89} into A and B. A is foliated by the straight segments l_α with angle α and B is foliated by the geodesic arcs l'_α.

Thus (5.27) leads to

$$\begin{aligned} S|_{\mathcal{C}_1}(\mathbf{p}_0^{-\alpha}) &= \frac{re^{-i\alpha} - \sqrt{1-4\sin^2\phi_1}}{\sqrt{1-4\sin^2\phi_1}re^{-i\alpha} - 1} \\ &= \frac{\sqrt{1-4\sin^2\phi_1}(r^2+1) - 2r\cos\alpha + 4\sin^2\phi_1 re^{i\alpha}}{(1-4\sin^2\phi_1)r^2 - 2r\cos\alpha\sqrt{1-4\sin^2\phi_1}+1} \\ &= \frac{4\sin^2\phi_1 re^{i\alpha}}{4\sin^2\phi_1} \\ &= re^{i\alpha}. \end{aligned}$$

This completes the result. □

Parameterization of the faces $\mathcal{F}_{234}$ and $\mathcal{F}_{345}$

We start to parameterize the triangular faces $\mathcal{F}_{234}$ and $\mathcal{F}_{345}$ by the meridian α-parameter.

We denote $\Pi_{\mathcal{C}_1}$ by the orthogonal projection onto $\mathcal{C}_1$. Recall, γ_{89} separates the leaf-shaped region into A and B. Then there exist two curves ℓ_{234} and ℓ_{345} such that ℓ_{234} and ℓ_{345} separate resepectively the faces $\mathcal{F}_{234}$ and $\mathcal{F}_{345}$ into two parts, one of which is projected to A and the other is projected to B. Moreover, $S(\ell_{234}) = \ell_{345}$ and then $\Pi_{\mathcal{C}_1}(\ell_{234}) = \Pi_{\mathcal{C}_1}(\ell_{345}) = \gamma_{89}$.

For $\alpha \in [-\phi_1, \phi_1]$, we consider the pre-image of $l_\alpha \cup l'_\alpha$ on $\mathcal{F}_{234}$, denoted by L^α_{234}. In other words, we have $\Pi_{\mathcal{C}_1}(L^\alpha_{234}) = l_\alpha \cup l'_\alpha$. Similarly, there is a curve L^α_{345} in $\mathcal{F}_{345}$ such that $\Pi_{\mathcal{C}_1}(L^\alpha_{345}) = l_\alpha \cup l'_\alpha$. For each $\alpha \in [-\phi_1, \phi_1]$, we see that L^α_{234} and ℓ_{234} (L^α_{345} and ℓ_{345}) intersect a point whose orthogonal projection on $\mathcal{C}_1$ is $\mathbf{p}_0^\alpha$.

In order to see this, we construct a family of Lagrangian planes which contain the geodesic segments connecting with $\mathbf{p}_0^\alpha$ and a point of $\mathcal{F}_{234}$ (or $\mathcal{F}_{345}$).

- Analysis of the pre-image $\Pi_{\mathcal{C}_1}^{-1}(l_\alpha) \subset L_{234}^\alpha$ and the case $\Pi_{\mathcal{C}_1}^{-1}(l_\alpha) \subset L_{345}^\alpha$ follows similarly. For $s \in [-\lambda, \lambda]$, a slice $\mathcal{C}_s$ of $\mathcal{B}_c$ corresponds to s being constant. We denote $\mathbf{p}_s$ by the intersection of the slice $\mathcal{C}_s$ with the edge γ_{16}. A bisector whose spine is the geodesic passing through 0 and $\mathbf{p}_s$ in $\mathcal{C}_2$ is denoted by $\mathcal{B}_s$. It follows that $\mathcal{C}_s$ and $\mathcal{C}_1$ turn out be two of the slices of $\mathcal{B}_s$. For a fixed $\alpha \in [-\phi_1, \phi_1]$, a meridian $L_{\alpha,s}$ of $\mathcal{B}_s$ containing l_α intersects with $\mathcal{C}_s$ and $\mathcal{F}_{234}$ at a point $\mathbf{q}_{\alpha,s}$. For $s = -\lambda$, we see that $\mathbf{q}_{\alpha,s} = \mathbf{p}_1^\alpha$ and $\Pi_{\mathcal{C}_1}([\mathbf{p}_1^\alpha, \mathbf{p}_0^\alpha]) = l_\alpha$. We can take $s_\alpha \in (-\lambda, \lambda)$ such that $\Pi_{\mathcal{C}_1}([\mathbf{q}_{\alpha,s_\alpha}, \mathbf{p}_0^\alpha]) = \mathbf{p}_0^\alpha$. Thus a curve consisting of points $\mathbf{q}_{\alpha,s}$ for $[-\lambda, s_\alpha]$ becomes $\Pi_{\mathcal{C}_1}^{-1}(l_\alpha) \subset L_{345}^\alpha$, drawn by the blue line in $\mathcal{F}_{234}$.

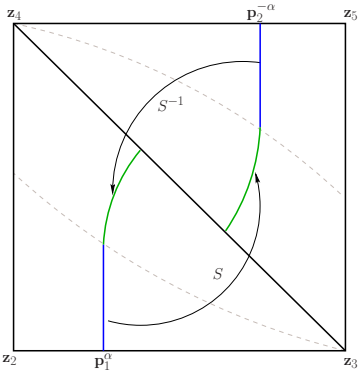

- Analysis of the pre-image $\Pi_{\mathcal{C}_1}^{-1}(l'_\alpha) \subset L_{234}^\alpha$. We denote $\mathbf{q}'_{-\alpha,s}$ by the intersection of $L_{-\alpha,s}$ with $\mathcal{C}_s$ and $\mathcal{F}_{345}$. For a fixed $\alpha \in [-\phi_1, \phi_1]$, we can take $s'_\alpha \in (-\lambda, \lambda)$ such that $\Pi_{\mathcal{C}_1}([\mathbf{q}'_{-\alpha,s'_\alpha}, \mathbf{p}_0^{-\alpha}]) = \mathbf{p}_0^{-\alpha}$ and $\Pi_{\mathcal{C}_1}([\mathbf{q}'_{-\alpha,\lambda}, \mathbf{p}_0^{-\alpha}]) = l_{-\alpha}$. Since the map S preserves $\mathcal{C}_1$, we have $\Pi_{\mathcal{C}_1}(S^{-1}([\mathbf{q}'_{-\alpha,s}, \mathbf{p}_0^{-\alpha}])) = S^{-1}(\Pi_{\mathcal{C}_1}([\mathbf{q}'_{-\alpha,s}, \mathbf{p}_0^{-\alpha}]))$. In particular, $\Pi_{\mathcal{C}_1}(S^{-1}([\mathbf{q}'_{-\alpha,s'_\alpha}, \mathbf{p}_0^{-\alpha}])) = S^{-1}(\mathbf{p}_0^{-\alpha}) = \mathbf{p}_0^\alpha$ and $\Pi_{\mathcal{C}_1}(S^{-1}([\mathbf{q}'_{-\alpha,\lambda}, \mathbf{p}_0^{-\alpha}])) = S^{-1}(l_\alpha) = l'_\alpha$. Thus we define a curve consisting of points $S^{-1}(\mathbf{q}'_{-\alpha,s})$ for $[s'_\alpha, \lambda]$, which is drawn by the green line in $\mathcal{F}_{234}$. In fact, the geodesic segment $S^{-1}([\mathbf{q}'_{-\alpha,s}), \mathbf{p}_0^{-\alpha}])$ is contained in the meridian $S^{-1}(L_{-\alpha,s})$ of bisector $S^{-1}(\mathcal{B}_s)$.

The same construction can be implemented for the face $\mathcal{F}_{345}$. This enables us to give the following proposition.

Proposition 5.3.21. *For $\alpha \in [-\phi_1, \phi_1]$, then $S(L_{234}^\alpha) = L_{345}^{-\alpha}$.*

Sides foliated by 2-dimensional cones

For each $\alpha \in [-\phi_1, \phi_1]$, we define a *sheet* $\mathfrak{X}_{234}^\alpha$ to be the geodesic cone from L_{234}^α to the point $\mathbf{p}_0^\alpha$. In other words, we join with each point of L_{234}^α to $\mathbf{p}_0^\alpha$ by a geodesic segment, that is

$$\mathfrak{X}_{234}^\alpha = \bigcup_{\mathbf{z} \in L_{234}^\alpha} [\mathbf{p}_0^\alpha, \mathbf{z}].$$

Analogously, the sheet $\mathfrak{X}_{345}^\alpha$ is defined to be the geodesic cone from L_{345}^α to the point $\mathbf{p}_0^\alpha$, that is

$$\mathfrak{X}_{345}^\alpha = \bigcup_{\mathbf{z} \in L_{345}^\alpha} [\mathbf{p}_0^\alpha, \mathbf{z}].$$

Proposition 5.3.22. *For $\alpha \neq \beta \in [-\phi_1, \phi_1]$, $\mathfrak{X}_{234}^\alpha$ (resp. $\mathfrak{X}_{345}^\alpha$) and $\mathfrak{X}_{234}^\beta$ (resp. $\mathfrak{X}_{345}^\beta$) are disjoint.*

Proof. It suffices to show that the orthogonal projection of $\mathfrak{X}_{234}^\alpha$ (or $\mathfrak{X}_{345}^\alpha$) onto $\mathcal{C}_1$ is $l_\alpha \cup l'_\alpha$. From Lemma 1.2.10, the projection of $[\mathbf{z}, \mathbf{p}_0^\alpha]$ is a geodesic segment joining $\mathbf{p}_0^\alpha$ and $\Pi_{\mathcal{C}_1}(\mathbf{z})$. Observe that both l_α and l'_α are geodesic segments with common endpoint $\mathbf{p}_0^\alpha$. For each point $\mathbf{z}$ of L_{234}^α, it follows that $\Pi_{\mathcal{C}_1}(\mathbf{z}) \in l_\alpha \cup l'_\alpha$ implies $\Pi_{\mathcal{C}_1}([\mathbf{z}, \mathbf{p}_0^\alpha])$ is contained in $l_\alpha \cup l'_\alpha$. For $\alpha \neq \beta \in [-\phi_1, \phi_1]$, therefore, $\{l_\alpha \cup l'_\alpha\} \cap \{l_\beta \cup l'_\beta\} = \emptyset$ implies that $\mathfrak{X}_{234}^\alpha \cap \mathfrak{X}_{234}^\beta = \emptyset$ (or $\mathfrak{X}_{345}^\alpha \cap \mathfrak{X}_{345}^\beta = \emptyset$). □

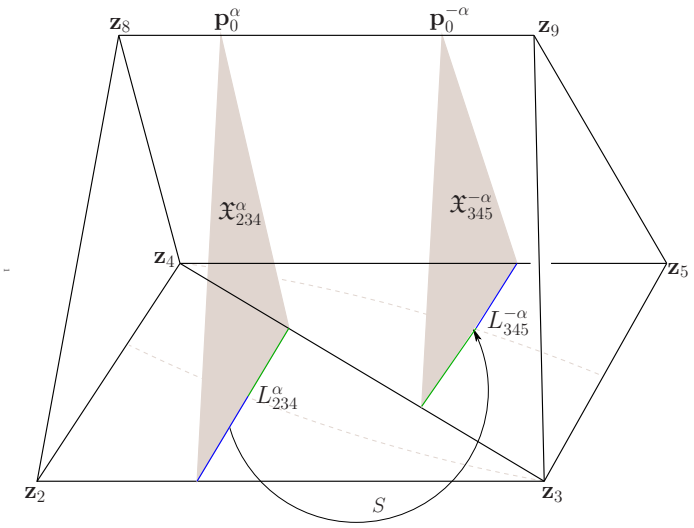

FIGURE 5.7: The schematic view of the sheets of two sides $\mathcal{S}_g$ and $\mathcal{S}'_g$. The action of S on a sheet $\mathfrak{X}_{234}^{\alpha}$ to $\mathfrak{X}_{345}^{-\alpha}$.

We are ready to describe the sides $\mathcal{S}_g$ and $\mathcal{S}'_g$, for the schematic view in Figure 5.7.

Definition 5.3.23. *The side S_g is made up of the sheets $\mathfrak{X}_{234}^{\alpha}$ for $\alpha \in [-\phi_1, \phi_1]$, namely,* $\mathcal{S}_g = \bigcup_{\alpha\in[-\phi_1,\phi_1]} \mathfrak{X}_{234}^{\alpha}$.

Definition 5.3.24. *The side S'_g is made up of the sheets $\mathfrak{X}_{345}^{\alpha}$ for $\alpha \in [-\phi_1, \phi_1]$, namely,* $\mathcal{S}'_g = \bigcup_{\alpha\in[-\phi_1,\phi_1]} \mathfrak{X}_{345}^{\alpha}$.

From Proposition 5.3.22, we remark that both $\mathcal{S}_g$ and $\mathcal{S}'_g$ are real analytic 3-submanifolds.

5.3.5 Construction of the polyhedron

In the previous sections we constructed eight 3-dimensional cells which are sides of our polyhedron. We define the polyhedron $\mathbf{D}$ to be the interior of the union of eight 3-cells, refer to Figure 5.7. It follows from Proposition 5.3.25 that $\mathbf{D}$ is well-defined a 4-dimensional domain.

Proposition 5.3.25. *$\mathcal{S}_c \cup \mathcal{S}'_c \cup \mathcal{S}_g \cup \mathcal{S}'_g \cup \mathcal{S}_{17} \cup \mathcal{S}_{67} \cup \mathcal{S}_{78} \cup \mathcal{S}_{79}$ is homeomorphic to S^3.*

Proof. Recall of the basic geometric fact that S^3 can be interpreted as the union of two 3-balls gluing along S^2. We see, up to homotopy, that the core prism $\mathcal{P}_c$ is a 3-ball with the boundary $\mathcal{F}_{123} \cup \mathcal{F}_{456} \cup \mathcal{F}_{1246} \cup \mathcal{F}_{1356} \cup \mathcal{F}_{234} \cup \mathcal{F}_{345}$. Another 3-ball is the union of $\mathcal{S}_g, \mathcal{S}'_g, \mathcal{S}_{17}, \mathcal{S}_{67}, \mathcal{S}_{78}, \mathcal{S}_{79}$ whose boundary is also $\mathcal{F}_{123} \cup \mathcal{F}_{456} \cup \mathcal{F}_{1246} \cup \mathcal{F}_{1356} \cup \mathcal{F}_{234} \cup \mathcal{F}_{345}$. In order to see this, we can think that two faces $\mathcal{F}_{123}$ and $\mathcal{F}_{456}$ are lying at both sides of the face $\mathcal{F}_{789}$. This completes the result. □

We also need to ensure that the interior of two sides $\mathcal{S}_g$ and $\mathcal{S}'_g$ cannot intersect the other sides contained in bisectors. This follows directly from the following proposition.

Proposition 5.3.26. *The interior of $\mathcal{S}_g$ and $\mathcal{S}'_g$ does not intersect with the sides contained in bisectors.*

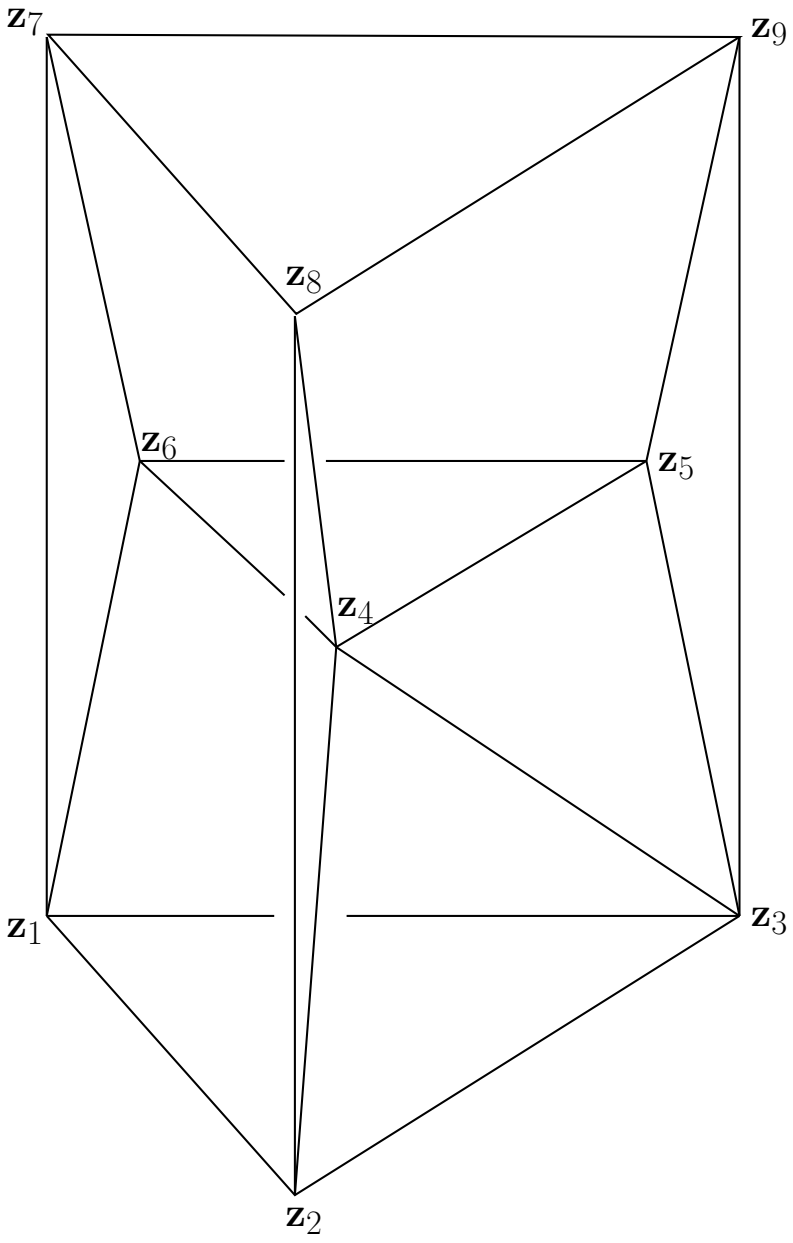

FIGURE 5.8: The schematic view of eight sides of the polyhedron **D** in the complex hyperbolic space. **D** is a 4-dimensional domain bounded by these eight sides.

Proof. It suffices to show the interior of each sheet $\mathfrak{X}^{\alpha}_{234}$ (or $\mathfrak{X}^{\alpha}_{345}$) does not meet with the sides contained in bisectors for $\alpha \in [-\phi_1, \phi_1]$. We only need to analyze the sheet $\mathfrak{X}^{\alpha}_{234}$ and the other follows similarly.

Recall, the bisectors containing the sides come in pairs so that the complex spines are the coordinate axes. As in the Proposition 1.2.28 of [Tho10] (or the Section 2.1.2), the number of intersection points between a geodesic and a bisector is equal to the number of intersection points between its spine and the projection of the geodesic onto its complex spine. Moreover, as in Section 1.2.4, we know that the projection of a geodesic σ to a complex line $\mathcal{C}$ is an arc of a geometrical circle (and in particular, this is also a geodesic arc if $\sigma \cap \mathcal{C} \neq \emptyset$) in $\mathcal{C}$. For the case that $\mathcal{C}$ is a coordinate axis, the projection of a geodesic segment $[\mathbf{z}, \mathbf{w}]$ is a shorter arc of a geometrical circle with endpoints $\Pi_{\mathcal{C}}(\mathbf{z})$ and $\Pi_{\mathcal{C}}(\mathbf{w})$ (the images of points under orthogonal projection onto $\mathcal{C}$).

For $\alpha \in [-\phi_1, \phi_1]$ and $\mathbf{z} \in L^{\alpha}_{234}$, we consider the projection of the geodesic segment $[\mathbf{p}^{\alpha}_0, \mathbf{z}]$ onto the coordinate axes $\mathcal{C}_1$ and $\mathcal{C}_2$. We denote Π_1, Π_2 by the orthogonal projection onto $\mathcal{C}_1$ and $\mathcal{C}_2$ respectively.

(i) Pair of sides $\mathcal{S}_{78}, \mathcal{S}_{79}$ are contained in bisectors $\mathcal{B}_{78}, \mathcal{B}_{79}$ whose spines contain γ_{78} and γ_{79}. Clearly, $\Pi_1([\mathbf{p}^{\alpha}_0, \mathbf{z}]) = l_{\alpha} \cup l'_{\alpha}$ does not intersect with γ_{78} and γ_{79}.

(ii) Pair of sides $\mathcal{S}_{17}, \mathcal{S}_{67}$ are contained in bisectors $\mathcal{B}_{17}, \mathcal{B}_{67}$ whose spines contain the straight segment γ_{17} and γ_{67}.

- For $\mathbf{z} \in \Pi_1^{-1}(l_{\alpha})$, the geodesic segment $[\mathbf{p}^{\alpha}_0, \mathbf{z}]$ is contained in a meridian of $\mathcal{B}_s$. Thus $\Pi_2([\mathbf{p}^{\alpha}_0, \mathbf{z}])$ is a straight segment with endpoints $\mathbf{z}_7$ and a point of γ_{16} and cannot intersect with γ_{17}, γ_{67}.
- For $\mathbf{z} \in \Pi_1^{-1}(l'_{\alpha})$, we see that $\Pi_1(\mathcal{S}_{17}) = \Pi_1(\mathcal{S}_{67})$ is the geodesic triangular face $\mathcal{F}_{789}$ and $\Pi_1([\mathbf{p}^{\alpha}_0, \mathbf{z}]) = l'_{\alpha}$. The interior of l'_{α} does not intersect with $\mathcal{F}_{789}$.

(iii) Pair of sides $\mathcal{S}_c, \mathcal{S}'_c$ are contained in bisector $\mathcal{B}_c$ whose spine contains γ_{16}.

- For $\mathbf{z} \in \Pi_1^{-1}(l_{\alpha})$, then $\Pi_2([\mathbf{p}^{\alpha}_0, \mathbf{z}])$ is a straight segment which intersects with γ_{16} only at $\Pi_2(\mathbf{z})$.
- We denote $(\mathbf{p}^{\alpha}_0, *)$ by the extension of $[\mathbf{p}^{\alpha}_0, \mathbf{z}]$ from $\mathbf{p}^{\alpha}_0$ to ∞ without $\mathbf{p}^{\alpha}_0$. For $\mathbf{z} \in \Pi_1^{-1}(l'_{\alpha})$, observe that $\Pi_1(\mathbf{p}^{\alpha}_0, *)$ is a geodesic ray from $\mathbf{p}^{\alpha}_0$ to the boundary passing through $S(0)$, see Figure 5.6. Non-intersection of $\Pi_1(\mathbf{p}^{\alpha}_0, *)$ and $\mathcal{F}_{789}$ shows that $(\mathbf{p}^{\alpha}_0, *)$ cannot intersect with the sides $\mathcal{S}_{17}$ and $\mathcal{S}_{67}$. Thus we know that $\Pi_2(\mathbf{p}^{\alpha}_0, *)$ does not intersect with γ_{17} and γ_{67}. From the geometric view, we claim that $\Pi_2([\mathbf{p}^{\alpha}_0, \mathbf{z}])$ intersects with γ_{16} only at $\Pi_2(\mathbf{z})$. In fact, the interior of $\Pi_2([\mathbf{p}^{\alpha}_0, \mathbf{z}])$ can only lie inside the angle region $-\phi_2 \leq \arg(z_2) \leq \phi_2$. Otherwise, it is not the shorter arc of a circle which is contradiction with Lemma 1.2.12. If $\Pi_2([\mathbf{p}^{\alpha}_0, \mathbf{z}])$ intersects with γ_{16} twice, then $\Pi_2(\mathbf{p}^{\alpha}_0, *)$ intersects with γ_{17} or γ_{67}, which is a contradiction.

From the above analysis, we see that the interior of $[\mathbf{p}^{\alpha}_0, \mathbf{z}]$ for $\alpha \in [-\phi_1, \phi_1]$ cannot intersect with the sides contained in bisectors. □

5.4 The main theorem

Our goal is to use Poincaré's polyhedron theorem to show that the polyhedron $\mathbf{D}$ is a fundamental domain and find a geometrical presentation although we already know both

that the group Γ_k is discrete and that a presentation of Γ_k (see [DFP05, Par06]). We will prove the following result:

Theorem 5.4.1. *Suppose that the ordered pair (k,l) is in the list*

$$(7,42),\ (8,24),\ (9,18),\ (10,15),\ (12,12),\ (15,10),\ (18,9),\ (24,8),\ (42,7),$$

that is, $l = 6k/(k-6)$. Then writing $\phi_1 = \pi/k$ and $\phi_2 = \pi/l$, the group Γ_k generated by the side pairings of $\mathbf{D}$ is a discrete subgroup of $PU(2,1)$ with fundamental domain $\mathbf{D}$ and presentation

$$\Gamma_k = \left\langle R, S, T, I_1 : \begin{array}{c} R^k = T^l = (R^{-1}S)^3 = (T^{-1}I_1)^3 = (S^{-1}I_1)^3 \\ = [R,T] = 1, \quad T = S^2, \quad R = I_1^2 \end{array} \right\rangle. \tag{5.28}$$

Remark 5.4.2. As the roles of k and l are actually symmetric, there are only 5 different groups Γ_k for $k = 7, 8, 9, 10, 12$. In particular, among them only Γ_9 and Γ_{12} are arithmetic, see the Table on the Page 27 of [Par09].

We will prove this theorem by verifying the conditions of the Poincaré's polyhedron theorem, following the strategy outlined below. For the case of $k = 6$, that is $l = \infty$, this makes T turn into a parabolic which gives rise to the disappearance of T^l in the presentation. Thus the group Γ_6 is exactly the same as G_2 (compare [Zh11]), up to conjugation.

Writing $J = S^{-1}I_1$, $R_1 = T^{-1}I_1$, $A_1 = R$ and $A_1' = JTJ^{-1}$, the presentation of Theorem 5.4.1 becomes

$$\left\langle J, R_1, A_1, A_1' : \begin{array}{c} J^3 = R_1^3 = A_1^k = {A_1'}^l = 1, \\ A_1 = (JR_1^{-1}J)^2, A_1' = (J^{-1}R_1^{-1}J^{-1})^2, \\ A_1R_1 = R_1A_1, A_1'R_1 = R_1A_1' \end{array} \right\rangle.$$

Note that $[A_1, R_1] = [R, T]$ follows from $R = I_1^2$ and $[A_1', R_1] = J[T,R]J^{-1}$ follows from $T = S^2$ and $R^{-1}S = J^{-1}R_1J$. This is the presentation in terms of R_1, J given in [Par09] with $p = 3$.

5.4.1 The side pairing maps

Let R, S, T and I_1 be given by (5.5), (5.11) and (5.12) respectively. In this section we show that these maps are the side-pairings of our polyhedron $\mathbf{D}$ and pair the sides of $\mathbf{D}$ as follows (see Figure 5.9).

$$R : \mathcal{S}_{78} \longrightarrow \mathcal{S}_{79}, \quad T : \mathcal{S}_{17} \longrightarrow \mathcal{S}_{67}, \quad S : \mathcal{S}_g \longrightarrow \mathcal{S}_g', \quad I_1 : \mathcal{S}_c \longrightarrow \mathcal{S}_c'.$$

We now verify these maps satisfy conditions (I) and (II) in Definition 2.3.3 for each side. It is clear that the side pairing maps R, S, T satisfy condition (I) and we give more details for the side pairing map I_1.

Recall that the map

$$I_1 = \frac{e^{-i\phi_1/3}}{2\sin\phi_2} \begin{bmatrix} -2\sin\phi_2 e^{i\phi_1} & 0 & 0 \\ 0 & 1 & -\sqrt{1-4\sin^2\phi_2} \\ 0 & \sqrt{1-4\sin^2\phi_2} & -1 \end{bmatrix}.$$

The action of I_1 on the bisector $\mathcal{B}_c$ (see (5.16)) is given by

$$\begin{aligned}\frac{e^{-i\phi_1/3}}{2\sin\phi_2}&\begin{bmatrix}-2\sin\phi_2 e^{i\phi_1} & 0 & 0\\ 0 & 1 & -\sqrt{1-4\sin^2\phi_2}\\ 0 & \sqrt{1-4\sin^2\phi_2} & -1\end{bmatrix}.\begin{bmatrix}\sqrt{1-\mu^2}re^{i\alpha}\\ \mu+is\\ 1+i\mu s\end{bmatrix}\\ &= -e^{-i\phi_1/3}\begin{bmatrix}\sqrt{1-\mu^2}re^{i(\alpha+\phi_1)}\\ \mu-is\\ 1-i\mu s\end{bmatrix}.\end{aligned}$$

We see that I_1 maps $\mathcal{B}_c$ to itself, sending the point with coordinates (r,s,α) to the point with coordinates $(r,-s,\alpha+\phi_1)$ when $-\pi/2\le\alpha<\pi/2-\phi_1$ or the point with coordinates $(-r,-s,\alpha+\phi_1-\pi)$ when $\pi/2-\phi_1\le\alpha<\pi/2$.

In terms of its action on the vertices of prism, we summarize as follows

$$I_1:\quad\begin{array}{ccc}\mathbf{z}_1&\longrightarrow&\mathbf{z}_6,\\ \mathbf{z}_2&\longrightarrow&\mathbf{z}_4,\\ \mathbf{z}_3&\longrightarrow&\mathbf{z}_5,\\ \mathbf{z}_4&\longrightarrow&\mathbf{z}_3,\\ \mathbf{z}_6&\longrightarrow&\mathbf{z}_1.\end{array}$$

By Lemmas 5.3.11 and 5.3.12, we can easily see that

$$I_1(\gamma_{16})=\gamma_{16},\ I_1(\gamma_{12})=\gamma_{46},\ I_1(\gamma_{13})=\gamma_{56},$$

$$I_1(\gamma_{24})=\gamma_{34},\ I_1(\gamma_{34})=\gamma_{35},$$

which implies that

$$I_1(\mathcal{F}_{1246})=\mathcal{F}_{1346},\qquad I_1(\mathcal{F}_{1346})=\mathcal{F}_{1356}.$$

We now concentrate on showing $I_1(\mathcal{F}_{234})=\mathcal{F}_{456}$ and $I_1(\mathcal{F}_{123})=\mathcal{F}_{456}$. Observe that the face $\mathcal{F}_{234}$ is contained in the intersection $\mathcal{B}_c\cap S^{-1}(\mathcal{B}_c)=\mathcal{B}_c\cap J(\mathcal{B}_c)$ that is a *Giraud disc*. Moreover, we have $J(\mathcal{F}_{234})\subset J(\mathcal{B}_c)\cap J^{-1}(\mathcal{B}_c)$ and $J^{-1}(\mathcal{F}_{234})\subset J^{-1}(\mathcal{B}_c)\cap\mathcal{B}_c$ since J is a regular elliptic element of order 3. As the permutation of J on the edges γ_{23},γ_{34} and γ_{24}, the triple intersection $\mathcal{B}_c\cap J(\mathcal{B}_c)\cap J^{-1}(\mathcal{B}_c)$ contains γ_{23},γ_{34} and γ_{24}. It follows that the third bisector containing the face $\mathcal{F}_{234}$ is $J^{-1}(\mathcal{B}_c)=I_1^{-1}S(\mathcal{B}_c)$. Obviously the map I_1 sends points of $\mathcal{B}_c\cap I_1^{-1}S(\mathcal{B}_c)$ to points of $\mathcal{B}_c\cap S(\mathcal{B}_c)$. Furthermore, the edge γ_{23} is contained in $\mathcal{B}_c\cap I_1^{-1}S(\mathcal{B}_c)$ with $s_0=-\lambda$ and the edge γ_{45} is contained in $\mathcal{B}_c\cap S(\mathcal{B}_c)$ with $s_0=\lambda$, which implies that $I_1(\gamma_{23})=\gamma_{45}$. From the above argument, we obtain $I_1(\mathcal{F}_{234})=\mathcal{F}_{456}$ and $I_1(\mathcal{F}_{123})=\mathcal{F}_{456}$. As a result, we prove that $I_1(\mathcal{S}_c)=\mathcal{S}'_c$.

We give the following lemma to verify condition (II) for each side.

Lemma 5.4.3. *If g is one of R,S,T,I_1, then $g^{-1}(\mathbf{D})\cap\mathbf{D}=g(\mathbf{D})\cap\mathbf{D}=\emptyset$. Moreover,*

$$\begin{array}{cccc}R^{-1}(\overline{\mathbf{D}})\cap\overline{\mathbf{D}}=\mathcal{S}_{78},&T^{-1}(\overline{\mathbf{D}})\cap\overline{\mathbf{D}}=\mathcal{S}_{17},&S^{-1}(\overline{\mathbf{D}})\cap\overline{\mathbf{D}}=\mathcal{S}_g,&I_1^{-1}(\overline{\mathbf{D}})\cap\overline{\mathbf{D}}=\mathcal{S}_c,\\ R(\overline{\mathbf{D}})\cap\overline{\mathbf{D}}=\mathcal{S}_{79},&T(\overline{\mathbf{D}})\cap\overline{\mathbf{D}}=\mathcal{S}_{67},&S(\overline{\mathbf{D}})\cap\overline{\mathbf{D}}=\mathcal{S}'_g,&I_1(\overline{\mathbf{D}})\cap\overline{\mathbf{D}}=\mathcal{S}'_c.\end{array}$$

Proof. • Consider the side $\mathcal{S}_{78}$ and other sides $\mathcal{S}_{79},\mathcal{S}_{17},\mathcal{S}_{67}$ follow similarly. If $\mathbf{z}\in\overline{\mathbf{D}}$ then $-\phi_1\le\arg(z_1)\le\phi_1$ with equality only when $\mathbf{z}\in\mathcal{B}_{78}$ (or $\mathcal{B}_{79}$). Likewise, if $\mathbf{w}=R(\mathbf{z})\in\overline{\mathbf{D}}$ then $-\phi_1\le\arg(e^{i2\phi_1}z_1)\le\phi_1$. Hence if $R(\mathbf{z})\in\overline{\mathbf{D}}$, or equivalently $\mathbf{z}\in R^{-1}(\mathbf{D})$, then $-3\phi_1\le\arg(z_1)\le-\phi_1$. Thus $\mathbf{z}\in\overline{\mathbf{D}}\cap R^{-1}(\overline{\mathbf{D}})$ if and only if $\mathbf{z}\in\mathcal{B}_{78}$ and precisely $\mathbf{z}\in\mathcal{S}_{78}$.

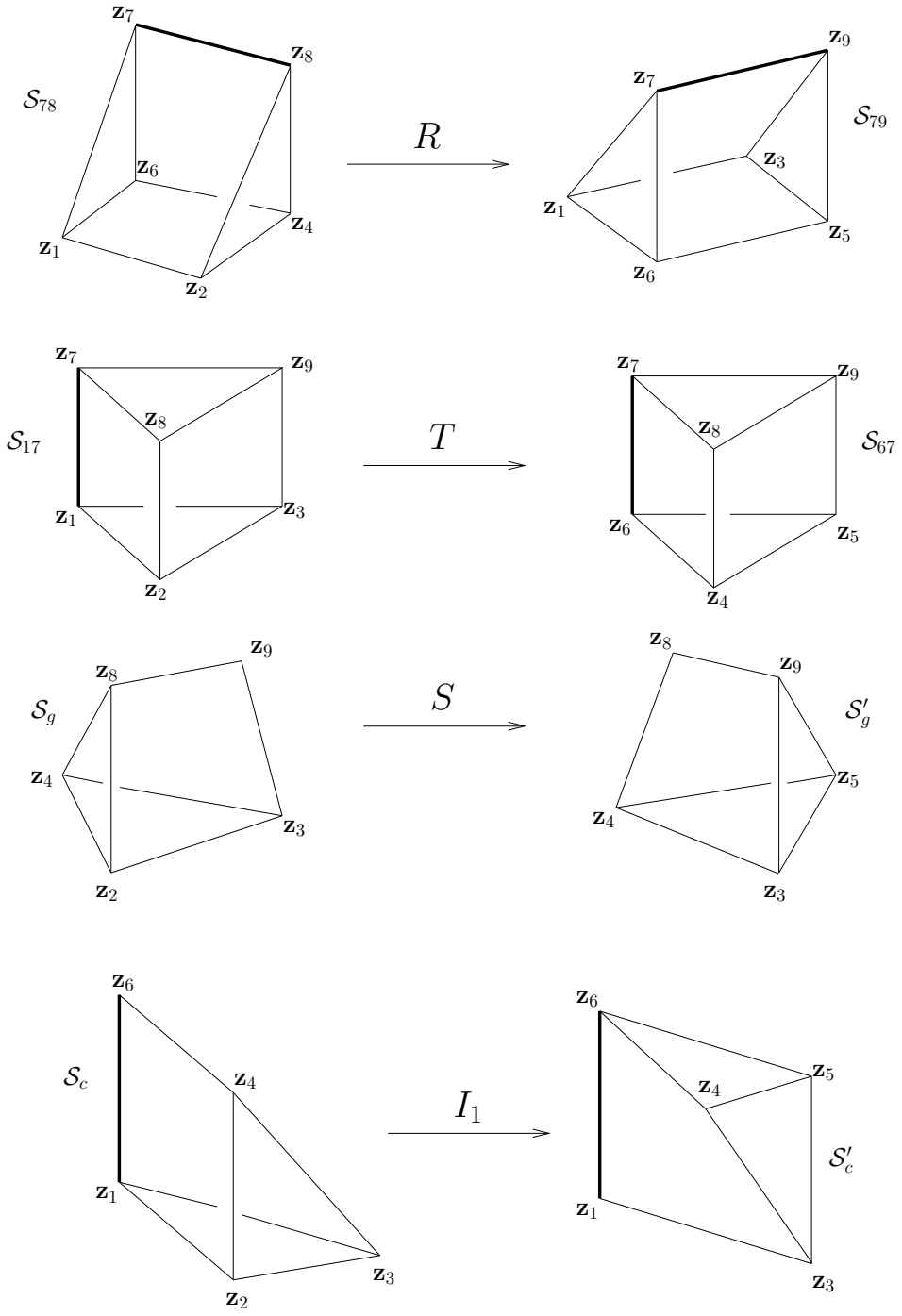

FIGURE 5.9: The sides of the polyhedron and side pairings. The bold lines denote the spines of the bisectors.

- Consider the core sides $\mathcal{S}_c$ and $\mathcal{S}'_c$. Observe that I_1 preserves $\mathcal{B}_c$ and swaps one side of $\mathcal{B}_c$ with the other. If $\mathbf{z} = (z_1, z_2) \in \overline{\mathbf{D}}$ then $2\sin\phi_2|z_2| \leq |z_2 - \sqrt{1-4\sin^2\phi_2}|$ with equality only when $\mathbf{z} \in \mathcal{S}_c \cup \mathcal{S}'_c$. If $\mathbf{z} \in \mathbf{D}$, then $\mathbf{w} = I_1(\mathbf{z})$ satisfying $2\sin\phi_2|w_2| > |w_2 - \sqrt{1-4\sin^2\phi_2}|$ does not intersect $\overline{\mathbf{D}}$. Only $\mathbf{z} \in \mathcal{S}_c$ (resp. $\mathbf{z} \in \mathcal{S}'_c$) then $I_1(\mathbf{z}) \in \mathcal{S}'_c$ (resp. $I_1^{-1}(\mathbf{z}) \in \mathcal{S}_c$).
- Consider the sides $\mathcal{S}_g$ and $\mathcal{S}'_g$. By construction, we see that $S(\mathcal{S}_g) = \mathcal{S}'_g$. It suffices to show that the images of other sides under S cannot intersect with the sides of $\mathbf{D}$ except for $\mathcal{S}'_g$. In order to see this, the spines of $S(\mathcal{B}_{78})$ and $S(\mathcal{B}_{79})$ are the geodesic segments connecting with $S(0)$ and $\mathbf{z}_8, \mathbf{z_9}$. It is easy to see that there is no intersection of the interior of $S(\mathcal{B}_{78})$ and $S(\mathcal{B}_{79})$ with the sides of $\overline{\mathbf{D}}$. The spines of $S(\mathcal{B}_{17})$ and $S(\mathcal{B}_{67})$ are the straight lines in common complex spine $S(\mathcal{C}_2)$. Their projection on $\mathcal{C}_1$ is a geodesic triangle with vertices $\mathbf{z}_8, \mathbf{z}_9, S(0)$. Thus they don't intersect with the sides of $\overline{\mathbf{D}}$. For the side $\mathcal{S}_g$, $T(\mathcal{S}'_g) \cap \mathcal{S}'_g = \emptyset$ implies that $S(\mathcal{S}'_g) \cap \mathcal{S}_g = \emptyset$. Moreover, $S(\mathcal{S}'_g) = T(\mathcal{S}_g)$ implies that this is the same projection of $\mathcal{S}_g$ on $\mathcal{C}_1$ and a rotation of the projection on $\mathcal{C}_2$ with angle ϕ_2.

□

5.4.2 The face cycles

We now write the face cycles induced by the side-pairings in terms of type of face and the label of face reflects the order of vertices.

- The $\mathbb{C}$-planar triangle cycles:

$$\mathcal{F}_{167} \xrightarrow{R} \mathcal{F}_{167},$$

$$\mathcal{F}_{789} \xrightarrow{T} \mathcal{F}_{789},$$

$$\mathcal{F}_{123} \xrightarrow{I_1} \mathcal{F}_{645} \xrightarrow{T^{-1}} \mathcal{F}_{123},$$

$$\mathcal{F}_{248} \xrightarrow{S} \mathcal{F}_{359} \xrightarrow{R^{-1}} \mathcal{F}_{248}.$$

- The $\mathbb{R}$-planar quadrilateral cycles:

$$\mathcal{F}_{1287} \xrightarrow{T} \mathcal{F}_{6487} \xrightarrow{R} \mathcal{F}_{6597} \xrightarrow{T^{-1}} \mathcal{F}_{1397} \xrightarrow{R^{-1}} \mathcal{F}_{1287}.$$

- The Giraud triangle cycles:

$$\mathcal{F}_{234} \xrightarrow{I_1} \mathcal{F}_{453} \xrightarrow{S^{-1}} \mathcal{F}_{342} \xrightarrow{I_1} \mathcal{F}_{534} \xrightarrow{S^{-1}} \mathcal{F}_{423} \xrightarrow{I_1} \mathcal{F}_{345} \xrightarrow{S^{-1}} \mathcal{F}_{234}.$$

- The generic quadrilateral cycles:

$$\mathcal{F}_{1246} \xrightarrow{I_1} \mathcal{F}_{6431} \xrightarrow{I_1} \mathcal{F}_{1356} \xrightarrow{R^{-1}} \mathcal{F}_{1246},$$

$$\mathcal{F}_{2398} \xrightarrow{S} \mathcal{F}_{3489} \xrightarrow{S} \mathcal{F}_{4598} \xrightarrow{T^{-1}} \mathcal{F}_{2398}.$$

5.4.3 Verifying the tessellation conditions

In this section we verify the cyclic condition of the Poincaré's polyhedron theorem, we refer more details to [DFP05] and [Par06]. Recall that for a face cycle

$$\mathcal{F}_1 \xrightarrow{g_1} \mathcal{F}_2 \xrightarrow{g_2} \cdots \longrightarrow \mathcal{F}_n \xrightarrow{g_n} \mathcal{F}_1.$$

The cycle transformation $g_n \circ g_{n-1} \cdots \circ g_1$ acts on $\mathcal{F}_1$ as the identity and there is a certain integer m such that $(g_n \circ g_{n-1} \cdots \circ g_1)^m = Id$. We call n the length of cycle and $n \cdot m$ its total length. In order to ensure condition cyclic we must show that there is a neighborhood U of the interior of the face such that U is covered by $\overline{\mathbf{D}}$ and its images under relevant sid pairings. Specifically, for the above face cycle, the following images of $\overline{\mathbf{D}}$:

$$g_1^{-1}(\overline{\mathbf{D}}),\ (g_2 \circ g_1)^{-1}(\overline{\mathbf{D}}),\ \cdots,\ ((g_n \circ g_{n-1} \cdots \circ g_1)^m)^{-1}(\overline{\mathbf{D}}) = \overline{\mathbf{D}}$$

cover a neighborhood of $\mathcal{F}_1$. We only sufficiently consider a neighborhood U of one member of a single face cycle and others are the images of U under suitable side-pairings.

Tessellation around $\mathbb{C}$-planar faces

In this section we consider the faces contained in a complex line. These are the faces $\mathcal{F}_{123}, \mathcal{F}_{456}, \mathcal{F}_{789}, \mathcal{F}_{167}, \mathcal{F}_{248}$ and $\mathcal{F}_{359}$. They form four face cycles described again as follows:

$$\mathcal{F}_{167} \xrightarrow{R} \mathcal{F}_{167}, \qquad \mathcal{F}_{789} \xrightarrow{T} \mathcal{F}_{789}.$$

The face $\mathcal{F}_{167}$ is in the intersection of two bisectors $\mathcal{B}_{78}$ and $\mathcal{B}_{79}$. If a point $z = (z_1, z_2) \in \overline{\mathbf{D}}$, then $-\phi_1 \leq \arg(z_1) \leq \phi_1$ and the face $\mathcal{F}_{167}$ is contained in $z_1 = 0$. We know R acts on z_1-plane as a rotation with the angle $2\phi_1$. Therefore, the union of the images of $\overline{\mathbf{D}}$ under R^i for $i = 1, 2, \cdots, k$ covers a sufficient small neighborhood of the face $\mathcal{F}_{167}$. Similarly, the union of the images of $\overline{\mathbf{D}}$ under T^j for $j = 1, 2, \cdots, l$ covers a sufficient small neighborhood of the face $\mathcal{F}_{789}$, we refer to the schematic view of their images in Figure 5.10. If the group is discrete, these elliptic elements are necessary to have finite order which gives rise to $k, l \in \mathbb{Z}$. Together with the condition $1/k + 1/l = 1/6$, we obtain the pairs (k, l) listed in Theorem 5.4.1. Otherwise the group is not discrete (see [Mos88]). From the geometrical point of view, in this case, $\mathbf{D}$ will intersect its image under some non-trivial power of R or T.

Proposition 5.4.4. *The polyhedron* $\mathbf{D}$ *and its images under the power of* R *(resp.* T*) tessellate around the face* $\mathcal{F}_{167}$ *(resp.* $\mathcal{F}_{789}$*). Moreover, the cycle transformation corresponding to the face* $\mathcal{F}_{167}$ *(resp.* $\mathcal{F}_{789}$*) is* R *(resp.* T*) and* $n = 1$*,* $m = k$ *(resp.* $m = l$*). This gives the cycle relation* $R^k = T^l = 1$*.*

The remaining two face cycles:

$$\begin{aligned} \mathcal{F}_{123} &\xrightarrow{I_1} \mathcal{F}_{456} \xrightarrow{T^{-1}} \mathcal{F}_{123}, \\ \mathcal{F}_{248} &\xrightarrow{S} \mathcal{F}_{359} \xrightarrow{R^{-1}} \mathcal{F}_{248}. \end{aligned}$$

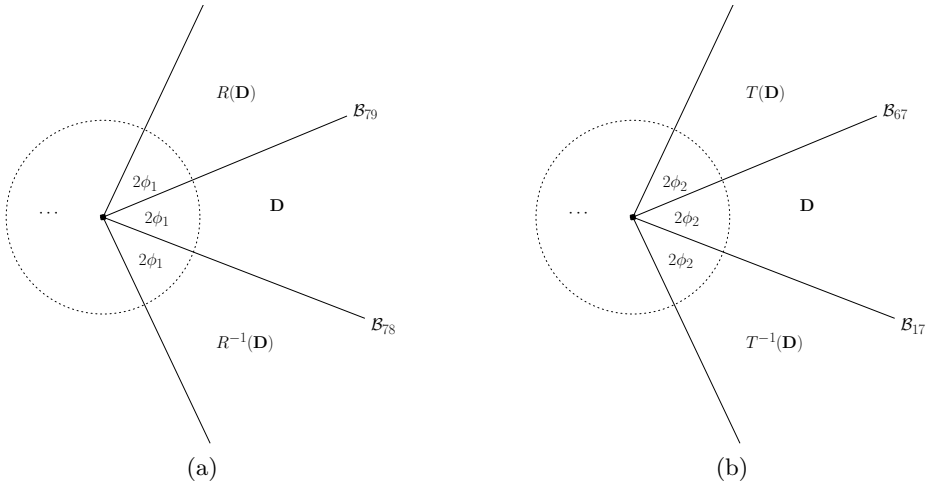

(a) (b)

FIGURE 5.10: (a) The images of $\overline{\mathbf{D}}$ under the power of R tiling a neighborhood of the face $\mathcal{F}_{167}$. (b) The images of $\overline{\mathbf{D}}$ under the power of T tiling a neighborhood of the face $\mathcal{F}_{789}$.

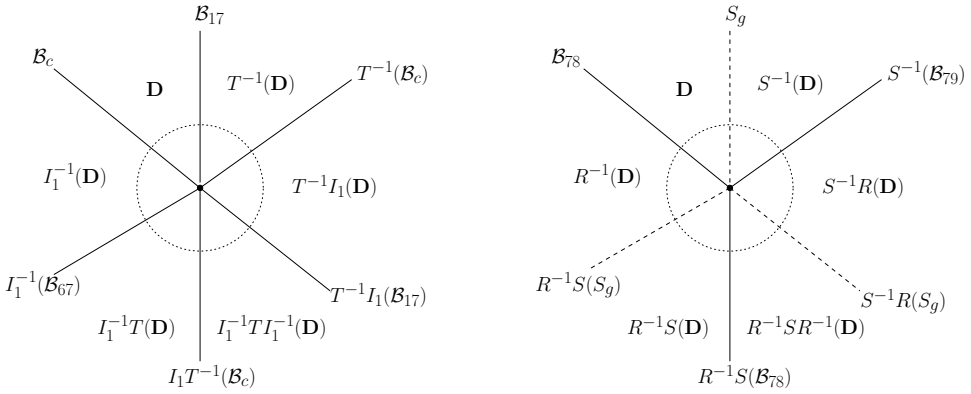

(a) (b)

FIGURE 5.11: (a) The images of $\overline{\mathbf{D}}$ covering a neighborhood of the face $\mathcal{F}_{123}$. (b) The images of $\overline{\mathbf{D}}$ covering a neighborhood of the face $\mathcal{F}_{248}$. The black points at the center indicate the corresponding faces.

Both of $T^{-1}I_1$ and $R^{-1}S$ are the complex reflections. The main difference between them is that the face $\mathcal{F}_{123}$ is in the intersection of two bisectors $\mathcal{B}_c, \mathcal{B}_{17}$ and the face $\mathcal{F}_{248}$ is in the intersection of a bisector $\mathcal{B}_{78}$ with a side S_g which is not contained in bisector. It is the same schematic 2-dimensional picture of covering a neighborhood of $\mathcal{F}_{123}$ and $\mathcal{F}_{248}$, see Figure 5.11.

Proposition 5.4.5. *The polyhedron* $\mathbf{D}$ *and its images under* I_1^{-1}, $I_1^{-1}T$, $I_1^{-1}TI_1^{-1}$, $T^{-1}I_1$ *and* T^{-1} *tessellate around the face* $\mathcal{F}_{123}$. *Moreover, the cycle transformation corresponding to the face* $\mathcal{F}_{123}$ *is* $T^{-1}I_1$ *and* $n = 2$, $m = 3$. *This gives the cycle relation* $(T^{-1}I_1)^3 = 1$.

Proposition 5.4.6. *The polyhedron* $\mathbf{D}$ *and its images under* R^{-1}, $R^{-1}S$, $R^{-1}SR^{-1}$, $S^{-1}R$ *and* S^{-1} *tessellate around the face* $\mathcal{F}_{248}$. *Moreover, the cycle transformation corresponding to the face* $\mathcal{F}_{248}$ *is* $R^{-1}S$ *and* $n = 2$, $m = 3$. *This gives the cycle relation* $(R^{-1}S)^3 = 1$.

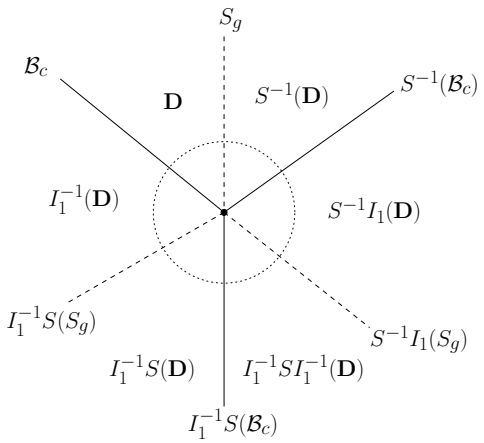

FIGURE 5.12: The images of $\overline{\mathbf{D}}$ covering a neighborhood of the face $\mathcal{F}_{234}$. The black point at the center indicates the face $\mathcal{F}_{234}$.

Tessellation around $\mathbb{R}$-planar faces

In this section we only consider a single face cycle in which the faces are all contained in Lagrangian planes. The associate face cycle is

$$\mathcal{F}_{1278} \xrightarrow{T} \mathcal{F}_{4678} \xrightarrow{R} \mathcal{F}_{5679} \xrightarrow{T^{-1}} \mathcal{F}_{1379} \xrightarrow{R^{-1}} \mathcal{F}_{1278}.$$

The schematic image of the tiling of a neighborhood of the face $\mathcal{F}_{1278}$:

$\mathbf{D}$	$R^{-1}(\mathbf{D})$
$T^{-1}(\mathbf{D})$	$T^{-1}R^{-1}(\mathbf{D})$

In fact that $\mathbf{D}$ and its images as above have disjoint interiors follows easily from Lemma 5.4.3. Moreover, the bisector $\mathcal{B}_{17}$ separates $\mathbf{D}$ and $T^{-1}(\mathbf{D})$, the bisector $\mathcal{B}_{78}$ separates $\mathbf{D}$ and $R^{-1}(\mathbf{D})$. Thus applying T^{-1} to $\mathbf{D}$ and $R^{-1}(\mathbf{D})$, we see that the bisector $T^{-1}(\mathcal{B}_{78})$ separates $T^{-1}(\mathbf{D})$ and $T^{-1}R^{-1}(\mathbf{D})$. Analogously, applying R^{-1} to $\mathbf{D}$ and $T^{-1}(\mathbf{D})$, the bisector $R^{-1}(\mathcal{B}_{17})$ separates $R^{-1}(\mathbf{D})$ and $R^{-1}T^{-1}(\mathbf{D}) = T^{-1}R^{-1}(\mathbf{D})$.

Proposition 5.4.7. *The polyhedron $\mathbf{D}$ and its images under T^{-1}, R^{-1} and $T^{-1}R^{-1}$ tessellate around the face $\mathcal{F}_{1278}$. Moreover, the cycle transformation corresponding to the face $\mathcal{F}_{1278}$ is $R^{-1}T^{-1}RT$ and $n = 4$, $m = 1$. This gives the cycle relation $[T, R] = 1$.*

Tessellation around the face $\mathcal{F}_{234}$

The face $\mathcal{F}_{234}$ is contained in a Giraud disc which is the intersection of $\mathcal{B}_c, S^{-1}(\mathcal{B}_c)$ and $I_1^{-1}S(\mathcal{B}_c)$. It is given by an equation of the form

$$|\langle \mathbf{z}, \mathbf{n}_0 \rangle| = |\langle \mathbf{z}, I_1^{-1}(\mathbf{n}_0) \rangle| = |\langle \mathbf{z}, I_1^{-1}SI_1^{-1}(\mathbf{n}_0) \rangle|.$$

As the arguments in Section 7.8 of [FFP10], we see that there are three regions where the first (resp. second and third) of these quantities as above is the smallest tessellate around the face $\mathcal{F}_{234}$.

Note that the points of $\mathbf{D}$ around the face $\mathcal{F}_{234}$ is bounded by $\mathcal{B}_c$ and the side $\mathcal{S}_g$ and the points of $S^{-1}(\mathbf{D})$ around the face $\mathcal{F}_{234}$ is bounded by $S^{-1}(\mathcal{B}_c)$ and the side $\mathcal{S}_g$. Thus the union of $\mathbf{D}$ and $S^{-1}(\mathbf{D})$ covers a neighborhood of $\mathcal{F}_{234}$ in the region where the first quantity is smallest. Applying the elements $S^{-1}I_1$ and $I_1^{-1}S$, we obtain the union $I_1^{-1}(\mathbf{D})$, $I_1^{-1}S(\mathbf{D})$, $I_1^{-1}SI_1^{-1}(\mathbf{D})$ and $S^{-1}I_1(\mathbf{D})$ covering the other two regions, see Figure 5.12. There is a difference around the faces $\mathcal{F}_{123}$ (or $\mathcal{F}_{248}$) and $\mathcal{F}_{234}$, that is not apparent from the 2-dimensional picture. We give the difference in the following proposition.

Proposition 5.4.8. *The polyhedron* $\mathbf{D}$ *and its images under* I_1^{-1}, $I_1^{-1}S$, $I_1^{-1}SI_1^{-1}$, $S^{-1}I_1$ *and* S^{-1} *tessellate around the face* $\mathcal{F}_{234}$. *Moreover, the cycle transformation corresponding to the face* $\mathcal{F}_{234}$ *is* $(S^{-1}I_1)^3$ *and* $n = 6$, $m = 1$. *This gives the cycle relation* $(S^{-1}I_1)^3 = 1$.

Tessellation around the generic quadrilateral faces

In this section we consider the faces of $\mathbf{D}$ that are neither contained in a complex line nor in a Lagrangian plane nor in a Giraud disc. These faces are regarded as the foliation of geodesics.

We first consider the face $\mathcal{F}_{1346}$, the associated face cycle is

$$\mathcal{F}_{1346} \xrightarrow{I_1} \mathcal{F}_{1356} \xrightarrow{R^{-1}} \mathcal{F}_{1246} \xrightarrow{I_1} \mathcal{F}_{1346}.$$

This is the same situation as in [Zh11]. We state again and refer to the 2-dimensional picture in Figure 5.13.

The face $\mathcal{F}_{1346}$ is the intersection of $\mathcal{S}_c$ and $\mathcal{S}'_c$ contained in the core bisector $\mathcal{B}_c$ and $\mathbf{D}$ covers the part of a neighborhood of $\mathcal{F}_{1346}$ at the side of $\mathcal{B}_c$ where $|\langle \mathbf{z}, \mathbf{n}_0\rangle| < |\langle \mathbf{z}, I_1^{-1}(\mathbf{n}_0)\rangle|$. Observe that I_1 or I_1^{-1} swaps one side of $\mathcal{B}_c$ and the other. Moreover, $I_1^{-1}(\overline{\mathbf{D}}) \cap \overline{\mathbf{D}} = \mathcal{S}_c$, $I_1(\overline{\mathbf{D}}) \cap \overline{\mathbf{D}} = \mathcal{S}'_c$ and $I_1^{-1}(\overline{\mathbf{D}}) \cap I_1(\overline{\mathbf{D}}) = I_1^{-1}(\mathcal{S}_{79}) = I_1(\mathcal{S}_{78})$. Therefore $\overline{\mathbf{D}} \cup I_1^{-1}(\overline{\mathbf{D}}) \cup I_1(\overline{\mathbf{D}})$ covers a neighborhood of $\mathcal{F}_{1346}$.

Proposition 5.4.9. *The polyhedron* $\mathbf{D}$ *and its images under* I_1^{-1} *and* I_1 *tessellate around the face* $\mathcal{F}_{1346}$. *Moreover, the cycle transformation corresponding to the face* $\mathcal{F}_{1346}$ *is* $I_1R^{-1}I_1$ *and* $n = 3$, $m = 1$. *This gives the cycle relation* $I_1R^{-1}I_1 = 1$.

For the face $\mathcal{F}_{3489}$, the associated face cycle is

$$\mathcal{F}_{3489} \xrightarrow{S} \mathcal{F}_{4589} \xrightarrow{T^{-1}} \mathcal{F}_{2389} \xrightarrow{S} \mathcal{F}_{3489}.$$

The face $\mathcal{F}_{1346}$ is the intersection of $\mathcal{S}_g$ and $\mathcal{S}'_g$. Since the map S (or S^{-1}) acts on the triangle $\mathcal{F}_{789}$ as rotation of π around its fixed point, the image $S(\mathbf{D})$ (or $S^{-1}(\mathbf{D})$) may be interpreted as lying in the other side of $\mathcal{S}_g \cup \mathcal{S}'_g$ by S or S^{-1}. Furthermore, it follows from Lemma 5.4.3 that $S^{-1}(\overline{\mathbf{D}}) \cap \overline{\mathbf{D}} = \mathcal{S}_g$, $S(\overline{\mathbf{D}}) \cap \overline{\mathbf{D}} = \mathcal{S}'_g$. It is obvious that $S^{-1}(\overline{\mathbf{D}}) \cap S(\overline{\mathbf{D}}) = S^{-1}(\mathcal{S}_{67}) = S(\mathcal{S}_{17})$ is contained in a bisector, and $\mathcal{S}_g \cap \mathcal{S}'_g \cap S^{-1}(\mathcal{S}_{67}) = \mathcal{F}_{1346}$, see Figure 5.14. The result follows from the same argument as above.

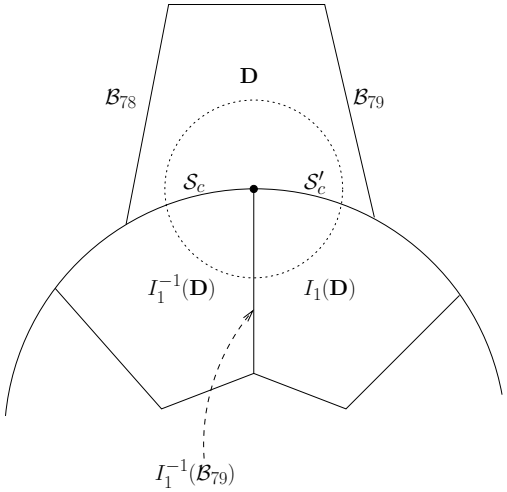

FIGURE 5.13: The images of $\overline{\mathbf{D}}$ covering a neighborhood of the face $\mathcal{F}_{1346}$. The black point at the center indicates the face $\mathcal{F}_{1346}$.

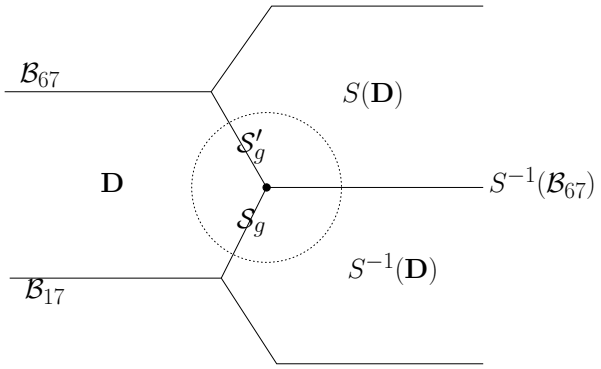

FIGURE 5.14: The images of $\overline{\mathbf{D}}$ covering a neighborhood of the face $\mathcal{F}_{3489}$. The black point at the center indicates the face $\mathcal{F}_{3489}$.

Proposition 5.4.10. *The polyhedron* $\mathbf{D}$ *and its images under* S^{-1} *and* S *tessellate around the face* $\mathcal{F}_{3489}$*. Moreover, the cycle transformation corresponding to the face* $\mathcal{F}_{3489}$ *is* $ST^{-1}S$ *and* $n = 3$*,* $m = 1$*. This gives the cycle relation* $ST^{-1}S = 1$*.*

This completes the proof of Theorem 5.4.1 by Poincaré's polyhedron theorem with Propositions 5.4.4-5.4.10.

5.4.4 Euler orbifold characteristics

We compute again their Euler orbifold characteristics $\chi(\mathbf{H}^2_{\mathbb{C}}/\Gamma_k)$ by analyzing the stabilizer of i-dimensional faces of our fundamental domain $\mathbf{D}$, which agrees with the formula in Page 38 of [Par09] by substituting $p = 3$, see also Theorem 5.1' of [Sau90]. The following table gives the order of the stabilizer for the vertices, 1-simplices, 2-simplices, 3-simplices and the only 4-cell, the whole of $\mathbf{D}$.

i-cells	Cycle	Stabilizer	Order
Vertices	$\mathbf{z}_1, \mathbf{z}_6$	$\langle T^{-1}I_1, R\rangle$	$3k$
	$\mathbf{z}_8, \mathbf{z}_9$	$\langle R^{-1}S, T\rangle$	$3l$
	$\mathbf{z}_7$	$\langle R, T\rangle$	kl
	$\mathbf{z}_2, \mathbf{z}_3, \mathbf{z}_4, \mathbf{z}_5$	$\langle I_1T^{-1}, S^{-1}R\rangle$	24
Edges	γ_{16}	$\langle I_1\rangle$	$2k$
	γ_{89}	$\langle S\rangle$	$2l$
	γ_{17}, γ_{67}	$\langle R\rangle$	k
	γ_{78}, γ_{79}	$\langle T\rangle$	l
	$\gamma_{23}, \gamma_{34}, \gamma_{45}, \gamma_{24}, \gamma_{35}$	$\langle R^{-1}S\rangle$	$2k$
	$\gamma_{28}, \gamma_{48}, \gamma_{39}, \gamma_{59}$	$\langle R^{-1}S\rangle$	$2k$
2-faces	$\mathcal{F}_{123}, \mathcal{F}_{456}$	$\langle T^{-1}I_1\rangle$	3
	$\mathcal{F}_{234}, \mathcal{F}_{345}$	$\langle S^{-1}I_1\rangle$	3
	$\mathcal{F}_{248}, \mathcal{F}_{359}$	$\langle R^{-1}S\rangle$	3
	$\mathcal{F}_{167}$	$\langle R\rangle$	k
	$\mathcal{F}_{789}$	$\langle T\rangle$	l
	$\mathcal{F}_{1246}, \mathcal{F}_{1346}, \mathcal{F}_{1356}$	$\langle Id\rangle$	1
	$\mathcal{F}_{1278}, \mathcal{F}_{4678}, \mathcal{F}_{1379}, \mathcal{F}_{5679}$	$\langle Id\rangle$	1
	$\mathcal{F}_{2389}, \mathcal{F}_{3489}, \mathcal{F}_{4589}$	$\langle Id\rangle$	1
3-faces	$\mathcal{S}_c, \mathcal{S}'_c$	$\langle Id\rangle$	1
	$\mathcal{S}_g, \mathcal{S}'_g$	$\langle Id\rangle$	1
	$\mathcal{S}_{78}, \mathcal{S}_{79}$	$\langle Id\rangle$	1
	$\mathcal{S}_{17}, \mathcal{S}_{67}$	$\langle Id\rangle$	1
Polyhedron	$\mathbf{D}$	$\langle Id\rangle$	1

Using $1/l = 1/6 - 1/k$, we compute the Euler orbifold characteristic to be

$$\begin{aligned}\chi(\mathbf{H}^2_{\mathbb{C}}/\Gamma_k) &= \frac{1}{3}\left(\frac{1}{k}+\frac{1}{l}\right)+\frac{1}{24}+\frac{1}{kl}-\frac{1}{2}\left(\frac{1}{k}+\frac{1}{l}\right)-\left(\frac{1}{k}+\frac{1}{l}\right)-1+\frac{25}{6}-4+1\\ &= \frac{1}{72}+\frac{1}{k}\left(\frac{1}{6}-\frac{1}{k}\right).\end{aligned}$$

5.5 Mostow groups of the second type

We review, in this section, the Mostow groups of the second type, which is written based on related materials in the Parker's survey paper [Par09]. It aims to explain briefly the previous construction of fundamental domains might be adapted for all Mostow groups of the second type.

Let $\Gamma(p,k)$ denote the equilateral triangle group $\langle R_1, R_2, R_3\rangle$ where each R_i is of order p. Mostow groups of the second type are the groups $\Gamma(p,k)$ where the values of p, k and $l = 1/(1/2 - 1/p - 1/k)$ are given in the following table.

p	3	3	3	3	3	4	4	4	5	5	6	6
k	7	8	9	10	12	5	6	8	5	5	4	6
l	42	24	18	15	12	20	12	8	20	10	12	6

In fact, the values of k and l can be interchanged.

We begin with the given geometric generators

$$R = (JR_1^{-1}J)^2, S = JR_1^{-1}, T = (JR_1^{-1})^2, I_1 = JR_1^{-1}J.$$

A conjectural presentation of $\Gamma(p,k)$ immediately follows from the above setting and the braid relations that

$$\Gamma(p,k) = \left\langle R,S,T,I_1 \left| \begin{array}{c} R^k = T^l = (R^{-1}S)^p = (T^{-1}I_1)^p = (S^{-1}I_1)^3 \\ = [R,T] = 1, \quad T = S^2, \quad R = I_1^2 \end{array} \right. \right\rangle. \tag{5.29}$$

To confirm that (5.29) is an exact presentation for $\Gamma(p,k)$, it needs to construct the same fundamental domains as the previous sections.

The key point of construction is to analyze the stabilizer group $\langle R,S,T\rangle$. As we computed in Section 5.2.2, the common eigenvector of R,S is

$$\mathbf{n} = \begin{bmatrix} u^2\overline{\tau} \\ \overline{u}^2\tau \\ -1 \end{bmatrix}$$

and T fixes the complex line to the polar vector $\mathbf{n}$.

By an easy calculation, we obtain

$$\begin{aligned} \langle \mathbf{n},\mathbf{n}\rangle_H &= \begin{bmatrix} \overline{u}^2\tau & u^2\overline{\tau} & -1 \end{bmatrix} H \begin{bmatrix} u^2\overline{\tau} \\ \overline{u}^2\tau \\ -1 \end{bmatrix} \\ &= 1 - u^3 + \overline{u}^6\tau^3 - \overline{u}^3\tau^3 + u^6\overline{\tau}^3 - u^3\overline{\tau}^3 + 1 - \overline{u}^3 \\ &= 2\left[1 - \cos\frac{2\pi}{p} - \cos(\frac{4\pi}{p} + \frac{2\pi}{k}) + \cos(\frac{2\pi}{p} + \frac{2\pi}{k})\right] \\ &\triangleq 2N(p,k). \end{aligned}$$

The basic construction requires us that the stabilizer group fixes a complex line. It suffices to analyze the norm of $\mathbf{n}$ and ask for the positive values.

- For $p = 4$,
$$N(4,k) = 1 - \sqrt{2}\sin(\frac{2\pi}{k} - \frac{\pi}{4}),$$
then $N(4,k) \geq 0$ if and only $k \geq 4$.

- For $p = 5$, then
$$N(5,k) = 1 - \cos\frac{2\pi}{5} + 2\sin(\frac{3\pi}{5} + \frac{2\pi}{k})\sin\frac{\pi}{5} > 0.$$

- For $p = 6$,
$$N(6,k) = \frac{1}{2} + \cos\frac{2\pi}{k}.$$
then $N(6,k) \geq 0$ if and only $k \geq 3$.

As T is a complex refection fixing the complex line $\mathbf{n}^{\perp}$, and

$$T = \begin{bmatrix} 0 & \overline{u}^2 & 0 \\ -\overline{u}^3\tau & \overline{u}^2\tau^2 + u\overline{\tau} & 0 \\ \overline{u} & -\tau & u\overline{\tau} \end{bmatrix},$$

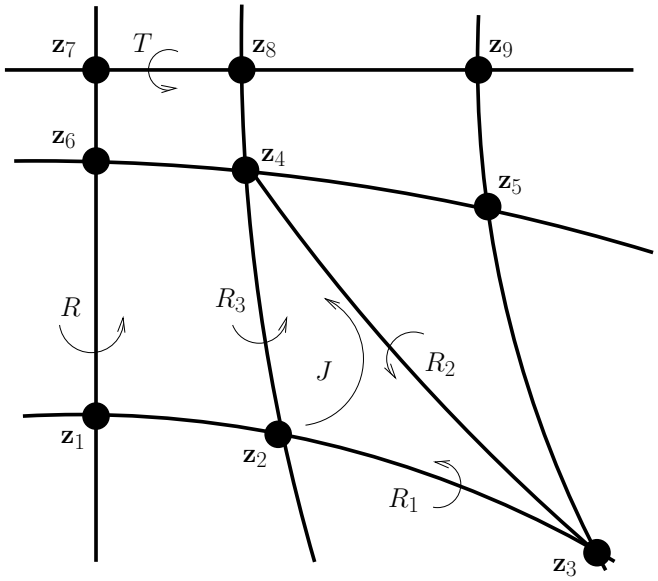

FIGURE 5.15: The schematic view of construction in 2-dimension. The bold lines are the complex lines. The bold points are the intersection of two complex lines which give rise to the vertices of polyhedron.

T has the eigenvalue $\overline{u}^2\tau^2$ corresponding to $\mathbf{n}$ and a repeated eigenvalue $u\overline{\tau}$. Thus the relation $T^l = 1$ implies that

$$\frac{1}{l} = \frac{1}{2} - \frac{1}{p} - \frac{1}{k} \tag{5.30}$$

for a positive integer l ($l = \infty$ if possible). Only possible values of k, l satisfying (5.30) listed in the table.

The construction of fundamental domains follows from the complex lines fixed by R, T, R_1, R_3, RR_3R^{-1} and TR_1T^{-1}, see Figure 5.15. The orthogonal properties of these complex lines come from the braid relations. A fundamental domain of the stabilizer group $\langle R, S\rangle$ acting on the complex line $\mathbf{n}^\perp$ is a geodesic hyperbolic triangle $\triangle(k/2, p, p)$ with the interior angles $2\pi/k, \pi/p, \pi/p$. As l tends to ∞, the complex line $\mathbf{n}^\perp$ degenerates to an ideal point. The action of the stabilizer group $\langle R, S\rangle$ on the boundary is almost-Euclidean, in other words, the triangle $\triangle(k/2, p, p)$ becomes an Euclidean triangle in a horizontal section of the Heisenberg group since $1/p + 1/k = 1/2$.

From the above arguments, the construction of fundamental domains for $\Gamma(3, k)$ can be implemented for all Mostow groups of the second type. Analogous to the case $G_2 = \Gamma(3, 6)$, the limiting configuration of fundamental domains for $\Gamma(4, k)$ and $\Gamma(6, k)$ turns out to be two of Mostow groups of the first type. In that case, T becomes to be a parabolic element. The presentation may be obtained by removing the relation $T^l = 1$. This gives a new approach to construct the fundamental domains for some of Mostow groups of the first type.

Chapter 6

Cohomology with local coefficients

In this chapter, we compute the cohomology of the Eisenstein-Picard modular surface and its sister with local coefficients. Our results follow the work by Yasaki [Yas08], where he constructed explicitly a spine for $SU(2,1;\mathbb{Z}[i])$ and used it to compute the cohomology for $SU(2,1;\mathbb{Z}[i])$.

6.1 Algorithm to compute the cohomology

This section recalls Dan Yasaki's work [Yas08], which describes − from the theoretical viewpoint − an algorithm to compute the cohomology of arithmetic groups as well as the quotient orbifolds.

6.1.1 Spines

Let G be a connected semisimple Lie group with finite center, and K a maximal compact subgroup of G. Then $X = G/K$ is a Riemannian symmetric space of noncompact type. Let Γ be an arithmetic subgroup of G, and $\Gamma\backslash X$ be the corresponding locally symmetric space. The special case of our interest is when G is the Lie group $SU(2,1)$ and Γ is a lattice. In that case, the associated symmetric space X will be the complex hyperbolic plane $\mathbf{H}^2_{\mathbb{C}}$.

Definition 6.1.1. *The virtual cohomological dimension (***vcd***) of* Γ *is the highest dimension of a space* X' *such that there exists a subgroup* $\Gamma' \subset \Gamma$ *of index finite, such that* Γ' *acts freely on* X' *and* $\Gamma'\backslash X'$ *is compact.*

Borel and Serre [BS73] showed that the discrepancy between the dimension of X and $\mathrm{vcd}(\Gamma)$ is given by the $\mathbb{Q}$-rank of Γ, the dimension of a maximal $\mathbb{Q}$-split torus in Γ. In our case, X is 4-dimensional, and $\mathrm{rank}_{\mathbb{Q}}(\Gamma) = 1$, then

$$\mathrm{vcd}(\Gamma) = \dim(X) - \mathrm{rank}_{\mathbb{Q}}(\Gamma) = 3.$$

This allows us to find a 3-dimensional Γ-equivariant deformation retract $X_0 \subset X$.

Definition 6.1.2. *A* ***spine*** *is a* Γ*-equivariant deformation retract* $X_0 \subset X$ *of dimension equal to the virtual cohomological dimension such that* $\Gamma\backslash X_0$ *is compact.*

Remark 6.1.3. A spine, in the previous chapters, is a geodesic in $\mathbf{H}^2_{\mathbb{C}}$ that determines a bisector. However, a spine in this chapter has a different sense that is a 3-dimensional subspace of $\mathbf{H}^2_{\mathbb{C}}$.

For the general case of $\mathbb{Q}$-rank 1 groups, Yasaki showed in [Yas06] the existence of spines. More precisely, a Γ-equivariant deformation retract of X was constructed by a family of exhaustion functions. Such exhaustion functions, from a geometric point of view, can be thought of as a measure of height with respect to a cusp or a rational parabolic subgroup. Recall that Busemann functions, in the same sense, can be also regarded as a distance of points between in the interior and on the boundary and its level set is a measure of height, called a *horosphere*. One can show that Busemann functions are a negative logarithm of these exhaustion functions, see Example 6.1.4 for the simple case.

Example 6.1.4. For $G = SL_2(\mathbb{R}), \Gamma = SL_2(\mathbb{Z})$ and the associated symmetric space is Poincaré's upper half-plane $\mathfrak{H}$. Let $z = x + iy \in \mathfrak{H}$ and $\lambda = p/q \in \mathbb{Q}$ in reduced form be a cusp.

- *Exhaustion functions* are given by

$$\begin{aligned} f_\infty(z) &= y, \\ f_\lambda(z) &= \frac{y}{(p-xq)^2+q^2y^2}. \end{aligned}$$

- Consider a unit-speed geodesic ie^t which converges to ∞, *Busmann function* with respect to ∞ is given by

$$\begin{aligned} h_\infty(z) &= d(z, ie^t) - t \\ &= \cosh^{-1}\left(1 + \frac{x^2+(y-e^t)^2}{2ye^t}\right) - t \\ &= \log(e^t/y) - t \\ &= -\log y. \end{aligned}$$

  In general, *Busmann function* with respect to λ is given by

$$h_\lambda(z) = h_\gamma \cdot \infty(z) = \Im(\gamma^{-1}\cdot z) = -\log\left[\frac{y}{(p-qx)^2+q^2y^2}\right]$$

  where γ has the matrix form as

$$\begin{pmatrix} p & * \\ q & * \end{pmatrix} \in SL_2(\mathbb{Z}).$$

In what follows, we will use Busemann functions as defined in Section 2.2.1 to describe a spine for $\Gamma \subset SU(2,1)$, that is a special case of $\mathbb{Q}$-rank 1 groups. Let $z = (\zeta, v, u) \in \mathbf{H}^2_{\mathbb{C}}$ be a point in horospherical coordinates and $\theta = (\zeta_0, v_0, 0)$ be a cusp. *Busmann functions* are given by

$$\begin{aligned} h_\infty(z) &= -\log u, \\ h_\theta(z) &= -\log\left[\frac{4u}{(|\zeta|^2+|\zeta_0|^2+u-2\Re(\overline{\zeta}_0\zeta))^2+(v-v_0+2\Im(\overline{\zeta}_0\zeta))^2}\right]. \end{aligned}$$

In order to define the spine, we need the following notions:

- Denote by $\mathcal{P}$ the set of fixed points by all parabolic subgroups of Γ.
- For $p \in \mathcal{P}$, we define

$$X_p = \{z \in \mathbf{H}^2_{\mathbb{C}} |\ h_p(z) \leq h_q(z) \text{ for every } q \in \mathcal{P}\backslash\{p\}\}.$$

- In general, for a subset $\mathcal{J} \subset \mathcal{P}$,

$$\begin{aligned} B(\mathcal{J}) &= \{z \in \mathbf{H}^2_{\mathbb{C}} |\ h_p(z) = h_q(z) \text{ for every pair } p, q \in \mathcal{J}\}, \\ X(\mathcal{J}) &= \bigcap_{p\in\mathcal{J}} X_p, \\ X'(\mathcal{J}) &= X(\mathcal{J})\backslash \bigcup_{\mathcal{J}'\supsetneq\mathcal{J}} X(\mathcal{J}'). \end{aligned}$$

  We call the set $X'(\mathcal{J})$ a *degenerate tile*.

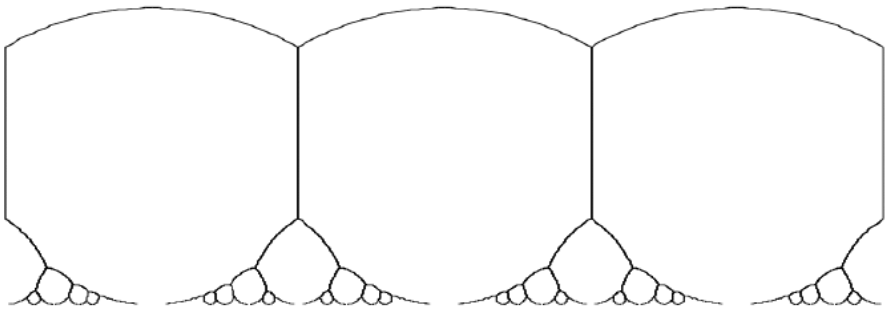

FIGURE 6.1: Spine for $SL_2(\mathbb{Z})$.

Remark 6.1.5.
- When $\mathcal{P}$ contains only a conjugacy class of parabolic fixed points, then X_p reduces to the *Ford domain* with respect to p.
- When $\mathcal{J} = \{p, q\}$ is of order 2, then $X(\mathcal{J}) = B(\mathcal{J})$ is the bisector between p and q. In this case, we can think of it by using Busemann function instead of Bergman metric in (2.1).

Definition 6.1.6. *A subset $\mathcal{J} \subset \mathcal{P}$ is called **admissible** if $X(\mathcal{J})$ is non-empty, and **strongly admissible** if $X'(\mathcal{J})$ is non-empty.*

Proposition 6.1.7. *[Yas06] Let $\mathscr{S}$ denote the collection of strongly admissible subsets of $\mathcal{P}$. Then the symmetric space X has a Γ-invariant degenerate tiling*

$$X = \coprod_{\mathcal{J} \in \mathscr{S}} X'(\mathcal{J})$$

such that $\gamma \cdot X'(\mathcal{J}) = X'(\gamma \cdot \mathcal{J})$ for all $\gamma \in \Gamma$ and $\mathcal{J} \in \mathscr{S}$.

The following definition enables us to give a spine for Γ, which is proved in [Yas06] as the main result.

Definition 6.1.8. *([Yas06]) We define a Γ-invariant subset $X_0 \subset X$ by*

$$X_0 = \coprod_{\substack{\mathcal{J} \in \mathscr{S} \\ |\mathcal{J}|>1}} X'(\mathcal{J}).$$

Note that $X_0 = X \setminus \bigcup_{p \in \mathcal{P}} X'(\{p\})$. In the special case of one cusp (only one conjugacy class of parabolic fixed points), the spine has a simple description which is the union of Γ-images of the boundary of the *Ford domain*. For example, for $G = SL_2(\mathbb{R})$, $\Gamma = SL_2(\mathbb{Z})$, a spine is the familiar infinite trivalent tree in upper half plane (Figure 6.1).

6.1.2 Connection with fundamental domain

As shown in [Yas06], the construction of the spine also gives a way to construct an exact fundamental domain for Γ. We investigate, on the contrary, the spine coming from the fundamental domain of Γ.

Example 6.1.9. For $G = SL_2(\mathbb{R})$ and $\Gamma = SL_2(\mathbb{Z})$ is a lattice of G acting on the upper half plane $\mathfrak{H}$. Then a fundamental domain for Γ is a familiar ideal geodesic triangle at the vertices $\infty, e^{i\pi/3}, e^{i2\pi/3}$ with the side pairing maps

$$z \to -\frac{1}{z}, \quad z \to z+1.$$

We define

$$\begin{aligned} a_1 &= \{e^{it} : \pi/3 \leq t \leq 2\pi/3\}, \\ a_{\frac{1}{2}} &= \{e^{it} : \pi/2 \leq t \leq 2\pi/3\}. \end{aligned}$$

It is immediately that $a_{\frac{1}{2}} \cong a_1/\langle z \to -\frac{1}{z}\rangle$ and a_1 can be regarded as the vertical geodesic retraction of fundamental domain. Obviously, the spine for $SL_2(\mathbb{Z})$ is the union of the Γ-images of $a_{\frac{1}{2}}$, and the arc $a_{\frac{1}{2}}$ is a fundamental domain for Γ in the spine.

Motivated by the example of $SL_2(\mathbb{R})$, it allows us to give the following lemma.

Lemma 6.1.10. *Let Γ be a lattice of $SU(2,1)$ with class number one. Suppose that a fundamental domain D of Γ is a geodesic cone based on connected compact set D_0, then a spine for Γ comes from the union of the Γ-images of D_0. In particular, a fundamental domain for Γ in the spine is contained in D_0.*

Proof. In the Siegel domain model of $\mathbf{H}^2_{\mathbb{C}}$, we define A_{D_0} to be the vertical geodesic projection along the u-coordinate onto D_0 in $\overline{D}$. Denote by

$$X_0 = \bigcup_{\gamma \in \Gamma} \gamma \cdot D_0.$$

It suffices to show X_0 is a Γ-equivariant deformation retract of $\mathbf{H}^2_{\mathbb{C}}$.

For $z \in \mathbf{H}^2_{\mathbb{C}}$, there exist a point $z_D \in \overline{D}$ and $\gamma_z \in \Gamma$ such that $\gamma_z \cdot z_D = z$. Define a family of maps $g_t : \mathbf{H}^2_{\mathbb{C}} \to \mathbf{H}^2_{\mathbb{C}}$ by

$$g_t(z) = \gamma_z \cdot [(1-t)z_D + tA_{D_0} \circ z_D].$$

It is clear that $g_0 = id$ and $g_1(\mathbf{H}^2_{\mathbb{C}}) \subset X_0$. For any $\gamma \in \Gamma$ and $z' = \gamma \cdot z$, then $\gamma_{z'} = \gamma \cdot \gamma_z$. It follows that

$$\gamma \cdot g_t(z) = g_t(\gamma \cdot z).$$

This g_t gives a Γ-equivariant deformation retract of $\mathbf{H}^2_{\mathbb{C}}$ onto X_0. □

Remark 6.1.11. For $\Gamma = SU(2,1;\mathbb{Z}[i])$, a fundamental domain of Γ constructed in [FFP10] consists of three compact sides (the core side and two pyramids) with the side pairings I_0 and S. Lemma 6.1.10 enables us to give a fundamental domain for Γ in the spine, which is made up of two 3-cells − a pyramid and half of the core side. This is similar to Yasaki's constructions of two conjugacy classes X, Y of 3-cells [Yas08]. For more details about these two constructions, we refer to the end of Section 8 in [FFP10].

Eisenstein-Picard modular surface and its sister

For the time being, we recall that the Eisenstein-Picard modular group and its sister are denoted by G_1 and G_2 respectively as in [Par98].

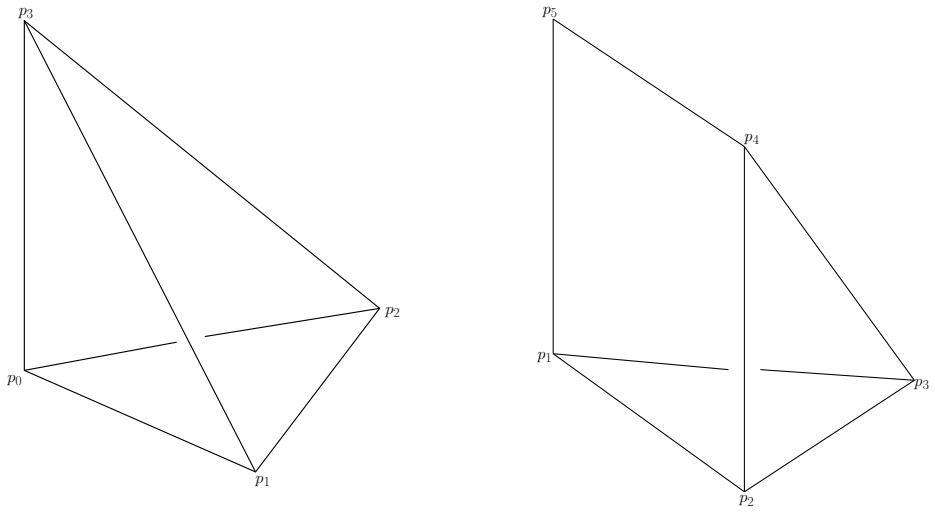

(a) $\Gamma = G_1$ (b) $\Gamma = G_2$

FIGURE 6.2: A fundamental domain for Γ in the spine.

- For $\Gamma = G_1$.

  Falbel and Parker [FP06] constructed a fundamental domain for the action of G_1 on $\mathbf{H}^2_{\mathbb{C}}$, which is a 4-simplex with one ideal vertex. Following their notations, G_1 is generated by the side pairing maps R, P and Q, where $\omega = (-1 + i\sqrt{3})/2$ is a cube root of unity and

$$R = \begin{bmatrix} 0 & 0 & 1 \\ 0 & -1 & 0 \\ 1 & 0 & 0 \end{bmatrix}, \; P = \begin{bmatrix} 1 & 1 & \omega \\ 0 & 1 & -\omega \\ 0 & 0 & 1 \end{bmatrix}, \; Q = \begin{bmatrix} 1 & 1 & \omega \\ 0 & -1 & 1 \\ 0 & 0 & 1 \end{bmatrix}.$$

  Lemma 6.1.10 enables us to give a fundamental domain for G_1 in the spine, which is a tetrahedron (see Figure 6.2(a)). The action on the vertices is given by

$$p_1 \xrightarrow{P} p_2 \xrightarrow{P} p_3,$$

$$(p_0, p_1, p_3) \xrightarrow{QP^{-1}} (p_0, p_2, p_3),$$

$$(p_0, p_1, p_2) \xrightarrow{R} (p_0, p_1, p_2).$$

- For $\Gamma = G_2$.

  A fundamental domain of G_2 constructed in Chapter 3 is a geodesic cone to infinity over a prism. This prism consists of two compact sides with side pairing map I_1. Recall that G_2 is generated by R, S, T and I_1, refer to the matrices in Section 3.2. (Here the capital R is not the same representative matrix as the one of G_1).

  One compact side, which is a wedge (see Figure 6.2(b)), gives a fundamental domain for G_2 in the spine by Lemma 6.1.10. We repeat the action of side pairing maps on the vertices:

$$p_2 \xrightarrow{S^{-1}I_1} p_3 \xrightarrow{I_1^{-1}S} p_4,$$

$$(p_1, p_2, p_4, p_5) \xrightarrow{I_1} (p_5, p_4, p_3, p_1),$$

TABLE 6.1: Representative cells and their stabilizers for G_1

Cell	Dimension	Stabilizer	Generators
$\mathbf{T}$	3	trivial	$\langle id \rangle$
$\triangle_{012}$	2	$\mathbb{Z}/2\mathbb{Z}$	$\langle R \rangle$
$\triangle_{013}$	2	trivial	$\langle id \rangle$
$\triangle_{123}$	2	trivial	$\langle id \rangle$
e_{03}	1	$\mathbb{Z}/6\mathbb{Z}$	$\langle PQ^{-1} \rangle$
e_{01}	1	$\mathbb{Z}/2\mathbb{Z}$	$\langle R \rangle$
e_{12}	1	$\mathbb{Z}/2\mathbb{Z}$	$\langle R \rangle$
p_0	0	$\mathbb{Z}/6\mathbb{Z} \times \mathbb{Z}/2\mathbb{Z}$	$\langle PQ^{-1}, R \rangle$
p_1	0	Group $\sharp 72$	$\langle PQ^{-1}P, R \rangle$

TABLE 6.2: Representative cells and their stabilizers for G_2

Cell	Dimension	Stabilizer	Generators
$\mathbf{W}$	3	trivial	$\langle id \rangle$
$\square_{1245}$	2	trivial	$\langle id \rangle$
$\triangle_{123}$	2	trivial	$\langle id \rangle$
$\triangle_{234}$	2	$\mathbb{Z}/3\mathbb{Z}$	$\langle S^{-1}I_1 \rangle$
e_{15}	1	$\mathbb{Z}/6\mathbb{Z}$	$\langle R \rangle$
e_{12}	1	$\mathbb{Z}/3\mathbb{Z}$	$\langle T^{-1}I_1 \rangle$
e_{23}	1	$\mathbb{Z}/2\mathbb{Z}$	$\langle T^{-1}I_1 \rangle$
p_1	0	$\mathbb{Z}/6\mathbb{Z} \times \mathbb{Z}/3\mathbb{Z}$	$\langle R, T^{-1}I_1 \rangle$
p_2	0	Group $\sharp 24$	$\langle R^{-1}S, T^{-1}I_1 \rangle$

$$(p_5, p_1, p_2) \xrightarrow{R} (p_5, p_1, p_3),$$

$$(p_1, p_2) \xrightarrow{T} (p_5, p_4).$$

Notation.

- Let $\mathbf{T}$ denote a tetrahedron with vertices p_0, p_1, p_2, p_3 and $\mathbf{W}$ denote a wedge with vertices p_1, p_2, p_3, p_4, p_5; see Figure 6.2.
- Let $\square_{ijkl}$ denote a quadrangle where the label is corresponding to its vertices.
- Let $\triangle_{ijk}$ denote a triangle where the label is corresponding to its vertices.
- Let e_{ij} denote an edge with endpoints p_i and p_j.

For $i = 0, 1, 2, 3$, we consider all the Γ-conjugacy classes of i-dimensional cells of X_0. For each Γ-conjugacy class, we fix a representative and compute the stabilizer. The results are given in Tables 6.1 and 6.2.

6.1.3 Cohomology computation from the cell structure

In the previous section, we obtain the cell structure of fundamental domain for Γ in the spine, which allows us to compute the cohomology of $\mathbf{H}^2_{\mathbb{C}}/\Gamma$ with local coefficients. The main reference for this section is [Yas08].

Orbifolds

We briefly review the basic definitions concerning orbifolds, or V-manifolds in the terminology of Satake (see [Sat56, Sat57]). Let Ω be a Hausdorff topological space.

- An *orbifold chart* on Ω is given by a connected open subset $\widetilde{U} \subseteq \mathbb{R}^n$ for some integer $n \geq 0$, a finite group $\Gamma_{\widetilde{U}}$ of C^∞-automorphisms of $\widetilde{U}$, and a map $\varphi : \widetilde{U} \to M$ such that φ is $\Gamma_{\widetilde{U}}$ -invariant ($\varphi \circ g = \varphi$ for all $g \in \Gamma_{\widetilde{U}}$) which induces a homeomorphism of $\widetilde{U}/\Gamma_{\widetilde{U}}$ onto a open subset $U = \varphi(\widetilde{U}) \subseteq M$;
- An *embedding* $\lambda : (\widetilde{U}, \Gamma_{\widetilde{U}}, \varphi) \hookrightarrow (\widetilde{V}, \Gamma_{\widetilde{V}}, \psi)$ between two charts is a smooth embedding $\lambda : \widetilde{U} \hookrightarrow \widetilde{V}$ such that for any $\gamma \in \Gamma_{\widetilde{U}}$, there exists a $\gamma' \in \Gamma_{\widetilde{V}}$ such that $\lambda \circ \gamma = \gamma' \circ \lambda$ and $\psi \circ \lambda = \varphi$;
- An *orbifold atlas* on Ω is a family $\mathcal{U} = \{(\widetilde{U}, \Gamma_{\widetilde{U}}, \varphi)\}$ of such charts, which cover Ω and are locally compatible in the following sense: given any two charts $(\widetilde{U}, \Gamma_{\widetilde{U}}, \varphi)$ for $U = \varphi(\widetilde{U}) \subseteq M$ and $(\widetilde{V}, \Gamma_{\widetilde{V}}, \psi)$ for $V = \varphi(\widetilde{V}) \subseteq M$, and a point $x = U \cap V$, there exists an open neighborhood $W \subseteq U \cap V$ of x and a chart $(\widetilde{W}, \Gamma_{\widetilde{W}}, \phi)$ for W such that there are embeddings $(\widetilde{W}, \Gamma_{\widetilde{W}}, \phi) \hookrightarrow (\widetilde{U}, \Gamma_{\widetilde{U}}, \varphi)$ and $(\widetilde{W}, \Gamma_{\widetilde{W}}, \phi) \hookrightarrow (\widetilde{V}, \Gamma_{\widetilde{V}}, \psi)$.

Definition 6.1.12. *An **orbifold** (of dimension n) is such a space Ω with an equivalence class of atlases $\mathcal{U}$. Two such atlases are said to be equivalent if they have a common refinement.*

Local system over $\Gamma\backslash X$

Since Γ acts properly discontinuously on X, $\Gamma\backslash X$ has a canonical structure of an orbifold. Let π denote the projection $X \to \Gamma\backslash X$. Since X_0 is a spine, there exists a Γ-equivariant deformation retract $g : X \to X_0$, which induces a deformation retract $\widetilde{g} : \Gamma\backslash X \to \Gamma\backslash X_0$. Then it is naturally that a projection $\pi_0 = \pi|_{X_0} : X_0 \to \Gamma\backslash X_0$.

Let E be a Γ-module with Γ-action given by $\rho : \Gamma \to GL(E)$. We define the Γ-equivariant presheaf $\mathcal{E}$ on $\Gamma\backslash X$. For every open set $U \subset M$,

$$\mathcal{E}_\Gamma(U) = \left\{ f : \pi^{-1}(U) \to E \;\middle|\; f(\gamma \cdot x) = \rho(\gamma) f(x), \forall \gamma \in \Gamma, x \in \pi^{-1}(U) \right\}.$$

Let $\mathbb{E}$ denote the sheafification of $\mathcal{E}_\Gamma$. We call $\mathbb{E}$ the sheaf associated to the local system on $\Gamma\backslash X$ defined by (E, ρ). We will extend this terminology to $\Gamma\backslash X_0$, where the sheaf associated to the local system defined by (E, ρ) is denoted by $\mathbb{E}_0$.

Considier a family of open sets $\mathcal{U} = \{U_i\}$ in an orbifold atlas on $\Gamma\backslash X$, we define the cohomology of $\Gamma\backslash X$ with local coefficients as follows.

- $C^0(\mathcal{U}; \mathbb{E}) = \{\alpha^0 \mid \alpha^0_i = \alpha^0|_{U_i} \in \mathcal{E}_\Gamma(U_i)\}$
- $C^q(\mathcal{U}; \mathbb{E}) = \{\alpha^q \mid \alpha^q_{i_0 i_1 \cdots i_q} = \alpha^0|_{U_{i_0} \cap U_{i_1} \cdots \cap U_{i_q}} \in \mathcal{E}_\Gamma(U_{i_0} \cap U_{i_1} \cdots \cap U_{i_q})\}$
- The differential operator d is defined by

$$d \cdot \alpha^q(U_{i_0} \cap U_{i_1} \cdots \cap U_{i_q} \cap U_{i_{q+1}}) = (-1)^j \sum_{j=0}^{q+1} \alpha^q_{i_0 i_1 \cdots \hat{i}_j \cdots i_{q+1}}.$$

Then the sequence

$$0 \to C^0(\mathcal{U};\mathbb{E}) \xrightarrow{d} C^1(\mathcal{U};\mathbb{E}) \xrightarrow{d} C^2(\mathcal{U};\mathbb{E}) \xrightarrow{d} \cdots$$

is exact and the cohomology of $\Gamma\backslash X$ is defined by

$$H^*(\Gamma\backslash X;\mathbb{E}) = \frac{\mathrm{Ker}(d)}{\mathrm{Im}(d)}.$$

To this end, we recall without proof a result which compares the cohomology of the whole space and its deformation retract (also see a proof in [Yas08]).

Theorem 6.1.13. *[Yas08]* $H^*(\Gamma\backslash X;\mathbb{E}) \cong H^*(\Gamma\backslash X_0;\mathbb{E}_0)$.

This theorem enables us to compute the cohomology of $\Gamma\backslash X$ from the structure of its spine.

Cohomology of regular cell complex

Definition 6.1.14. *A **finite regular cell complex** is a finite CW complex where the attaching map from each closed cell into the complex is a homeomorphism onto its image.*

Definition 6.1.15. *For a finite regular cell complex C, the **face poset** of C is the set of closed cells with the partial ordering derived from containment. Given a face poset $(P,<)$, the **order complex** of P is the simplicial complex whose vertices are the elements of P and the k-simplices of P are $(k+1)$-flags $p_0 < p_1 < \cdots < p_k$ with $p_i \in P$.*

Let $\mathcal{F}$ denote the order complex of the face poset of X_0 and $\mathcal{F}^k$ denote the set of k-simplices of $\mathcal{F}$. We can take, up to normalization, a Γ-equivariant homeomorphism $\Phi : \mathcal{F} \to X_0$ satisfying

- $\Phi(\gamma \cdot x) = \gamma \cdot \Phi(x)$ for all $\gamma \in \Gamma$ and $x \in \mathcal{F}$.
- $\Phi(\sigma_0 < \sigma_1 < \cdots < \sigma_k) \subset \sigma_k$ for all $\sigma_0 < \sigma_1 < \cdots < \sigma_k$ ordered simplices of $\mathcal{F}$.

Let $\mathfrak{U}_{\mathcal{F}}$ denote the open cover of $\mathcal{F}$ consisting of open star neighborhoods of each vertex in $\mathcal{F}$. Using the Γ-equivariant homeomorphism Φ, we get an open cover $\mathfrak{U}_0 = \Phi(\mathfrak{U}_{\mathcal{F}})$ of X_0 so that there is an open set $U_\sigma \in \mathfrak{U}_0$ for each cell σ. For each p, denote $\mathcal{R}_p$ a set of representatives of Γ-conjugacy classes of p-cells of X_0. Let $[\sigma]$ denote the representative of the conjugacy class of σ.

Čech cohomology $\check{H}^*(\mathfrak{U}_0;\mathbb{E}_0)$ is defined by the cochain complex and codifferential as follows:

$$\begin{aligned} C^0(\mathfrak{U}_0;\mathbb{E}_0) &= \bigoplus_{[\sigma]\in\mathcal{R}_0} \mathbb{E}_0(U_{[\sigma]}) \\ &= \bigoplus_{[\sigma]\in\mathcal{R}_0} \left\{ f : \pi_0^{-1}(U_{[\sigma]}) \to E \mid f(\gamma\cdot x) = \rho(\gamma) f(x),\ \forall \gamma \in \Gamma, x \in \pi_0^{-1}(U_{[\sigma]}) \right\} \\ &= \{ f : \mathcal{F}^0 \to E |\ f(\gamma \cdot F) = \rho(\gamma) f(F), \quad \forall \gamma \in \Gamma, F \in \mathcal{F}^0 \}. \end{aligned}$$

$$C^k(\mathfrak{U}_0;\mathbb{E}_0) = \{ f : \mathcal{F}^k \to E |\ f(\gamma \cdot F) = \rho(\gamma) f(F), \quad \forall \gamma \in \Gamma, F \in \mathcal{F}^k \}.$$

For $f \in C^k(\mathfrak{U}_0;\mathbb{E}_0)$, $df \in C^{k+1}(\mathfrak{U}_0;\mathbb{E}_0)$ is given by

$$df(\sigma_0 < \cdots < \sigma_{k+1}) = \sum_{i=0}^{k+1} (-1)^i f(\sigma_0 < \cdots < \hat{\sigma}_i < \cdots < \sigma_{k+1}).$$

Proposition 6.1.16. *[Yas05] Let $\mathbb{E}_0$ be the sheaf associated to the local system on $\Gamma\backslash X_0$ defined by (E,ρ) and $\mathfrak{U}_0$ be defined as above. Then $H^*(\Gamma\backslash X_0;\mathbb{E}_0)=\check{H}^*(\mathfrak{U}_0;\mathbb{E}_0)$.*

Proposition 6.1.16 gives the computation of the cohomology of $\Gamma\backslash X_0$ with local coefficients from the Čech cohomology for the cover $\mathfrak{U}_0$. An implementation of method for computing the cohomology is given in Theorem 6.1.18. It is useful to introduce the following notions for computation.

We define $\mathrm{Top}:\mathcal{F}\to X_0$ to be the map which sends a flag $\sigma_0<\cdots<\sigma_k$ to σ_k. For a cell $\sigma\in X_0$, let $\mathcal{F}_\sigma=\mathrm{Top}^{-1}(\sigma)$, which is the set of maximal flags terminating at σ. For each representative $[\sigma]$, we fix a distinguished maximal flag of cells $F_{[\sigma]}=\sigma_0<\sigma_1<\cdots<\sigma_p$ where σ_k is an k-cell and $\sigma_p=[\sigma]$. For each $\sigma\in X_0$, there exists a unique simplex F_σ that is Γ-conjugate to $F_{[\sigma]}$. In other words, there is a unique element $\gamma_\sigma\in\Gamma$, up to $\mathrm{Stab}_\Gamma(\sigma)$, such that

$$\gamma_\sigma\cdot F_{[\sigma]}=F_\sigma.$$

For each fixed p-cell, let S_σ denote the simplicial complex arising from the face poset of cells in σ. More precisely, the vertices of S_σ are the cells contained in σ and the k-simplices are the $(k+1)$-flags $\sigma_0<\sigma_1<\cdots<\sigma_k$.

Proposition 6.1.17. *[Yas05] Let σ be a p-cell and S_σ the corresponding complex defined above. Choose an orientation of S_σ. Then there exists a map*

$$n_\sigma:\{p\text{-simplices of } S_\sigma\}\to\{\pm1\}$$

such that $\partial S_\sigma=\sum_{F\in S_\sigma^p} n_\sigma(F)\partial F$. Furthermore, if F and H intersect in a $(p-1)$-face, then $n_\sigma(F)=-n_\sigma(H)$.

After fixing the distinguished maximal flag $\{F_{[\sigma]}\}$ for each p-cell $\sigma\in\mathcal{R}_p$, we define a function $\mathrm{sgn}_\sigma:\partial\sigma\to\{\pm1\}$. Choose the orientation of S_σ so that the map $n_\sigma(F_{[\sigma]})=(-1)^p$. Then for $\tau\in\partial\sigma$, we define

$$\mathrm{sgn}_\sigma(\tau)=n_\sigma(F_\tau<\sigma).$$

For convenience, we explain how to determine the sgn_σ from an intuitive point of view, see Figure 6.3.

We now ready to give the main theorem for computing the cohomology from the cell structure.

Theorem 6.1.18. *([Yas08]) The cohomology $H^*(\Gamma\backslash X_0;\mathbb{E}_0)$ can be computed from the complex*

$$0\to\bigoplus_{\sigma\in\mathcal{R}_0}E^{\mathrm{Stab}_\Gamma(\sigma)}\to\bigoplus_{\sigma\in\mathcal{R}_1}E^{\mathrm{Stab}_\Gamma(\sigma)}\to\cdots\to\bigoplus_{\sigma\in\mathcal{R}}E^{\mathrm{Stab}_\Gamma(\sigma)}\to0$$

where the differential

$$\delta:\quad\bigoplus_{\sigma\in\mathcal{R}_{p-1}}E^{\mathrm{Stab}_\Gamma(\sigma)}\to\bigoplus_{\sigma\in\mathcal{R}_p}E^{\mathrm{Stab}_\Gamma(\sigma)}$$

is given by

$$(\delta v)_\sigma=\sum_{\tau\in\partial\sigma}\mathrm{sgn}_\sigma(\tau)\rho(\gamma_\tau)v_{[\tau]}.$$

Here γ_τ, sgn, and $[\cdot]$ defined above and the vector $v_{[\tau]}$ is the $[\tau]$-component of the vector $v\in\bigoplus_{\sigma\in\mathcal{R}_{p-1}}E^{\mathrm{Stab}_\Gamma(\sigma)}$.

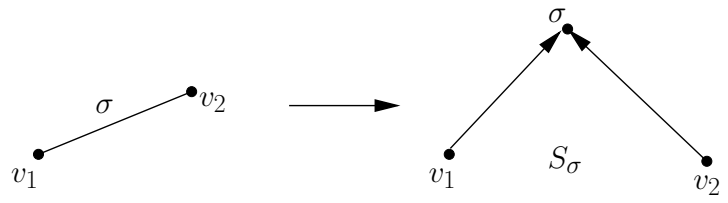

(a) 1-cell

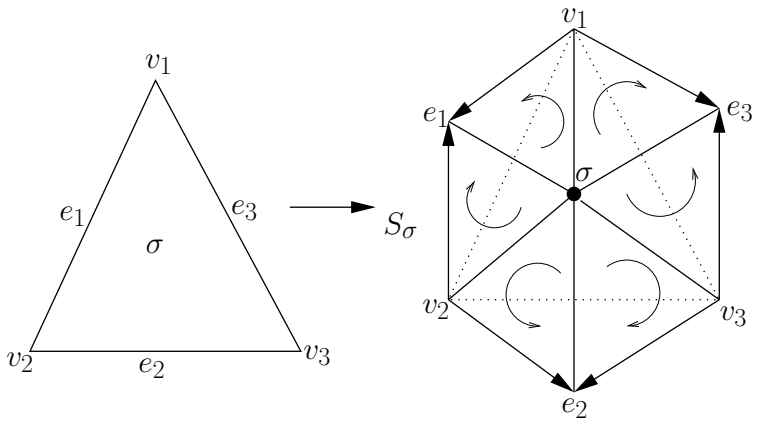

(b) 2-cell

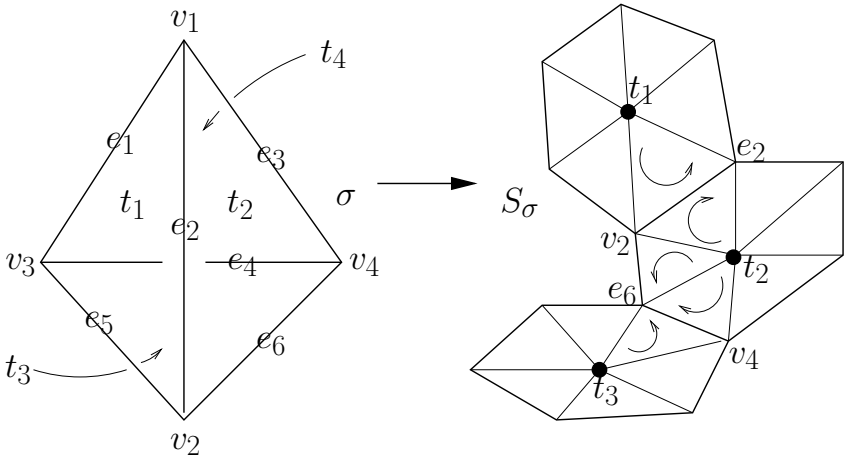

(c) 3-cell

FIGURE 6.3: The simplicial complex S_σ arising from the cell σ.

TABLE 6.3: Distinguished maximal flags

3-cells	2-cells	1-cells	0-cells
$\mathbf{T} > \triangle_{012} > e_{01} > p_0$	$\triangle_{012} > e_{01} > p_0$	$e_{03} > p_0$	p_0
	$\triangle_{013} > e_{01} > p_0$	$e_{01} > p_0$	p_1
	$\triangle_{123} > e_{12} > p_1$	$e_{12} > p_1$	

TABLE 6.4: $\mathbf{T}$ Data

$\sigma \in \partial\mathbf{T}$	F_σ	γ_σ	$\mathrm{sgn}(\sigma)$
$\triangle_{012}$	$\triangle_{012} > e_{01} > p_0$	id	-1
$\triangle_{013}$	$\triangle_{013} > e_{01} > p_0$	id	$+1$
$\triangle_{023}$	$\triangle_{023} > e_{02} > p_0$	QP^{-1}	-1
$\triangle_{123}$	$\triangle_{123} > e_{12} > p_1$	id	$+1$

6.2 The cohomology of $\mathbf{H}^2_{\mathbb{C}}/G_1$

As an application of Theorem 6.1.18, we choose the distinguished maximal flags given in Table 6.3. With this choice of distinguished flags, we compute γ_σ, F_σ and sgn_σ for each cell given in Tables 6.4 − 6.7. Combining with Table 6.1, Theorem 6.1.18 enables us to give the following theorem.

Theorem 6.2.1. *Let E be a G_1-module with the action of G_1 given by $\rho_1 : G_1 \to \mathrm{GL}(E)$. Then $H^*(\mathbf{H}^2_{\mathbb{C}}/G_1; \mathbb{E})$ can be computed from the following cochain complex.*

$$0 \to \mathscr{C}^0 \to \mathscr{C}^1 \to \mathscr{C}^2 \to \mathscr{C}^3 \to 0.$$

where

$$\begin{aligned}
\mathscr{C}^0 &= E^{\langle \rho_1(PQ^{-1}), \rho_1(R)\rangle} \bigoplus E^{\langle \rho_1(PQ^{-1}P), \rho_1(R)\rangle}, \\
\mathscr{C}^1 &= E^{\rho_1(PQ^{-1})} \bigoplus E^{\rho_1(R)} \bigoplus E^{\rho_1(R)}, \\
\mathscr{C}^2 &= E^{\rho_1(R)} \bigoplus E \bigoplus E, \\
\mathscr{C}^3 &= E.
\end{aligned}$$

Then $(\lambda_i) \in \mathscr{C}^0, (\mu_i) \in \mathscr{C}^1, (\nu_i) \in \mathscr{C}^2$, the differentials are given by

$$\begin{aligned}
\delta_0^{(1)}(\lambda) &= \begin{bmatrix} -\lambda_1 + \rho_1(P^2)\lambda_2 \\ -\lambda_1 + \lambda_2 \\ (\rho_1(QP^{-1}) - 1)\lambda_2 \end{bmatrix}, \\
\delta_1^{(1)}(\mu) &= \begin{bmatrix} (1 - \rho_1(QP^{-1})\mu_2 + \mu_3 \\ -\mu_1 + \mu_2 + \rho_1(PQ^{-1}P)\mu_3 \\ (1 - \rho_1(PQP^{-1}) + \rho_1(P))\mu_3 \end{bmatrix}, \\
\delta_2^{(1)}(\nu) &= \begin{bmatrix} -\nu_1 + (1 - \rho_1(QP^{-1}))\nu_2 + \nu_3 \end{bmatrix}.
\end{aligned}$$

Consider the trivial representation $E = \mathbb{Z}$, then the cohomology of $\mathbf{H}^2_{\mathbb{C}}/G_1$ with $\mathbb{Z}$-coefficients is isomorphic to the singular cohomology of $\mathbf{H}^2_{\mathbb{C}}/G_1$. Theorem 6.2.1 enables us to compute explicitly the cohomology from the chain complex

$$0 \to \mathbb{Z}^2 \to \mathbb{Z}^3 \to \mathbb{Z}^3 \to \mathbb{Z} \to 0$$

TABLE 6.5: $\triangle_{012}$ and $\triangle_{013}$ Data

$\sigma \in \partial\triangle_{012}$	F_σ	γ_σ	$\mathrm{sgn}(\sigma)$	$\sigma \in \partial\triangle_{013}$	F_σ	γ_σ	$\mathrm{sgn}(\sigma)$
e_{01}	$e_{01} > p_0$	id	$+1$	e_{01}	$e_{01} > p_0$	id	$+1$
e_{02}	$e_{02} > p_0$	QP^{-1}	-1	e_{03}	$e_{03} > p_0$	id	-1
e_{12}	$e_{12} > p_1$	id	$+1$	e_{12}	$e_{13} > p_1$	$PQ^{-1}P$	$+1$

TABLE 6.6: $\triangle_{123}$ Data

$\sigma \in \partial\triangle_{123}$	F_σ	γ_σ	$\mathrm{sgn}(\sigma)$
e_{12}	$e_{12} > p_1$	id	$+1$
e_{13}	$e_{13} > p_1$	PQP^{-1}	-1
e_{23}	$e_{23} > p_2$	P	$+1$

with the differentials given by

$$\delta_0^{(1)} = \begin{bmatrix} -1 & 1 \\ -1 & 1 \\ 0 & 0 \end{bmatrix}, \quad \delta_1^{(1)} = \begin{bmatrix} 0 & 0 & 1 \\ -1 & 1 & 1 \\ 0 & 0 & 1 \end{bmatrix}, \quad \delta_2^{(1)} = \begin{bmatrix} -1 & 0 & 1 \end{bmatrix}.$$

Theorem 6.2.2. *Let $\mathbb{Z}$ denote the constant sheaf of integers on $\mathbf{H}^2_{\mathbb{C}}/G_1$. Then*

$$H^i(\mathbf{H}^2_{\mathbb{C}}/G_1; \mathbb{Z}) = \begin{cases} \mathbb{Z}, & i = 0 \\ 0, & i \geq 1. \end{cases}$$

6.3 The cohomology of $\mathbf{H}^2_{\mathbb{C}}/G_2$

Analogue to Theorem 6.2.1, Theorem 6.3.1 follows from all the data for representatives of cells, distinguished flags, γ_σ, F_σ and sgn_σ in Table 6.2 and Tables 6.8 − 6.12.

Theorem 6.3.1. *Let E be a G_2-module with the action of G_2 given by $\rho_2 : G_2 \to \mathrm{GL}(E)$. Then $H^*(\mathbf{H}^2_{\mathbb{C}}/G_2; \mathbb{E})$ can be computed from the following cochain complex.*

$$0 \to \mathscr{C}^0 \to \mathscr{C}^1 \to \mathscr{C}^2 \to \mathscr{C}^3 \to 0.$$

where

$$\begin{aligned} \mathscr{C}^0 &= E^{\langle \rho_2(R), \rho_2(T^{-1}I_1)\rangle} \bigoplus E^{\langle \rho_2(R^{-1}S), \rho_2(T^{-1}I_1)\rangle}, \\ \mathscr{C}^1 &= E^{\rho_2(R)} \bigoplus E^{\rho_2(T^{-1}I_1)} \bigoplus E^{\rho_2(T^{-1}I_1)}, \\ \mathscr{C}^2 &= E \bigoplus E \bigoplus E^{\rho_2(S^{-1}I_1)}, \\ \mathscr{C}^3 &= E. \end{aligned}$$

TABLE 6.7: e_{03}, e_{01} and e_{12} Data

$\sigma \in \partial e_{03}$	γ_σ	$\mathrm{sgn}(\sigma)$	$\sigma \in \partial e_{01}$	γ_σ	$\mathrm{sgn}(\sigma)$	$\sigma \in \partial e_{12}$	γ_σ	$\mathrm{sgn}(\sigma)$
p_0	id	-1	p_0	id	-1	p_1	id	-1
p_3	P^2	$+1$	p_1	id	$+1$	p_2	QP^{-1}	$+1$

TABLE 6.8: Distinguished maximal flags

3-cells	2-cells	1-cells	0-cells
$\mathbf{W} > \square_{1245} > e_{12} > p_1$	$\square_{1245} > e_{12} > p_1$	$e_{15} > p_1$	p_1
	$\triangle_{123} > e_{12} > p_1$	$e_{12} > p_1$	p_2
	$\triangle_{234} > e_{23} > p_2$	$e_{23} > p_2$	

TABLE 6.9: $\mathbf{W}$ Data

$\sigma \in \partial\mathbf{W}$	F_σ	γ_σ	$\mathrm{sgn}(\sigma)$
$\square_{1245}$	$\square_{1245} > e_{12} > p_1$	id	-1
$\square_{1345}$	$\square_{1345} > e_{45} > p_5$	I_1	-1
$\triangle_{123}$	$\triangle_{123} > e_{12} > p_1$	id	$+1$
$\triangle_{234}$	$\triangle_{234} > e_{23} > p_2$	id	-1

Then $(\alpha_i) \in \mathscr{C}^0, (\beta_i) \in \mathscr{C}^1, (\kappa_i) \in \mathscr{C}^2$*, the differentials are given by*

$$\begin{aligned}
\delta_0^{(2)}(\alpha) &= \begin{bmatrix} (\rho_2(T)-1)\alpha_1 \\ -\alpha_1+\alpha_2 \\ (\rho_2(S^{-1}I_1)-1)\alpha_2 \end{bmatrix}, \\
\delta_1^{(2)}(\beta) &= \begin{bmatrix} -\beta_1+(1-\rho_2(T))\beta_2-\rho_2(I_1^{-1}S)\beta_3 \\ (1-\rho_2(R))\beta_2+\beta_3 \\ (1+\rho_2(S^{-1}I_1)+\rho_2(I_1^{-1}S))\beta_3 \end{bmatrix}, \\
\delta_2^{(2)}(\kappa) &= \begin{bmatrix} -(1+\rho_2(I_1))\kappa_1+\kappa_2-\kappa_3 \end{bmatrix}.
\end{aligned}$$

Similarly, Theorem 6.3.1 gives us to explicitly compute the cohomology $H^*(\mathbf{H}^2_{\mathbb{C}}/G_2;\mathbb{Z})$ from the chain complex

$$0 \to \mathbb{Z}^2 \to \mathbb{Z}^3 \to \mathbb{Z}^3 \to \mathbb{Z} \to 0$$

with the differentials given by

$$\delta_0^{(2)} = \begin{bmatrix} 0 & 0 \\ -1 & 1 \\ 0 & 0 \end{bmatrix}, \quad \delta_1^{(2)} = \begin{bmatrix} -1 & 0 & -1 \\ 0 & 0 & 1 \\ 0 & 0 & 3 \end{bmatrix}, \quad \delta_2^{(2)} = \begin{bmatrix} -2 & 1 & -1 \end{bmatrix}.$$

Theorem 6.3.2. *Let* $\mathbb{Z}$ *denote the constant sheaf of integers on* $\mathbf{H}^2_{\mathbb{C}}/G_2$*. Then*

$$H^i(\mathbf{H}^2_{\mathbb{C}}/G_2;\mathbb{Z}) = \begin{cases} \mathbb{Z}, & i = 0, 2 \\ 0, & i = 1 \text{ or } i \geq 3. \end{cases}$$

TABLE 6.10: $\square_{1245}$ Data

$\sigma \in \partial\square_{1245}$	F_σ	γ_σ	$\mathrm{sgn}(\sigma)$
e_{12}	$e_{12} > p_1$	id	$+1$
e_{24}	$e_{24} > p_4$	$I_1^{-1}S$	-1
e_{45}	$e_{45} > p_5$	T	-1
e_{15}	$e_{15} > p_1$	id	-1

TABLE 6.11: $\triangle_{123}$ and $\triangle_{234}$ Data

$\sigma \in \partial\triangle_{123}$	F_σ	γ_σ	$\mathrm{sgn}(\sigma)$	$\sigma \in \partial\triangle_{234}$	F_σ	γ_σ	$\mathrm{sgn}(\sigma)$
e_{12}	$e_{12} > p_1$	id	$+1$	e_{23}	$e_{23} > p_2$	id	$+1$
e_{23}	$e_{23} > p_2$	id	$+1$	e_{34}	$e_{34} > p_3$	$S^{-1}I_1$	$+1$
e_{13}	$e_{13} > p_1$	R	-1	e_{24}	$e_{24} > p_4$	$I_1^{-1}S$	$+1$

TABLE 6.12: e_{15}, e_{12} and e_{23} Data

$\sigma \in \partial e_{15}$	γ_σ	$\mathrm{sgn}(\sigma)$	$\sigma \in \partial e_{12}$	γ_σ	$\mathrm{sgn}(\sigma)$	$\sigma \in \partial e_{23}$	γ_σ	$\mathrm{sgn}(\sigma)$
p_1	id	-1	p_1	id	-1	p_2	id	-1
p_5	T	$+1$	p_2	id	$+1$	p_3	$S^{-1}I_1$	$+1$

Proof. We only compute the 2-dimensional cohomology $H^2(\mathbf{H}^2_{\mathbb{C}}/G_2)$. The others are easier. It suffices to show $H^2(\mathbf{H}^2_{\mathbb{C}}/G_2) = \mathrm{Ker}(\delta_2^{(2)})/\mathrm{Im}(\delta_1^{(2)})$ is isomorphic to $\mathbb{Z}$. Note that

$$\mathrm{Ker}(\delta_2^{(2)}) = \{(\kappa_1, \kappa_2, \kappa_3) \in \mathbb{Z}^3 |\ \kappa_2 = 2\kappa_1 + \kappa_3\} \cong \{(\kappa_1, \kappa_3) \in \mathbb{Z}^2\}$$

and

$$\mathrm{Im}(\delta_1^{(2)}) = \{(\kappa_1, \kappa_2, \kappa_3) \in \mathbb{Z}^3 |\ \kappa_3 = 3\kappa_2\} = \{(\kappa_1, \kappa_3) \in \mathbb{Z}^2 |\ 3\kappa_1 + \kappa_3 = 0\}.$$

Consider a homomorphism

$$\begin{array}{rcl} \mathbb{Z}^2 & \stackrel{\phi}{\longrightarrow} & \mathbb{Z} \\ (\kappa_1, \kappa_3) & \longrightarrow & 3\kappa_1 + \kappa_3, \end{array}$$

then ϕ is surjective implies that

$$\mathrm{Ker}(\delta_2^{(2)})/\mathrm{Im}(\delta_1^{(2)}) = \mathbb{Z}^2/\mathrm{Ker}(\phi) \cong \mathbb{Z}.$$

□

Bibliography

[As77] A. Ash; *Deformation retracts with lowest possible dimension of arithmetic quotients of self-adjoint homogeneous cones*, Math. Ann., 225(1) (1977), 69-76.

[As80] A. Ash; *Cohomology of congruence subgroups $SL_n(\mathbb{Z})$*, Math. Ann., 249(1) (1980), 55-73.

[As84] A. Ash; *Small-dimensional classifying spaces for arithmetic subgroups of general linear groups*, Duke Math. J., 51(2) (1984), 459-468.

[BGS85] W. Ballmann, M. Gromov and V. Schroeder; *Manifolds of Non-positive curvature*, Progress in Mathematics, **61**, Birkhäuser, Basel, 1985.

[BHC62] A. Borel and Harish-Chandra; *Arithmetic subgroups of algebraic groups*, Ann. Math., **75** (1962), 485-535.

[Bo11] R. K. Boadi; *New cone metrics on the sphere*, Ph. D thesis, KUNUST Kumasi, Ghana 2011.

[BS73] A. Borel and J. P. Serre; *Corners and arithmetric groups*, Comment. Math. Helv. **48** (1973), 436-491.

[CG74] S. S. Chen and L. Greenberg; *Hyperbolic spaces. In: Contributions to Analysis*, ed. L.V. Ahlfors et al. Academic Press, 1974.

[Coh68] P. M. Cohn; *A presentation for SL_2 for Euclidean quadratic imaginary number fields*, Mathematika, **15** (1968), 156-163.

[Cor92] K. Corlette; *Archimedean superrigidity and hyperbolic geometry*, Annals of Math., **135** (1992), 165-182.

[Dek96] K. Dekimpe; *Almost-Bieberbach groups: Affine and polynomial structures*, Lecture Notes in Mathematics, 1639, Springer-Verlag, Berlin, 1996.

[Der05] M. Deraux; *Dirichlet domains for the Mostow lattices*, Experimental Maths., **14** (2005), 467-490.

[Der06] M. Deraux; *Deforming the $\mathbb{R}$-Fuchsian $(4;4;4)$-triangle group into a lattice*, Topology **45** (2006), 989-1020.

[DFP05] M. Deraux, E. Falbel and J. Paupert; *New constructions of fundamental polyhedra in complex hyperbolic space*, Acta Math., **194** (2005), no. 2, 155-201.

[DM86] P. Deligne and G. D. Mostow; *Monodromy of hypergeometric functions and non-lattice integral monodromy*, Publ. Math. IHES., **63** (1986), 5-89.

[Feu84] J. M. Feustel; *Zur groben Klassifikation der Picardschen Modulflächen*, Math. Nachr., **118** (1984), 215-251.

[FFLP11] E. Falbel, G. Francsics, P. Lax and J. R. Parker; *Generators of a Picard modular group in two complex dimensions*, Proc. Amer. Math. Soc. **139** (2011), 2439-2447.

[FH83] J. M. Feustel and R. P. Holzapfel; *Symmetry points and Chern invariants of Picard modular surfaces*, Math. Nachr., **111** (1983), 7-40.

[Fin89] B. Fine; *Algebraic theory of the Bianchi groups*, Marcel Dekker Inc., (1989).

[FK94] J. Faraut and A. Korányi; *Analysis on symmetric cones*, Oxford Math. Monographs, Oxford Univ. Press, New York, 1994.

[FP06] E. Falbel and J. R. Parker. *The Geometry of Eisenstein-Picard Modular Group*, Duke Math. J., **131**(2006), no. 2, 249-289.

[FFP10] E. Falbel, G. Francsics and J. R. Parker; *The geometry of the Gauss-Picard modular group*, Math Annalen., **349** (2010), 459-508.

[FL05] G. Francsics and P. Lax. *A semi-explicit fundamental domain for the Picard Modular Group in complex hyperbolic space*, Contemporary Mathematics., **368**(2005), 211-226.

[FLa05] G. Francsics and P. Lax; *An explicit fundamental domain for the Picard Modular Group in two complex dimensions*, (Preprint 2005).

[FZ99] E. Falbel and V. Zocca; *A Poincaré's polyhedron theorem for complex hyperbolic geometry*, J. Reine Angew. Math., **516** (1999), 133-158.

[Gir21] G. Giraud; *Sur certaines fonctions automorphes de deux variables*, Ann. Ec. Norm., **38** (1921), no. 3, 43-164.

[Gol99] W. M. Goldman; *Complex Hyperbolic Geometry*, Oxford Mathematical Monographs, Oxford University Press (1999).

[GPS87] M. Gromov and I. Piatetski-Shapiro; *Non-arithmetic groups in Lobachevsky spaces*, Publ. Math. IHES., **66** (1987), 93-103.

[GR70] H. Garland and M. S. Raghunathan; *Fundamental domains for lattices in (**R**-)rank 1 semisimple Lie groups*, Ann. of Math., **92** (1970), no.2, 279-326.

[GS92] M. Gromov and R. Schoen; *Harmonic maps into singular spaces and p-adic superrigidity for lattices in groups of rank one*, Publ. math. IHES., **76** (1992), 165-246.

[Kir92] F. Kirwan; *Complex algebraic curves*, London Mathematical Society Student Texts **23**, Cambridge University Press, (1992).

[Hol80] R.-P. Holzapfel; *A class of minimal surfaces in the unknown region of surface geography*, Math. Nachr., **98** (1980), 211-232.

[Hol98] R. P. Holzapfel, *Ball and surface arithmetics*, Aspects of Mathematics, E29. Friedr. Vieweg & Sohn, Braunschweig, 1998.

[Liv81] R. A. Livné; *On Certain Covers of the Universal Elliptic Curve*, Ph.D. Thesis, Harvard University, 1981.

[Loc61] E. H. Lockwood; *A book of curves*, Cambridge University Press, 1961.

[Mar84] G. Margulis; *Arithmeticity of the irreducible lattices in the semisimple groups of rank greater than 1*, Invent. Math., **74** (1984), 93-120.

[Men79] E. R. Mendoza; *Cohomology of PGL_2 over imaginary quadratic integers*, Bonner Math. Schriften 128, Univ, Bonn, 1979.

[Mos83] G. D. Mostow; *Strong rigidity of locally symmetric spaces*, Annals of Maths. Studies. **78**, Princeton University Press (1973).

[Mos80] G. D. Mostow; *On a remarkable class of polyhedra in complex hyperbolic space*, Pacific J. Math., **86** (1980), 171-276.

[Mos86] G. D. Mostow; *Generalized Picard lattices arising from half-integral conditions*, Publ. Math. IHES., 63 (1986), 91-106.

[Mos88] G. D. Mostow; *On discontinuous action of monodromy groups on the complex n-ball*, J. Amer. Math. Soc., **1** (1988), 555-586.

[Par10] J. R. Parker; *Complex hyperbolic kleinian groups*, Cambridge University press., (to appear).

[Par98] J. R. Parker; *On the volumes of cusped, complex hyperbolic manifolds and orbifolds*, Duke Math. J., **94** (1998), No. 3, 433-464.

[Par06] J. R. Parker; *Cone metrices on the sphere and Livné's lattices*, Acta Math., **196** (2006), 1-64.

[Par09] J. R. Parker; *Complex hyperbolic lattices*, Contemporary Mathematics., **501** (2009), 1-42.

[Pic83] É. Picard; *Sur des fonctions de deux variables indépendentes analogues aux fonctions modulaires*, Acta Math., **2** (1883), 114-135.

[Pic84] É. Picard; *Sur des formes quadratiques ternaires indéfinies indéterminées conjuguées et sur les fonctions hyperfuchsiennes correspondantes*, Acta Math., **5** (1884), 121-182.

[Pic85] É. Picard; *Sur les fonctions hyperfuchsiennes provenant des séries hypergéométriques de deux variables*, Ann. Sci. École Norm.Sup., **62** (1885), 357-384.

[PPa09] J. R. Parker and J. Paupert; *Unfaithful complex hyperbolic triangle groups II: Higher order reflections*, Pacific J. Math., **239** (2009), 357-389.

[PPl06] J. R. Parker and I. D. Platis; *Open sets of maximal dimension in complex hyperbolic quasi-Fuchsian space*, J. Differential Geometry., **73** (2006), 319-350.

[PT10] J. R. Parker and J. M. Thompson; *A fundamental domain for Deraux's lattice*, (preprint) 2010.

[Sat56] I. Satake; *On a generalization of the notion of manifold*, Proc. of the Nat. Acad. of Sc. U.S.A, **42** (1956), 359-363.

[Sat57] I. Satake; *The Gauss-Bonnet theorem for V-manifolds*, J. Math. Soc. of Japan, **9** (1957), 464-492.

[Sau90] J. K. Sauter; *Isomorphisms among monodromy groups and applications to lattices in $PU(1;2)$*, Pacific J. Math., **146** (1990), 331-384.

[Sco83] G. P. Scott; *The geometries of 3-manifolds*, Bull. London Math. Soc., **15**(1983), 401-487.

[Sou78] C. Soulé; *The cohomology of $SL_3(\mathbb{Z})$*, Topology, **17** (1978), 1-22.

[STa79] I. N. Stewart and D. O. Tall; *Algebraic number theory*, Chapman and Hall Ltd., (1979).

[Sto10] M. Stover; *Cusps and volumes of Picard modular surfaces*, to appear in Proc. Amer. Math. Soc., (2010).

[Swa71] R. G. Swan; *Generators and relations for certain special linear groups*, Adv. in Math., **6** (1971), 1-77.

[SV83] J. Schwermer and K. Vogtmann; *The integral homology of SL2 and PSL_2 of Euclidean imaginary quadratic integers*, Comment. Math. Helv., **58** (1983), 573-598.

[Tho10] J. M. Thompson; *Complex hyperbolic triangle groups*, Ph. D thesis in Durham University, 2010.

[Yas05] Dan Yasaki; *On the existence of spines for $\mathbb{Q}$-rank 1 groups*, Ph. D thesis in Duke University, 2005.

[Yas06] Dan Yasaki; *On the existence of spines for $\mathbb{Q}$-rank 1 groups*, Sel. math. New ser., **12** (2006), 541-564.

[Yas08] Dan Yasaki; *An explicit spine for the Picard modular group over the Gaussian integers*, J. Number. Theory., **128** (2008), 207-237.

[Zh11] T. Zhao; *A minimal volume arithmetic cusped complex hyperbolic orbifold*, Math. Proc. Camb. Phil. Soc., **150** (2011), 313-342.

[Zin79] T. Zink; *Über die Anzahl der Spitzen einiger arithmetischer Untergruppen unitäer Gruppen*, Math. Nachr., **89** (1979), 315-320.